RADC-TR-88-97
Final Technical Report
July 1988

RELIABILITY PREDICTION MODELS FOR DISCRETE SEMICONDUCTOR DEVICES

IIT Research Institute

David W. Coit and Mary G. Priore

APPROVED FOR PUBLIC RELEASE; DISTRIBUTION UNLIMITED.

ROME AIR DEVELOPMENT CENTER
Air Force Systems Command
Griffiss Air Force Base, NY 13441-5700

This report has been reviewed by the RADC Public Affairs Division (PA) and is releasable to the National Technical Information Service (NTIS). At NTIS it will be releasable to the general public, including foreign nations.

RADC-TR-88-97 has been reviewed and is approved for publication.

APPROVED: James J. Dobson

JAMES J. DOBSON
Project Engineer

APPROVED: John J. Bart

JOHN J. BART
Technical Director
Directorate of Reliability & Compatibility

FOR THE COMMANDER: John A. Ritz

JOHN A. RITZ
Directorate of Plans and Programs

If your address has changed or if you wish to be removed from the RADC mailing list, or if the addressee is no longer employed by your organization, please notify RADC (RBER) Griffiss AFB NY 13441-5700. This will assist us in maintaining a current mailing list.

Do not return copies of this report unless contractual obligations or notices on a specific doucment require that it be returned.

REPORT DOCUMENTATION PAGE

Form Approved OMB No. 0704-0188

1a. REPORT SECURITY CLASSIFICATION UNCLASSIFIED	1b. RESTRICTIVE MARKINGS N/A
2a. SECURITY CLASSIFICATION AUTHORITY N/A	3. DISTRIBUTION/AVAILABILITY OF REPORT Approved for public release; distribution unlimited.
2b. DECLASSIFICATION/DOWNGRADING SCHEDULE N/A	
4. PERFORMING ORGANIZATION REPORT NUMBER(S) N/A	5. MONITORING ORGANIZATION REPORT NUMBER(S) RADC-TR-88-97
6a. NAME OF PERFORMING ORGANIZATION IIT Research Institute 6b. OFFICE SYMBOL (If applicable)	7a. NAME OF MONITORING ORGANIZATION Rome Air Development Center (RBER)
6c. ADDRESS (City, State, and ZIP Code) Beeches Technical Campus Route 26 Rome NY 13440	7b. ADDRESS (City, State, and ZIP Code) Griffiss AFB NY 13441-5700
8a. NAME OF FUNDING/SPONSORING ORGANIZATION Rome Air Development Center 8b. OFFICE SYMBOL (If applicable) RBER	9. PROCUREMENT INSTRUMENT IDENTIFICATION NUMBER F30602-85-C-0131
8c. ADDRESS (City, State, and ZIP Code) Griffiss AFB NY 13441-5700	10. SOURCE OF FUNDING NUMBERS PROGRAM ELEMENT NO. 62702F; PROJECT NO. 2338; TASK NO. 02; WORK UNIT ACCESSION NO. 2P

11. TITLE (Include Security Classification)
RELIABILITY PREDICTION MODELS FOR DISCRETE SEMICONDUCTOR DEVICES

12. PERSONAL AUTHOR(S)
David W. Coit, Mary C. Priore

13a. TYPE OF REPORT	13b. TIME COVERED	14. DATE OF REPORT (Year, Month, Day)	15. PAGE COUNT
Final	FROM Jul 85 TO Feb 87	July 1988	348

16. SUPPLEMENTARY NOTATION
N/A

17. COSATI CODES		
FIELD	GROUP	SUB-GROUP
13	08	

18. SUBJECT TERMS (Continue on reverse if necessary and identify by block number)
Reliability; Failure Rate; MIL-HDBK-217; Discrete Semiconductor; Diode; Transistor; Thyristor; Opto-electronic; Microwave Transistor

19. ABSTRACT (Continue on reverse if necessary and identify by block number)

The objective of this study was to update and revise the failure rate prediction models for discrete semiconductor devices currently in Section 5.1.3 of MIL-HDBK-217E, "Reliability Prediction of Electronic Equipment." GaAs Power FETS, Transient Suppressor Diodes, Infrared LEDs, Diode Array Displays and Current Regulator Devices.

The proposed prediction models provide the ability to predict total device failure rate (both catastrophic and drift) for all military environments for both operating and non-operating modes. The updated models are formatted to be compatible with MIL-HDBK-217E and are included as an appendix to the Final Technical Report.

Significant factors found to influence failure rate were device construction, semiconductor material, junction temperature, electrical stress, circuit application, application environment, package type and screen class.

20. DISTRIBUTION/AVAILABILITY OF ABSTRACT ☒ UNCLASSIFIED/UNLIMITED ☐ SAME AS RPT. ☐ DTIC USERS	21. ABSTRACT SECURITY CLASSIFICATION UNCLASSIFIED
22a. NAME OF RESPONSIBLE INDIVIDUAL James J. Dobson	22b. TELEPHONE (Include Area Code) (315) 330-2951 22c. OFFICE SYMBOL RADC (RBER)

DD Form 1473, JUN 86 *Previous editions are obsolete.*

PREFACE

This Final Technical Report was prepared by IIT Research Institute Rome, NY for the Rome Air Development Center, Griffiss AFB, New York under Contract F30602-85-C-0131. The RADC technical contract monitor for this program is Mr. James Dobson. This final report covers the work performed from July 1985 to February 1987.

The principal investigators for this program were David W. Coit and Mary G. Priore. Other members of the IITRI project team providing valuable assistance are John Carroll, William K. Denson, William H. Crowell, Alex J. Recchio, James P. Carey and Michael J. Rossi. Report preparation was coordinated by Pamela J. Meus. Also providing document production support were Patti McQuinn and Steven Lorraine.

MANAGEMENT SUMMARY

The objective of this study was to update and revise the failure rate prediction models for discrete semiconductor devices currently in Section 5.1.3 of MIL-HDBK-217E, "Reliability Prediction of Electronic Equipment."

In addition, new failure rate prediction models were developed for the following devices:

- o GaAs Power FETs
- o Transient Suppressor Diodes
- o Infrared LEDs
- o Diode Array Displays
- o Current Regulator Diodes

The proposed prediction models provide the ability to predict total device failure rate (both catastrophic and drift) for all military environments for both operating and nonoperating modes. The updated models are formatted to be compatible with MIL-HDBK-217E and are included as an appendix to this Final Technical Report.

Significant factors found to influence failure rate were device construction, semiconductor material, junction temperature, electrical stress, circuit application, application environment, package type and screen class.

As a result of this effort, the efficiency and usability of the discrete semiconductor section was greatly improved by:

- o Consolidation of redundant quality factor tables
- o Consolidation of redundant environmental factor tables
- o Definition of a separate (from the base failure rate) temperature factor

- Junction temperature estimation based on package thermal resistances
- Elimination of insignificant model factors

As a result of this study, all discrete semiconductor models were revised. No device types or models were deleted. Consideration was given to eliminating Germanium devices from MIL-HDBK-217E because they are in the process of becoming obsolete. However, it was decided to retain these devices since they continue to be used in small quantitites.

TABLE OF CONTENTS

TABLE OF CONTENTS (CONT'D)

LIST OF FIGURES

LIST OF FIGURES (CONT'D)

LIST OF TABLES

LIST OF TABLES (CONT'D)

LIST OF TABLES (CONT'D)

1.0 INTRODUCTION

1.1 OBJECTIVE

The objective of this study was to update and revise the discrete semiconductor device failure rate prediction models for inclusion into MIL-HDBK-217E, "Reliability Prediction of Electronic Equipment." The proposed models provide the ability to predict total device failure rate (both catastrophic and drift) for all military environments for both operating and nonoperating modes.

The proposed prediction models predict component failure rates as a function of the characteristics of the device, the technology employed in producing the device, and the external factors such as operational and environmental stresses which have a statistically significant effect on device failure rate. The prediction models are presented in a form compatible with MIL-HDBK-217E in Appendix A.

The study objectives were met by defining and implementing a four-phase study approach. The four phases are as follows:

- Evaluation of existing MIL-HDBK-217E discrete semiconductor models
- Data/information collection
- Data analysis/model development
- Final technical report preparation

These study phases are described in detail in the major sections of this technical report.

1.2 BACKGROUND

Accurate reliability prediction models are essential tools in the development, design, manufacture, and maintenance of military electronic

equipments and systems. Prior to this study, the MIL-HDBK-217E failure rate prediction models for discrete semiconductors had not formally been investigated since 1978. Since that time, many of the reference tables for discrete semiconductors have become inadequate in regard to the full range of values, such as electrical ratings and frequency ranges. In addition, there are many new devices that are not properly addressed in MIL-HDBK-217E, such as GaAs power FETs. Additionally, models were updated to reflect advances in design and processing technology.

1.3 ABBREVIATIONS/ACRONYMS

The following abbreviations and acronyms are used throughout the report:

AF	Air Force
AFWAL	Air Force Wright Aeronautical Laboratory
AIA	Aerospace Industries Association
AIA	Airborne Inhabited Attack
AIB	Airborne Inhabited Bomber
AIC	Airborne Inhabited Cargo
AIF	Airborne Inhabited Fighter
AIT	Airborne Inhabited Trainer
ARW	Airborne Rotory Wing
AUA	Airborne Uninhabited Attack
AUB	Airborne Uninhabited Bomber
AUC	Airborne Uninhabited Cargo
AUF	Airborne Uninhabited Fighter
AUT	Airborne Uninhabited Trainer
CL	Cannon Launch
CW	Continuous Wave
DF	Duty Factor
DH	Double Heterostructure
DSCS	Defense Satellite Communications Systems
DTIC	Defense Technical Information Center
EIA	Electronic Industries Association
FET	Field Effect Transistor
GB	Ground Benign
GF	Ground Fixed
GIDEP	Government Industry Data Exchange Program
GM	Ground Mobile
GP	General Purpose
HEMT	High Electron Mobility Transistor
IMPATT	Impact Avalanche Transit Time
IRED	Infrared Emmitting Diode

JFET	Junction Field Effect Transistor
JPL	Jet Propulsion Laboratory
JTIDS	Joint Tactical Information Distribution System
LASER	Light Amplification by Stimulated Emission of Radiation
LED	Light Emmiting Diode
MDC	Maintenance Data Collection
MFA	Airbreathing Missile, Flight
MFF	Missile, Free Flight
ML	Missile, Launch
MMIC	Monolithic Microwave Integrated Circuits
MOS	Metal-Oxide-Semiconductor
MOV	Metal Oxide Varistor
MP	Manpack
MTBF	Mean Time Between Failure
MTTF	Mean Time To Failure
NASA	National Aeronautics and Space Administration
NH	Naval, Hydrofoil
NRL	Naval Research Laboratories
NS	Naval, Sheltered
NSIA	National Security Industrial Association
NSB	Naval, Submarine
NU	Naval, Unsheltered
NUU	Naval, Undersea, Unsheltered
PIN	P-type, Intrinsic, N-Type
PPAC	Product Performance Agreement Center
PW	Pulse Width
RAC	Reliability Analysis Center
RADC	Rome Air Development Center
RF	Radio Frequency
RIW	Reliability Improvement Warranty
SCR	Silicon Controlled Rectifier
TED	Transferred Electron Device
TRAPATT	Trapped Plasma Avalanche Triggered Transit
USL	Undersea, Launch

2.0 DATA/INFORMATION COLLECTION

The basis for reliability prediction model development is the establishment of a comprehensive knowledge-base consisting of empirical failure data, together with qualitative reliability assessments of discrete semiconductor part types. IITRI conducted an exhaustive data/information collection task to obtain the requisite information. This was accomplished with two distinct subtasks: a literature search and empirical data collection. Additionally, potential deficiencies with the collected data were studied to further understand the implications of the data analysis tasks.

2.1 LITERATURE SEARCH

A thorough literature review was performed to identify all current published information relevant to the reliability of discrete semiconductors. Results from the literature search were used to identify additional data sources, to develop theoretical failure rate prediction models, to evaluate proposed models and to complement the data analyses for part families where only limited data resources were available. Additionally, discrete semiconductor reliability prediction references were examined to aid in determining deficiencies (where there were any) in current prediction methods.

The following technical areas warranted particular emphasis during the literature search:

(1) Reliability and device characterization of high frequency discrete semiconductor devices (GaAs FETs, Bipolar Microwave Transistors, Detector/Mixer Diodes, Schottky Detector Diodes, IMPATT Diodes, PIN Diodes, Gunn Diodes, Varactors, Tunnel Diodes and Step Recovery Diodes)

(2) Documented temperature relationships

(3) Time-to-failure test data

(4) Comparisons of predicted to observed failure rates

(5) References to field reliability data reporting systems

To ensure an efficient and effective literature search, an organized search methodology was followed. Hundreds of documents or technical articles were identified and critiqued to determine applicability to this study. Important literature resources are presented in Table 2.1-1. Over 100 relevant document or technical articles were found; these are listed in the References and Bibliography sections of this final report.

TABLE 2.1-1. LITERATURE REVIEW RESOURCES

Resource	Description
Defense Technical Information Center	DTIC maintains a large computerized database of technical documents produced by government sponsored efforts.
Reliability Analysis Center (RAC)	RAC is a DoD Information Analysis Center primarily concerned with electronic component and system reliability. The center has an automated library and database with numerous hardware reliability references.
Government Industry Data Exchange	The GIDEP database contains four separate databanks. Of these, the Engineering Databanks, the Reliability-Maintainability Data-bank, and the Failure Experience Databank were most relevant to this study.
Published Authors	Published authors identified in the literature as being experts in the field were contacted for further data and information relevant to the reliability of discrete semiconductor devices, particularly state-of-the-art device types.

Government organizations that perform or fund research in relevant technical areas were queried to identify ongoing or completed studies. Technical reports from the following organizations were particularly helpful.

USAF RADC
USAF Space Division
Air Force Wright Aeronautical Laboratories (AFWAL)
Jet Propulsion Laboratories (JPL)
Naval Research Laboratories (NRL)
NASA Marshall Space Flight Center

The information gathered from the literature search was particularly important to the development of failure rate prediction models for GaAs power FETs and other state-of-the-art and/or low-population, low-usage part types. Such part types have not usually been exposed to enough field usage to base a failure rate prediction model entirely on statistical analyses. Therefore, test data, knowledge of failure mechanisms, accelerating stresses and activation energies from the literature are particularly important for these devices. Included in this category of parts are microwave devices and high power devices.

2.2 EMPIRICAL DATA COLLECTION

IITRI conducted a highly successful data collection effort to identify data sources and to collect empirical discrete semiconductor failure data. The data collection effort provides the required baseline used for subsequent data analyses. A preferred data collection approach was determined in the early stages of this study to facilitate planning, to provide direction to data collection activities, and to ensure that adequate time was available for reacting to unforeseen difficulties or data deficiencies. A detailed listing of the collected data is presented in Appendix B of this report. The data is summarized in Table 2.2-1.

TABLE 2.2-1. DISCRETE SEMICONDUCTOR FIELD FAILURE DATA SUMMARY

Part Class	Failures	Part Hours ($\times 10^6$)
Switching Diode	86	916.91
Rectifier Diode	471	7745.48
Voltage Regulator Diode	228	1154.84
Voltage Reference Diode	282	2951.22
Current Regulator Diode	2	13.54
Transient Suppressor Diode	7	6.58
PNP Transistor, <5W	2330	24706.61
NPN Transistor, <5W	246	1845.35
PNP Transistor, ≥ 5W	52	75.10
NPN Transistor, ≥ 5W	89	112.24
Dual Transistor	1	7.05
Darlington Transistor	57	76.58
JFET	878	5177.81
MOSFET	209	431.77
Unijunction Device	19	68.23
Thyristor	245	1013.18
Schottky Microwave Diode	18	129.39
Tunnel Diode	72	234.45
Varactor	30	173.29
PIN Diode	1857	13413.37
Microwave Power Transistor	2612	1138.70
LED	22	4827.08
Infrared Emitting Diode (IRED)	0	39.19
Alphanumeric Display (Segment)	144	636689.67
Alphanumeric Display (Diode Array)	4	646.09
Photodetector	7	47.02
Opto-isolator	170	595.96

Table 2.2-1 presents a complete summary of all collected field data. In several categories there was insufficient data to determine statistically relevant failure rates. The precision with which failure rates can be estimated is dependent on the quantity of observed failures. Failure rate estimation precision is suspect for part categories where there were a small (i.e., less than five) number of failures. Part types with less than five failures are current regulator diodes, dual transistor devices, infrared emitting diodes and diode array alphanumeric displays. For these part types the best estimate failure rates were used by dividing the number of failures by the part hours. It is recommended that more data be collected and the proposed prediction models checked for validity for these parts.

Four specific data collection tasks were defined. The first task was a system/equipment identification process. A survey of numerous military equipments was conducted to identify system/equipments meeting predetermined criteria established to ensure plentiful and accurate data. The second task was an extensive survey of discrete semiconductor manufacturers and users. The survey was conducted by mail and over the telephone. The third task was in-person visits to organizations where data could not be accessed by other means. The final data collection task was the compilation of data referenced in the literature and documented technical studies. Also as part of this task, additional contact was made to the authors and/or study sponsors to determine whether more data were available. Results of the four specific data collection tasks were described in the following sections.

System/Equipment Identification

Discrete semiconductors, in one or more of a multitude of different design options, are used in essentially all military electronic equipments. The sheer magnitude of the available equipments, each a potential candidate for discrete semiconductor data collection, presented a problem to IITRI data collectors. It would be terribly inefficient to arbitrarily choose equipments with discrete semiconductors and pursue relevant failure data. Instead, the system/equipment identification task was specifically defined to review numerous potential equipments, using a predetermined set of evaluation criteria. After reviewing many candidates, an optimal group of equipments was selected which would result in accurate, meaningful data and represent diverse application and environmental conditions.

Five minimum criteria were established to define an acceptable data source. Each potential equipment selection was evaluated with these

criteria before proceeding with data summarization. These five criteria are:

(1) Data available to the part level

(2) Primary failures can be separated from total maintenance actions

(3) Sufficient detail, including stress levels, can be identified for the components

(4) Part hours can be precisely determined

(5) Sufficient equipment hours to expect discrete semiconductor failures

In addition to this criteria, the following factors were considered:

- Number of different discrete semiconductor part types
- Existence of low population and state-of-the-art parts
- Application environment
- Age of data

Since verified part failures are essential to develop meaningful failure rate prediction models, a major area of interest was Reliability Improvement Warranty (RIW) program data. Equipments procured under RIW contract are subjected to more thorough failure diagnosis. Also, failure documentation is much more complete than the data available through the automated military data retrieval systems. IITRI established contact at the Product Performance Agreement Center (PPAC), Wright Patterson AFB, to aid in the equipment selection process. PPAC monitors RIW programs for the Air Force. Applicable RIW equipments used for this study are the AN/ARN-118, the F-16 heads-up-display and the F-16 flight control computer.

The military equipments selected after the evaluation process are as follows:

AN/FPS-115 PAVE PAWS
AN/FPS-117 SEEK IGLOO
AN/TPS-59
JTIDS
F-16 flight control computer
F-16 heads-up-display
AN/ARN-118
AN/ARC-164
AN/BRD-7

IITRI successfully collected data on each of these systems with the exception of the JTIDS and AN/ARC-164. Data was not available on the JTIDS despite determined efforts, including written requests and a trip to the equipment prime contractor. This was unfortunate because this system was considered a major source of microwave device failure data. The AN/ARC-164 data consisted of insufficient device hours to be useful for this study.

The above group of equipments represent diverse application and environmental conditions. Environmental factors could be properly evaluated and refined because of the range of environmental stresses represented by this set of equipments. Applications range from ground to helicopter. The AN/ARN-118 is a particularly useful candidate for evaluating and developing environmental factors because it is installed in thirteen different aircraft types representing each major category (i.e., attack, fighter, cargo, trainer, bomber and helicopter). Additionally, the AN/BRD-7 was extremely useful for evaluating naval environmental factors.

The equipment selection task favored equipments designed with bipolar microwave transistors and other low population and state-of-the-art part types since there are a limited number of equipments designed with microwave transistors. To quantify a failure rate prediction model, it was necessary to identify candidate equipments and collect data for a

range of the key parameters which affect failure rate, namely frequency, power, duty factor and pulse width. For example, the AN/FPS-117 and AN/FPS-115 phased array modules are designed with microwave transistors which operate with different pulse width and at different frequency-power characteristics. Failures of microwave devices are generally tracked more accurately by both the government user and the contractor because of the relatively higher rate of failure and the costs involved. General Electric, Syracuse, NY, supplied failure data on the AN/FPS-117 and AN/TPS-59. Raytheon was contacted over the telephone and in-person and has submitted data on the AN/FPS-115 phased array modules. This data consists of 521 part failures in 439.84 x 10^6 part hours for microwave transistors.

The principal sources of field data used by IITRI were from recent data sources. The data collection time domain for the major sources are as follows:

F-16 HUD	1979 - 1983
F-16 FCC	1979 - 1983
AN/BRD-7	1974 - 1976
Commercial Equipment Manufacturer Data	1979 - 1986
AN/FPS-115	1983 - 1986
AN/TPS-59	1983 - 1985
AN/ARN-118	1976 - 1979

No fielded equipments meeting the defined criteria could be identified which utilize GaAs power FETs. The MILSTAR and Defense Satellite Communications Systems (DSCS) III were identified as systems with GaAs power FETs. However, it is too early for the collection of field data.

The system/equipment selection task resulted in selection of a core group of equipments with known failure reporting accuracy. The successful completion of this task ensures that engineering and data summarization time is spent wisely and that excessive effort was not spent summarizing equipments in one application at the expense of others.

Selection of this core group of equipments did not mean that other data sources were not sought after. In fact, as the study progressed, data was collected from other equipments including the B3D radar and the ITT Vortac system and a variety of commercial electronic equipments.

Discrete Semiconductor User/Vendor Survey

A thorough discrete semiconductor reliability survey was conducted to:

(1) Identify additional sources of data
(2) Expand the scope of the data collection effort
(3) Obtain objective outside opinions and assistance
(4) Assist the MIL-HDBK-217E evaluation task

More than 160 discrete semiconductor vendors and 160 user organizations were queried. Survey participants were asked to critique the existing MIL-HDBK-217E failure rate prediction methodology and to determine whether failure data were available. Survey participants were selected using GIDEP ALERTs, part manufacturer catalogs (i.e., Goldbook, EEM) and IITRI's extensive collection of contacts developed through the successful completion of other reliability modeling efforts. A portion of this task was also subcontracted to the Reliability Analysis Center (RAC). A copy of the survey for discrete semiconductor users is presented in Figure 2.2-1. Organizations who have participated in the survey are listed in Table 2.2-2.

Results from the user/vendor survey were used to complement the equipment selection task and corresponding data summarization. The user/vendor survey is a flexible data collection tool because they are inexpensive to distribute and have proven to be invaluable in identifying new sources of data and new approaches to collect data. Surveys were sent to a wide variety of government and commercial industries representing many different applications. Upon receipt of a completed survey, the organization was contacted to determine the availability of data and/or the identification of potential sources.

MIL-HDBK-217E DISCRETE SEMICONDUCTOR SURVEY

Name: _____

Title: _____

Organization: _____

Address: _____

_____

_____

Telephone No.: _____

(1) What discrete semiconductor part types are being used in equipment designs but are not included in MIL-HDBK-217D? _____

_____

(2) What discrete semiconductor part types included in MIL-HDBK-217D do not have adequate parameter table ranges? Which specific tables are inadequate? _____

_____

_____

(3) What factors included in the MIL-HDBK-217D discrete semiconductor failure rate prediction models do not have a significant effect on reliability in your opinion? _____

_____

_____

(4) What factors are not included in the MIL-HDBK-217D models that you feel do have a significant effect on reliability? _____

_____

_____

(5) What other problems or comments do you have with the MIL-HDBK-217D discrete semiconductor section? _____

_____

_____

(6) Does your organization have discrete semiconductor field, test or failure analysis data to support your opinions? _____

(7) Please return the completed survey to the following address:

IIT Research Institute
P.O. Box 180
Turin Road, North
Rome, NY 13440

Figure 2.2-1. MIL-HDBK-217E Discrete Semiconductor Survey

TABLE 2.2-2. MIL-HDBK-217E DISCRETE SEMICONDUCTOR SURVEY RESPONDEES

ACDC Electronics
Oceanside, CA

Albert Hayes & Associates
Yucca Valley, CA

Boeing Military Airplane Company
Wichita, KS

Eaton Corporation, AIL Division
Hauppauge, NY

Fisher Controls
Marshalltown, IA

GEC Avionics LTD
Rochester, Kent, England

General Electric Ordinance
Systems Division
Pittsfield, MA

General Semiconductor

Intersil
Cupertino, CA

Lorain Products
Lorain, OH

Magnovox Electronic Systems Company
Ft. Wayne, IN

Naval Ordinance Station
Louisville, KY

Northrop Precision Products Division
Norwood, MA

Raytheon Equipment Division
Marlboro, MA

Rockwell International
Albuquerque, NM

Rohm Corporation
Irvine, CA

Sperry Flight Systems
Phoenix, AZ

Sprague Electric Company
Concord, NH

Westinghouse Electric Corporation
Baltimore, MD

Data Collection Trips

Many sources of failure data can only be accessed through in-person visits because of the proprietary nature of many internal databases, the need to specifically describe required data characteristics and the need to "sell" the study program to organizations who provide data without charge. The data collection trips performed to support the discrete semiconductor reliability study were carefully planned to maximize the probability of obtaining relevant data.

Table 2.2-3 presents a summary of the organizations visited by IITRI engineers to collect discrete semiconductor failure data. Most organizations who routinely perform reliability predictions were enthusiastic to the revision of the MIL-HDBK-217E discrete semiconductor section and were receptive to the data collection request. As a direct result of the data collection trips, 521 failures in 439.84 x 10^6 part hours were collected from Raytheon, and 60 failures in 299 x 10^6 part hours of life test data was collected from Unitrode.

TABLE 2.2-3. DATA COLLECTION TRIPS

ORGANIZATION	LOCATION	USER/ VENDOR	DATE OF VISIT
Magnavox	Torrance, CA	User	3 October 1985
Hughes Aircraft Co.	Fullerton, CA	User	21 January 1986
Northrup Corp.	Hawthorne, CA	User	22 January 1986
Sanders Associates	Nashua, NH	User	10 February 1986
Silicon Transistor Corp.	Chelmsford, MA	Vendor	10 February 1986
Raytheon Co.	Wayland, MA	User	11 February 1986
Semicon Inc.	Burlington, MA	Vendor	12 February 1986
M/A COM	Burlington, MA	Vendor	12 February 1986
Unitrode	Watertown, MA	Vendor	13 February 1986

Life Test Data

The data collection efforts for this study were concentrated on the collection of field experience data; however, life test and other forms of test data have not been ignored. Life test data was the only source of quantitative reliability data for GaAs power FETs. Additionally, test data is an excellent source of time-to-failure, failure mode/mechanism and temperature dependence data. Test data was pursued by making telephone contact with manufacturers and testing facilities, and by identifying documented sources of life test data.

A high priority was placed on the collection of life test data for GaAs power FETs. Although several systems (i.e., MILSTAR, DSCS III) are

designed with GaAs power FETs, no field data was available; thus, collection of quality life test data was imperative.

In general GaAs FET life testing is performed for one of two reasons: either (1) testing is done in support of an existing equipment development program as part of a design trade-off or as part of reliability qualification, or (2) testing is only one aspect of a technology development program designed to develop devices at unique frequency and/or power ranges.

Air Force Space Division (AFSC) has sponsored several programs which involve life testing of GaAs FETs. In one Space Division program, Jet Propulsion Laboratories (JPL) has tested GaAs FETs at 7.5 GHz and 2 watts, and at 7.5 GHz and 6 watts. In another Space Division program, 20 GHz FETs and IMPATT diodes are being tested and the results compared. This testing, performed by RCA David Sarnoff Laboratories, is anticipated to be completed by the end of 1987.

Air Force Wright Aeronautical Laboratories (AFWAL) has also been active in the development of GaAs power FETs and have sponsored programs which have included life testing. In one AFWAL program, "GaAs Power FET Technology Improvement" performed by Hughes Aircraft Co., life testing and development activities were performed to support a goal of 10 watt GaAs power FETs operating in the 9 to 10 GHz frequency range. Observed failure mechanisms were gold electromigration and tin diffusion through via holes. AFWAL has also sponsored technology development work in the 5 GHz range and other related technical areas.

Other organizations contacted by IITRI who are sponsoring GaAs power FET life testing are NASA Goddard Space Flight Center, Naval Research Laboratories (NRL) and RCA David Sarnoff Laboratories. Additionally, numerous part vendors (i.e., Avantek, Microwave Associates, etc.) were contacted to identify sources of life test data.

Table 2.2-4 presents a summary of the discrete semiconductor data identified in the literature. Table 2.2-5 presents a listing of all collected life test data. After identifying a potential data source in the literature, IITRI contacted the author and/or the sponsoring agency to determine:

(1) More specific information regarding the testing

(2) Whether there has been additional testing since the publication date

(3) Whether there has been similar testing on other discrete semiconductor part types

TABLE 2.2-4. DISCRETE SEMICONDUCTOR LIFE TEST DATA EXTRACTED FROM LITERATURE

Part Type	Number Tested	Failures	Part Hours ($\times 10^6$)
Bipolar Transistor	219	21	0.494
FET	851	224	9122.691
Microwave Transistor	101	26	1.099
Schottky Barrier Diode	150	52	62.313
PIN Diode	(1)	1326	8438.136
Varactor	(1)	0	38.715
GUNN Diode	(1)	40	4.727
IMPATT Diode	290	90	0.640
LED	60	39	1.023
LED Array	352	237	0.447
Laser Diode	874	442	4.646
Photodiode	16	0	0.077
Photocoupler	669	337	2.152
	>3582	2834	17677.160

NOTES: (1) The total number of devices tested could not be determined because of the format of the submitted data.

TABLE 2.2-5. DISCRETE SEMICONDUCTOR HIGH TEMPERATURE LIFE TEST FAILURE DATA

Part Type	Junction/Channel Temperature(°C)	Failures	Part Hours (x 10^6)	Failure Rate (failure/10^6 hours)
Transient	100	-	-	63
Suppressor	125	-	-	158
Diode	145	-	-	631.0
(Varistor)	150	-	-	562.0
	125	-	-	56
	100	-	-	18
	125	-	-	126
	100	-	-	13
Si FET, <5W	191	24	.44	-
Si FET, ≥5W	200	9	.12	-
Si FET, 90W	200	3	.12	-
Si FET, 125W	200	2	.12	-
Si FET, 150W	200	5	.25	-
Si FET, 6W	200	5	.13	-
Si FET, 12.5W	200	6	.13	-
Si FET, 5W	200	1	.13	-
Bipolar Trans.	131	1	.17	-
	191	6	.13	-
	291	14	.10	-
Thyristor	373	-	-	4800
	348	-	-	1600
Si Schottky	210	10	.263	-
Microwave	240	16	.263	-
Diode	270	23	.109	-
GaAs Schottky	136	0	.413	-
Microwave	141	0	.019	-
Diode				
Si IMPATT Diode	203	1	.031	-
	210	0	.163	-
	218	0	.031	-
	219	2	.019	-
	221	0	.143	-
	232	2	.028	-
	312	32	.064	-
	332	32	.015	-
	256	5	.01189	-
	280	20	.08031	-
	300	10	.00017	-
	312	7	.00004	-
	325	13	.01006	-
	350	12	.00224	-
	290	8	.00168	-

TABLE 2.2-5. DISCRETE SEMICONDUCTOR HIGH TEMPERATURE LIFE TEST FAILURE DATA (CONT'D)

Part Type	Junction/Channel Temperature(°C)	Failures	Part Hours ($\times 10^6$)	Failure Rate (failure/10^6 hours)
GaAs IMPATT Diode	220	17	.030	-
	235	1	.006	-
	350	14	.076	-
	400	14	.014	-
	215	1	.070	-
GaAs Gunn Diode	275	9	.00004	-
	300	9	.00002	-
	325	9	.00003	-
	-	0	.118	-
	-	2	.300	-
	-	4	1.114	-
	-	29	1.809	-
	-	4	1.112	-
	-	1	.247	-
GaAs FET (<100mw)	200	27	.037	-
	220	40	.029	-
	240	29	.028	-
	260	33	.016	-
	230	-	-	610
	255	-	-	3937
	275	-	-	9174
GaAs Power FET	150	8	.014	-
	190	11	.004	-
	225	6	.001	-
	180	8	.068	-
	240	8	.027	-
	270	8	.006	-
	228	4	.008	-
	280	7	.0008	-
	218	0	.003	-
	265	66	.088	-
	208	8	.032	-
	160	4	.146	-
	225	4	.077	-
	250	10	.105	-
	275	13	.008	-
	200	-	-	454
	218	-	-	555
	249	-	-	1613
	274	-	-	4545
	274	-	-	7407
	274	-	-	2128

TABLE 2.2-5. DISCRETE SEMICONDUCTOR HIGH TEMPERATURE LIFE TEST FAILURE DATA (CONT'D)

Part Type	Junction/Channel Temperature(°C)	Failures	Part Hours ($\times 10^6$)	Failure Rate (failure/10^6 hours)
LED, GaAs	10	41	.333	-
	70	1	.003	-
	130	1	.003	-
	170	15	.003	-
	190	5	.003	-
LED, Si	210	62	.034	-
	250	69	.017	-
	170	43	.054	-
Infrared Emitting Diode	-	39	1.023	-
Opto-isolator, Si	10	103	0.647	-
	130	60	.810	-
	190	53	.256	-
	230	41	.312	-
	250	80	.128	-
Laser Diode, AlGaAs	22	13	1.035	-
	70	205	1.402	-
	70	0	.3	-
Laser Diode, GaAs	22	0	.637	-
	65	0	.091	-

For some sources of test data; only the resulting failure rate was available and not the specific number of failures and device hours. In these instances more detailed information was requested from the data source. In general, the data was not used if the specific number of failures and hours could not be identified. For part types where data was scarce or the part type was of particular interest, it was necessary to use these data entries during model development. They are presented in Table 2.2-5 as entries with a failure rate but no corresponding failures and part hours.

Data Summarization

Data summarization consists of the extraction and compilation of the desired data elements from the source reports and/or supporting

documentation, and coding the data for computer entry. Data summarization consisted of the following five tasks for sources of field data:

(1) Identification of discrete semiconductor part types within the chosen equipment

(2) Determination of part characterization information

(3) Identification of relevant part failures

(4) Determination of applicable electrical and environmental stress levels

(5) Determination of equipment operating histories

Each of these tasks is essential to properly summarize the data and the identification of failed parts requires the most effort and technical skill. For example, to identify the quantity of discrete semiconductor failures for the AN/ARN-118, over 3,500 RIW failure reports were manually evaluated.

Specific electrical and environmental stress levels can be difficult to determine. An approach which has been successfully used by IITRI is to obtain the detailed MIL-HDBK-217E part stress reliability prediction reports from the equipment manufacturer or the government project office. The detailed part stress reports provide the inputs to the reliability prediction, and thereby include the electrical stress and application information required to properly characterize the device usage. Detailed parts stress reliability predictions were received for the AN/ARN-118 and the F-16 HUD. For other systems, part stress information was solicited from the equipment manufacturers. Applied power and frequency were obtained for the microwave bipolar transistors in the AN/FPS-117, AN/FPS-115, ITT Vortac, DME, TACAN and AN/TPS-59.

2.3 DATA DEFICIENCIES

It is important to understand the characteristics of available failure data to fully appreciate the meaning of the resultant failure rate prediction models. The available data does have limitations, and it is

necessary to identify and evaluate these limitations so that precautionary or compensatory measures can be taken. This section explores these apparent data deficiencies and explains the implications regarding prediction model accuracy.

The available discrete semiconductor data was generally either high temperature life test data or field experience data. In general, the field experience data is preferable for model development purposes; however, both types of data have relative merits for use in this study.

Life test data is generally of a high statistical quality because there is very little uncertainty regarding estimation of failure quantity, failure definition, number of parts on test, test time, and test conditions. Life test data is often the only available source of data for the determination of component failure rate time dependency and temperature relationships. Additionally, life test data is available sooner then field data for emerging technologies such as GaAs power FETs and may be the only source for these devices. The major deficiencies with life test data are (1) the test periods are relatively short, and (2) the test conditions are not representative of the actual usage environment. Life test data was only used in this study as a complement to the field experience data except for GaAs FETs and laser diodes where life test data was the only type available.

Collection and analysis of field experience data was the major emphasis in this study. Models based on field data more accurately reflect the actual usage environment. Deficiencies with this type of data can be categorized into three areas:

(1) Data Reporting System Characteristics

- Availability of reliability data
- Failure definition
- Grouped data

(2) Application Characterization

- Operating time estimation
- Mission profile categorization

- Environmental/electrical stress determination

(3) Effects of Design Practices

- Natural correlation of variables
- Model availability paradox
- High integration/low failure rate trends

Data Reporting System Characteristics

The first group of data deficiencies relate to characteristics of field data reporting systems. These systems are often constructed as a means of documenting maintenance activity and not specifically to provide data to reliability analysts. Tracing on-equipment maintenance activities to piece-part component replacements is difficult and often impossible because of incomplete reporting at the depot. For this reason (and others), large automated data collection systems, such as the U.S. Air Force Maintenance Data Collection (MDC) system or the U.S. Navy 3M, were not used in this study.

There is a notable lack of dedicated reliability data tracking systems (i.e., systems whose primary intent is to measure field reliability as opposed to documenting maintenance activity). A good example of a system more oriented toward reliability concerns is the CDS system dedicated to the F-16 Falcon. More emphasis in the development of reliability dedicated systems is highly recommended and would facilitate reliability modeling efforts such as the one described here.

Another deficiency with automated data reporting systems is the ability with which failures can be separated from non-failure part replacements. Parts are often replaced as a result of secondary failures or shoddy maintenance. It is not unusual for several components to be replaced in a single repair action; however, the primary failures must be segregated from the non-failure part replacements for a meaningful data set. This can be a difficult process with even the most detailed reporting format and is an inexact practice, using existing automated databases. For this reason, IITRI focused on RIW data sources, where the

maintenance activity can be traced and more detailed failure analysis is performed.

A third data deficiency is the failure definition. For many intermittent or drift failures, the definition of failure may vary based on the particular equipment function and application, or may be dependent on the tolerance of the equipment user. It is therefore important to collect data from a cross-section of equipment types and applications so the data represents average failure conditions.

Blind usage of automated data tracking systems can lead to invalid analyses. IITRI carefully chose data sources in this study to ensure high integrity of the collected data set.

Application Definition

Additional problems are introduced by the requirement to characterize the usage application. Observed failure rates are mathematically related to failure-accelerating stresses as an integral part of the model development process. The ability to accurately model the device failure rate is directly related to the ability to define those stresses. It is often impossible to precisely define all application stresses because of the diversity of mission scenarios, the failure of equipment operaters to track all essential information and the inaccessibility of some key information.

Generally, airborne equipments either (1) do not have elapsed time meters, or (2) the operating time is not recorded as part of maintenance reporting. As a result, it is necessary to estimate the equipment operating time based on the flight hours. Research by Hughes (Ref. 1) presents a methodology to compute operating hours based on flight hours, pre-flight and post-flight checkout times, mission duration and duty cycle. An example of an equipment where the operating time was faithfully recorded was the AN/ARN-118. Unfortunately, this example represents an exception and not the standard practice.

For ground equipments, precise readings of the operating times are not available. For this reason, IITRI pursued data from large ground based radar units (e.g., PAVE PAWS) which operate 24 hours per day (23 hours was assumed, to account for downtimes associated with maintenance).

Another product of the operating time estimation process is the existence of "window" style data. In this data format, data is available in the form of X failures in Y part hours. The part hours represent a cumulative count of hours accrued from the individual components. The issue of "window" data and its implications have been studied by IITRI (Ref. 2). One result of this data deficiency is that only the exponential time-to-failure distribution with its underlying constant failure rate could be assumed. To check the validity of this assumption, test data was collected and analyzed to identify trends with time. This analysis is described in greater detail in Section 4.7 of this report. It was concluded that the exponential distribution could not be rejected, and it was therefore recommended for use in this study.

Another deficiency relates to the grouping of mission profiles into environment categories (e.g., ground fixed, airborne uninhabited fighter). Specific missions can deviate significantly from the norm. Unfortunately, this deviation usually cannot be extracted from the data source or be predicted in the equipment design phase (where these models will ultimately be used). Since discrete semiconductor failure rate is dependent on temperature cycling and other environmental stresses, the extent which these stresses deviate from the norm impacts the model accuracy.

Similarly, the determination of electrical stress levels for fielded equipments can be difficult to obtain. The equipment designers are reluctant to compile this information because of the effort required. IITRI solved this problem by obtaining the detailed part stress reliability prediction (if performed). The Air Force maintains no central library for the storage of this material, and therefore the predicted data was requested from the equipment manufacturer. When the detailed

predictions could not be found, the manufacturer's derating design guidelines were assumed to be applicable.

Effects of Design Practices

The nature of equipment design can distort the collected data set and can create some difficulties for discrete semiconductor data analysis.

Potential variables often have undesirable (from a statistical viewpoint) natural correlations. A good example is in the design of microwave bipolar transistors where design trade-offs are performed by altering frequency, power, duty factor and pulse width to achieve desired output characteristics. These trade-offs create natural correlations in the data set (i.e., frequency is negatively correlated with power). Another example is in more stressful environments where equipment designers use highly screened components. This makes good sense from a design perspective; however, it creates a correlation between environment and screen class variables, thereby preventing independent evaluation and quantification of the respective effects on failure rate.

Other trends in equipment design are to use higher integration devices, and to improve manufacturing processes and design practices, thereby decreasing failure rate. As a result, equipments include fewer devices with lower failure rates. Therefore, it becomes more difficult to accumulate the large quantities of observed failures required for statistical analysis of failure rate. These trends also lead to the presence of "zero" failure data records; the standard method of dividing the number of observed failures by the part hours resulted in a failure rate value of zero. Zero failures can be the result of (1) a low inherent failure rate, or (2) insufficient part hours recorded. It is desirable but often difficult to separate the "zero" failure data records into one of these categories.

Finally, development of timely reliability prediction models presents an interesting paradox to the reliability analyst. Applicable and accurate reliability prediction models are required when an emerging

technology initially sees widespread usage, and yet the data to develop the required models will not be available for some time (i.e., several years) after the new technology is widely used. Within the context of this study, this paradox is particularly true for GaAs power FETs where there is an urgent need for an accurate failure rate prediction model, but the requisite field data to develop the model does not exist.

Conclusions

Several deficiencies with data collection systems and other factors have been identified. By properly identifying and studying these effects, IITRI was able to select a data collection plan to minimize the deleterious effects. IITRI is confident that the data collected for this study is of high statistical quality and that it accurately reflects the field reliability of discrete semiconductors.

3.0 CRITIQUE OF EXISTING MIL-HDBK-217E DISCRETE SEMICONDUCTOR MODELS

Prior to formal model development activities, IITRI completed an in-depth review and evaluation of MIL-HDBK-217E, Section 5.1.3, "Discrete Semiconductors," to identify potential deficiencies with the existing failure rate prediction methodology. Several emerging technologies were identified which were not currently addressed. Additionally, many of the power rating and application tables were determined to be inadequate because of limited parameter ranges. This section presents a complete description of the evaluation process and the resulting conclusions.

The review of the MIL-HDBK-217E failure rate prediction models was completed with four distinct tasks. The first task was a review of the existing failure rate prediction models and corresponding modifying factors. The existing factors were investigated to determine whether the range of available parameter values was sufficient in regard to all discrete semiconductor design options currently used in equipment designs. Additionally, the magnitudes of the modifying factors were investigated to determine their relative effect on the resultant failure rate prediction. Secondly, an intensive investigation of state-of-the-art part types and technologies was conducted to identify part types not currently addressed by MIL-HDBK-217E. The third task was to scrutinize the existing section to determine which models, if any, are obsolete and should be deleted from MIL-HDBK-217E. An objective evaluation of the model groupings was the fourth task. The intent of this task was to determine whether a more logical part grouping could be determined to improve the usability of the discrete semiconductor section.

3.1 EXAMINATION OF PRESENT MODEL PARAMETERS

Analysis of the MIL-HDBK-217E models yielded a number of inconsistencies and shortcomings. Table 3.1-1 summarizes for each group of devices the ranges of Pi factors for each reliability model modifying factor. Since there are many factors influencing the reliability of a

TABLE 3.1-1. MIL-HDBK-217E PI FACTOR RANGES

Group	Description	Environment (Excluding C_L)	Appli.	Quality	Current or Power Rating	Stress	Complex.	Contact Construction	Operating Power & Frequency	Matching Network
1	Transistors (Si, Ge, NPN, PNP)	1-65	.7-15	.12-12	1-5	.3-3	.7-1.2			
2	FETs	1-65	.7-50	.12-12			.7-1.1			
3	Unijunction (JFET)	1-65		.5-50						
4	Diodes (Si, Ge)	1-50		.15-15	1-10	.7-1.0		1-2		
5	Diode, Regulator & Ref.	1-70	1-1.5	.3-30						
6	Thyristors	1-65		.5-50	1-15					
7	Diodes (Microwave)	1-120		1-5						
8	Varactor, etc.	1-70	.5-2.5	.5-25	.5-2.4					
9	Microwave Transistors	1-25	1-4	1-10					1-30	1-4
10	Optoelectronics	1-26		.01-1.0						

device (many more than can possibly be accounted for in the models), it was the intent of this study to identify those factors having the most influence on reliability and which are accessible to engineers in the design phase. It can be seen from Table 3.1-1 that some Pi factors have a very small range, insignificant relative to the expected precision of the models. It is doubtful that inclusion of such a factor improves prediction accuracy. For example, the application factors for zener/avalanche diodes (Table 5.1.3.5-2 in MIL-HDBK-217E) ranges from a value of 1.0 to 1.5. Inclusion of any variable with such a narrow range of values has two effects on a prediction model:

(1) Indicates a high level of precision in the models which in reality does not (and cannot) exist because of data limitations and natural variability.

(2) Adds to the complexity of the models without adding additional information.

Special emphasis was placed on inspection of the RF diode and transistor sections. Examination of these sections illustrates how rapidly the technology in these areas has been expanding. The models in these sections have serious deficiencies in relation to state-of-the-art technology. First, GaAs power FETs are not included in Group IX, Microwave Transistors, and GaAs technology is not included in Group VII, Microwave Diodes. Second, the operating frequency and power values in MIL-HDBK-217E Table 5.1.3.9-3 for Group IX transistors fall well below current levels. Third, advances in device design and construction within the last eight years are expected to have had a significant effect on inherent device failure rates. One report (Ref. 39) states that failure rates for state-of-the-art Si bipolar microwave power transistors are 20 times lower than those reported ten years ago.

The primary failure mechanism of earlier devices was electromigration of the Al metalization. The more recent Au metalization systems are less susceptible to electromigration. These systems employ a refractory metal barrier layer that inhibits alloying of Au and the semiconductor. The electromigration problem remains, though less pronounced, as a result of such processing problems as thin spots or pin holes in the refractory layer. Although the newer metalization systems have improved reliability, this has necessarily been a trade-off with more complex processing techniques.

Another observation regarding the present models is that the models have a relatively complex equation for the base failure rate as a function of temperature, electrical stress, and various shaping parameter constants. A more usable model form will consist of a constant base failure rate for each part type with a separate multiplicative factor for temperature, normalized to unity at a default temperature (of possibly 25°C) and stress (of possibly .5). This method will yield results mathematically similar to that of the current models, although possibly increasing its utility.

Those factors identified in both the model review effort and the industry survey (described in Section 2.2), needing tables with higher electrical stress rating or similar expansion, are given in Table 3.1-2. Additionally IITRI personnel attended the MIL-HDBK-217E coordination meeting dealing with discrete semiconductors. The meeting took place in December 1985. This provided additional information into the limitations of the existing models and model parameters. Table 3.1-3 provides a summary of relevant comments from the MIL-HDBK-217E coordination meeting.

Other general comments/opinions from the user/vendor survey, although not necessarily endorsed by IITRI, are presented as a faithful recording of opinions expressed by the survey participants. All comments were given due consideration. Asterisks indicate those comments which significantly impacted study results.

TABLE 3.1-2. DEVICES WITH INADEQUATE PARAMETER TABLE RANGES

TRANSISTORS

- Group I - Table 5.1.3.1-4 needs expanded power ratings and associated π_R factor
- Group II - separate consideration of power FETs
- Group II - Table 5.1.3.2-2 needs application categories for GaAs devices >100mW and associated π_A factors
- Group II - Table 5.1.3.2-2 existing driver (<100mW) π_A factor (50.0) should be reevaluated
- Group II - Table 5.1.3.2.4 quality factor for GaAs FETs needs expanding

DIODES

- Group IV - separate consideration for power diodes
- Group IV - Table 5.1.3.4-3 increase current ratings to 500A
- Group VI - Table 5.1.3.6-3 increase current ratings to 500A
- Group VIII - Table 5.1.3.8-3 increase power rating

MICROWAVE TRANSISTORS

- Group IX - Table 5.1.3.9-3 needs expanded peak operating power (watts) and frequency (GHz) and associated π_F factors

OPTO-ELECTRONIC DEVICES

- Group X - increase the number of characters for alphanumeric displays

TABLE 3.1-3. MIL-HDBK-217E COORDINATION MEETING COMMENTS

	Source	Comments
1.	EIA	Change failure rate temperature dependency to an approach based on power dissipation and thermal resistance.
2.	AIA	Power ratings for the Group I power rating factor should be increased to include 2000 and 3000 watt devices.
3.	AIA	The FET model should be expanded to include GaAs driver devices with power ratings greater than 100mW.
4a.	EIA	The FET model should be expanded to include GaAs driver devices with power greater than 100mW.
4b.	EIA	Failure rate model is required for Power Schottky diodes used in power supplies.
5.	EIA	Change upper power level constraint for analog circuit diodes to avoid confusion with power rectifier.
6.	EIA	Consider redundancy for HV stack power rectifiers.
7.	AIA	Increase the current ratings for Group IV diodes to include devices rated between 50 to 80 amps.
8a.	EIA	Include Triacs in the handbook.
8b.	EIA	Increase the current ratings for thyristors.
9.	NSIA	Relabel the thyristor model to include both thyristors and SCRs.
10.	EIA	Expand coverage of the microwave diode model to include silicon Schottky mixers. The failure rate should be similar to silicon Schottky detectors.
11.	AIA	The Microwave transistor model needs to be revised because technology in this area has been rapidly expanding.

TABLE 3.1-3. MIL-HDBK-217E COORDINATION MEETING COMMENTS

	Source	Comments
12.	EIA	Quality factor for microwave transistors should be expanded to include nonhermetic parts.
13a.	AIA	Change failure rate dependency for microwave transistors from peak operating power to average operating power.
13b.	AIA	Expand table for microwave transistors to include devices operating at frequencies above 4.0 GHz.
14.	EIA	Group semiconductor laser devices with lasers instead of discrete semiconductor devices.
15.	AF(RADC)	Simplify the laser diode model. Failure rates seem too high.
16.	AF(RADC)	Simplify the laser diode model.
17.	AIA	Change the range of temperature factor values to provide compatibility between text and table.
18.	AIA	In Example 6, change peak power to average power.

- Factors found not to have a significant effect on reliability:
  - * The difference between 'lower' and 'JAN' quality factors is too large
  - Power/current rating - High power/current devices are only less reliability as a group because they tend to be more highly stressed in use
  - The difference between NPN vs PNP transistors is no longer significant
  - * The difference between hermetically sealed packages and those encapsulated in organic materials is smaller
- Factors not found in the discrete semiconductor section that have a significant effect on reliability:
  - Beam lead construction and surface mount construction
  - A ground commercial environment between present ground benign and ground fixed
  - Voltage stress and voltage rating for FETs
  - Quality factor for SCD parts between JAN and JANTX
  - Power rating of FETs
  - Hot/cold starts - power cycling
  - * Junction temperatures
  - Complexity factor for series combinations of zener diodes in a single package
- General comments:
  - Environmental factor should have a vibration range, number of power on's and life thermal cycles
  - Table 5.1.3.1-2, Si low noise factor seems high
  - Table 5.1.3.2-2, GaAs driver seems high
  - * Commercial transistors (Group I) show higher failure rates than given
  - * Diodes (Group VII) and Transistors (Group IX) should be reviewed for realism

3.2 NEW PART IDENTIFICATION

The review of the MIL-HDBK-217E models included an analysis of part types not addressed or insufficiently addressed. The parts identified are listed in Table 3.2-1. The list was determined from telephone records (both from IITRI and RADC) and information from the survey used to solicit information from device manufacturers and users.

TABLE 3.2-1. PART TYPES TO BE ADDRESSED

- GaAs Power FETs
- Transient Suppressors
- MOV's
- Power Schottky Diodes
- Varistors
- GaAs Diodes
- Variations on MOSFET's
- Current Regulators
- Laser Diodes
- Photothyristors
- Photovoltaic Cells
- Diode Arrays

3.3 OBSOLETE PART IDENTIFICATION

IITRI also conducted a review of the MIL-HDBK-217E discrete semiconductor section to identify part types which are presently included in the document but are no longer used in electronic equipment designs. The intent of this study task was to identify and remove obsolete part types to improve the organization, clarity and consistency of the section. This study task was accomplished by surveying reliability engineers at the largest equipment manufacturers.

At this point there are no part types for which it can be absolutely stated that they will never be included in any forthcoming electronic equipment design. Therefore, the result of this task was to recommend that no part types be removed from MIL-HDBK-217E. Several part categories including Germanium devices are seeing declining usage for general

applications, although specialized applications persist. The corresponding models may become obsolete at some future time; however, to maintain the present utility of the discrete semiconductor section, no part types are recommended for deletion at this time.

3.4 MODEL GROUPING

Table 3.4-1 lists the ten groups of device types in the current MIL-HDBK-217E Discrete Semiconductor section. A more logical grouping scheme would be advantageous to improve the organization and clarity of the overall failure rate prediction process. Consideration of alternate groupings was accomplished as part of the MIL-HDBK-217E review process.

The following discrete semiconductor device grouping factors were considered:

- Generic part type (transistor, diode, etc.)
- Construction (FET, bipolar, etc.)
- Semiconductor Material (Si, Ge, GaAs)
- Device function
- Frequency
- Power
- Combinations of the above

As an example, microwave diode groupings by function and by construction are presented in Table 3.4-2. The examples indicate variations between possible grouping options.

Each of the seven factors above were examined qualitatively with respect to their relative importance in a device grouping schema. Criteria which were considered desirable for a grouping schema were:

1. logical/easy to use
2. physically correct (with regard to both physics of failure and construction)
3. supports statistical findings

TABLE 3.4-1. PRESENT DISCRETE SEMICONDUCTOR GENERIC GROUPS

Part Type	Group
A. Transistors	
Silicon NPN Silicon PNP Germanium PNP Germanium NPN	I
Field Effect Transistors	II
Unijunction	III
B. Diodes and Rectifiers	
Silicon (General) Germanium (General)	IV
Voltage Regulator (Zener, Avalanche) Voltage Reference (Temp. Comp. Zener, Avalanche)	V
Thyristors	VI
C. Microwave Semiconductors and Special Devices	
Detectors Mixers	VII
Varactors, IMPATT, Gunn, PIN Step Recovery, Tunnel	VIII
Microwave Transistors	IX
D. Opto-electronic Devices	X

TABLE 3.4-2. MICROWAVE DIODES GROUPED BY FUNCTION AND CONSTRUCTION

1. Microwave Diodes Grouped by Function

"Microwave" Power Generation

- Power Multiplication: Varactor, Step Recovery
- Power Amplification, Oscillator: Gunn, Avalanche (IMPATT, TRAPATT) Tunnel, Back, Varactor, Step Recovery

Receiving, Detection, Mixing

- Detecting and Mixing: Schottky Barrier Point Contact, Tunnel, Back
- Rectifying: Schottky Barrier

Control of "Microwave" Power

- Tuning: Varactor
- Attenuation and Limiting, Switching and Phase Shifter: PIN

2. Microwave Diodes Grouped by Construction

- Schottky Barrier, Point Contact
- PIN
- Varactor, Step Recovery
- Gunn (TED, Bulk effect)
- IMPATT, TRAPATT, BARITT
- Tunnel, Back, Mixer, Detector

It was quickly determined that a device grouping schema based on any one of the seven factors would be overly simplified and that some logical combination of the above was necessary. A number of prioritized cuts would have to be made before a suitable schema resulted.

The first cut was made based upon generic part type. This factor satisfied all three criteria listed above and resulted in:

Group I	Diodes
Group II	Transistors
Group III	Unijunction Devices
Group IV	Thyristors
Group V	Optoelectronics

The second cut was based upon operating frequency range, since this variable has a profound effect on the physical aspects of the device, and was supported in the statistical findings of the study. This resulted in:

Group I	Low Frequency Diodes
Group II	High Frequency (Microwave/RF) Diodes
Group III	Low Frequency Transistors
Group IV	High Frequency (Microwave/RF) Transistors
Group V	Unijunction Devices
Group VI	Thyristors
Group VII	Optoelectronics

The third and final cut was based upon device construction (FET vs. bipolar) since this factor is logical, physically correct and was significant based on the study findings. Thus, the final grouping schema was:

Group I	Low Frequency Diodes
Group II	High Frequency (Microwave, RF) Diodes
Group III	Low Frequency Bipolar Transistors
Group IV	Low Frequency FETs
Group V	Unijunction Devices
Group VI	High Frequency (Microwave, RF) Bipolar Transistors
Group VII	High Frequency (Microwave, RF) FETs
Group VIII	Thyristors
Group IX	Optoelectronics

The remaining factors: function, power, and semiconductor material were accounted for within the individual device groups by either separate models (i.e., semiconductor material) or pi factors within the same model (such as function and rated power).

4.0 FAILURE RATE MODELING CONCEPTS

4.1 FAILURE RATE MODELING APPROACH

A general failure rate modeling approach was defined to provide the basic structure for the discrete semiconductor failure rate prediction model development process. The use of a general modeling approach for all device types resulted in models which are consistent and complementary. Figure 4.1-1 presents the model development approach graphically. The following paragraphs briefly describe the general modeling approach.

Identify Potential Variables

The first step of the model development process was to identify variables which could potentially have an effect on discrete semiconductor failure rates. These variables were limited to information that would be readily available to engineers during the equipment design phase. Determination of these variables was based on a thorough literature search and on information obtained through the discrete semiconductor user and vendor surveys. Tables 4.1-1, 4.1-2 and 4.1-3 list the potential model input parameters identified for transistors, diodes, and optoelectronic devices, respectively. Parameters are either a result of device construction/design, circuit application, application environment, or a combination of these. The identification of these parameters serves to focus the data collection efforts and refine the theoretical models.

Theoretical Model Development

A series of theoretical failure rate prediction models was hypothesized to provide the resultant models with a sound theoretical/engineering backing. Basically, theoretical model development involved evaluation of the effects of the parameters identified in the previous phase. In addition, the optimal model form (i.e., additive,

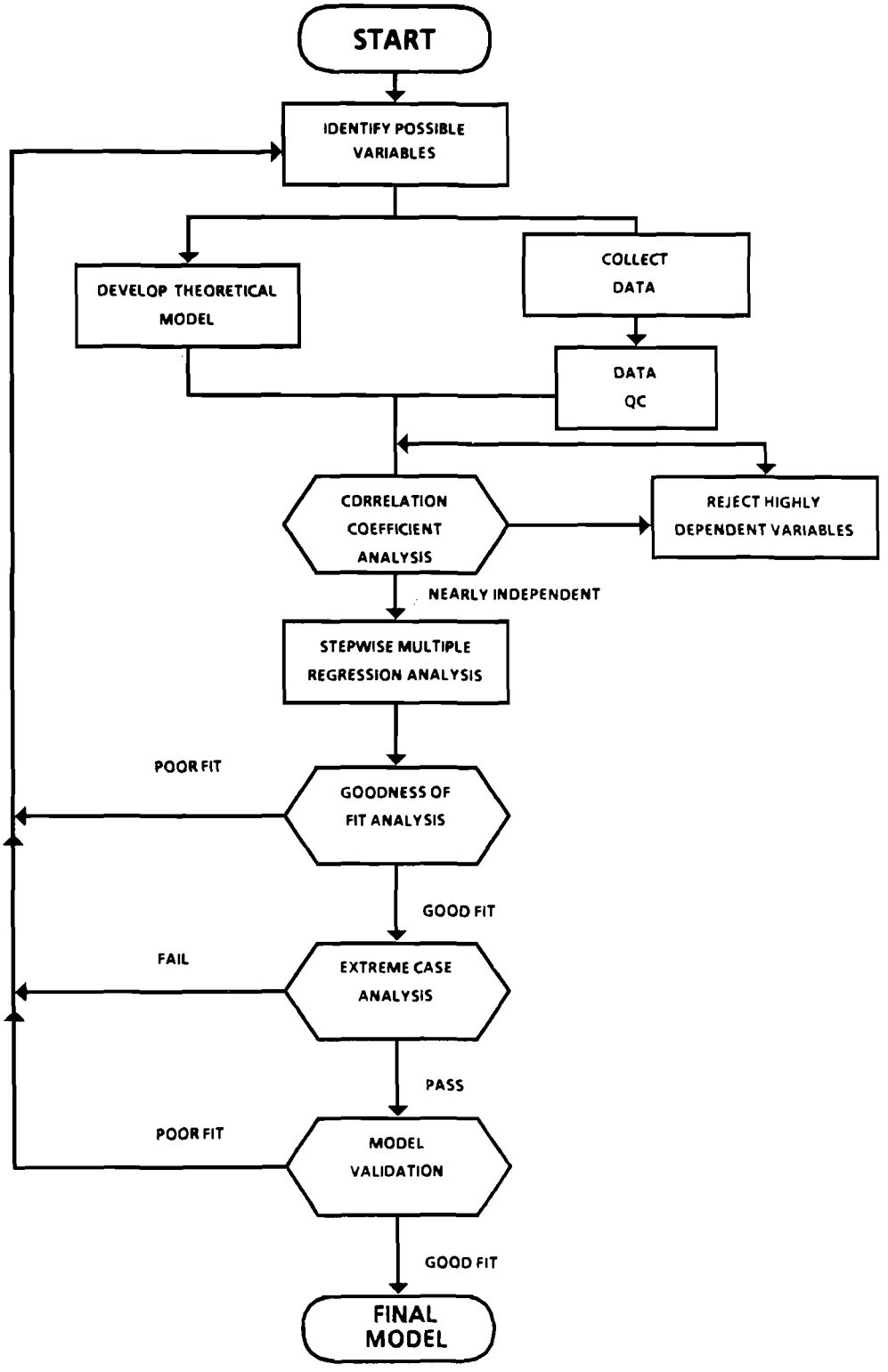

Figure 4.1-1. Model Development Flow Chart

TABLE 4.1-1. POTENTIAL MODEL INPUT VARIABLES FOR TRANSISTORS (1)

Device Style (C)	Quality Level (C)
Power Rating (C)	Duty Cycle (A)
Package Type (C)	Operating Frequency (A)
Semiconductor Material (C)	Junction Temperature (A,C,E)
Structure (NPN, PNP) (C)	Application Environment (E)
Electrical Stress (A)	Complexity (C)
Circuit Application (A)	Power Cycling (A)

TABLE 4.1-2. POTENTIAL MODEL INPUT VARIABLES FOR DIODES (1)

Device Style (C)	Quality Level (C)
Current Rating (C)	Duty Cycle (A)
Package Type (C)	Operating Frequency (A)
Contact Construction (C)	Junction Temperature (A,C,E)
Semiconductor Material (C)	Application Environment (E)
Electrical Stress (A)	Complexity (C)
Circuit Application (A)	Power Cycling (A)

TABLE 4.1-3. POTENTIAL MODEL INPUT VARIABLES FOR OPTOELECTRONICS (1)

Device Style (C)	Duty Cycle (A)
Package Type (C)	Junction Temperature (A,C,E)
Semiconductor Material (C)	Application Environment (E)
Electrical Stress (A)	Complexity (C)
Circuit Application (A)	Power Cycling (A)
Quality Level (C)	

Note 1: (C) = construction/design variable

(A) = circuit application variable

(E) = application environment variable

multiplicative, combination) was determined and the time dependency of discrete semiconductor failure rate was studied.

Development of the theoretical models relied heavily on published literature. The literature included many instances of mathematical models relating failure rate (or mean-time-to-failure) to temperature, power, derating and other factors. Many other technical articles or documents provided a qualitative assessment of reliability influences. These were useful to define the relative effect of numerous variables. In very general terms, the theoretical models were of the following form.

$$\lambda_t = \lambda_b \, \pi_T \, \pi_E \, \pi_Q \prod_{i=1}^{n} \pi_i$$

where

λ_t = theoretical failure rate prediction

λ_b = base failure rate, dependent on device style

π_T = temperature factor (presented in Section 4.4)

$$= \exp\left(-A\left(\frac{1}{T_j} - \frac{1}{T_r}\right)\right)$$

where

A = constant

T_j = junction temperature

T_r = reference temperature

π_E = environment factor based upon device application environment (presented in Section 4.6)

π_Q = quality factor based upon device screen level and hermiticity

$\prod_{i=1}^{n} \pi_i$ = the product of Pi factors based upon variables from the list of potential model input variables found to have a significant effect on discrete semiconductor failure rate

The development of theoretical device failure rate prediction models was an integral part of the overall model development process.

Information collected through the literature search and discrete semiconductor user and vendor surveys was reviewed and evaluated to aid in the development of theoretical models for each discrete semiconductor device group. The theoretical models serve the following functions:

- Assure prediction models conform to physical and chemical principles
- Select variables when not possible by purely statistical techniques

Data Analysis

The next phase of the modeling approach was data analysis using the failure rate data collected through an intensive data collection effort (described in Section 2.0). Techniques used were correlation coefficient analysis, regression analysis, goodness-of-fit testing and others. These are described in the following paragraphs.

The first data analysis task was correlation coefficient analysis. The objective of this analysis was to identify highly correlated variables. As part of this task, correlation coefficients were computed for each pair of independent variables. The correlation coefficient is a measure of the relation between two variables and varies between -1 and 1 (from perfect negative to perfect positive correlation). Regression analysis requires that all independent variables are uncorrelated; therefore, the effects of correlated variables could not be simultaneously quantified. If the variables were correlated inherently (e.g., junction temperature and power), a decision was made to include only the most significant variable in the regression analysis. If the variables were correlated due to chance (e.g., quality vs. temperature), then several options were considered. If a valid theoretical or empirical relationship was found for one of the correlated variables, then the effect of that variable was removed from the data by assuming the relationship to be

correct. If this assumption was correct, then the effect of the remaining correlated variable could be accurately assessed by data analysis.

The next step in the model development process was to apply stepwise multiple regression analysis. Regression analysis is described in detail in Draper and Smith (Ref. 61). This technique was used to compute the coefficients of an assumed model form in a least squares fit to the data. Regression solutions were found for decreasing confidence limits beginning with 90%. In addition, standard error statistics were computed for each significant variable to obtain an indication of the accuracy of coefficient estimates. Additionally, upper and lower 90% confidence interval values were determined for each coefficient. In general, variables were not included in the proposed model if they did not significantly affect failure rate with at least 70% confidence. However, if a variable such as device screening was known to influence failure rate from an engineering perspective, then coefficients were computed with less than 70% confidence and a corresponding factor was proposed. In these instances, the resultant factor should be considered approximate. This was necessary only occasionally, and no factors were proposed with less than 50% confidence.

Generally, transformations were performed on the data to give multiplicative model forms. For example, the effect of junction temperature is often modeled by use of the equivalent Arrhenius relationship, which takes the form,

$$\lambda = A \exp(-B/T)$$

where T is the independent variable, λ is the dependent variable and A and B are constants. By taking the natural logarithm of each side, the equation becomes

$$\ln\lambda = \ln A - \frac{B}{T}$$

which can be solved by regression analysis with 1/T the independent variable and $\ln\lambda$ the dependent variable.

In addition to quantitative regression that was used to relate failure rate to variables such as temperature and rated power, qualitative regression techniques were also employed. Qualitative regression (often termed covariance analysis) is used to model the effect of variables which cannot be measured on a numerical scale (e.g., screen class). A matrix of indicator variables (0 or 1) is defined and used as the independent variables to represent the qualitative variable.

The F-ratio and Critical F are parameters which are used in conjunction with regression analysis to determine significance of independent variables. The Critical F value corresponds to the degrees of freedom of the model (equal to the number of data points minus the number of b_i coefficients minus one) and a specified confidence limit. This number may be used to test the significance of each variable as it is considered for addition to or deletion from the model. The F-ratio value for a regression is the quotient of the mean square due to regression and the mean square due to residual variation. If the F-ratio value for any independent variable is greater than the Critical F value, then it was considered a significant factor influencing failure rate and was included in the regression solution.

Model Evaluation

The goodness-of-fit of the regression solution was then measured using the R-squared statistic. The R^2 coefficient or multiple coefficient of determination is equal to the ratio of the sum of squares of the deviations explained by the regression to the sum of the squares of the deviations of the observed data. The R^2 value was used as a means to determine the ability of the regression model to predict the observed results. The coefficient ranges from 0 to 1.0. A coefficient value of 1.0 indicates a perfect fit between the model and the observed data.

No absolute acceptable limit was defined to determine what constituted a "good fit" because of the relative variability between part classes and because of different sample sizes. For example, the acceptable R-squared value for microwave transistors would have been unacceptable for general purpose diodes because of the smaller lot-to-lot variability and more standardized design and manufacturing processes.

The next phase of the general model development process was to perform an extreme case analysis. Predictions were made using the proposed model for parameters beyond the ranges found in the data. The intent of the extreme case analysis was two-fold: (1) to identify any set of conditions which cause the proposed model to numerically "blow up," (2) to identify any set of conditions which predict a failure rate which is intuitively incorrect. For instance, a model that predicted an unscreened device with a lower failure rate than a similar screened device or that predicted a negative failure rate would be examples of an intuitively incorrect model. Reasons for failing the extreme case analysis primarily involve an incorrect choice of model form. If the extreme case analysis indicated that the proposed model was unacceptable, then the entire model development process was begun again.

The final phase of the model evaluation task consisted of an engineering peer review. Engineers who were not directly involved with the model development process, yet who are cognizant in the areas of component reliability and prediction models, critically evaluated the resultant failure rate prediction models to determine whether the model properly addressed known failure modes/mechanisms and activating stresses.

4.2 TEMPERATURE EFFECTS

An investigation into the effects of temperature was a crucial part of the discrete semiconductor device failure rate modeling effort. Based on the published literature, the impact of device temperature was determined

to be one of the most important variables affecting discrete semiconductor device failure rates.

Based on historical data, the Arrhenius relationship adequately models the reaction rate of discrete semiconductor failure mechanisms within a specific temperature range. The Arrhenius model is based on empirical data and predicts that the rate of a given chemical or physical reaction, in this case a failure mechanism, will be exponential with the inverse of temperature. Conceptually, the Arrhenius model is given by:

$$\text{Reaction Rate} \propto \exp(-E_a/KT)$$

where

E_a = activation energy (eV)
K = Boltzman's constant
= 8.63×10^{-5} (eV/^{o}K)
T = temperature (^{o}K)

Every chemical reaction has a unique activation energy associated with it. During the life of discrete semiconductor components there may be several such reactions proceeding simultaneously, each capable either individually and/or jointly of causing a part failure. However, consideration of each reaction separately would be too complex to analyze with the available data. It has been found, however, that for general classes of components with similar failure mechanism distributions the cumulative effects of the various reactions can be approximated by an Arrhenius model for a specified temperature range. This relationship has been designated as the "equivalent Arrhenius relationship." Because of the documented accuracy of this approach and the limitations of the available data, it was decided to investigate the effects of temperature using the equivalent Arrhenius relationship. It must be emphasized that beyond the range of normal usage temperatures, this relationship will no longer be applicable.

The form of the temperature factor for the discrete semiconductor theoretical failure rate prediction models is thus based on the equivalent Arrhenius relationship and is given by

$$\pi_T = \exp(-A(\frac{1}{T_j} - \frac{1}{T_r}))$$

where

T_j = junction temperature (^oK)

T_r = reference temperature

A = equivalent activation energy divided by Boltzman's constant

It was decided to include a reference temperature for two reasons:

(1) A proposed model with the reference temperature term provides more information. The base failure rate would be equal to the device failure rate at the reference temperature. Thus, inspection of the base failure rate value provides meaningful information for quick analyses.

(2) A proposed model with the reference temperature term would minimize the need for exponential numbers (e.g. 7×10^{34}) and would therefore result in models which are easier to use. The temperature factor would be equal to one when the ambient temperature equals the reference temperature, and would generally be below 100 for even the highest possible temperatures found in operating applications.

The value of 298^oK (25^oC) was chosen as a reference since this is most often the point at which derating begins for discrete semiconductors. When the junction temperature approaches the reference temperature, the value of multiplicative temperature factor approaches unity.

Mathematically, adding the reference temperature term to the proposed model will have no effect on the resultant failure rate prediction. Relative differences caused by selection of the reference temperature will be compensated by corresponding changes in the base failure rate.

The proposed temperature factor is based on the device junction temperature (T_j). Generally, the junction temperature cannot be determined directly but must be estimated based on the case temperature, electrical application parameters and construction characteristics of the device.

There are two primary methods used to compute the junction temperature, each with a certain degree of precedence and relative merits. The first method is based on electrical stress ratios. This method is utilized in the current discrete semiconductor model where junction temperature is estimated by,

$$T_j = 273 + T + S\Delta T$$

where

T_j = junction temperature in ^{o}K

T = operating temperature in ^{o}C (ambient or case)

S = stress ratio (equal to operating stress divided by rated stress)

ΔT = difference between typical maximum allowable temperature with no current or power (total derating) and the typical maximum allowable temperature with full rated junction current or power.

The $(\Delta T)S$ term is an estimation of the rise in junction temperature because of applied stress and is based upon device derating curves. A typical device derating curve is shown in Figure 4.2-1. The slope of the derating curve is theoretically based upon the device thermal resistance; that is, the derating curve indicates the amount applied power must be lowered for a given application temperature. This is necessary since the device junction temperature must not exceed a manufacturer-specified limit. The rate at which this trade-off occurs is determined by the device thermal resistance, which is proportional to the rise in temperature corresponding to a particular rise in applied power.

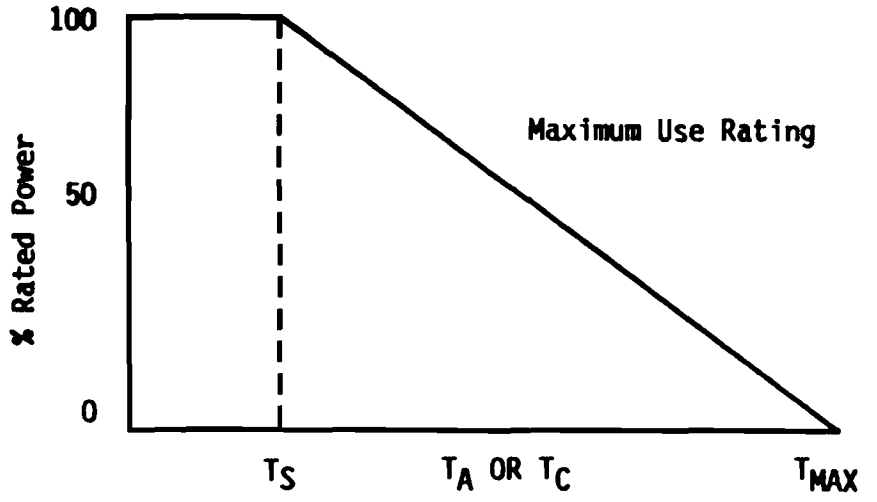

NOTE:

(1) T_S = temperature at which derating begins
T_{MAX} = maximum rated junction temperature
T_A = ambient temperature
T_C = case temperature
P_{OP} = actual power dissipated
P_{MAX} = maximum rated power at T_S

(2) Maximum junction temperature (T_{MAX}) is normally 175 or 200°C for silicon and 100°C for germanium devices. T_S is usually 25°C, but it can be higher.

Figure 4.2-1. Conventional Derating Curve

The second option for representing junction temperature is:

$$T_J = 273 + T + \theta P$$

where

T_J = junction temperature (°K)

T = temperature ambient or case as appropriate (°C)

θ = junction to case or ambient thermal resistance of the device (°C/watt or °C/Amp)

P = device power (current for some diodes when the thermal resistance is given in °C/Amp)

In this case, the rise in junction temperature due to applied power is given directly by the θP term. This method is used in MIL-HDBK-217E to compute junction temperature for microcircuits.

The benefit of the "$(\Delta T)S$" method is that it demonstrates the effects of electrical stress levels outright, encouraging the use of derating principles. However, the benefits of the "θP method" outweigh this. First, the use of the θP method for discrete semiconductors will be consistent with the other microelectronic failure rate prediction models in MIL-HDBK-217E. Secondly, it is a more direct and intuitively correct approach since it is based on physical principles--the θ values are based upon measurable thermal properties of the device materials and construction. The derating curves used in the current method are then derived based upon the observed thermal resistance values. Finally, with the increased development and usage of power devices, the presence of a heat sink becomes increasingly important to part failure rate. Although derating curves do not exist or make sense for heat sinks, the heat sink thermal resistances are often available. Thus, to keep consistency within the model when taking into account the effects of a heat sink, the θP method is preferable and was selected to be included in the proposed discrete semiconductor models.

The proposed temperature factor form is markedly different from the existing MIL-HDBK-217E temperature factor form. The temperature factor in the MIL-HDBK-217E discrete semiconductor failure rate prediction models is built into the base failure rate and is given by:

$$\lambda_b \propto \exp\left[\left(\frac{N_T}{273 + T + (\Delta T)S}\right) + \left(\frac{273 + T + (\Delta T)S}{T_m}\right)^P\right]$$

where

λ_b = base failure rate

N_T, T_m, P = shaping parameters

T = operating temperature in ^{o}C (ambient or case)

ΔT = difference between typical maximum allowable temperature with no junction current or power (total derating) and the typical maximum allowable temperature with full rated junction current or power

S = stress ratio of operating electrical stress to rated electrical stress

There are two obvious differences between the proposed temperature factor and the existing temperature relationship. The first difference is the method to determine junction temperature, which has already been described. The second major difference relates to model complexity. The existing model includes factors (i.e., T_m, P) which are not addressed in the proposed model form, and the present model also includes several parameters twice. IITRI determined that the streamlined model format was preferable after an intensive exercising of the existing models for different applications and different junction temperatures.

Intuitively the T_m and P constant values are justified. From a physical perspective, the T_m constant is the temperature (in ^{o}K) where the predicted failure rate begins to deviate from the equivalent Arrhenius relationship. The P constant is indicative of the rate of deviation. This is seemingly satisfactory because the equivalent Arrhenius relationship is only expected to be accurate over a limited temperature range.

Despite the apparent physical correctness of the complex temperature factor format, it is needlessly complex from a pragmatic viewpoint. Over the range of junction temperatures found during normal usage, the extra temperature factor term (following the plus sign in the base failure rate equation) rarely resulted in a meaningful difference.

As an initial step into the investigation of temperature effects, all available temperature data and information for the various part categories was gathered and compiled. As the study progressed, it was quickly

determined that it would be necessary to examine and make use of all available data and information. Activation energy information was sought for each part type in the following forms:

1. Current MIL-HDBK-217E equivalent activation energies
2. Life test data
3. Activation energies from the literature
4. Field data
5. Any of the above on similar part types where necessary

Current MIL-HDBK-217E activation energies were considered to hold precedence for parts where either the technology has not changed significantly, or little to no new (since the preceeding modeling study) information was available. To obtain the current activation energy, a simple transformation was performed on the MIL-HDBK-217E N_T constant due to the differences between the current and the proposed temperature factor forms described above. In all cases, the current values were checked against all new data and information for consistency.

High temperature life test data and activation energies were gathered from the literature. Data was available for test temperatures ranging from 55°C to 400°C.

Test data was particularly useful for the determination of temperature effects. The range of temperatures found during field usage is often insufficient to confidently model temperature effects. The life test data (at elevated temperatures) complements the field data in these instances. This data was previously presented in Tables 2.2-4 and 2.2-5. It must be emphasized, however, that no data was used where the test temperature exceeded design limits or where the range of test temperatures was small.

Table 4.2-1 shows activation energies reported in the literature for the various discrete semiconductor devices. In some cases only the activation energies were reported and in some cases, the raw data supporting the activation energies were available.

An estimate of activation energy was calculated from field data for part types where (1) sufficient information was available to make a estimate of junction temperatures for a majority of data points and (2) a broad range of junction temperatures was available. This estimate was used primarily for comparison purposes against current MIL-HDBK-217E values. All requisite information was available to calculate π_T for approximately 75% of the data points since device thermal resistance (θ), applied power, rated power, applied current, rated current, and ambient temperature were tracked for each device in the database. Of the remaining 25%, an estimate of junction temperature was computed by assuming typical thermal resistances and/or power derating (for the specific part class and application). For approximately 5% of the data records insufficient information was available to estimate junction temperature and these records were deleted from subsequent analyses.

It was difficult to distinguish from the available data whether a given component was accompanied by a heat sink or not. The assumption was made that high power devices were accompanied by a heat sink and low power devices were not. Although, specific instances can be found where this assumption is invalid, these cases do not severely impact the analysis because of the magnitude of the collected data set. In the case of heat sinks, the total device thermal resistance is given by:

$$\theta_{JA} = \theta_{JC} + \theta_{CA}$$

where

θ_{JA} = total junction-to-ambient thermal resistance

TABLE 4.2-1. DISCRETE SEMICONDUCTOR REPORTED ACTIVATION ENERGIES

Device Type	Reference	Test Temperatures(°C)(1)	Activation Energy (eV)
Si IMPATT Diode	3	210,220 (A)	>1.07
	4	256 - 312 (J)	3.50
	5	280 - 350 (J)	1.60
GaAs IMPATT Diode	6	<300 (J)	.2-.4
	6	<300 (J)	1.60
	5	350 - 400 (J)	1.8
	7	180 - 260 (J)	1.36
Si Schottky Barrier	8	238 - 298 (C)	1.6
	9	210 - 270 (A)	.62
Gunn Diode	10	275 - 325 (J)	2.03
GaAs FET	11	218 - 280 (J)	1.0
	12	175 - 250 (J)	1.2 - 1.8
	13	160 - 265 (J)	.96 - 1.6
	14	---	1.8
	15	---	1.0 - 1.1
	16	---	.67 - 2.3
	17	227 - 295 (A)	1.8
	18	230 - 275 (J)	1.5 (Au)
	18	230 - 275 (J)	1.0 (Al)
	19	200 - 231 (A)	1.0
	20	185 - 215 (A)	1.4 - 1.9
	21	170 - 220 (J)	.8 - .84
	22	85 - 240 (J)	1.5
Si, GP Transistor	23	---	2.0 (Au)
		---	1.2 (Al)
Diode, GP	24	---	.75
Avalanche Photo-Diode	25	55 - 150 (A)	.8
	26	---	.7

TABLE 4.2-1. DISCRETE SEMICONDUCTOR REPORTED ACTIVATION ENERGIES (CONT'D)

Device Type	Reference	Test Temperatures (°C)(1)	Activation Energy (eV)
GaAs LED	27	65 - 185 (J)	.65 - .75
	28	88 - 167 (J)	.3
	29	---	.8
GaP LED	29	---	.93
Si LED	26	---	.7
	30	100 - 200 (A)	.6 - .75
GaAs Laser	31	25 - 90 (A)	.8
	29	---	.75
	32	50 - 70 (A)	.62
	33	70 (A)	.7
	34	60 - 100 (A)	.9 - 1.3
	35	40 - 70 (C)	.34

NOTE (1): (A) = Ambient
(C) = Case
(J) = Junction
--- = Not reported

θ_{JC} = device junction-to-case thermal resistance

θ_{CA} = thermal resistance of the heat sink to ambient

Thermal resistances for heat sink types were found in the literature (Ref. 36). The mean of the values for high power ($\geq$5W) device heat sinks was 2.4°C/W. The mean of all low power device (<5W) heat sinks was 7.5°C/W. These values include the washer and heat sink compound.

Where values for power or current were not available, it was assumed devices were derated according to MIL-HDBK-338 and RADC-TR-84-254 (Ref. 37) as follows:

	Derating Factors	
Transistors	Power	Current
FETS and Microwave Transistors	.50	---
Others	.50	.75
Diodes		
High Frequency Diodes	.50	.50
Switching, Signal	.50	.50
Rectifiers	.65	.75
Voltage Reference	.65	.50
Voltage Regulator	.50	.50
Opto Electronics		
All	.50	.50

In the few cases where ambient temperatures were not available, temperature values corresponding to the application environment of the data point were taken from MIL-HDBK-217E, Table 5.2-34, Ambient Temperature For All Parts. The table is reproduced here as Table 4.2-2. These values were chosen as a best estimate because of their precedence.

TABLE 4.2-2. TYPICAL AMBIENT TEMPERATURE FOR ALL ENVIRONMENTS

Environment	T_A (°C)	Environment	T_A (°C)
A_{IA}	55	G_F	40
A_{IB}	55	G_M	55
A_{IC}	55	M_{FA}	45
A_{IF}	55	M_{FF}	45
A_{IT}	55	M_L	55
A_{RW}	55	M_P	35
A_{UA}	71	N_H	40
A_{UB}	71	N_S	40
A_{UC}	71	N_{SB}	40
A_{UF}	71	N_U	75
A_{UT}	71	N_{UU}	20
C_L	40	S_F	30
G_B	30	U_{SL}	35

Individual device thermal resistances were generally available from the manufacturer's specification sheet either directly or by virtue of the derating curve. When they were not given, values were either (1) taken from the Electronics Engineer's Handbook (Ref. 36) as follows:

Thermal Resistance in °C/W in Still Air

Package Type	θ_{JA}	θ_{JC}
TO-3	40	1.85
TO-5	200	60.00
TO-18	450	200.00
TO-66	40	5.75
TO-99, TO-100	197	---

or (2) typical values for θ were extracted from the database for similar devices in similar packages.

A table of default values for device and heat sink thermal resistances are given with the prediction models in Appendix A. These values are a result of taking the geometric mean of values for similar devices in similar packages from the data collected for this effort, plus values from the Electronic Engineer's Handbook (Ref. 36).

It should be mentioned that junction temperatures calculated based upon such thermal resistances are simply best estimates of the true junction temperature. Several references (Ref. 38,39) point out discrepancies between manufacturer's published thermal resistances and actual test-measured thermal resistances. The fact that different manufacturers use difference measurement techniques also confounds results. (Ref. 40,41). In fact, the accurate measurement of device thermal resistance is not a trivial task (Ref. 40). In addition, it has been reported that device thermal resistance is not actually a constant as the values infer, but rather a function of temperature (Ref. 20,42). For example, the thermal conductivity of GaAs decreases with increasing temperature at a rate of about .3%/^{o}C. Additionally, the use of generic device thermal resistances may add error since device thermal resistance is a function of the individual device materials and the thermal conductivities of these materials at specific temperatures, heat flow area, and material thicknesses. Despite these deficiencies, the θP method provides an accurate measure of the rise in junction temperature on average.

In the case of both life test and field data, the individual device temperature constants were developed as follows. Failure data was entered into a regression with the natural logarithm of failure rate as the dependent variable and the inverse of temperature as the independent variable. The slope of such a regression line is then given by,

$$b_1 = \frac{-Ea}{K}$$

where

b_1 = the slope of the regression line
E_a = equivalent activation energy
K = Boltzman's constant

Table 4.2-3 presents activation energy estimates for all part types made 1) from life test and field data, 2) those reported in the literature, 3) the current MIL-HDBK-217E values and 4) the resulting proposed activation energy.

Current MIL-HDBK-217E values were assumed to hold precedence for all part types with the exception of those technologies which were known to have evolved significantly since the last modeling effort, and/or for which significant new data was available. These technologies inlcude:

Si IMPATT Diodes
GaAs FETs
LEDs and Alpha-numeric Displays
Photodetectors/Opto-isolators

For each of these part types, the proposed activation energies were based upon recent life test data.

In the following cases, no current MIL-HDBK-217 activation energy exists:

Current Regulator Diodes
Transient Suppressor Diodes
Gunn Diodes

In the case of current regulator diodes, no new temperature effects data was available. Since these diodes are essentially FETs with the gate and source connected, the current MIL-HDBK-217E FET activation energy was assumed as a best estimate until further data is available.

For varistor/transient suppressor diodes, the proposed E_a was based upon estimates from life test data. However, since the life test point estimate value was intuitively high and since the data it was based upon was strictly on the high end of device temperature limits, the lower 95% confidence bound value was assumed until further information is available.

TABLE 4.2-3. ACTIVATION ENERGY (E_a) DATA SUMMARY FOR ALL PART TYPES

Part Type	Proposed Ea (eV)	Current Ea (eV)	Literature Reported Ea (eV)	Field Data Ea (eV) -95%	Point Est.	+95%	Life Test Data Ea (eV) -95%	Point Est.	+95%
Si GP Diode	.27	.27	.75	.02	.10	.19		N/A	
Ge GP Diode	.42	.42	N/A		N/A			N/A	
Voltage Regulator/Voltage Reference Diode	.15	.15	N/A	.03	.12	.28		N/A	
Current Regulator Diode	.17	N/A	N/A		N/A			N/A	
Transient Suppressor/Varistor Diode	.33	N/A	N/A		N/A		.33	.78	1.2
PIN Diode	.18	.18	N/A		N/A			N/A	
TUNNEL Diode	.18	.18	N/A		N/A			N/A	
Si IMPATT Diode	.45	.18	1.07-3.50		N/A		.01	.45	.95
Si Schottky Microwave Diode	.13	.13	.62-1.6		N/A		-1.8	.63	3.1
Varactor	.18	.18	N/A		N/A			N/A	
Gunn Diode	.22	N/A	2.03		N/A		.97	2.7	4.45
Si Bipolar Transistor	.18	.18	1.2-2.0	-1.14	.44	2.0		N/A	
Ge Bipolar Transistor	.30	.30	N/A		N/A			N/A	
Si FET	.17	.17	N/A	- .03	.15	.33		N/A	
Unijunction Transistor	.21	.21	N/A		N/A			N/A	
Thyristor/SCR	.27	.27	N/A		N/A		.64	.72	.80
GaAs FET (< 100 mW)	.39	.17	.67-2.3		N/A		.19	.39	.59
GaAs FET (≥ 100 mW)	.46	N/A	.67-2.3		N/A		.14	.46	.78
Microwave Bipolar Transistor	.25	.25(Au) .50(Al)	.3-2.0	- .32	.11	.55		N/A	
LED and Display	.23	.70	.3-.93		N/A		.07	.20	.32
Photodetector/Opto-isolator	.24	.70	.7-.8		N/A		-.16	.24	.64
GaAs/AlGaAs Laser Diode	.40	.40	.34-1.3		N/A		.12	.28	.45
InGaAs/InGaAsP Laser Diode	.50	.50	.34-1.3		N/A			N/A	

In the case of Gunn diodes, the current MIL-HDBK-217E activation energy for other high frequency diodes was assumed until further temperature effects data becomes available.

For the balance of the part types, the current MIL-HDBK-217E activation energy was compared with the upper and lower 95% confidence values about the value estimated from the life test and field data. In all cases the MIL-HDBK-217E value compared favorably with these values and was retained.

4.3 ENVIRONMENTAL FACTOR ANALYSIS

The general modeling approach described in Section 4.1 was applied to the discrete semiconductor failure data collected to determine the effects of environment (humidity, temperature cycles, vibration, shock, etc.) on discrete semiconductor failure rates. Values were developed for all 26 environmental categories presently in MIL-HDBK-217E.

Data was available from 15 environment categories, including all airborne environments, all ground environments and naval submarine. This represents a wide range of environmental stress levels which was sufficient to evaluate and update the environmental factors. For environmental categories where no data could be collected, the existing environmental factors were used to scale the updated factors.

Initially, consideration was given to the development of environmental factor equations as a function of specific environmental stress measurements (i.e., relative humidity, "g" force, etc.). An environmental factor of this form would provide maximum sensitivity to changes in environmental stress and would increase reliability prediction accuracy for specific applications. However, after carefully considering this issue, IITRI decided to maintain the existing method of unique, constant

environmental factor values for all missions falling within a defined environmental category for the following reasons:

(1) For most sources of field data, the specific environmental stress values are unknown and therefore derivation of environmental factor equations using empirical techniques would be difficult.

(2) One of the major objectives of this study effort was to develop reliability prediction models that are usable and that include model input parameters which are accessible to the handbook user. In the design phase of equipment development, many specific environmental stress parameters generally would not be known; therefore, the anticipated increase in prediction accuracy would be negated by a decrease in model usability.

The investigation of environmental factors began with a thorough examination of the existing factors. The present MIL-HDBK-217E models have ten separate environmental series, one for each of the ten device groups. Table 4.3-1 presents the environmental factors for each device group and each environment. Additionally, the mean and variance for each environment class are included in the table.

Initial inspection of the environmental factor matrix revealed that little variation existed for several of the categories. For example, seven of the ten environmental factors for manpack are the same value (i.e., 12). In other environmental categories, the calculated variance is high but this was due to one or two outliers. It is unclear whether the outliers are due to an increased (or decreased) sensitivity to environmental stress or are a statistical aberration. It was noticed that little variation existed between different environmental categories. For example, the values for N_U, N_H and N_{UU} are generally indistinguishable (from a statistical perspective). Based on these observations, it was necessary to perform an analysis to determine whether the effects of environmental stress could be adequately modeled with fewer factors, thereby improving the efficiency of the prediction process without degrading prediction accuracy.

TABLE 4.3-1. EXAMINATION OF MIL-HDBK-217E DISCRETE SEMICONDUCTOR ENVIRONMENTAL FACTOR SERIES

	G_B	G_F	G_M	M_P	M_{SB}	M_S	M_U	M_H	M_{UU}	A_{RW}	A_{IC}	A_{IT}	A_{IB}	A_{IA}	A_{IF}	A_{UC}	A_{UT}	A_{UB}	A_{UA}	A_{UF}	S_F	M_{FF}	M_{FA}	U_{SL}	M_L	C_L
Transistors Group I	1	5.8	18	12	9.8	9.8	21	19	20	27	9.5	15	35	20	40	15	25	60	35	65	0.4	12	17	36	41	690
Transistors Group II	1	4.0	18	12	6	8.6	21	19	20	27	7.5	9	35	30	40	10	15	55	50	65	0.6	12	17	36	41	690
Transistors Group III	1	4	18	12	9.3	9.3	21	19	20	27	9.5	15	35	20	40	15	25	60	35	65	1	12	17	36	41	690
Transistors Group IV	1	3.9	18	12	4.8	4.8	21	19	20	27	15	20	30	25	35	25	30	50	40	50	1	12	17	36	41	690
Diodes Group V	1	3.9	18	12	5.8	8.7	21	19	20	27	4.5	6.5	45	25	45	7.5	10	70	40	70	1	12	17	36	41	690
Diodes Group VI	1	3.9	18	12	5.8	8.7	21	19	20	27	9.5	15	35	20	40	15	25	60	35	65	1	12	17	36	41	690
Diodes Group VII	1	6.4	31	35	8	11	33	54	58	78	30	40	65	50	70	50	60	105	80	110	1	36	50	110	120	2000
Diodes Group VIII	1	3.9	18	12	5.8	8.7	21	19	20	27	4.5	6.5	45	25	45	7.5	10	70	40	70	1	12	17	36	41	690
Transistors Group IX	1	2	7.8	7.4	3.6	4.7	11	11	12	16	2.5	3.5	6	3.5	6	5	7	10	7	10	1	7.5	11	22	25	250
Opto Semiconductors Group X	1	2.4	7.8	7.7	3.7	5.7	11	12	13	17	2.5	3.5	5.5	3.5	8	3	5.5	8	5.5	10	1	7.8	11	23	26	450
Mean	1	4.02	17.26	13.41	6.26	8	20.2	21	22.3	30	9.5	13.4	33.6	22.2	36.9	15.3	21.3	54.8	36.8	58	.9	13.5	19.1	40.7	45.8	753
Variance	0	1.74	41.34	60.97	4.58	4.69	37.51	144.2	167.1	17.4	66.9	118.82	313.1	174.6	339.9	189.5	262.6	809.3	438.7	873.3	.05	65.6	124.1	624.5	721.3	214K

There are currently ten unique series of environmental factors and 26 environmental categories for a total of 260 environmental factor options in the MIL-HDBK-217E discrete semiconductor section. It was important to determine whether this high degree of model sensitivity is justified or meaningful. Analysis of variance (ANOVA) and regression analysis were performed on the failure data from the AN/ARN-118 to further study the environmental factor issue. The AN/ARN-118 data was selected because (1) this equipment operates in all avionic environments both inhabited and uninhabited, (2) the use of one high quality data set eliminates much of variability associated with factors other than environmental stress, and (3) the AN/ARN-118 includes a large cross-section of discrete semiconductor device types. The objective of this analysis was to determine:

- Whether the existing 10 series of environmental factors are all justified
- The effect of inhabited vs uninhabited
- The effect of aircraft type

To test the effect of environment, two ANOVAs were performed. Initially, the data was sorted by aircraft type, inhabited vs. uninhabited, and part class and ANOVA was performed. The results of this analysis are presented in Table 4.3-2. This analysis indicated that device construction, aircraft type and inhabited vs. uninhabited are all important variables influencing failure rate. However, this analysis does not determine whether the relative effect of environment is dependent on device construction or whether 10 unique environmental factor series are justified. The analysis indicated that part style and inhabited/uninhabited are highly significant factors in the prediction of field failure rate. Aircraft type was less significant, but was still an apparent influencing factor.

TABLE 4.3-2. ANOVA FOR AN/ARN-118 DATA

RESPONSE VARIABLE: LOG (FAILURE RATE)					
Source of Variation	Sum of Squares	D.F.	Mean Square	F-Ratio	Prob(>F)
Main Effects	45.627619	9	5.0697354	14.503353	.0000
Part Type	36.552728	4	9.1381819	26.142247	.0000
Inhabited	1.844054	1	1.8440543	5.2754174	.0307
Aircraft	2.711760	4	.6779401	1.9394315	.1364
Residual	8.389346	24	.3495561		
TOTAL (Corr.)	54.016965	33			

A second ANOVA was then performed where failure rates for each part class group (composed of observed data for the ten avionic environments) were divided by the average failure rate for the group. This action numerically removed the effect of part class from the analysis to more closely focus on environmental factor sensitivity. If the results of the second ANOVA indicated that part class was still a significant variable, then this would serve as evidence that environmental sensitivity varied significantly for the different part classes and that different environmental factor series were justified for each part class. However, the second analysis indicated that part class did not have a significant effect on environmental factor determination, and thus a single series of environmental factors could be proposed without introducing significant error. The results of the second ANOVA are presented in Table 4.3-3. The results can be justified physically since (1) environmental stresses predominately accelerate package related failure mechanisms and (2) packaging techniques are similar for many of the device types.

TABLE 4.3-3. ANOVA FOR NORMALIZED AN/ARN-118 DATA

RESPONSE VARIABLE: LOG (NORMALIZED FAILURE RATE)					
Source of Variation	Sum of Squares	D.F.	Mean Square	F-Ratio	Prob(>F)
Main Effects	4.5560198	9	.5062244	1.4481922	.2235
Part Type	.4887523	4	.1221881	.3495521	.8417
Inhabited	1.8440543	1	1.8440543	5.2754174	.0307
Aircraft	2.7117604	4	.6779401	1.9394315	.1364
Residual	8.3893464	24	.3495561		
TOTAL (Corp.)	12.945366	33			

Another result of the environmental factor analysis was that the ratio of uninhabited-to-inhabited discrete semiconductor failure rates was determined to be 1.84. This result is consistent with existing prediction procedures, although slightly lower that the commonly believed 2-to-1 ratio. The observed ratio differences between diodes and transistors was small (i.e., statistically insignificant), and therefore it was assumed that the ratio of uninhabited-to-inhabited failure rate was the same for the discrete semiconductor family of devices.

The regression solution for the AN/ARN-118 discrete semiconductor data analysis is given by the following equation,

$$\lambda_{ARN\text{-}118} = .225 \left\{ \begin{array}{l} 1.0, \text{ transistors} \\ 1.23, \mu \text{ transistors} \\ 0.62, \text{ diodes} \\ 0.31, \mu \text{ diodes} \\ 14.81, \text{ thyristors} \end{array} \right\} \left\{ \begin{array}{l} 1.0, \text{ A} \\ 0.926, \text{F} \\ 0.578, \text{C} \\ 0.770, \text{B} \\ 0.474, \text{T} \end{array} \right\} \left\{ \begin{array}{l} 1.0, \text{ inhabited} \\ 1.84, \text{ uninhabited} \end{array} \right\}$$

Rearranging this solution into a format which is more familiar to MIL-HDBK-217E users results in the following relationship for environmental factor. The environmental factor for airborne inhabited attack was assumed to be equal to 25 for this demonstration. In practice, determination of the actual factor values was performed by analyzing the AN/ARN-118 data mixed together with data from other environments.

$$\pi_E = .25 \left\{ \begin{array}{l} 1.0, \text{ A} \\ 0.926, \text{F} \\ 0.578, \text{C} \\ 0.770, \text{B} \\ 0.474, \text{T} \end{array} \right\} \left\{ \begin{array}{l} 1.0, \text{ inhabited} \\ 1.84, \text{ uninhabited} \end{array} \right\}$$

π_E = 46.0, AUA	= 25.0, AIA
= 42.6, AUF	= 23.2, AIF
= 26.6, AUC	= 14.5, AIC
= 35.4, AUB	= 19.3, AIB
= 21.8, AUT	= 11.9, AIT

As the model development process further proceeded, it became apparent that the difference between cargo, bomber and trainer aircrafts was small and that in several instances, the ranking of aircraft influences seemed inconsistent. For example in the AN/ARN-118 data analysis, cargo failure rate were observed to be higher than trainer failure rates. To remedy this situation, the same factor was proposed for these three aircraft types.

As a by-product of this analysis it was noticed that the environmental sensitivity of microwave diodes and transistors was consistently different that other discrete part classes (although not a highly significant difference). It was determined that the best method to predict environmental effects is to propose three environmental factor series. Separate factors were determined for microwave and non-microwave discrete semiconductors. Additionally, a unique series was proposed for optoelectronics. This action results in a overall decrease in factor permutations from 260 to 78. The new factors are presented in Appendix A and in the appropriate sections of Section 5.0 of this report.

4.4 QUALITY FACTOR ANALYSIS

An important aspect of this study was to investigate the effects on failure rate caused by device quality. The applicable device quality level depends upon the type and amount of screening performed on discrete semiconductors and the package type. MIL-S-19500, "General Specification

for Semiconductor Devices," is the appropriate military specification for transistors and diodes and includes the specific requirements for a quality level. Discrete semiconductor quality levels as specified by MIL-HDBK-217E are:

(1) JANTXV
(2) JANTX
(3) JAN
(4) Lower (Commercial Hermetic)
(5) Plastic (Commercial Plastic)

Initially, the existing MIL-HDBK-217E discrete semiconductor quality factors were categorized and studied. MIL-HDBK-217E currently includes ten unique quality factors to model the effects of screening and package type on discrete semiconductor failure rate. These factors are presented in Table 4.4-1.

There are eight unique quality factor series. Initially, it was believed that this indicated different degrees of screening sensitivity for the various discrete semiconductor part families. The factors can vary by a factor as large as 100 for a given screen class, depending on the part category. However, after close examination, it was determined that the factors were not necessarily sensitive but were needlessly repetitious. Since the models are multiplicative, it is the relative difference which is important and not the absolute magnitude of the factors. Table 4.4-2 presents the relative quality factor tables. These values were computed by dividing each series by the JANTX quality factor (in effect, normalizing each series to a JANTX quality factor equal to one). Examination of this table reveals that the factors are very similar; in fact, eight of the ten are identical.

Based on the previously described findings, it was determined that one series of quality factors would be sufficient to model the effects of part quality for all non-RF devices. This assumption is consistent with the microcircuit failure rate models in MIL-HDBK-217E. For RF devices (Groups

TABLE 4.4-1. QUALITY FACTOR MATRIX

	JANTXV	JANTX	JAN	Lower	Plastic
Transistors Group I	.12	.24	1.2	6.0	12.0
Transistors Group II (1)	.12	.24	1.2	6.0	12.0
Transistors Group III	.5	1.0	5.0	25.0	50.0
Transistors Group IV	.15	.3	1.5	7.5	15.0
Diodes Group V	.3	.6	3.0	15.0	30.0
Diodes Group VI	.5	1.0	5.0	25.0	50.0
Diodes Group VII	1.0	2.0	3.5	5.0	--
Diodes Group VIII (2)	.5	1.0	5.0	25.0	--
Transistors Group IX (3)	1.0	2.0	4.0	10.0	--
Opto Semiconductors Group X	.01	.02	0.1	0.5	1.0

Notes: (1) Factors are for Si devices only
(2) Factors do not apply to GUNN and IMPATT devices
(3) Factors correspond to equivalent screen classes
-- Not applicable

TABLE 4.4-2. NORMALIZED QUALITY FACTOR MATRIX

	JANTXV	JANTX	JAN	Lower	Plastic
Transistors Group I	0.5	1.0	5.0	25	50
Transistors Group II (1)	0.5	1.0	5.0	25	50
Transistors Group III	0.5	1.0	5.0	25	50
Transistors Group IV	0.5	1.0	5.0	25	50
Diodes Group V	0.5	1.0	5.0	25	50
Diodes Group VI	0.5	1.0	5.0	25	50
Diodes Group VII	0.5	1.0	1.8	2.5	--
Diodes Group VIII (2)	0.5	1.0	5.0	25	--
Transistors Group IX (3)	0.5	1.0	2.0	5.0	--
Opto Semiconductors Group X	0.5	1.0	5.0	25	50

Notes: (1) Factors are for Si devices only
(2) Factors do not apply to GUNN and IMPATT devices
(3) Factors correspond to equivalent screen classes
-- Not applicable

VII, VIII, and IX), no changes were made to the existing factors because there was a lack of empirical data in a wide range of screen classes upon which to base new factors. It would be inappropriate to propose new factors without proper backing data. A cosmetic change consisting of normalizing the factors to a JANTX value equal to one was made to provide consistency among the discrete semiconductor sections.

An intuitive evaluation of quality factor trends was also completed to complement forthcoming statistical investigations. Based on this evaluation, it was anticipated that advances in manufacturing and processing will tend to lessen the immediate effects of screening. These technological advances result in lower percentages of defective or weak devices. The intended effects of screening are to lower the rate of failure for the surviving population by removing the defective and weak devices. Since this segment of the device population is naturally shrinking, it is anticipated that the numerical values for quality factor will tend to become less sensitive.

Screen class was initially introduced into the regression as a qualitative variable. On average the results were encouraging. However the individual values did not consistently conform to the anticipated ranking (i.e., devices with more screening showed a higher failure rate). Therefore, to promote smoothing and to ensure an updated quality factor series with physically correct rankings, the present MIL-HDBK-217E quality factor was introduced into the regression model as a independent variable while observed failure rate were the dependent variable. The updated factors were therefore given by:

$$\lambda_p \propto (\pi_{Q,old})^n$$

$$\pi_{Q,updated} = (\pi_{Q,old})^n$$

where

λ_p = predicted failure rate

$\pi_{Q,old}$ = existing MIL-HDBK-217E quality factor

$\pi_{Q,updated}$ = proposed updated quality factors

n = shaping parameter (regression coefficient)

Results of the quality factor analysis for non-RF devices are as follows:

Quality Level	Updated Factor
JANTXV	0.7
JANTX	1.0
JAN	2.4
Lower (Commercial Hermetic)	5.5
Plastic (Commercial Plastic)	8.0

It was also desired to develop factors for JANS screen class. However, a complete lack of observed data for this screen class prevented the development of updated factors.

4.5 DETERMINATION OF PREDICTION MODEL FORM - TIME DEPENDENCY

An objective of this study was to develop discrete semiconductor failure rate prediction models to predict both catastrophic and drift failures as a function of time for inclusion in MIL-HDBK-217E, Reliability Prediction of Electronic Equipment. To establish a uniform failure criterion for drift component failures, some assumptions regarding failure criterion had to be made.

The primary purpose of the MIL-HDBK-217E device failure rate prediction models is to estimate the reliability of military equipment and systems. With this purpose in mind, the definition of "failure" resulting from drift in an electronic part must include any drift failure which causes the equipment employing the failed device to cease to function satisfactorily. Although this assumption makes the time-to-failure circuit dependent and in some cases a matter of judgement, it is assumed

that the field usage data collected for this study will be statistically representative of the total population, and therefore the failure criteria used by the data sources are assumed to be typical to those throughout the industry. The drift failures shall be considered jointly with catastrophic failures. The resulting prediction models will thereby take into account the effects of both catastrophic and drift failures on overall system or equipment reliability. This assumption will simplify calculation and implementation of the models while allowing for realistic prediction of electronic equipment reliability.

With the inclusion of drift failures in the total failure population, the question of a time-dependent hazard rate arises. Unlike the randomness associated with catastrophic failures (homogenous Poisson process), which results in the generally-accepted constant failure rate assumption, drift failure rates are generally time-dependent. Furthermore, drift failures are sometimes reversible. For these reasons the following investigation was conducted to determine the influence of drift failures on the total device failure population.

A thorough examination of the application of a time-dependent failure rate to the MIL-HDBK-217E discrete semiconductor failure rate prediction models was completed. One reference from the literature indicated that semiconductor device time-to-failure data fits the exponential distribution (Ref. 3), indicating a constant failure rate. Conversely, several other sources showed the log normal failure distribution to be applicable, indicating a time-dependent failure rate (Ref. 7,11,12,13,19,28).

There are many practical reasons why the assumption of a constant failure rate in time is preferred to a time-dependent failure rate for the MIL-HDBK-217E discrete semiconductor failure rate prediction models.

- Simplicity

  The mean time between failure (MTBF) of a system whose component parts exhibit constant hazard rates is not time dependent, where as for a system made up of components having nonconstant failure rates, the system MTBF will be time-dependent and is therefore undefined unless a particular mission time is specified. The assumption of exponentiality allows for failure rates to be summed in a series reliability network.

- Precedent

  The exponential assumption is used for the electronic components currently in MIL-HDBK-217E.

- Data Availability

  If any distribution other than an exponential is assumed, the parameters of the distribution must be determined by analysis of cumulative time-to-failure data. This detailed information is seldom available for field data sources. The exponential distribution allows population parameter estimates to be made based upon total part operating hours and total number of failures.

- Accuracy

  When developing models such as those employed in MIL-HDBK-217E, any improvement in model accuracy resulting from the use of a more complex distribution (than exponential) may be insignificant when compared to the inherent variability associated with reliability prediction and the "statistical noise" in the data.

An objective analysis of constant versus time-dependent failure rate distributions was undertaken, using observed time-to-failure data. However, for the above mentioned reasons, it was predetermined that if MIL-HDBK-217E discrete semiconductor failure rate prediction models could be established as accurately by assuming an exponential failure distribution as by a lognormal or other time dependent failure distribution, the former would be implemented.

The following paragraphs describe the analysis procedure followed.

All time-to-failure data was extracted from the available literature. This collected data consisted of life test results at high temperatures. Ideally, it would have been preferrable to analyze time-to-failure field data since such data would more closely approximate the actual usage environments. However, such data is simply not available. High temperature life test time-to-failure data was available for the following device types:

Low Noise GaAs FETs
High Power GaAs FETs
General Purpose Transistors (NPN & PNP)
GaAs Laser Diodes
IMPATT Diodes
Schottky Diodes

Weibull analysis was then applied. The Weibull distribution is particularly useful in analyzing life data since (1) it has repeatedly been observed to provide a good fit to the data, and (2) it is a flexible distribution which can approximate many other statistical distributions, depending upon the value of β, the shape parameter. Table 4.5-1 gives some shapes of the Weibull distribution depending upon various values of β. The two-parameter Weibull distribution was chosen for this analysis. The form of the Weibull distribution varies between texts, but a common one is given by the probability density function:

$$f(t) = \frac{\beta}{\alpha} \left(\frac{t}{\alpha}\right)^{\beta-1} \exp\left(-\left(\frac{t}{\alpha}\right)^{\beta}\right)$$

where

α = scale parameter (characteristic life)
β = shape parameter

TABLE 4.5-1. WEIBULL SHAPE PARAMETERS (REFERENCE 43)

Shape Parameter, β	Distribution Type
$\beta < 1$	Gamma ($k < 1$)
$\beta = 1$	Exponential
$\beta = 2$	Rayleigh
$\beta = 3.44$	Normal (approx.)

Each individual data set (there were 21 in all) was plotted on Weibull probability paper, and the value of β was determined. Figures 4.5-1 through 4.5-21 illustrate the Weibull plots of the data. The results of this step of the analysis were encouraging since, as can be seen from the plots, the values of β seemed to center around 1.0. Table 4.5-2 presents of a summary of the best fit Weibull parameters.

The next step of the analysis was to force the best line with $\beta = 1.0$ through the observed data points. This is also illustrated in the figures. The Kolmogorov-Smirnov (K-S) goodness-of-fit test was then applied to the forced line. The intent of this step was to determine the degree of error resulting from the exponential assumption. None of the data sets was significantly different from the exponential model at 20% significance. This implies that the available data does not indicate deficiencies with the exponential assumption. The results of the Kolmogorov-Smirnov test are presented in Table 4.5-3.

Based on the results of the K-S test, it was assumed that the failure distributions of the semiconductor devices analyzed could be described by a Weibull with a slope of 1.0. Assuming anything other than a constant failure rate would introduce unnecessary complexity into the models. The observed time-to-failure distributions were accurately represented by an exponential distribution over the range of variables in the data. Time-to-failure data was not available for all discrete semiconductor device types under investigation. It was therefore necessary to make the assumption that the times-to-failure of other discrete semiconductor part

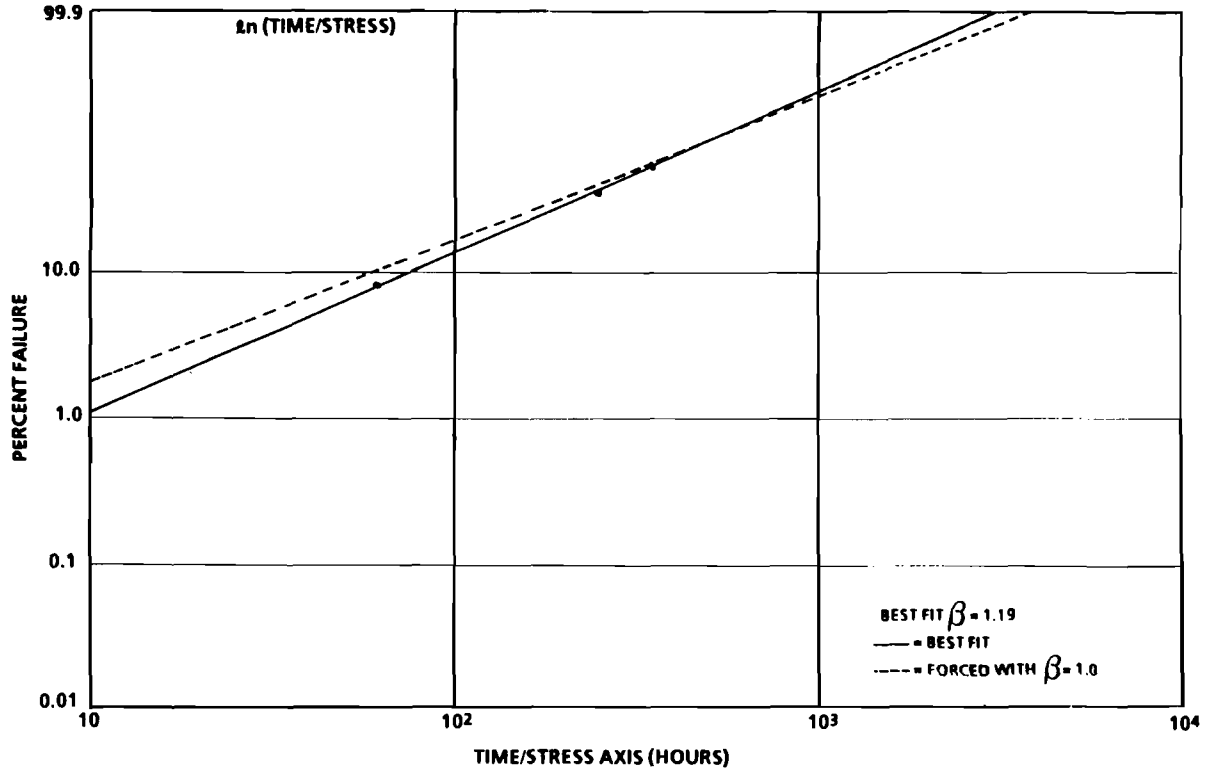

Figure 4.5-1. Weibull Plot of High Temperature Operating Life Data for GaAs FETs I

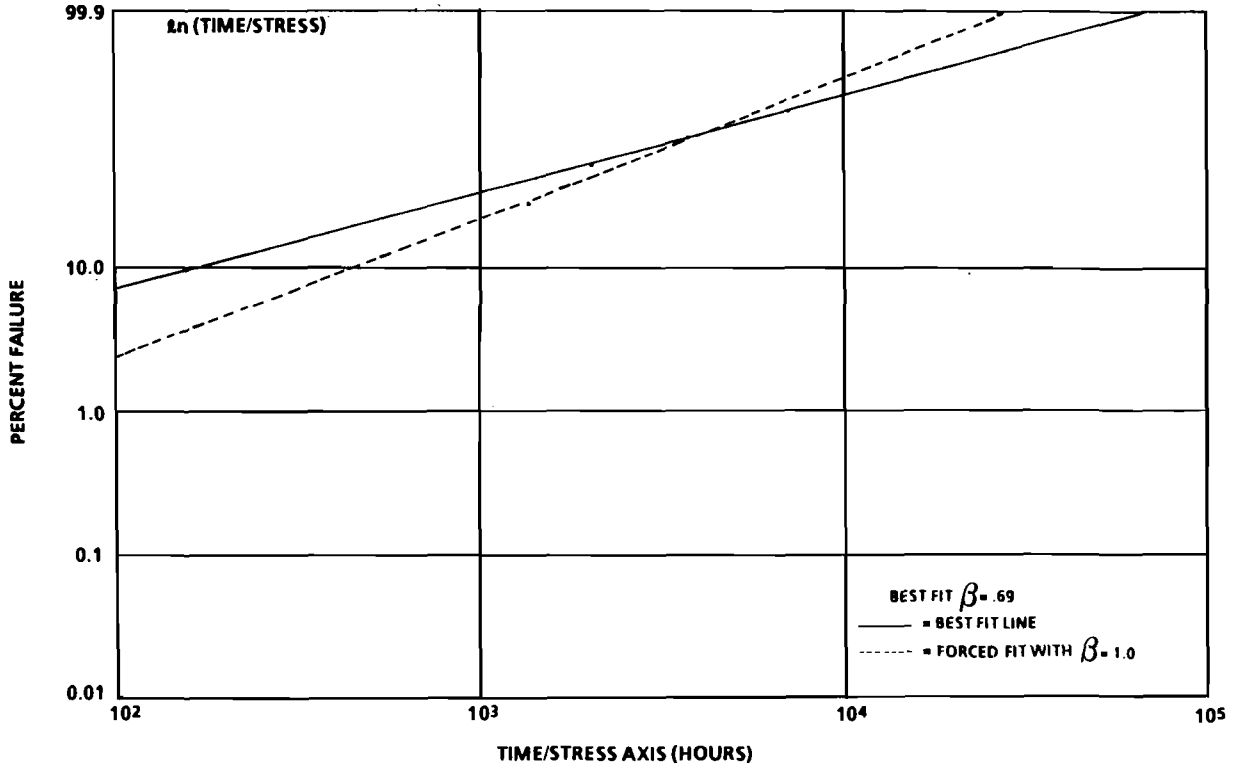

Figure 4.5-2. Weibull Plot of High Temperature Operating Life Data For GaAs Laser Diodes I

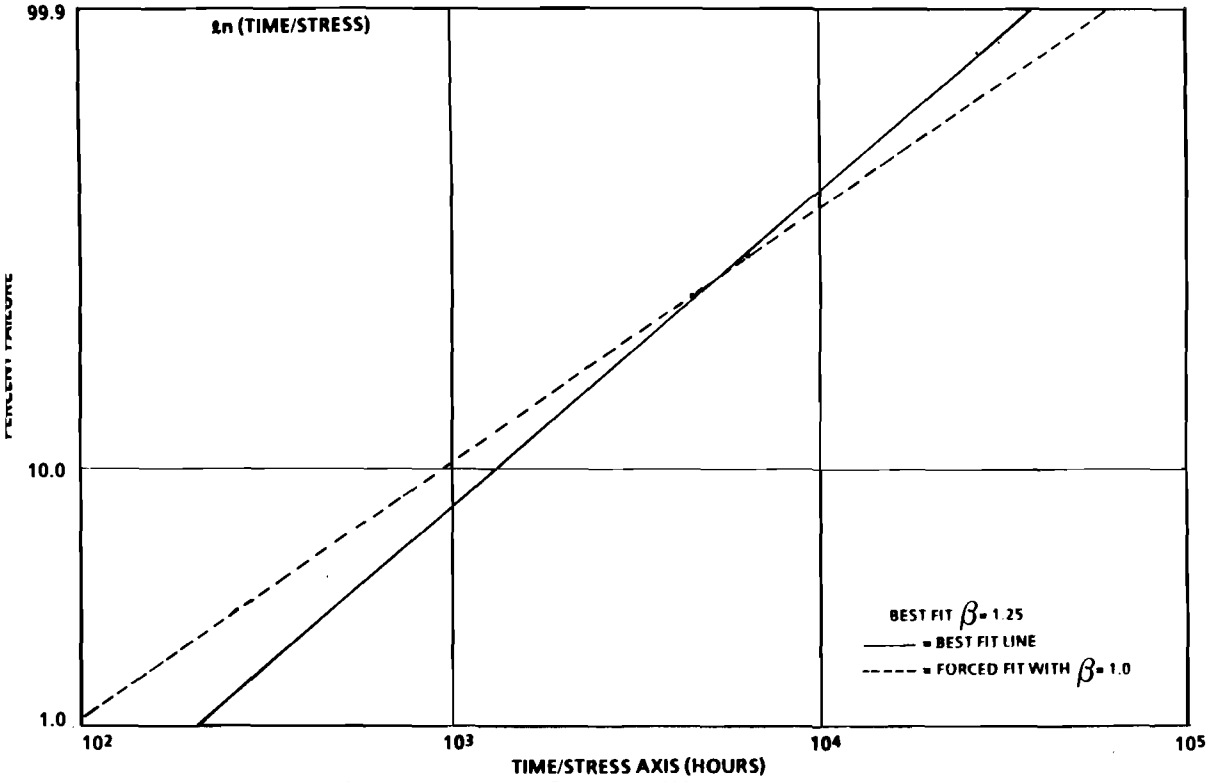

Figure 4.5-3. Weibull Plot of High Temperature Operating Life Data For GaAs Laser Diodes II

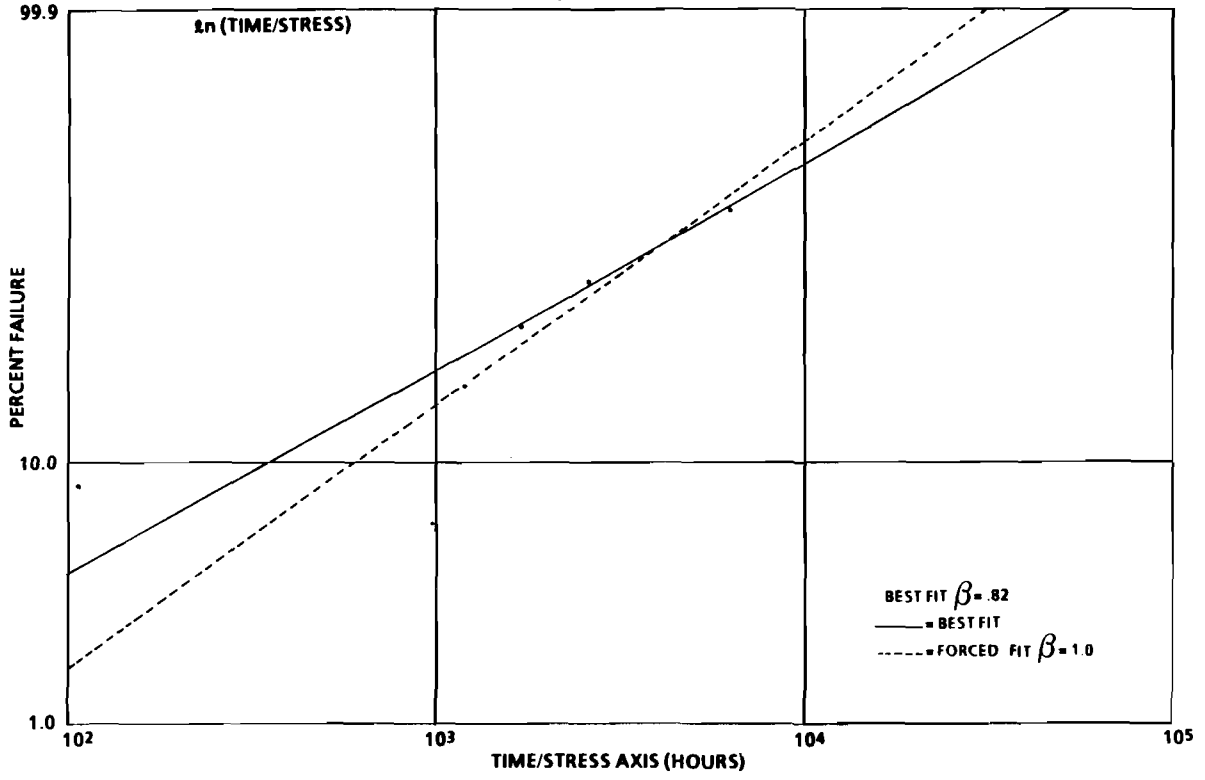

Figure 4.5-4. Weibull Plot of High Temperature Operating Life Data For GaAs Laser Diodes III

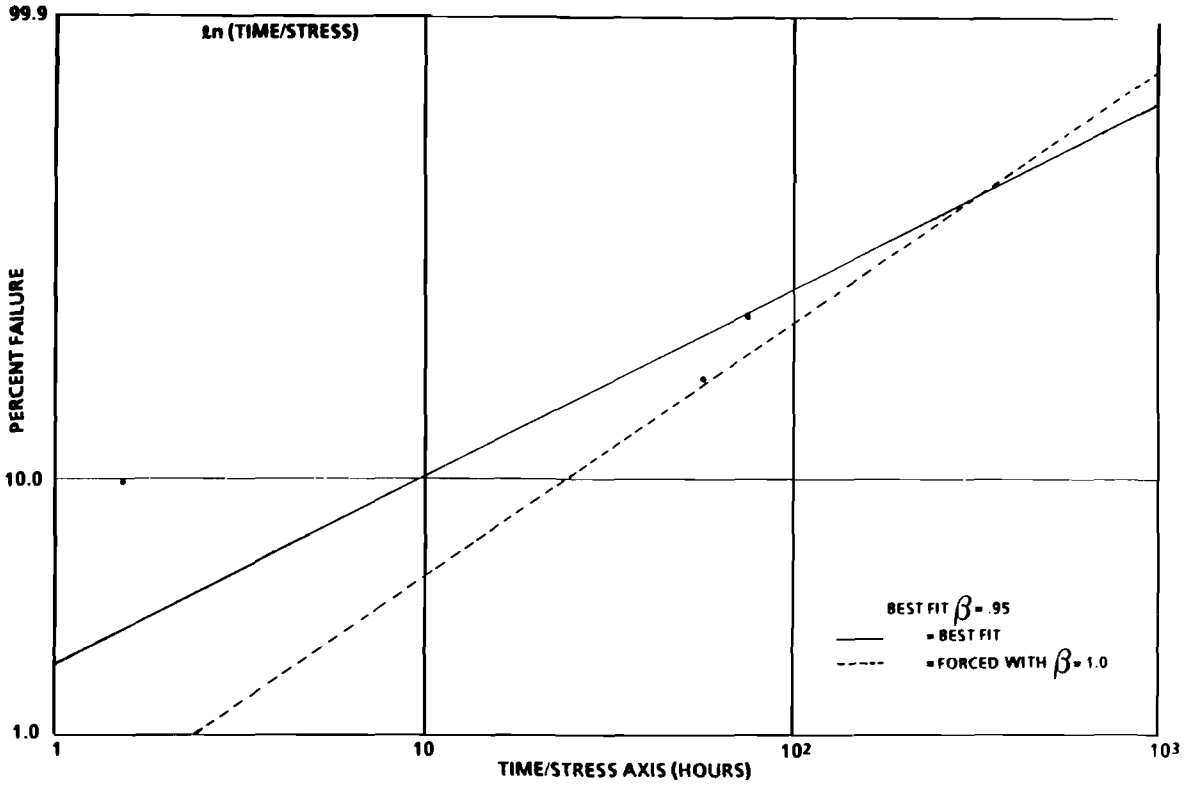

Figure 4.5-5. Weibull Plot of High Temperature Operating Life Data For GaAs Laser Diodes IV

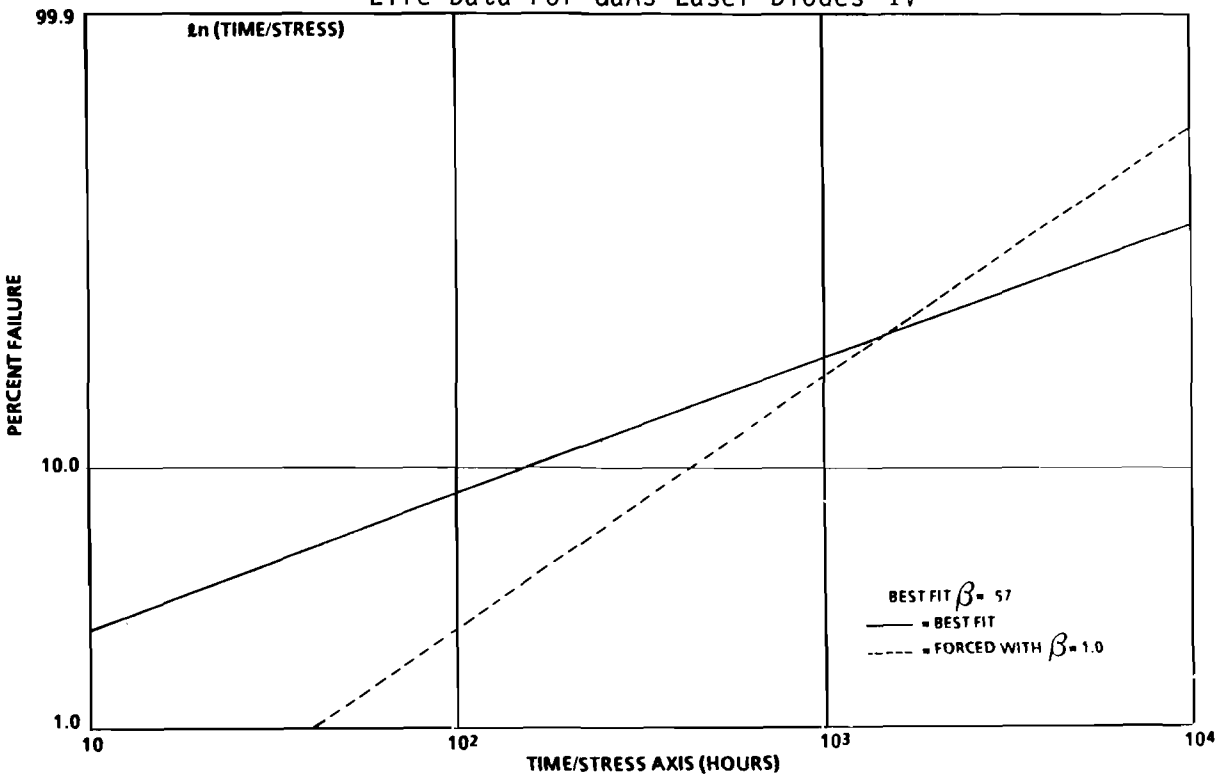

Figure 4.5-6. Weibull Plot of High Temperature Operating Life Data For GaAs Laser Diodes V

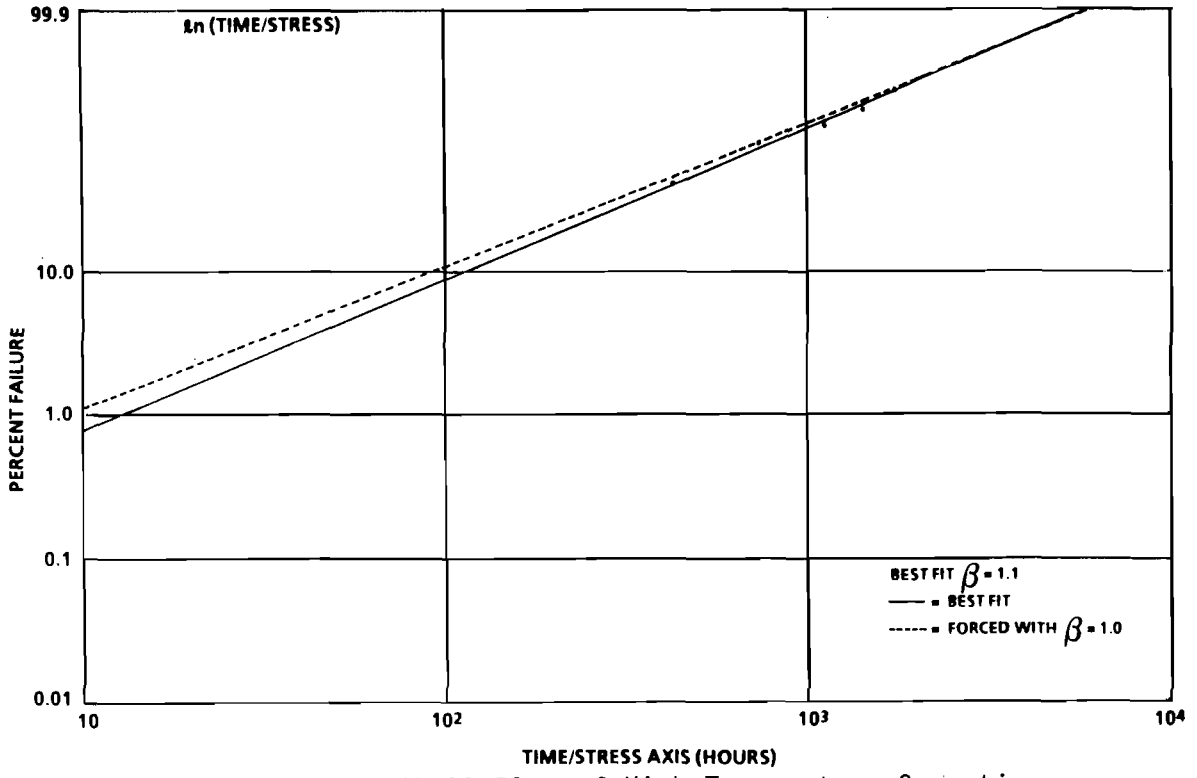

Figure 4.5-7. Weibull Plot of High Temperature Operating Life Data For GaAs FETs II

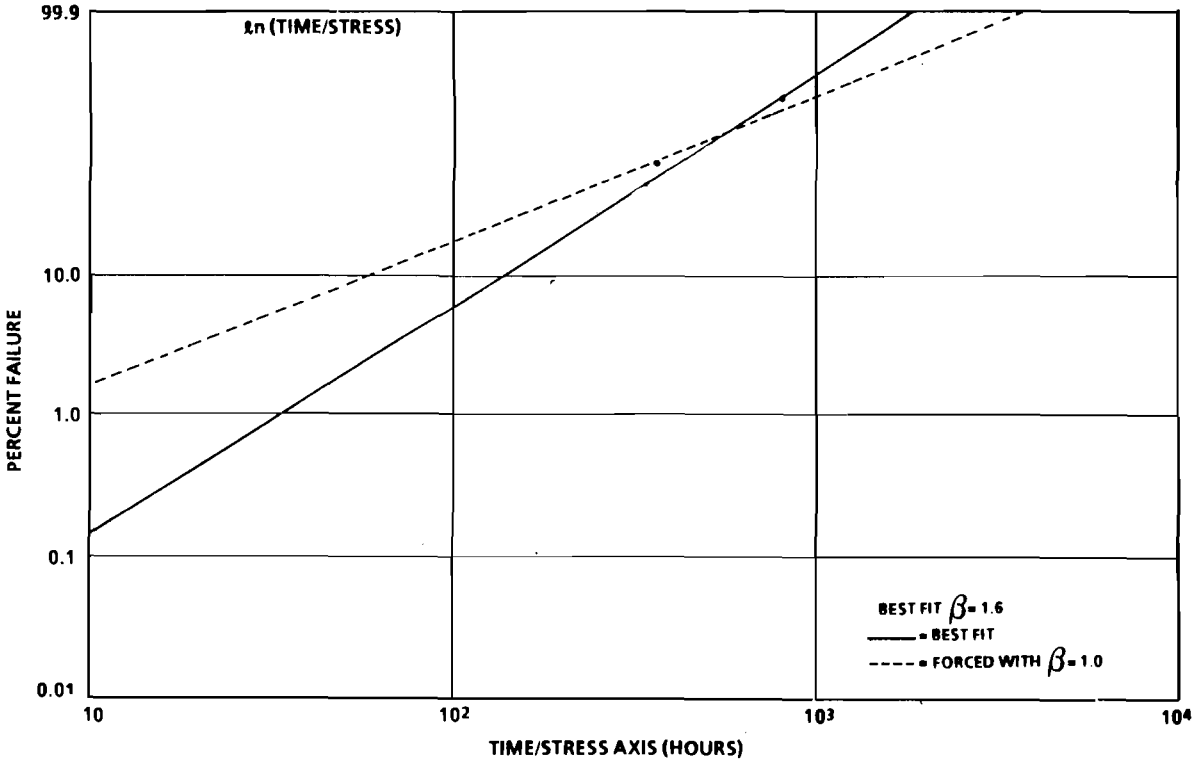

Figure 4.5-8. Weibull Plot of High Temperature Operating Life Data For GaAs FETs III

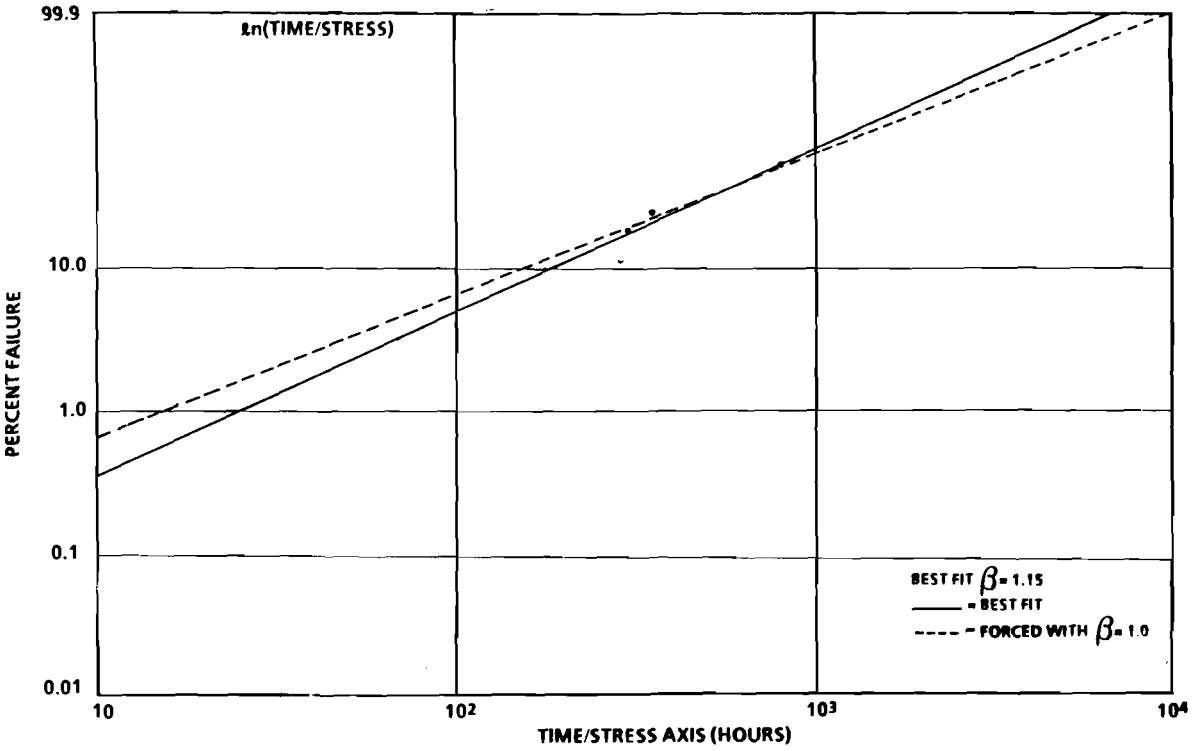

Figure 4.5-9. Weibull Plot of High Temperature Operating Life Data For High Power Pulsed IMPATT Diodes I

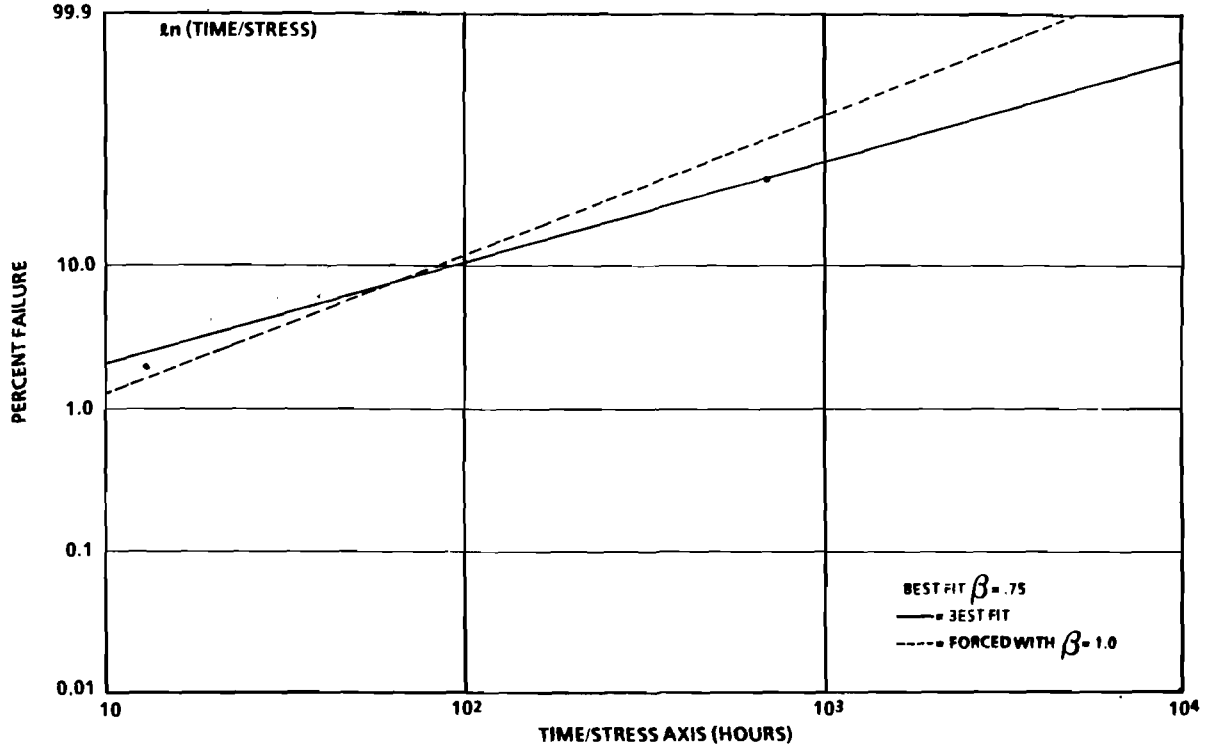

Figure 4.5-10. Weibull Plot of High Temperature Operating Life Data For High Power Pulsed IMPATT Diodes II

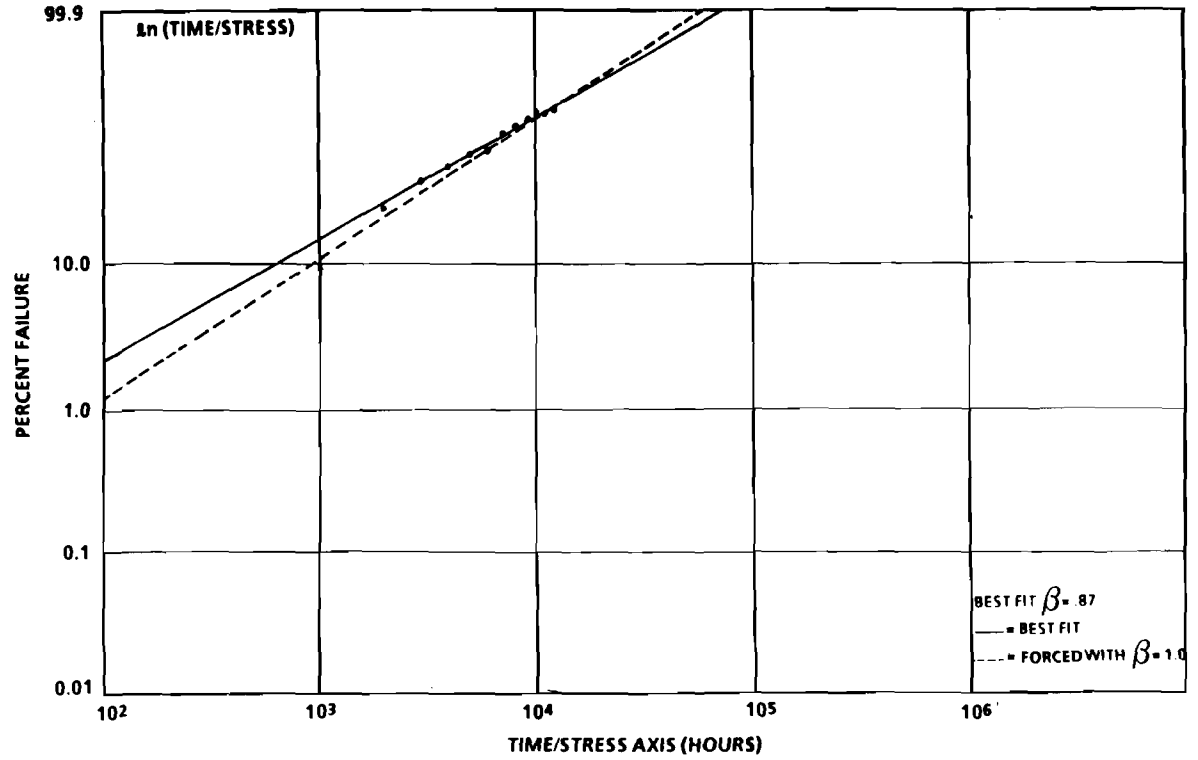

Figure 4.5-11. Weibull Plot of High Temperature Operating Life Data For AlGa As Lasers

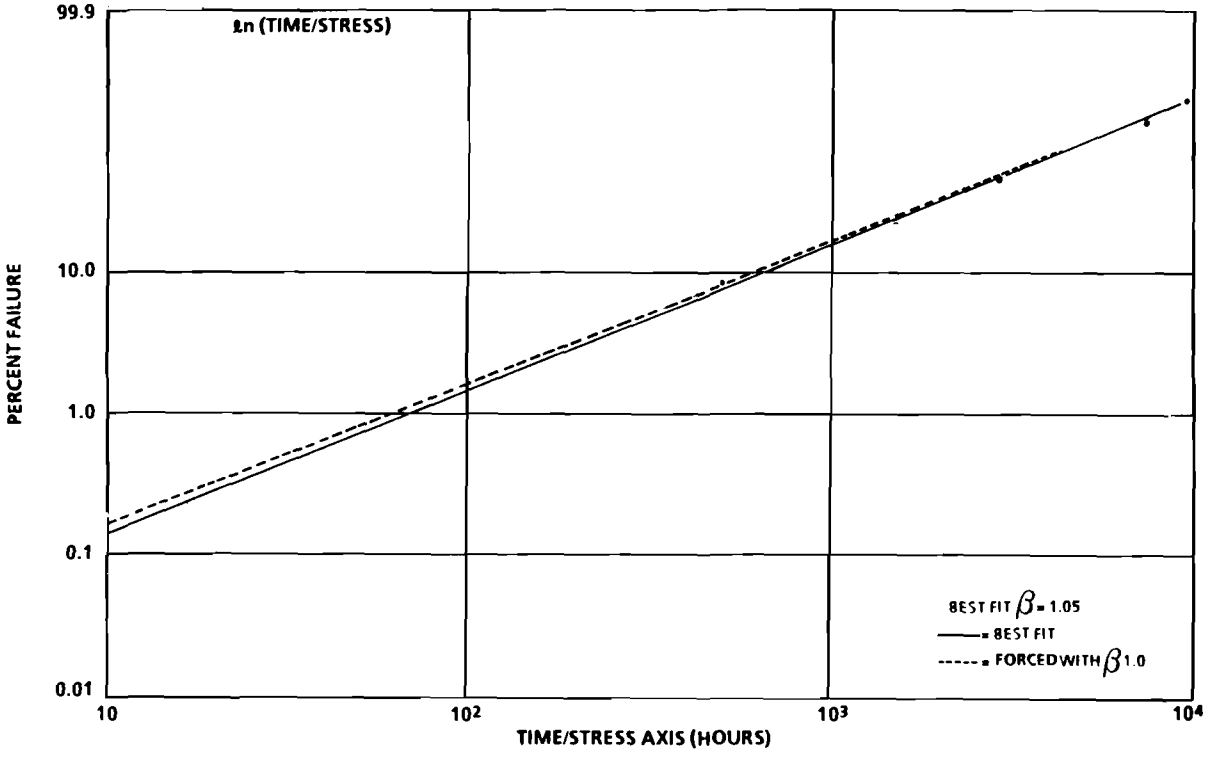

Figure 4.5-12. Weibull Plot of High Temperature Operating Life Data For InGaAs/InGaAsP DH Lasers

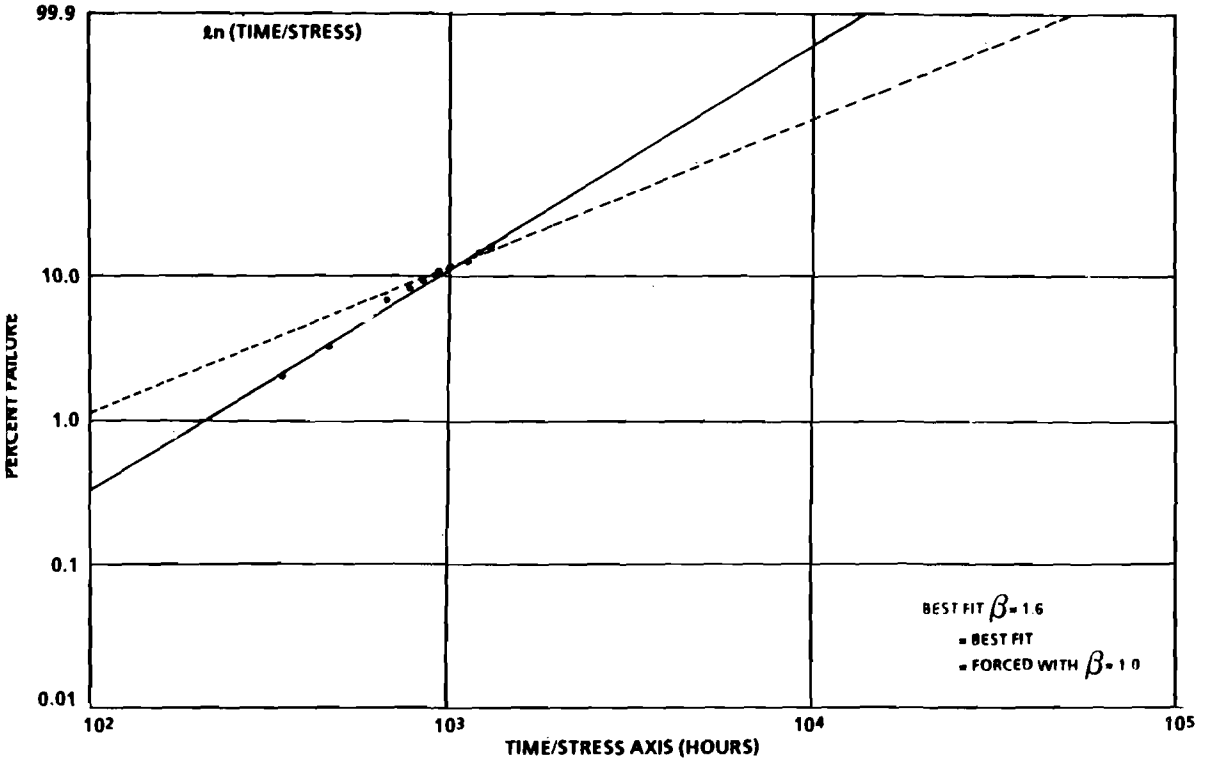

Figure 4.5-13. Weibull Plot of High Temperature Operating Life Data For JAN 2N918

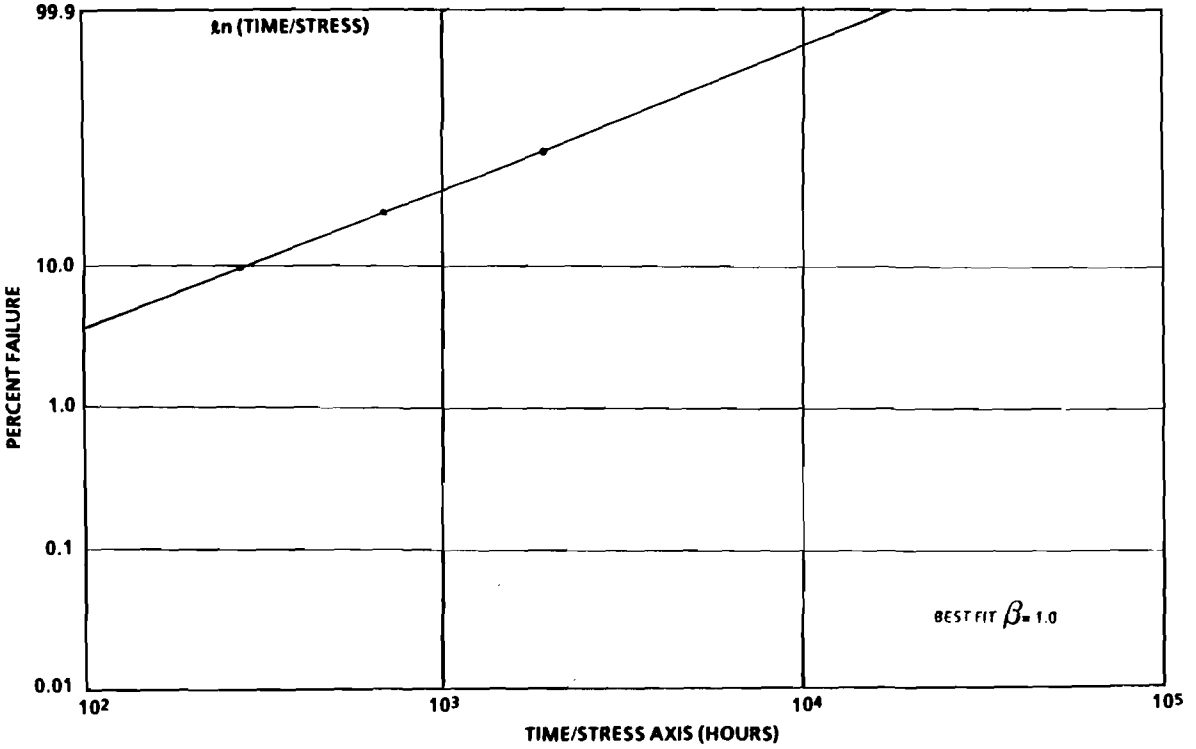

Figure 4.5-14. Weibull Plot of High Temperature Operating Life Data For GaAs Power FETs

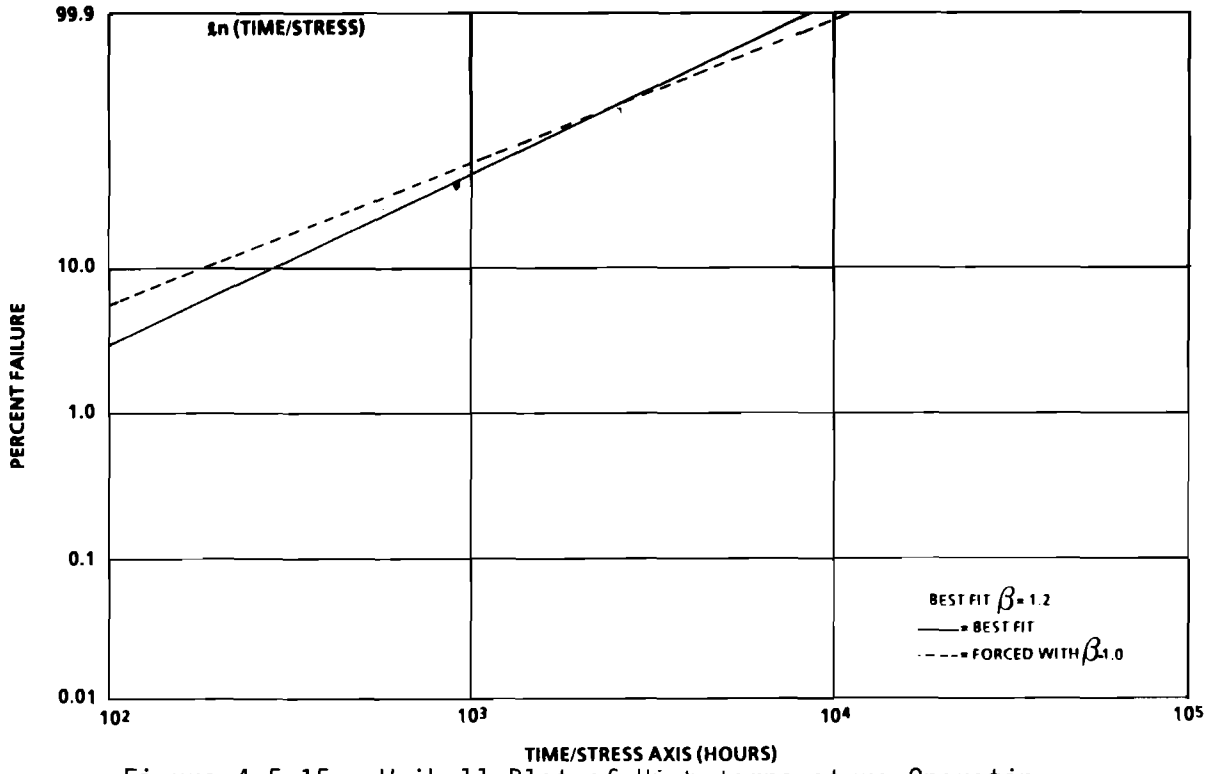

Figure 4.5-15. Weibull Plot of High Temperature Operating Life Data For Low Noise GaAs FETs I

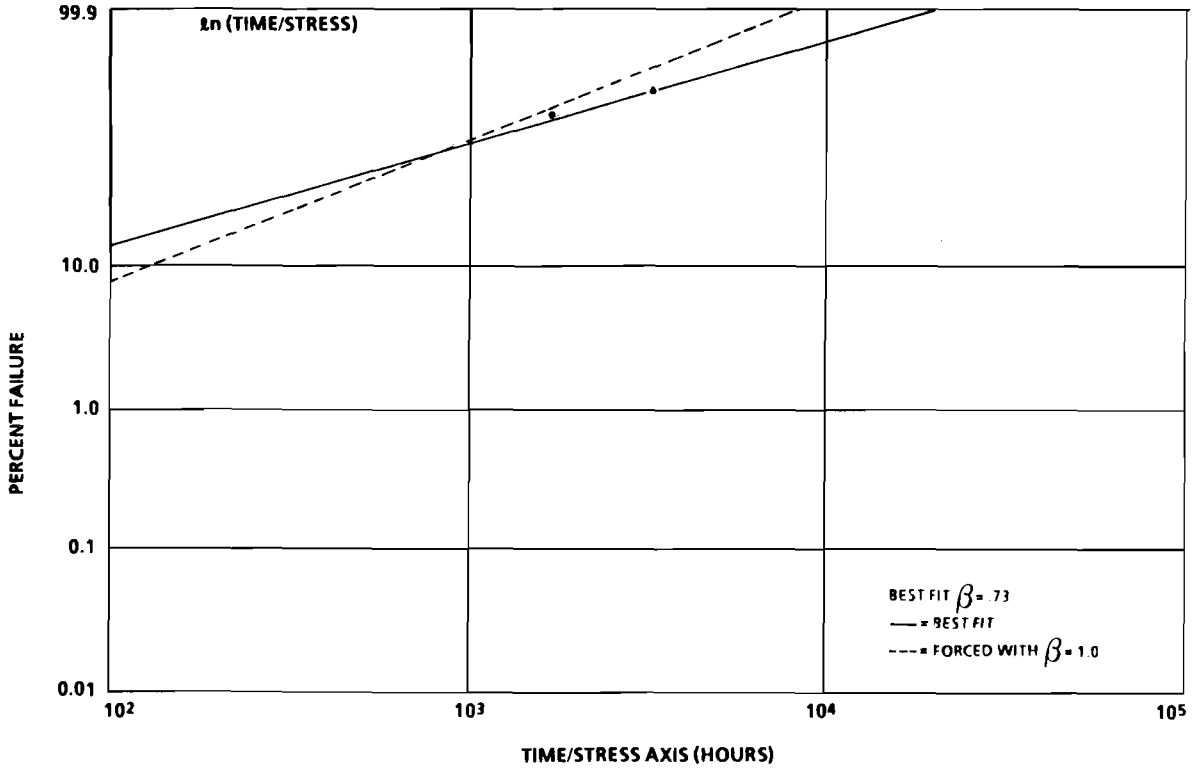

Figure 4.5-16. Weibull Plot of High Temperature Operating Life Data For Low Noise GaAs FETs II

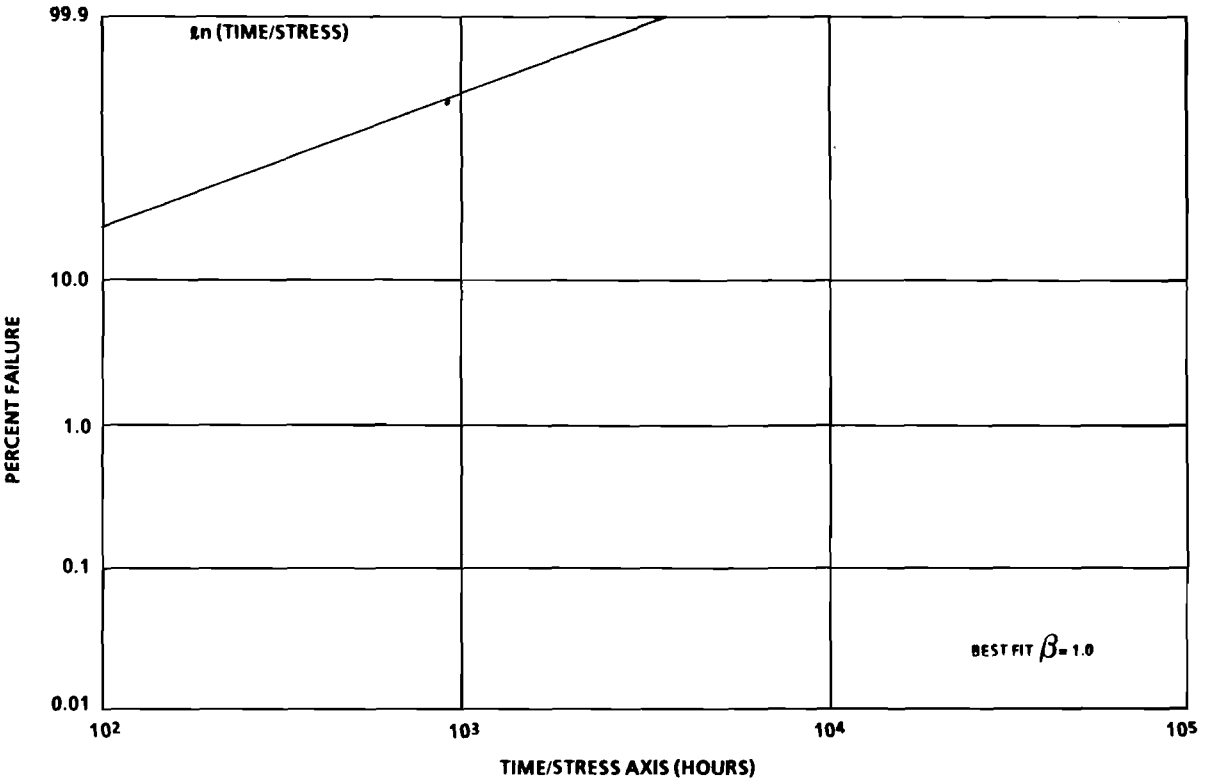

Figure 4.5-17. Weibull Plot of High Temperature Operating Life Data For Low Noise GaAs FETs III

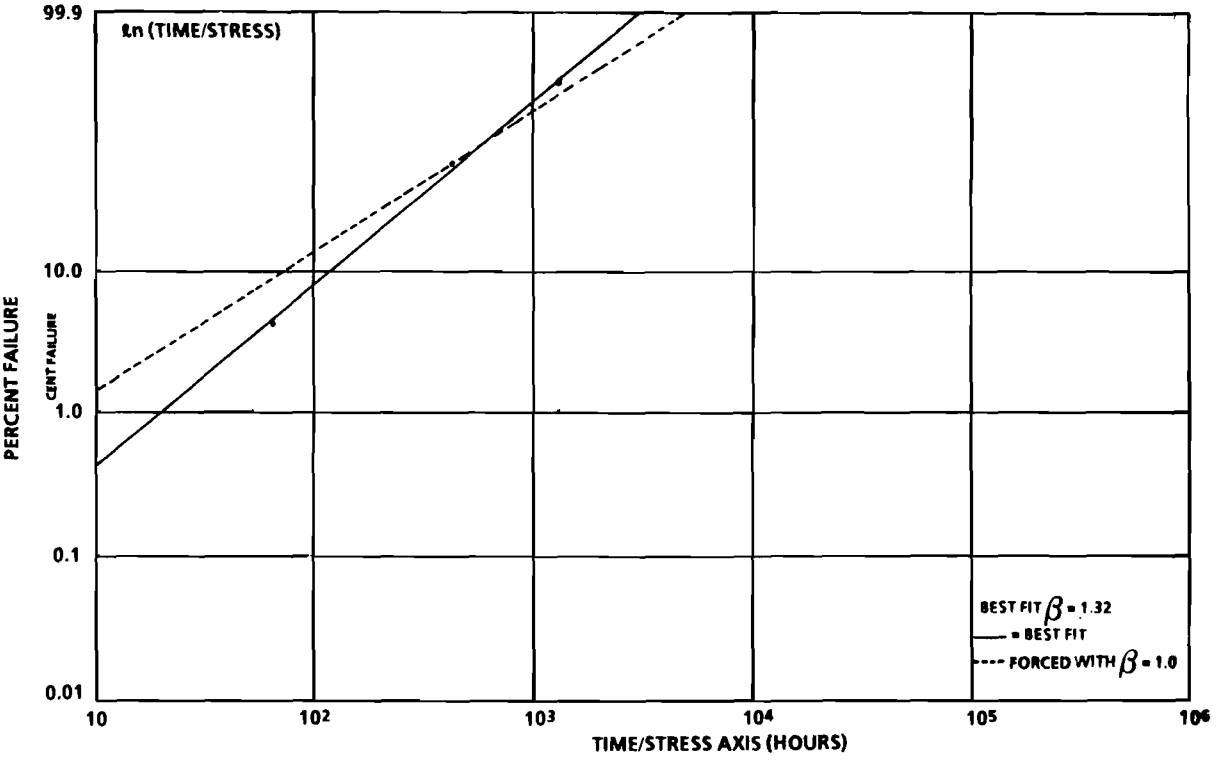

Figure 4.5-18. Weibull Plot of High Temperature Operating Life Data For Low Noise GaAs FETs IV

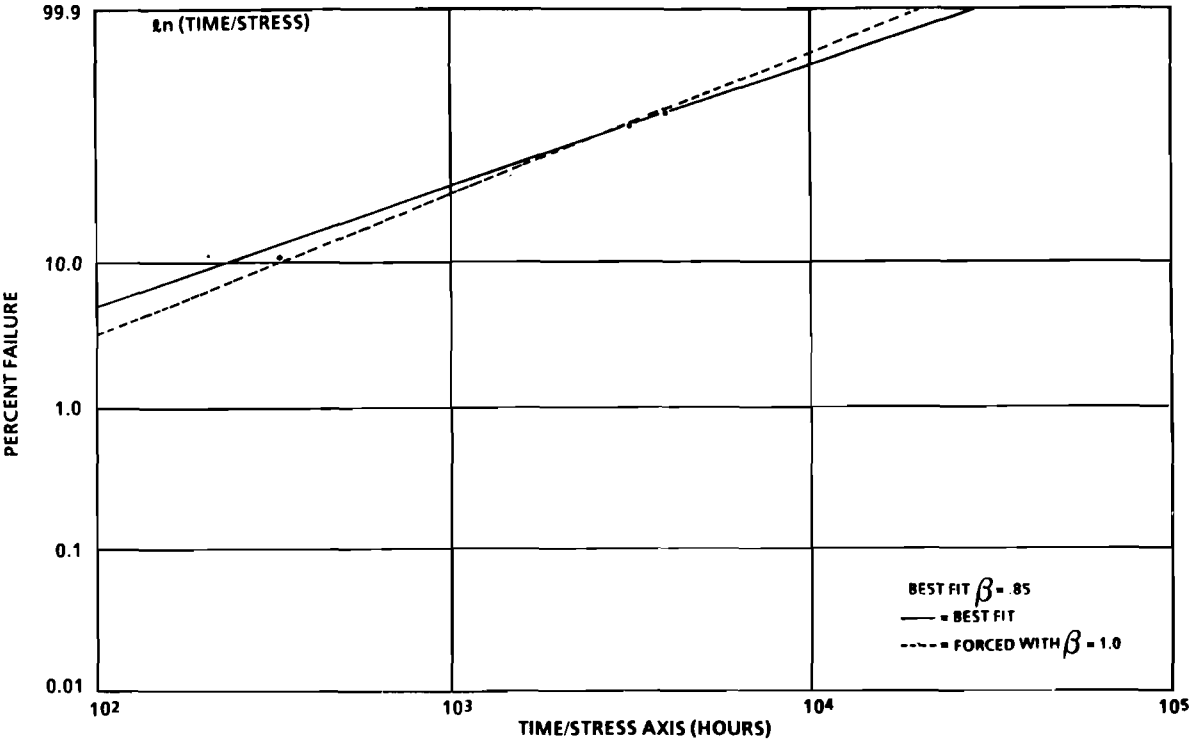

Figure 4.5-19. Weibull Plot of High Temperature Operating Life Data For Low Noise GaAs FETs V

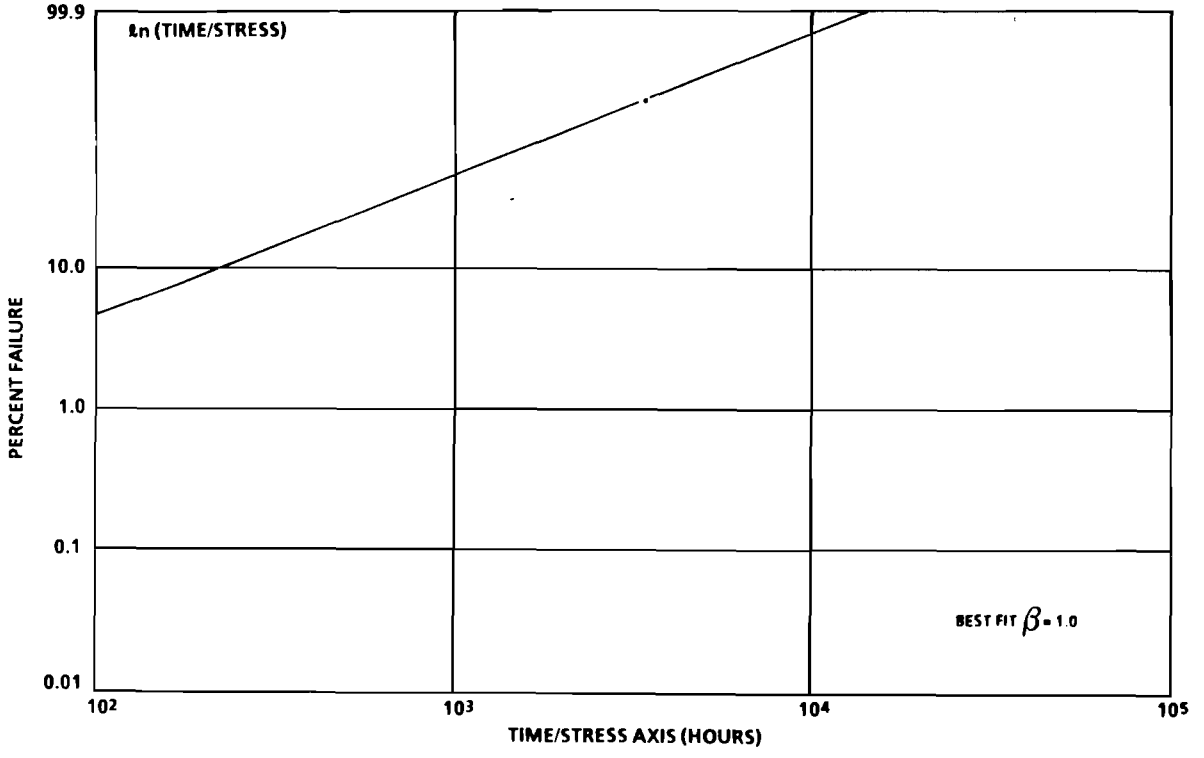

Figure 4.5-20. Weibull Plot of High Temperature Operating Life Data For Low Noise GaAs FETs VI

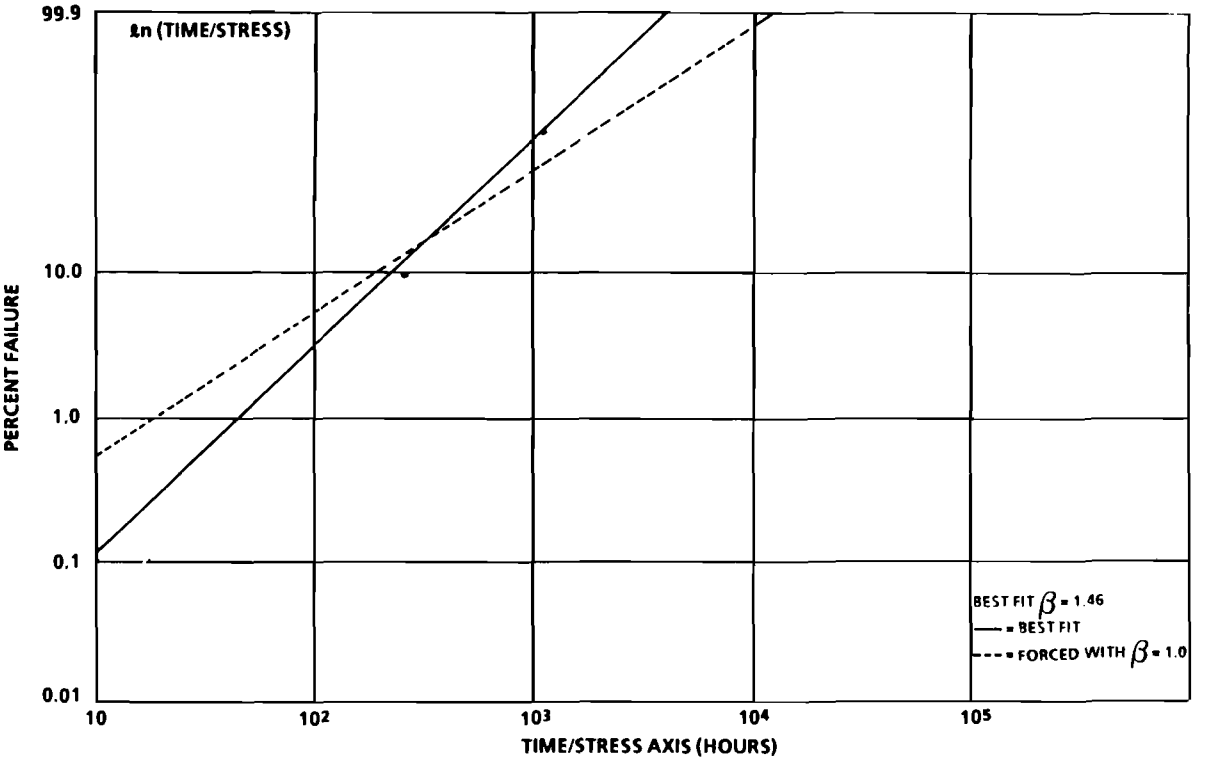

Figure 4.5-21. Weibull Plot of High Temperature Operating Life Data For Low Noise GaAs FETs VII

TABLE 4.5-2. OBSERVED WEIBULL PARAMETERS

Figure #	Ref #	Temperature (°C)(1)	β	α
4.5-1	20	200 (Tc)	1.15	600
4.5-2	35	70 (Tc)	.69	4,400
4.5-3	35	55 (Tc)	1.25	8,000
4.5-4	35	70 (Tc)	.82	5,200
4.5-5	35	70 (Tc)	.95	230
4.5-6	35	40 (Tc)	.57	10,000
4.5-7	19	245 (Ta)	1.10	950
4.5-8	19	231 (Ta)	1.60	580
4.5-9	44	90 (Tc) 220 (Tj)	1.15	1,300
4.5-10	44	90 (Tc) 220 (Tj)	.75	2,000
4.5-11	33	70 (Ta)	.87	8,000
4.5-12	45	20 (Tc)	1.05	6,000
4.5-13	42	300 (Tj)	1.60	4,000
4.5-14	11	228 (Tj)	1.00	2,700
4.5-15	22	200 (Ta)	1.20	1,600
4.5-16	22	200 (Ta)	.73	1,500
4.5-17	22	220 (Ta)	1.00	500
4.5-18	22	220 (Ta)	1.32	700
4.5-19	22	85 (Ta)	.85	3,100
4.5-20	22	120 (Ta)	1.00	2,100
4.5-21	22	240 (Ta)	1.46	1,200

NOTES: (1) Tc = case temperature
Ta = ambient temperature
Tj = junction temperature

TABLE 4.5-3. K-S TEST RESULTS

igure #	Ref. #	# of Fail.	Maximum Deviation	K-S Statistic (0.2 Significance Level)	Conclusion
4.5-1	20	4	.022	.494	Fits $\beta = 1.0$
4.5-2	35	5	.078	.446	Fits $\beta = 1.0$
4.5-3	35	5	.054	.446	Fits $\beta = 1.0$
4.5-3	35	6	.200	.410	Fits $\beta = 1.0$
4.5-5	35	7	.083	.381	Fits $\beta = 1.0$
4.5-6	35	4	.116	.494	Fits $\beta = 1.0$
4.5-7	19	9	.090	.339	Fits $\beta = 1.0$
4.5-8	19	7	.227	.381	Fits $\beta = 1.0$
4.5-9	44	11	.055	.323	Fits $\beta = 1.0$
4.5-10	44	15	.231	.276	Fits $\beta = 1.0$
4.5-11	33	74	.118	.124	Fits $\beta = 1.0$
4.5-12	45	7	.140	.381	Fits $\beta = 1.0$
4.5-13	42	13	.025	.297	Fits $\beta = 1.0$
4.5-14	11	4	.080	.494	Fits $\beta = 1.0$
4.5-15	22	11	.250	.323	Fits $\beta = 1.0$
4.5-16	22	13	.040	.297	Fits $\beta = 1.0$
4.5-17	22	15	.090	.276	Fits $\beta = 1.0$
4.5-18	22	14	.060	.274	Fits $\beta = 1.0$
4.5-19	22	11	.090	.323	Fits $\beta = 1.0$
4.5-20	22	16	.190	.258	Fits $\beta = 1.0$
4.5-21	22	10	.250	.322	Fits $\beta = 1.0$

types would follow the same distribution. There was no evidence in the literature that any discrete semiconductor part types should differ from those with available times-to-failure. Furthermore, the part types analyzed represent a diverse cross-section of all part types, since they include both FET and Bipolar devices and members from the transistor, diode, and optoelectronic groups.

5.0 ANALYSIS RESULTS

This section presents the model development and data analysis results. The section is divided into seven subsections, each addressing a unique discrete semiconductor group or application as follows:

5.1 Low Frequency Diodes
5.2 Low Frequency Transistors
5.3 Thyristors
5.4 High Frequency Diodes
5.5 High Frequency Transistors
5.6 Optoelectronics
5.7 Nonoperating Failure Rates

Within each subsection, the final proposed failure rate prediction model is presented first, followed by a detailed discussion of the analysis process by which it was obtained.

5.1 LOW FREQUENCY DIODES

The methodology discussed in Section 4.0 was implemented to develop a failure rate prediction model for low frequency diodes. In contrast to the current MIL-HDBK-217E groupings, all low frequency diodes are in one group for improved model utility. Diode types include:

Switching diodes
Analog diodes
Power rectifiers
High voltage rectifiers
Fast recovery diodes
Schottky rectifier diodes
Current regulator diodes
Voltage reference diodes
Voltage regulator diodes
Varistors (transient suppressors)

5.1.1 Low Frequency Diode Failure Rate Prediction Models

This section presents the failure rate prediction models developed for low frequency diodes. The models are presented in Appendix A in a form compatible with MIL-HDBK-217E.

The final failure rate prediction model for low frequency diodes is a function of device style, temperature, voltage stress, contact construction, screen level, package hermeticity and application environment:

$$\lambda_p = \lambda_b \pi_S \pi_C \pi_Q \pi_T \pi_E$$

where

λ_p = predicted diode failure rate (failures/10^6 operating hours)

λ_b = base failure rate (failures/10^6 operating hours)
= .0038, analog
= .0023, switching
= .069, fast recovery
= .011, power rectifier diodes including schottky power diodes
= .019/junction, power rectifier HV stack
= .0047, voltage regulator, voltage reference
= .0013, transient suppressor diode, varistors
= .0034, current regulator

π_S = voltage stress factor

= 1.0 current regulator, voltage reference, voltage regulator, transient suppressors, varistors

$$= .054 \quad \left(\text{for } \frac{V_R \text{ applied}}{V_R \text{ rated}} \leq .3\right)$$

$$= \left(\frac{V_R \text{ applied}}{V_R \text{ rated}}\right)^{2.43} \quad \left(\text{for } \frac{V_R \text{ applied}}{V_R \text{ rated}} > .3\right)$$

where

V_R = diode reverse voltage (volts)

π_C = contact construction factor
= 1.0, metallurgically bonded
= 2.0, non-metallurgically bonded (spring loaded contacts)

π_Q = quality factor
= .7, JANTXV
= 1.0, JANTX
= 2.4, JAN
= 5.5, Lower
= 8.0, Plastic

π_T = temperature factor

$$= \exp\left(-\frac{E_a}{K}\left(\frac{1}{T_j + 273} - \frac{1}{298}\right)\right)$$

where

T_j = junction temperature (^oC)

$\frac{E_a}{K}$ = equivalent activation energy divided by Boltzman's constant

= 3091, Si analog, switch, fast recovery rectifier and power rectifiers, and HV stack diodes

= 4914, Ge analog, switch, fast recovery, rectifier/power, and HV stack diodes

= 1718, voltage reference and voltage regulator diodes

= 1925, current regulator diodes

= 3810, varistors, transient suppressor diodes

π_E = environment factor

= 1.0, GB	= 30, AIA
= 1.6, GMS	= 28, AIF
= 5.5, GF	= 20, AUC
= 17, GM	= 20, AUT
= 13, MP	= 20, AUB
= 8.0, NSB	= 45, AUA
= 9.5, NS	= 41, AUF
= 19, NU	= 1.0, SF
= 19, NH	= 12, MFF
= 19, NUU	= 16, MFA
= 24, ARW	= 30, USL
= 13, AIC	= 33, ML
= 13, AIT	= 320, CL
= 13, AIB	

5.1.2 Diode Model Development

The failure rate prediction model for diodes was developed by hypothesizing a theoretical model based upon the results of the literature search and by empirical data analysis using stepwise multiple linear regression to quantify model parameters.

As a first step, application and construction parameters which could potentially impact failure rate were identified from the literature and are presented in Table 5.1-1. Parameter values were determined whenever possible for all data records in the diode database. If sufficient detail could not be determined, then the data record was not used in the analysis. Table 5.1-2 summarizes the diode field failure data collected.

The next step in the model development process was the development of a theoretical model in which factors having the most significant effect on diode failure rates were identified based upon published physics of failure data and information (Ref. 8,24,36,46,47). Only factors available to potential failure rate prediction model users were included.

These factors were determined to be junction temperature, electrical stress, maximum electrical ratings, screen class, package hermeticity, application environment and contact construction.

The resulting theoretical model for all low frequency diodes follows:

$$\lambda_p = \lambda_b \, \pi_S \, \pi_r \, \pi_C \, \pi_Q \, \pi_T \, \pi_E$$

where

λ_p = predicted diode failure rate

λ_b = base failure rate
= f_1(device style, application)

π_S = electrical stress factor
= f_2(stress)

TABLE 5.1-1. DIODE CHARACTERIZATION VARIABLES

I. Device Style
   1. Switching Diode
   2. General Purpose Diode
   3. Rectifier
   4. High Voltage Rectifier
   5. Power Rectifier/Schottky Power Diodes
   6. Fast Recovery
   7. Voltage Regulator Diode
   8. Voltage Reference Diode
   9. Current Regulator Diode
   10. Transient Suppressor Diode/Varistor

II. Semiconductor Material

III. Package Type (Drawing Number)

IV. Contact Construction
   A. Metallurgically Bonded
   B. Nonmetallurgically Bonded
   C. Whisker
   D. Stud
   E. Point
   F. Ribbon

V. Maximum Electrical Ratings
   A. Power
   B. Current
   C. Voltage

VI. Applied Electrical Stress
   A. Power
   B. Current
   C. Voltage

VII. Screening Level

VIII. Package Hermeticity

IX. Temperature
   A. Actual Junction
   B. Rated Junction

X. Device Thermal Resistance

XI. Application Environment

TABLE 5.1-2. DIODE FIELD DATA

Diode Type	Quality Level	Environment	Failures	Part Hours ($\times 10^6$)
Switching	Lower	GB	2	83.56
	JANTX	NSB	6	2.61
	JANTX	AIC	1	14.98
	JANTX	AIT	2	18.84
	JANTX	AIB	0	3.98
	JANTX	AIA	1	3.53
	JANTX	AIF	11	8.01
	JANTX	AUC	13	286.87
	JANTX	AUT	11	187.90
	JANTX	AUB	3	77.35
	JANTX	AUA	7	68.68
	JANTX	AUF	29	160.60
Rectifier	Lower	GB	426	7567.77
	JANTX	NSB	3	1.16
	JANTX	NSB	2	12.00
	JANTX	AIC	1	4.28
	JANTX	AIF	2	4.14
	JANTX	AUC	18	72.78
	JANTX	AUT	8	37.30
	JANTX	AUA	4	17.17
	JANTX	AUF	7	28.88
Voltage Regulator	Plastic	GB	192	911.65
	JANTX	GF	3	3.36
	JANTX	NSB	1	9.35
	JANTX	AIC	3	8.56
	JANTX	AIT	0	10.76
	JANTX	AIB	0	2.28
	JANTX	AIA	0	2.01
	JANTX	AIF	12	21.17
	JANTX	AUC	7	72.77
	JANTX	AUT	2	46.94
	JANTX	AUB	2	19.93
	JANTX	AUA	2	17.16
	JANTX	AUF	4	28.89

TABLE 5.1-2. DIODE FIELD DATA (CONT'D)

Diode Type	Quality Level	Environment	Failures	Part Hours ($\times 10^6$)
Voltage Reference	Lower	GB	16	232.01
	Plastic	GB	266	2687.66
	JANTX	NSB	0	3.56
	JANTX	AIC	0	.77
	JANTX	AUC	0	10.70
	JANTX	AUT	0	6.90
	JANTX	AUB	1	2.85
	JANTX	AUA	0	2.52
	JANTX	AUF	0	4.25
Current Regulator	Plastic	GB	2	13.54
Varistor	JANTX	AUC	1	2.14
	JANTX	AUT	0	1.38
	JANTX	AUA	1	.51
	JANTX	AUF	5	2.55
		TOTALS	1180	13852.62

π_r = electrical rating factor
= $f_3(i_{rated})$

π_C = contact construction factor

π_Q = quality factor
= f_4(screen level, hermeticity)

π_T = temperature factor

$$= \exp(-\frac{E_a}{K}(\frac{1}{T_j}))$$

where

E_a = equivalent activation energy
K = Boltzman's constant
T_j = device junction temperature (^oK)

π_E = environment factor

Applying regression analysis, the base failure rate was determined as a function of device style and application. A separate base failure rate was determined empirically for each diode style.

The final temperature factor was of the following form

$$\pi_T = \exp(-\frac{E_a}{K}\ (\frac{1}{T_j + 273}\ -\ \frac{1}{T_r}))$$

where

E_a = equivalent activation energy
= f_5(device style, materials)

K = Boltzman's constant
= 8.63×10^{-5} eV/^oK

T_j = junction temperature (^oC)

T_r = reference temperature = 298^oK

This temperature factor form was assumed for all diodes as discussed in Section 4.4. The reference temperature was added for convenience (such that π_T = 1 at 25°C) and has no impact on model validity. As a result of the literature search, it was observed that diode high temperature life testing performed after 1978, when the last models were developed, was dominated by the testing of high frequency diodes. Because of the lack of new information, previous MIL-HDBK-217E temperature factors for low frequency diodes were assumed. These values were checked against estimates made from the field data. This approach was possible for two reasons:

(1) Predominant changes in diode technology since 1978 have not been in the area of low frequency diodes, therefore the current temperature factors for low frequency devices are expected to remain representative.

(2) A wide range of ambient temperatures were available for these devices. Additionally, values for device thermal resistance and applied electrical stresses could often be accurately determined or estimated, allowing for a high confidence estimate device junction temperature in field devices.

Recent life test data was available for varistor transient suppressor diodes (Ref. 24) and is presented in Table 5.1-3. The varistor activation energy was determined from this data by performing regression analysis with $\ln(\lambda)$ as the dependent variable and $\frac{1}{T_j}$ as the independent variable. This resulted in a slope (i.e., activation energy divided by Boltzman's constant) of 3810.

TABLE 5.1-3. TRANSIENT SUPPRESSOR (VARISTOR) LIFE TEST DATA

Junction Temperature (°C)	Failure Rate (failures/10^6 hours)
100	63
125	158
150	562
125	56
100	18
145	631
125	126
100	13

The previous MIL-HDBK-217E activation energy for Si general purpose (GP) diodes is .27eV, for Ge general purpose diodes is .42eV, and for zener diodes (voltage regulator/voltage reference) is .15eV. There was no recent data for Ge general purpose diodes, therefore the current activation energy was retained. The current value for Si general purpose diodes was checked against the value obtained from field failure data. The activation energy value resulting from the data analysis is .10 with lower and upper 95% confidence bounds of -.02 and .19 respectively. Although the current value did not lie within this interval, it was retained since it is reasonably close to the value, particularly since the range of junction temperatures from the field data was relatively limited as compared with typical life test temperatures. The current MIL-HDBK-217E activation energy for zener diodes is .15eV, which compared favorably to the value of .12eV estimated from the field data. Lower and upper 95% confidence bounds were -.03 and .28eV.

There was no life test data and insufficient field data available to determine an activation energy for current regulator diodes, for which there was also no previous MIL-HDBK-217E model. However, since a current regulator diode is essentially a field effect transistor with gate and source connected, the MIL-HDBK-217E FET activation energy was assumed as a best estimate.

Electrical stress was expected to have a significant effect on predicted diode failure rate, since the effects of derating are well documented. It was thus imperative that a stress factor be examined in a failure rate prediction model development process. Based upon derating guidelines (Ref. 37,46), reverse voltage and forward current stresses were examined for switching diodes, rectifiers and transient suppressors; and power dissipation for voltage reference and regulator diodes. These electrical stress variables represent stress factor model inputs. An electrical stress factor was significant for all diodes except voltage reference and voltage regulator diodes. No stress data or information was

available for current regulators. Additionally, no stress factor was applied to transient suppressors.

The maximum rated electrical parameters factor was also included in the diode theoretical model. Device absolute maximum voltage, current, and power ratings are not to be exceeded under any conditions. The designer has the responsibility of determining an average design value for each device rating by using a safety factor that assures that the absolute values will never be exceeded. Logically, one might say that devices with higher electrical ratings are able to withstand higher electrical levels, thereby having an inverse relationship with failure rate. However, in practice, high power devices are generally put in more demanding applications. Additionally, the higher electrical levels a design requires, the less room there is for derating. In general, based upon past experience and on the data gathered for this effort, devices at the upper end of commercially available electrical parameter levels are stressed at higher levels than other devices. Rated current was chosen for the maximum rated parameter analysis subsequent to the examination of diode failure mechanisms, distributions and accelerating stresses compiled from the composite of the literature, including recent RADC sponsored studies (Ref. 9,24,48,49). Additionally, the previous MIL-HDBK-217E Group IV models contain a rated current factor as a precedent. As a result of the regression analysis, rated current was not found to be a significant factor. Since the diode data provided a wide range of the maximum rated average forward current variable (.001 to 250 Amperes), and since there may be some correlation between the effects of stress and electrical rating level on failure rate as discussed above, rated current factor was not included in the prediction model.

Application environment and device quality were expected to be significant factors and were quantified for diodes as described in Sections 4.5 and 4.6. As in the past, screening effects and package hermeticity were maintained in a single factor.

Device contact construction was also investigated as a potential model input parameter. Correlation between contact construction and failure rate in our dataset was very low (.036), and the resulting factor when forced into a regression was very small (1 to 1.17). However, upon examination of the dataset with respect to this variable, it was observed that the data was not balanced. The metallurgically bonded data far outweighed the non-metallurgically bonded data, and a positive conclusion based upon the analysis results was not possible. Therefore, the previous factor of 1 for metallurgically bonded and 2 for non-metallurgically bonded was retained.

5.2 LOW FREQUENCY TRANSISTORS

Failure rate prediction models for low frequency bipolar, field effect, and unijunction transistors were successfully developed according to the modeling methodology described in Section 4.0.

5.2.1 Transistor Failure Rate Prediction Models

This section presents the failure rate prediction models developed for low frequency transistors. The models are presented in a form compatible with MIL-HDBK-217E in Appendix A.

The unijunction transistor failure rate prediction model was found to be a function of junction temperature, screen level, package hermeticity and application environment:

$$\lambda_p = \lambda_b \pi_Q \pi_T \pi_E$$

where

λ_p = predicted component failure rate (failures/10^6 operating hours)

λ_b = base failure rate (failures/10^6 operating hours)
= .0083

π_Q = quality factor
= .7, JANTXV
= 1.0, JANTX
= 2.4, JAN
= 5.5, Lower
= 8.0, Plastic

π_T = temperature factor

$$= \exp\left[-2483\left(\frac{1}{T_j + 273} - \frac{1}{298}\right)\right]$$

where

T_j = junction temperature (^oC)

π_E = environment factor (see Table 5.2-1)

TABLE 5.2-1. TRANSISTOR ENVIRONMENTAL FACTOR

Environment	π_E	Environment	π_E
GB	1.0	AIA	30
GMS	1.6	AIF	28
GF	5.5	AUC	20
GM	17	AUT	20
MP	13	AUB	20
NSB	8.0	AUA	45
NS	9.5	AUF	41
NU	19	SF	1.0
NH	19	MFF	12
NUU	19	MFA	16
ARW	24	USL	30
AIC	13	ML	33
AIT	13	CL	320
AIB	13		

The Si FET transistor model was determined to be a function of technology (MOSFET vs JFET), channel temperature, component complexity, circuit application, screen level, package hermeticity and application environment:

$$\lambda_p = \lambda_b \pi_A \pi_Q \pi_T \pi_E$$

where

λ_p = predicted failure rate (failures/10^6 operating hours)

λ_b = base failure rate (failures/10^6 operating hours)
= .012, MOSFET
= .0048, JFET

π_A = application factor
= 1.5, linear
= .7, switch
= 5.0, high frequency (> 400 MHz and average power < 300 mW)
= 10.0, power FET (average power > 250 W)

π_Q = quality factor
= .7, JANTXV
= 1.0, JANTX
= 2.4, JAN
= 5.5, Lower
= 8.0, Plastic

π_T = temperature factor

$$= \exp\left[-1925\left(\frac{1}{T_j + 273} - \frac{1}{298}\right)\right]$$

where

T_j = channel temperature

π_E = environmental factor (see Table 5.2-1)

The model for bipolar transistors was found to be a function of junction temperature, voltage stress, rated power, component complexity, circuit application, screen level, package hermeticity and application environment:

$$\lambda_p = \lambda_b \pi_S \pi_r \pi_A \pi_Q \pi_T \pi_E$$

where

λ_p = predicted component failure rate (failures/10^6 operating hours)

λ_b = base failure rate (failures/10^6 operating hours)
= .00074

π_S = voltage stress factor
= .045 exp(3.1 (V_{CE} applied/V_{CE} rated))

where

V_{CE} = collector-to-emitter voltage (volts)

π_r = power rating factor
= 0.43, $P < .1W$
= $(P)^{0.37}$, $P \geq .1W$

where

P = rated power (watts)

π_A = application factor
= 1.5, linear
= .7, switch

π_Q = quality factor
= .7, JANTXV
= 1.0, JANTX
= 2.4, JAN
= 5.5, Lower
= 8.0, Plastic

π_T = temperature factor

$$= \exp[-2114(\frac{1}{T_j + 273} - \frac{1}{298})], \text{ Si}$$

$$= \exp[-3521(\frac{1}{T_j + 273} - \frac{1}{298})], \text{ Ge}$$

π_E = environment factor (see Table 5.2-1)

5.2.2 Low Frequency Transistor Model Development

Failure rate prediction models for unijunction, bipolar, and Si FET transistors were developed by hypothesizing a theoretical model based on the results of the literature search and intuitive reliability relationships and by statistical analysis of empirical component failure data to quantify model parameters.

As a first step, application and construction variables which characterize transistors and could potentially impact failure rate were identified and are presented in Table 5.2-2. These factors were determined whenever possible for transistor data collected. Data points with insufficient detail were excluded from the analysis. Tables 5.2-3 through 5.2-5 summarize the unijunction, bipolar and field effect transistor field data collected.

TABLE 5.2-2. TRANSISTOR CHARACTERIZATION VARIABLES

I. Device Style
   A. bipolar
   B. FET
   C. unijunction

II. Semiconductor Material

III. Structure/Type
   A. NPN vs. PNP
   B. JFET vs. MOSFET
   C. N-Channel vs. P-Channel

IV. Power Rating

V. Electrical Stress

VI. Circuit Application

VII. Quality Level

VIII. Duty Cycle

IX. Junction Temperature

X. Device Thermal Resistance

XI. Application Environment

XII. Complexity

XIII. Package Type (Drawing Number)

TABLE 5.2-3. UNIJUNCTION TRANSISTOR FIELD DATA SUMMARY

Quality Level	Environment	Failures	Part Hrs ($\times 10^6$)
JANTX	Ground Fixed	0	.14
Plastic	Ground Benign	19	62.64
JANTX	AUF	0	.85
JANTX	AUC	0	2.14
JANTX	AUT	0	1.38
JANTX	AUB	0	.57
JANTX	AUA	0	.51
TOTALS		19	68.23

TABLE 5.2-4. BIPOLAR TRANSISTOR FIELD DATA SUMMARY

Style	Environment	Quality	Failures	Part Hrs ($\times 10^6$)
Single Transistor, PNP, <5W	GB	Plastic	2214	24278.35
	GF	JANTX	0	1.19
	AIC	JANTX	1	4.28
	AIT	JANTX	0	5.38
	AIB	JANTX	0	1.14
	AIA	JANTX	0	1.01
	AIF	JANTX	49	14.56
	AUC	JANTX	26	164.23
	AUT	JANTX	12	100.03
	AUB	JANTX	4	43.86
	AUA	JANTX	15	31.11
	AUF	JANTX	9	62.61
Single Transistor, NPN, <5W	GF	JANTX	9	1230.18
	NSB	JAN	0	5.69
	NSB	JANTX	3	45.53
	AIC	JANTX	1	20.70
	AIT	JANTX	0	13.46
	AIB	JANTX	1	2.84
	AIA	JANTX	0	2.52
	AIF	JANTX	12	27.09
	AUC	JANTX	142	201.17
	AUT	JANTX	24	128.21
	AUB	JANTX	12	51.03
	AUA	JANTX	18	46.89
	AUF	JANTX	24	70.04
Single Transistor, PNP, ≥5W	GB	Plastic	19	36.28
	GF	JANTX	0	.07
	NSB	JAN	0	.35
	NSB	JANTX	3	3.20
	AIF	JANTX	19	1.55
	AUC	JANTX	4	12.84
	AUT	JANTX	4	8.29
	AUB	JANTX	2	3.41
	AUA	JANTX	2	3.02
	AUF	JANTX	1	5.09

TABLE 5.2-4. BIPOLAR TRANSISTOR FIELD DATA SUMMARY (CONT'D)

Style	Environment	Quality	Failures	Part Hrs ($x10^6$)
Single Transistor, NPN, ≥5W	GF	JANTX	0	.07
	NSB	JAN	0	.70
	NSB	JANTX	0	2.31
	AIC	JANTX	0	2.14
	AIT	JANTX	0	2.60
	AIB	JANTX	0	.57
	AIA	JANTX	0	.50
	AIF	JANTX	23	3.61
	AUC	JANTX	32	38.52
	AUT	JANTX	7	24.85
	AUB	JANTX	11	10.24
	AUA	JANTX	4	9.08
	AUF	JANTX	12	17.05
Dual Transistor	GF	JANTX	0	.28
	AIF	JANTX	1	.28
	NSB	JANTX	0	6.49
Darlington	AUC	JANTX	22	32.07
	AUT	JANTX	15	16.70
	AUB	JANTX	1	10.23
	AUA	JANTX	7	7.56
	AUF	JANTX	12	10.02
	TOTALS		2776	26804.23

TABLE 5.2-5. FIELD EFFECT TRANSISTOR FIELD DATA SUMMARY

Type	Environment	Quality	Failures	Part Hrs ($x10^6$)
JFET	GB	Plastic	843	5088.75
JFET	GF	Lower	0	.14
	NSB	JANTX	0	1.87
	AIF	JANTX	16	5.44
	AUC	JANTX	10	32.11
	AUT	JANTX	4	20.72
	AUB	JANTX	0	8.52
	AUA	JANTX	2	7.57
	AUF	JANTX	3	12.69
MOSFET	GB	Plastic	209	431.77
	TOTALS		1087	5609.58

The next step in the model development process was the compilation of a theoretical model, comprising the factors from Table 5.2-2 which were determined to have the most significant effect on component failure rate. Only factors which are readily available to prediction model users are included. The form of the various factors (i.e., additive, multiplicative, etc.) was chosen based upon findings of the literature search and established reliability relationships (Ref. 24,47).

The theoretical model for unijunction transistors follows:

$$\lambda_p = \lambda_b \pi_S \pi_r \pi_Q \pi_T \pi_E$$

where

λ_p = predicted unijunction transistor failure rate (failures/10^6 operating hours)

λ_b = base failure rate

π_S = electrical stress factor

π_r = maximum electrical rating factor

π_Q = quality factor = f(screen level, package hermeticity)

π_T = temperature factor

$$= \exp\left(\frac{-E_a}{K}\left(\frac{1}{T_j}\right)\right)$$

where

E_a = equivalent activation energy
K = Boltzman's constant
T_j = component junction temperature (^oK)

π_E = environment factor

The theoretical model for bipolar transistors follows:

$$\lambda_p = \lambda_b \pi_S \pi_r \pi_C \pi_A \pi_Q \pi_T \pi_E$$

where

λ_p = predicted bipolar transistor failure rate (failures/10^6 operating hours)

λ_b = base failure rate
= f_1(NPN vs. PNP)

π_S = voltage stress factors
= $C_1 \exp(C_2(\frac{V_{CE\ applied}}{V_{CE\ rated}}))$, C_1, C_2 = constants

π_r = power rating factors
= (rated power)^n, n = constant

π_C = complexity factor
= f_3(component complexity)

π_A = application factor
= A_1, linear
= A_2, switch
= A_3, low noise RF

π_Q = quality factor
= f_4(screen level, package hermeticity)

π_T = temperature factor
= $\exp(\frac{-E_a}{K}(\frac{1}{T_j}))$

where

E_a = activation energy
= f_2(semiconductor material)
K = Boltzman's constant
T_j = component junction temperature (^oK)

π_E = environment factor

The theoretical model for Si Field Effect Transistors (FET) is:

$$\lambda_p = \lambda_b \pi_S \pi_r \pi_d \pi_C \pi_A \pi_Q \pi_T \pi_E$$

where

λ_p = predicted component failure rate (failures/10^6 operating hours)

λ_b = base failure rate
= f_1(MOSFET vs. JFET)

π_S = stress factor
= $C_1 \exp(C_2(\frac{V_{CE\ actual}}{V_{CE\ rated}}))$

π_r = power rating factor

π_d = channel doping factor
= f_2(N-channel vs. P-channel)

π_C = complexity factor
= f_3(device complexity)

π_A = application factor
= A_1, linear
= A_2, switch
= A_3, low noise RF
= A_4, power

π_Q = quality factor
= f_4(screen level, package hermeticity)

π_T = temperature factor

$$= \exp\left(\frac{-E_a}{K}\left(\frac{1}{T_j}\right)\right)$$

where

E_a = equivalent activation energy
K = Boltzman's constant
T_j = component channel temperature (^oK)

π_E = environment factor

The quality and environment factors for unijunction, Si FET, and low frequency bipolar transistors were developed according to the methodologies described in Sections 4.5 and 4.6.

Temperature factors for all transistor types were developed according to the methodologies described in Section 4.2. No recent high temperature life test data/activation energies were located for unijunction transistors. Thus, the current MIL-HDBK-217E temperature factor was assumed. In doing so, a transformation (described in Section 4.4) was performed on the "N_T" constant in Table 5.1.3-2 of MIL-HDBK-217E for agreement with the new form of the temperature factor.

The high temperature life test data collected for Si FETs is listed in Table 5.2-6. The data was insufficient to determine a new temperature

factor, since testing at only one temperature for low power and one temperature for high power devices was available. The current MIL-HDBK-217E equivalent activation energy (.17eV) was therefore assumed for Si FETs. This value compared favorably with estimates made from field data points where reasonable approximations for junction temperature could be made. The activation energy estimated from the field data was .15eV with lower and upper 95% confidence bands of -.03 and .33eV.

TABLE 5.2-6. LOW FREQUENCY TRANSISTOR HIGH TEMPERATURE LIFE TEST DATA

Device Type	Junction/Channel Temperature (^{o}C)	Failures	Part Hours ($x10^{6}$)
FET, Si, <5W	191	24	.44
FET, Si, >5W	200	9	.12
FET, Si, 90W	200	3	.12
FET, Si, 125W	200	2	.12
FET, Si, 150W	200	5	.25
FET, Si, 6W	200	5	.128
FET, Si, 12.5W	200	6	.127
FET, Si, 5W	200	1	.125
Bipolar	131	1	.17
	191	6	.13
	291	14	.10

High temperature life test data collected for low frequency (<200MHz) Si bipolar transistors is listed in Table 5.2-6. The data corresponds to an activation energy of .45 eV. However, since this value was based upon limited data, the geometric mean of the current MIL-HDBK-217E equivalent activation energies for Si NPN and PNP silicon bipolar transistors, .18 eV, was compared to the upper and lower 95% confidence intervals of the activation energy estimated from field data, which were 2.0 and -1.14. Since the current factor lies within this interval, it was decided to retain the current factor because the new data could not

disprove this value. The geometric mean of the values for NPN and PNP were used since there is little physical evidence that a meaningful difference exists and because polarity was examined as part of the base failure rate in the theoretical model. The modeling was performed with the polarity factor in both the base failure rate and in the temperature factor, and the best fit was chosen as a final model.

There was no new high temperature life test/activation energy data available for Ge bipolar transistors and insufficient data to make estimations from field data, thus, the current MIL-HDBK-217E activation energy was assumed correct. Again the geometric mean of the NPN and PNP activation energies was used.

The polarity factor for bipolar transistors was defined as part of the base failure rate in the theoretical model. In the current MIL-HDBK-217E model, different base failure rates are provided for NPN and PNP devices; however, upon closer examination, there was only a small numerical difference. The data analysis for this study was inconclusive regarding polarity. It was decided, however, to propose a single base failure rate for both NPN and PNP devices.

Despite many efforts to collect circuit application information for the low frequency transistor data, it was generally unattainable. The current MIL-HDBK-217E factors for both FET and bipolar devices were thus retained. The bipolar transistor model presented in Section 5.2.1 included an application factor for Si low noise RF devices. The collected data and model development activities for these devices are presented in Section 5.5 of this report. The failure rate predictions for these devices are grouped with other bipolar transistors for convenience.

The benefits of electrical parameter derating on semiconductor components are well documented (Ref. 37,46). Electrical stress was considered an important factor in the FET and Bipolar transistor theoretical models. Data collected on the ARN-118 was complemented with a

part stress MIL-HDBK-217E failure rate prediction performed on that same equipment. Voltage stress level (i.e., Applied V_{CE}/Rated V_{CE}) data was thus available for the individual bipolar transistors in that equipment, resulting in a highly significant voltage stress factor for high power ($\geq$5W) bipolar transistors. Voltage stress was not found to be a significant factor for low power bipolar transistors. However, from a theoretical perspective, derating should also benefit low power devices and the voltage stress factor was applied to all bipolar transistor devices. It was hypothesized that the low failure rates (and the associated higher failure rate variability) of low power transistors prevented validation or confirmation of the stress factor developed from the high power devices.

Despite many attempts, insufficient data was available to determine an electrical stress factor for Si FETs. Additionally, insufficient electrical stress and maximum rating information was available for the unijunction transistor data collected. However, since these devices are relatively simple devices, the addition of two more factors may have overly complicated the model.

Data was available on single device complexity Si FETs only. Thus, the current MIL-HDBK-217E complexity factor could neither be adjusted nor refuted. One data point was collected for a dual bipolar transistor; however, this data point was a gross outlier and was deleted from the analysis. Approximately 76 x 10^6 part hours were collected for bipolar darlington transistors. The factor resulting from this data supported the current MIL-HDBK-217E complexity factor for bipolar transistors. However, since one of the main thrusts of this effort was to eliminate unrealistic implied precision in the models, and the range of the present complexity factor is so small, this factor was deleted from both the FET and bipolar transistor models.

Si FET field data was collected on devices with rated power ranging to 5 Watts, making it impossible to address power FETs by analysis of field

data. Operating life test data at 200°C junction temperature on 5W to 150W VMOS and VDMOS devices was previously presented in Table 5.2-6. Since test conditions were carefully selected so as to avoid causing failure mechanisms not indicative of normal long term usuage, the reported failure rates of the device on test were examined for a relationship between failure rate and rated power by means of regression analysis. The data showed no relation between failure rate and rated power, thus a factor could not be applied to the model based on this data.

Since power FETs are being used at low frequencies at power levels beyond that found in the data, it was decided to assume an application factor for power FETs based on physical similarities to bipolar transistors. Rated power was a highly significant variable for bipolar transistors and is included in the final model form for these devices. An application factor (π_A) for high power ($\geq$250 watt) FETs was determined based on this relationship, since FETs are expected to be at least as sensitive to power as bipolar devices. A factor of 10.0 was computed for a power rating of 500 watts. This is, of course, an approximate value but it is recommended that it be included in the FET model because it improves the usability of the models for equipments with power FETs.

5.3 THYRISTORS (SCRs)

Failure rate prediction models were successfully developed for thyristors according to the methodology described in Section 4.0. The proposed thyristor model is now in a separate section for handbook uniformity; since two layer (diode) and three layer (transistor) devices are segregated, it follows that four layer (thyristors) devices should also be segregated.

5.3.1 Thyristor Failure Rate Prediction Models

This section presents the final form of the proposed failure rate prediction models for thyristor devices. The model is presented in a form

compatible with MIL-HDBK-217E in Appendix A. The proposed model is a function of junction temperature, blocking voltage stress, rated forward current (RMS), screen level, package hermeticity and application environment.

$$\lambda_p = \lambda_b \pi_S \pi_r \pi_Q \pi_T \pi_E$$

where

λ_p = predicted thyristor (SCR) failure rate (failures/10^6 operating hours)

λ_b = base failure rate (failures/10^6 operating hours)
= .0022

π_S = voltage stress factor

$$= \left(\frac{\text{V blocking applied}}{\text{V blocking rated}}\right)^{1.9}$$

π_r = rated current factor (for $0 \leq I_f \leq 175$ amps)

$= (I_f(\text{rms}))^{.40}$, I_f = rated forward current (amps)

π_Q = quality factor
= .7, JANTXV
= 1.0, JANTX
= 2.4, JAN
= 5.5, Lower
= 8.0, Plastic

π_T = temperature factor

$$= \exp\left(-3082\left(\frac{1}{T_j + 273} - \frac{1}{298}\right)\right)$$

π_E = environment factor

= 1.0, GB	= 30, AIA
= 1.6, GMS	= 28, AIF
= 5.5, GF	= 20, AUC
= 17, GM	= 20, AUT
= 13, MP	= 20, AUB
= 8.0, NSB	= 45, AUA
= 9.5, NS	= 41, AUF
= 19, NU	= 1.0, SF
= 19, NH	= 12, MFF
= 19, NUU	= 16, MFA
= 24, ARW	= 30, USL
= 13, AIC	= 33, ML
= 13, AIT	= 320, CL
= 13, AIB	

5.3.2 Thyristor Model Development

Failure rate prediction models for thyristors were developed by hypothesizing a theoretical model based on the results of the literature search and intuitive reliability relationships, and by statistical analysis of empirical component failure data to quantify model parameters.

Application and construction variables identified as a result of the literature search that could potentially impact thyristor failure rate are presented in Table 5.3-1. These factors were determined wherever possible for all thyristor data collected. Only one reference (Ref. 51) was located, which specifically addressed thyristor failure mechanisms. This reference was also the source for the life test data presented in Table 5.3-2. Basically, thyristors were assumed to be susceptible to failure modes and mechanisms common to other semiconductor junction devices. Table 5.3-3 summarizes the thyristor field data collected.

TABLE 5.3-1. THYRISTOR CHARACTERIZATION VARIABLES

I. Rated Forward Current (RMS)
II. Electrical Stress
III. Duty Cycle
IV. Junction Temperature
V. Device Thermal Resistance
VI. Quality Level
VII. Application Environment
VIII. Package Type

TABLE 5.3-2. THYRISTOR LIFE TEST DATA

Failure Rate (Failures/10^6 Hours)	Junction Temperature (^oC)	Voltage Stress ($\frac{V\ Block\ Applied}{V\ Block\ Rated}$)
.0026	373	.25
.0042	373	.50
.0057	373	.75
.0085	373	1.00
.0011	348	.25
.0016	348	.50
.0019	348	.75

TABLE 5.3-3. THYRISTOR FIELD DATA

Failures	Part Hours ($x10^6$)	Rated Current (I (rms)) (amps)	Environment	Quality Level
31	218.30	2.0	G_B	Plastic
24	304.54	8.0	G_B	Plastic
44	179.96	12.5	G_B	Plastic
4	2.55	1.6	G_B	Plastic
4	3.05	110.	G_B	Plastic
3	47.46	10.0	G_B	Plastic
1	5.66	.2	G_B	Plastic
3	36.65	.8	G_B	Plastic
2	9.75	5.0	G_B	Plastic
19	6.96	175.0	G_B	Plastic
4	51.78	.8	G_B	Plastic
28	88.53	5.0	G_B	Plastic
27	38.82	40.0	G_B	Plastic
0	8.28	30.0	G_B	Plastic
7	1.01	100.0	A_{UA}	JANTX
2	1.14	100.0	A_{UB}	JANTX
16	2.76	100.0	A_{UT}	JANTX
8	1.70	100.0	A_{UF}	JANTX
18	4.28	100.0	A_{UC}	JANTX

The next step in the model development process was the compilation of a theoretical model, comprised of the factors in Table 5.3-1 that were determined to have a significant effect on thyristor failure rate. Factors which would be available to prediction model users are included. The model is given by,

$$\lambda_p = \lambda_b \pi_S \pi_r \pi_Q \pi_T \pi_E$$

where

λ_p = predicted thyristor failure rate (failures/10^6 operating hours)

λ_b = base failure rate

π_r = rated current factor
= (rated forward current (RMS))^n, n = constant

π_S = voltage stress factor

$$= \left(\frac{\text{V blocking applied}}{\text{V blocking rated}}\right)^m, \text{ m = constant}$$

π_Q = quality factor

π_T = temperature factor

$$= \exp\left(-\frac{E_a}{K}\left(\frac{1}{T_J}\right)\right)$$

where

E_a = equivalent activation energy
K = Boltzman's constant
T_j = device junction temperature (^oK)

π_E = environment factor

The quality and environment factors for thyristors were developed according to the methodologies described in Sections 4.5 and 4.6. Multiple linear regression analysis was performed against the life test data presented in Table 5.3-2 to determine a voltage stress and temperature factors. Both voltage stress and temperature were highly significant variables at a greater than 90% significance level. As with other device types where an estimate of activation energy from data was available, the current MIL-HDBK-217E temperature acceleration factor (.27eV) was compared with the upper and lower 95% confidence level of the value estimated from the life test data. The temperature factor obtained directly from the data was:

$$\pi_T = \exp\left(-8371\left(\frac{1}{T_j + 273} - \frac{1}{298}\right)\right)$$

which corresponds to an activation energy of .72eV. Lower and upper confidence bounds are .64 and .80. The current MIL-HDBK-217E value of .27eV was not overruled for two reasons: First, life test data consistently results in higher activation energies than are seen in the field, and third, the test data for thyristors was available at only two temperatures and thus, inconclusive.

A factor for rated forward current (RMS) was obtained from regression analysis of the field data presented in Table 5.3-3. Although this factor was only significant at a 30% significance level, this was not sufficient

rationale to reject the current MIL-HDBK-217E factor. Additionally, maximum electrical rating was determined to be an important factor for semiconductor junction devices in general as a result of the literature search.

5.4 HIGH FREQUENCY (RF, MICROWAVE, MILLIMETER WAVE) DIODES

The category of high frequency diodes includes several unique and specialized devices with diverse characteristics. Depending upon their general microwave application, these devices can be thought of in three groups: Generation, Receiving/Detection, and Control of High Frequency Energy. The distribution of high frequency diodes into these groups is shown in Table 5.4-1. In reality, there is some overlap between groups. For example, varactors can function in both voltage control and power multiplier applications. Tunnel and back diodes can be used as detectors and mixers as well as amplifiers. Because of this overlap, care was taken to assure that only one model would describe each diode type. For example, currently there are separate models for detectors/mixers and for tunnel diodes. However, since tunnel diodes can serve as detectors and mixers, some confusion exists. For this reason, a proposed model was developed for each individual microwave diode type, and any application/function information was made a factor in the model where such data was available.

High frequency diodes, although similar in basic operating principles to their low frequency counterparts, have unique construction characteristics which enable them to accomplish specific microwave functions. Variations between diode types include semiconductor material, doping level, etc. There is much variation even within specific diode families. For example, with the IMPATT diodes, there are variations in doping profile, for example Read vs. Non-Read. Within the transferred electron device family there are bulk GUNN GaAs devices, planar epitaxial devices, and planar ion-implanted devices.

TABLE 5.4-1. HIGH FREQUENCY DIODE GROUPS

Power Generation

(Multipliers, Amplifiers and Oscillators)
- Gunn
- Avalanche (IMPATT, TRAPATT)

Receiving, Detecting, and Mixing

(Detecting, Mixing, and Rectifying)
- Schottky Barrier
- Schottky Point Contact
- Tunnel
- Back

Power Control

(Tuning, Attenuation, Limiting, Switching and Phase Shifting)
- PIN
- Varactor
- Step Recovery

Based upon the results of the literature search, data collection effort, and conversations with field experts, it is apparent that high frequency diodes constitute a very specialized and dynamic technology. RF testing of devices is complex and costly, and consequently failure mechanism information is scarce. Based upon these observations, resulting high frequency diode failure rate prediction models are different from the models developed for traditional devices and received much emphasis in this effort. Full-scale prediction models were developed strictly for specific devices represented in the dataset and within the range of variables available, with few generalizations. The models were developed to be easily expandable and updatable as more data and information becomes available.

5.4.1 High Frequency Diode Failure Rate Prediction Models

This section presents the failure rate prediction models developed for high frequency diodes (defined here as 200 MHz operating frequency and greater). The models are presented in Appendix A in a form compatible with MIL-HDBK-217E.

The final model for Si Schottky and Point Contact ($\leq$ 35 GHz operating frequency) microwave diodes is:

$$\lambda_p = \lambda_b \pi_Q \pi_T \pi_E$$

where

λ_p = predicted Schottky barrier and point contact failure rate (failures/10^6 operating hours)

λ_b = base failure rate = .0272 failures/10^6 operating hours

π_Q = quality factor
= .5, JANTXV
= 1.0, JANTX
= 1.75, JAN
= 2.5, Lower

π_T = temperature factor

$$= \exp\left(-1522\left(\frac{1}{T_j + 273} - \frac{1}{298}\right)\right), \; T_j = \text{junction temperature } (^oC)$$

π_E = environmental factor (see Table 5.4-2)

TABLE 5.4-2. HIGH FREQUENCY ENVIRONMENTAL FACTORS

Environment	π_E	Environment	π_E
GB	1	AIA	4.6
GF	2.0	AIF	4.6
GM	4.9	AUC	7.0
MP	4.9	AUT	7.0
NSB	3.6	AUB	7.0
NS	4.7	AUA	12.0
NU	11	AUF	12.0
NH	11	SF	1
NUU	11	MFF	7.5
ARW	16	MFA	11
AIC	3.7	USL	22
AIT	3.7	ML	55
AIB	3.7	CL	250

The final model for Varactor and Step Recovery diodes is:

$$\lambda_p = \lambda_b \pi_A \pi_Q \pi_T \pi_E$$

where

λ_p = predicted Varactor and Step Recovery microwave diode failure rate (failures/10^6 operating hours)

λ_b = base failure rate = .0025 failures/10^6 operating hours

π_A = application factor
= .5, voltage control
= 2.5, multiplier

π_Q = quality factor

$\pi_T = \exp\left(-2100\left(\frac{1}{T_j + 273} - \frac{1}{298}\right)\right)$, T_j = junction temperature (^oC)

π_E = environmental factor (see Table 5.4-2)

The final model for Tunnel/Back Diodes is:

$$\lambda_p = \lambda_b \pi_Q \pi_T \pi_E$$

where

λ_p = predicted Tunnel/Back diode failure rate (failures/10^6 operating hours)

λ_b = base failure rate (failures/10^6 operating hours)
= .0025

π_Q = quality factor
= .5, JANTXV
= 1.0, JANTX
= 5.0, JAN
= 25, Lower

π_T = temperature factor

$$= \exp\left(-2100\left(\frac{1}{T_j + 273} - \frac{1}{298}\right)\right)$$

π_E = environmental factor (see Table 5.4-2)

The final model for Gunn (bulk effect) diodes is:

$$\lambda_p = \lambda_b \pi_Q \pi_T \pi_E$$

where

λ_p = predicted failure rate (failures/10^6 operating hours)

λ_b = base failure rate = .6 failures/10^6 operating hours

π_Q = quality factor
= .5, JANTXV or equivalent
= 1.0, JANTX or equivalent
= 5.0, JAN or equivalent
= 25, Lower

π_T = temperature factor

$$= \exp\left(-2562\left(\frac{1}{T_j + 273} - \frac{1}{298}\right)\right), \quad T_j = \text{junction temperature } (^oC)$$

π_E = environmental factor (see Table 5.4-2)

The final model for Si IMPATT diodes ($\leq$ 35 GHz operating frequency) is:

$$\lambda_p = \lambda_b \pi_Q \pi_T \pi_E$$

where

λ_p = predicted failure rate (failures/10^6 operating hours)

λ_b = base failure rate (failures/10^6 operating hours)
= .2235

π_Q = quality factor
= .5, JANTXV or equivalent
= 1.0, JANTX or equivalent
= 5.0, JAN or equivalent
= 25, Lower

π_T = temperature factor

$$= \exp\left(-5260\left(\frac{1}{T_j + 273} - \frac{1}{298}\right)\right), \quad T_j = \text{junction temperature } (^oC)$$

π_E = environmental factor (see Table 5.4-2)

The final model for PIN diodes is:

$$\lambda_p = \lambda_b \pi_r \pi_Q \pi_T \pi_E$$

where

λ_p = predicted PIN diode failure rate (failure/10^6 operating hours)

λ_b = base failure rate (failures/10^6 operating hours)
= .0148

π_r = power rating factor
= .5, 0 < Rated Power ≤ 10W
= .326(ln(Rated Power)) - .25; 10W < Rated Power < 500W

π_Q = quality factor
= .5, JANTXV
= 1.0, JANTX
= 5.0, JAN
= 25, Lower

π_T = temperature factor

$$= \exp\left(-2100\left(\frac{1}{T_j + 273} - \frac{1}{298}\right)\right), \; T_j = \text{junction temperature } (^oC)$$

π_E = environmental factor (see Table 5.4-2)

5.4.2 High Frequency Diode Model Development

Failure rate prediction models for high frequency diodes were developed by hypothesizing a theoretical model and by analyzing empirical data to quantify model parameters. Factors for temperature were assumed based upon available physics of failure information and high temperature test data. Factors for application environment were based upon universal factors developed from the composite of the databases, described in Section 4.6.

As a first step, application and construction variables which characterize high frequency diodes and could potentially impact failure rate were identified and are presented in Table 5.4-3. These factors were

TABLE 5.4-3. HIGH FREQUENCY DIODE CHARACTERIZATION VARIABLES

I. Device Style

- a. Tunnel
- b. Back
- c. PIN
- e. Schottky Point Contact
- f. Varactor
- g. Gunn (Bulk Effect)
- h. IMPATT
- i. TRAPATT
- j. Step Recovery

II. Semiconductor Material

- a. GaAs
- b. Si
- c. GaP
- d. Ge
- e. InP

III. Package (Drawing number)

IV. Contact Construction

- a. Metallurgically Bonded
- b. Nonmetallurgically Bonded
- c. Whisker
- d. Stud
- e. Point
- f. Ribbon

V. Maximum Electrical Ratings

- a. Power Dissipation
- b. Voltage (Reverse/Breakdown as applicable)
- c. Forward Current

VI. Applied Electrical Stress

- a. Power
- b. Voltage (Reverse/Breakdown as applicable)
- c. Forward Current

VII. Application

- a. Multiplication
- b. Amplification
- c. Oscillator
- d. Receiving
- e. Detecting
- f. Mixing
- g. Rectifying
- h. Tuning
- i. Attenuation
- j. Limiting
- k. Switching
- l. Phase shifting

VIII. Duty Factor/Pulse Width

IX. Screening Level

X. Package Hermeticity

XI. Operating Frequency

XII. Temperature

- a. Actual Ambient
- b. Rated Junction

XIII. Device Thermal Resistance

XIV. Application Environment

determined whenever possible for all data in the failure rate prediction model database. Table 5.4-4 summarizes the high frequency diode field data collected.

TABLE 5.4-4. HIGH FREQUENCY DIODE FIELD DATA SUMMARY

Device Type	Quality Level	Environment	Failures	Part Hrs ($x10^6$)
Si Schottky	JANTX	AUA	0	7.58
	JANTX	AUB	0	8.53
	JANTX	AUT	3	20.72
	JANTX	AUF	2	12.75
	JANTX	AUC	1	32.11
	Unknown	NS	2	16.55
	Unknown	GF	10	31.16
Ge Tunnel	Lower	GB	72	234.45
Varactor	Plastic	GB	30	130.91
	JANTX	NS	0	1.78
	JANTX	AUA	0	.51
	JANTX	AUB	0	.57
	JANTX	AUT	0	1.38
	JANTX	AUF	0	.85
	JANTX	AUC	0	2.14
	Unknown	SF	0	35.17
PIN (>500W)	JAN	GF	1298	8291.84
PIN (<10W)	Lower	GF	28	145.15
PIN (>400W)	JANTX	GF	33	2322.31
PIN (<.1W)	JANTX	GF	498	2654.07

The next step was the development of a theoretical model, which was accomplished in two steps. First, factors which have the most significant effect on high frequency device failure rates were identified based on published physics of failure data and information (Refs. 3,6,7,52) and on intuitive reliability relationships. Only factors available to potential failure rate prediction model users were considered. Next, a study of the various model forms was undertaken to determine the best possible form as

applicable to high frequency diode failure rate prediction. Possible model forms included multiplicative, additive, and nonlinear.

A single theoretical model was applicable to all high frequency diodes. This does not imply that the same failure mechanisms act on all high frequency diodes or that changes in model factors have the same effect on all device types. This action only implies that the same general factors influence high frequency diode failure rate (to different degrees) and that a single theoretical model format can be adopted for convenience. The model is multiplicative in agreement with the current MIL-HDBK-217E models and is of the form:

$$\lambda_p = \lambda_b \pi_f \pi_p \pi_A \pi_D \pi_Q \pi_T \pi_E$$

where

λ_p = predicted device failure rate (failures/10^6 operating hours)

λ_b = base failure rate
= f_1(device style, semiconductor material)

π_f = frequency factor
= $a(f)^b$

where

a,b = constants
f = operating frequency (GHz)

π_p = power factor
= $(P_a/P_r)^m$

where

P_a = applied power
P_r = rated power
m = shaping factor

π_A = application factor

π_D = duty factor
= f_2(duty cycle, pulse width)

π_Q = quality factor
= f_3(screen level, package hermeticity)

π_T = temperature factor

$$= \exp\left(\frac{-E_a}{K}\left(\frac{1}{T_j}\right)\right)$$

where

E_a = equivalent activation energy, dependent on device material
K = Boltzman's constant
T_j = junction temperature (^oK)

π_E = environmental factor

The rationalization behind the selection of these factors is discussed in the following paragraphs.

Semiconductors materials currently employed in high frequency diode fabrication primarily include Si, an elemental semiconductor, and GaAs a compound semiconductor. (Ge, InP and GaP have also been used to some degree.) From a materials point of view, GaAs claims certain advantages over Si; however, from a reliability viewpoint, investigations have not kept pace with performance gains. It was thus necessary to examine differences between semiconductor materials from a reliability viewpoint. This was accomplished through the device base failure rates.

Based upon the results of the literature search, temperature was determined to be the most significant variable influencing device failure rate. It was assumed that the equivalent Arhennius relationship (discussed in Section 5.4) was applicable to high frequency diode failure rates. It was also assumed that the effects of temperature could be different for the various types of diodes and also for the different semiconductor materials. The preliminary form of the temperature factor was:

$$\pi_T = \exp\left[\frac{-E_a}{K}\left(\frac{1}{T_j + 273} - \frac{1}{T_r}\right)\right]$$

where

E_a = equivalent activation energy
= f_4(device type, materials)

K = Boltzman's constant = 8.63×10^5 eV/°K

T_j = junction temperature (°C)

T_r = reference temperature = 298°C

The reference temperature is added for convenience. When the ambient temperature equals the reference temperature (i.e., equals 25°C), which is generally the maximum temperature at which full rated operation is allowed (according to derating guidelines), the temperature factor equals one. The addition of this reference factor allows consistency with the current MIL-HDBK-217E microcircuit models.

This information complemented the high temperature life test data obtained in the data and information collection tasks. This data is summarized in Table 5.4-5. For devices where insufficient temperature effects information could be obtained, present MIL-HDBK-217E temperature factor values were assumed to be correct.

Failure data reported in the literature indicated that operating frequency may be a significant variable impacting the reliability of IMPATT diodes. It was logical to include a frequency factor in the theoretical failure rate prediction model because as the frequency of a diode increases above a certain level, the diode design becomes complicated since conventional processing techniques reach their limitations. Also, it has been reported (Ref. 58) that GaAs Schottky mixer diode burn out from RF pulses greater than 1 watt is a significant problem at frequencies above 36 GHz, implying a dependence on operating frequency. Since there was no rationale for excluding this factor for other diode types, a factor for operating frequency was included in the theoretical failure rate prediction model for all high frequency diodes. Additionally, duty factor and pulse width factors were added to the model, along with a frequency factor, because these variables define the amount of time a device is stressed with a certain pulse.

TABLE 5.4-5. HIGH TEMPERATURE LIFE TEST DATA FOR HIGH FREQUENCY DIODES

Device Type	Junction Temperature (°C)	Failures	Part Hours ($\times 10^6$)
Si Schottky Barrier	240	16	.263
	270	23	.109
	210	10	.263
GaAs Schottky Barrier	136	0	.413
	141	0	.019
Si IMPATT	203	1	.031
	210	0	.163
	218	0	.031
	219	2	.019
	221	0	.143
	232	2	.028
	312	32	.064
	332	32	.015
	256	5	.01189
	280	20	.08031
	300	10	.00017
	312	7	.00004
	325	13	.01006
	350	12	.00224
	290	8	.00168
GaAs IMPATT	220 (Case)	17	.030
	235 (Case)	1	.006
	350	14	.076
	400	14	.014
	215	1	.070
GaAs Gunn	275	9	.0004
	300	9	.000002
	325	9	.0000003
	---	0	.118
	---	2	.300
	---	4	1.114
	---	29	1.809
	---	4	1.112
	---	1	.247

Electrical stress was also determined to be a significant factor influencing high-frequency diode failure rates. The benefits of electrical derating have been well documented (Refs. 37,46). Ballamy and Kimerling (Ref. 6) identified a failure mechanism at junction temperatures less than 300°C in Schottky IMPATT diodes with thick platinum layers called recombination-enhanced diffusion. Defects produced at the GaAs-Pt interface by interface reaction diffuse into the GaAs under recombination stimulation. The effect is not seen in devices exposed to temperature stress alone, thus making the investigation of electrical stress important. This failure mechanism has also been reported in ion-implanted Gunn diodes.

Namordi and Sokolov (Ref. 52) report on the effect of current bias on the reliability of Read-type Schottky Barrier GaAs IMPATTs. The efficiency of Read-type GaAs IMPATTs has been shown to be critically dependent on the width of the avalanche region; thus, junction motion seriously impairs both efficiency and output power. By analyzing life test data, the change in junction position was found to be proportional to the product of current density and time.

Based upon the information available in the literature, it was deemed necessary to examine the effects of electrical stress on high frequency device reliability. Power was chosen as an appropriate measure for the following reasons: first, regression analysis requires that all independent variables be uncorrelated, and there was often a correlation between power and other electrical ratings; second, if only one measure could be chosen, partially as a result of this correlation, power would best model the effect of electrical stress-related failure mechanisms on device reliability.

Environmental and quality factors included in the high frequency diode failure rate prediction models were analyzed from the composite discrete semiconductor database as discussed in detail in Section 4.6.

The results of the regression analyses for each high frequency diode type follow.

5.4.3 High Frequency Diode Analysis Results

This section presents the analysis results for high frequency diodes. Devices considered include: IMPATT diodes, Gunn diodes, Schottky diodes, PIN diodes, Varactor and Step Recovery diodes, and Tunnel, Mixer and Detector diodes.

IMPATT Diodes

The failure rate prediction model for IMPATTs is based solely on the analysis of life test data, since despite many efforts no field data was available. The life test environment was assumed to be equal to a ground benign environment with extremely high ambient temperatures.

Insufficient data was available to quantify a duty factor or a pulse width variable. Also, since the data was life test data, in which devices are generally highly stressed, there was an insufficient range of electrical stress levels to quantify a stress variable. The rated power data was unbalanced with 13 out of 16 data points having a rated power of .5 watts. Data was available on both X-band and KA-band devices; however, regression results with the frequency variable were inconsistent with theoretical relationships. This is probably because either duty factor or pulse width or both variables were unknown for many of the data points. It is expected that both the failure rate and the operating frequency would be correlated with duty factor and/or pulse width. Thus the effect of frequency could not be independently evaluated because of the uncertainty regarding these parameters.

The semiconductor material factor (Si vs. GaAs) was significant at greater than a 90% significance level, resulting in the following base failure rates:

λ_b = .2235 failures/10^6 operating hours, Si
= .0540 failures/10^6 operating hours, GaAs

However, since this factor was based upon extremely limited data for GaAs devices, it was felt presumptuous to make the GaAs base failure rate less than 25% of the Si failure rate. Although GaAs claims advantages over Si from a materials viewpoint, reliability investigations have not kept pace with performance gains. Until further, more conclusive data is available for GaAs IMPATT devices, attempts to predict their reliability would be incorrect and misleading. Therefore, the resulting prediction model is based solely upon the Si IMPATT data, and is only applicable to Si IMPATT devices.

The temperature factor developed is:

$$\pi_T = \exp\left(-5260\left(\frac{1}{T_j + 273} - \frac{1}{298}\right)\right)$$

This factor was the result of the analysis of IMPATT life test data collected. The current MIL-HDBK-217 factor was based upon minimal data and was a generic factor applied to all high frequency diodes, and was therefore replaced with the new factor.

An equivalent quality factor was included in the model based on the assumption that screening of these devices would affect the device failure rate in a means similar to the screening of other high frequency diodes (where a quality factor has been established). It was felt that this option (i.e., assuming a quality factor) would provide a better design tool than the option of ignoring the effects of screening.

Gunn Diodes

Although the data collection effort described in Section 2.0 included a search for Gunn diode data, little new failure data subsequent to the previous microwave modeling effort (Ref. 53) was available. Thus, the current MIL-HDBK-217E model for Gunn diodes could not be refuted. The environment factor for this model was updated based upon the collected discrete semiconductor data as described in Section 4.6.

A quality factor was included in the model based on the assumption that screening would affect Gunn diode failure rate in a manner similar to other high frequency diodes, where a quality factor has already been established. It was again felt that this option (i.e., assuming a quality factor) would provide a better design tool than the option of ignoring the effects of screening.

Although there was insufficient data to quantitatively develop a temperature factor for Gunn diodes, an estimated relationship was applied to the model to provide consistency with the other high frequency diode models. The assumed relationship was based upon the geometric mean of the Schottky, IMPATT, tunnel and varactor temperature constants. It is strongly recommended that this assumption be checked with actual test data when further, more conclusive information is available.

The Gunn diode life test data presented in Table 5.4-5 was not included in the calculation of a temperature constant for two reasons. First, the small number of part hours makes the significance of the data questionable; and second, the extremely high test temperatures are probably indicative of a single, dominant failure mechanism, which is not characteristic of failure tendencies at lower operating temperatures. Therefore, extrapolation to operating temperatures is questionable at best and most likely, invalid. This data indicates an activation energy of 3.1eV.

Finally, it was necessary to make an adjustment to the original base failure rate to compensate for the addition of the temperature factor. The junction temperatures could not be identified for the original data sources which yielded the MIL-HDBK-217E base failure rate of 0.6. A junction temperature of 75°C was then assumed and the base failure rate was adjusted to a value of 0.18. In this manner, the updated base failure rate multiplied by the new temperature factor (for the average junction temperature of 75°C) is equal to the old base failure rate.

Schottky Diodes

Despite many efforts, failure data was not available for GaAs Schottky diodes; thus, the proposed model applies to Si Schottky diodes only. A unique base failure rate was obtained from the available data. An analysis of the life test data for Si Schottky diodes resulted in a temperature factor of:

$$\pi_T = \exp\left(-7416\left(\frac{1}{T_j + 273} - \frac{1}{298}\right)\right)$$

This corresponds to an activation energy of .63. Lower and upper 95% confidence bounds were -1.8 and 3.1 respectively. Since the current MIL-HDBK-217E temperature factor was within the upper and lower 95% confidence interval of this variable, and the factor was based on the analysis of only three data points, the current MIL-HDBK-217E factor was not refuted. Since all Schottky diode data was a JANTX quality level, a new quality factor was not derived and the current MIL-HDBK-217E factor was assumed to be correct.

No circuit application or device electrical information such as maximum rated electrical parameters, electrical stress, pulse width, duty factor, or operating frequency were available for these diodes. Therefore, these parameters could not be included in the failure rate prediction model.

The model developed based upon Schottky diode data will be applicable to point contact diodes as well, since these diodes are similar in materials and application, and differ only in contact type. This assumption represents the "best estimate" given the available data/information.

Varactor and Step Recovery Diodes

Since Varactor and Step Recovery diodes are similar in construction and application, these diodes are merged into one model, as they are in the current MIL-HDBK-217E models. Unlike the current models, however, sufficient data was available to develop unique base failure rates for Varactor/Step Recovery as well as each of the other microwave diode types. Since the varactor data collected is believed to be entirely from voltage control applications, a new application factor for varactors could not be developed and the current application factor was retained.

No circuit application or device electrical information, such as maximum rated electrical parameters, electrical stress, pulse width, duty factor, or operating frequency, was available for these devices.

Additionally, no life test data was available, so the current MIL-HDBK-217E value for equivalent activation energy was retained. The current MIL-HDBK-217E quality factor series for these, as well as the other high frequency diodes, were retained because of inconsistent results.

PIN Diodes

A unique base failure rate was developed for PIN diodes. Since no life test data was available, the current temperature factor was assumed to be correct. Results of the regression analysis for quality level were inconsistent due to the lack of sufficient data, therefore, current quality factors were also assumed.

No circuit application information, such as electrical stress, pulse width, duty factor, or operating frequency, was available for these devices and as a result, they could not be included in the final failure rate model.

PIN diode data was collected for both high power (400 to 500 watts) and low power (<.1w) devices. However, power rating was not a statistically significant variable based on analysis of the available dataset. When the variable was forced into the regression, results were inconsistent with accepted reliability relationships. Since available data was of limited quantity this result was insufficient evidence to disprove the current MIL-HDBK-217E factor, which was retained.

Tunnel, Mixer and Detector Diodes

A unique base failure rate was developed for Tunnel, Mixer and Detector diodes. Because of the lack of available data, the current MIL-HDBK-217E factors for quality level and temperature effects for Tunnel diodes were assumed. The current temperature factor for tunnel diodes was also assumed correct for mixer and detector diodes, since insufficient data was available to distinguish between them, and the devices are similar enough in construction and application. The new environment factor series was also applicable to this model.

No circuit application or device electrical information, such as maximum rated electrical parameters, electrical stress, pulse width, duty factor, or operating frequency, was available to quantify, the effects of these variables on device failure rate. Therefore, these factors were not included in the prediction model.

5.5 HIGH FREQUENCY TRANSISTORS

Failure rate prediction models for RF bipolar power transistors, low noise RF transistors, GaAs FETs and GaAs power FETs were determined. GaAs power FETs were defined as devices with output power $\geq$ 100 mW.

5.5.1 High Frequency Transistors Models

This section presents the failure rate prediction models for "high frequency" transistors. The models are presented in a format compatible with MIL-HDBK-217E in Appendix A.

The prediction model for RF transistors with frequency $\geq$ 200 MHz and average power $\geq$ 1 watt is as follows. The model is applicable for devices with frequency less than 5 GHz and output power less than 600 watts.

$$\lambda_p = \lambda_b \pi_A \pi_{pw} \pi_m \pi_Q \pi_T \pi_E$$

where

λ_p = predicted failure rate (failures/10^6 operating hours)

λ_b = base failure rate (failures/10^6 operating hours)
$= .032 \exp(.354(f) + .00558(P))$

where

f = frequency (GHz)
P = average output power (watts)

π_A = application factor
= .06(DF) + .40, pulsed applications, DF = duty cycle (%)
= .40, CW

π_{pw} = pulse width factor (equal to one for CW applications)
= 1.0, pulse width (PW) $\leq$ .5 ms
= .937 + .127(PW), PW > .5 ms

π_m = matching network factor
= 1.0, input and output internal matching
= 2.0, input internal matching
= 4.0, no internal matching

π_Q = quality factor
= 0.5, JANTXV with IR scan for die attach and screen for barrier pinholes on gold metalized devices
= 1.0, JANTX or equivalent
= 2.0, JAN or equivalent
= 5.0, lower quality

π_T = temperature factor

$$= 6.7((V_{CE}/BV_{CES}) - .35)\ \exp(-2903(\frac{1}{T_j+273} - \frac{1}{373}))$$

where

V_{CE} = operating voltage (volts)
BV_{CES} = collector-emitter breakdown with base emitter shorted (volts)
T_j = peak operating temperature (^oC)

π_E = environmental factor (see Table 5.5-1)

TABLE 5.5-1. RF TRANSISTOR ENVIRONMENTAL FACTORS

Environment	π_E	Environment	π_E
GB	1	AIA	4.6
GMS	1.1	AIF	4.6
GF	2	AUC	7.0
GM	4.9	AUT	7.0
MP	4.9	AUB	7.0
NSB	3.6	AUA	12
NS	4.7	AUF	12
NU	11	SF	1
NH	11	MFF	7.5
NUU	11	MFA	11
ARW	16	USL	22
AIC	3.7	ML	55
AIT	3.7	CL	250
AIB	3.7		

The failure rate prediction model for low noise RF transistors (< 1 watt) is as follows.

$$\lambda_p = \lambda_b\ \lambda_r\ \pi_s\ \pi_Q\ \pi_T\ \pi_E$$

where

λ_p = predicted failure rate (failures/10^6 operating hours)

λ_b = base failure rate (failures/10^6 operating hours)
= .18

π_r = power rating factor
= .43, R $\leq$ .1W

= $(R)^{.37}$, R > .1W

where

R = rated power (watts)

π_S = voltage stress factor

$$= .045 \exp\left(3.1\left(\frac{\text{Applied } V_{CE}}{\text{Rated } V_{CEO}}\right)\right)$$

π_Q = quality factor
= 0.5, JANTXV
= 1.0, JANTX
= 2.0, JAN
= 5.0, Lower

π_T = temperature factor

$$= \exp\left(-2214\left(\frac{1}{T_j + 273} - \frac{1}{298}\right)\right), \; T_j = \text{junction temperature } (^oC)$$

where

T_j = junction temperature (^oC)

π_E = environmental factor (see Table 5.5-1)

The failure rate prediction model for GaAs FETs (output power $\leq$ 100 mW) is as follows.

$$\lambda_p = \lambda_b \, \pi_A \, \pi_Q \, \pi_T \, \pi_E$$

where

λ_p = predicted failure rate (failures/10^6 operating hours)

λ_b = base failure rate (failures/10^6 operating hours)
= .052

π_A = application factor
= 1.0, low noise
= 7.1, driver ($\leq$ 100 mW)

π_Q = quality factor
= 0.5, JANTXV or equivalent
= 1.0, JANTX or equivalent
= 2.0, JAN or equivalent
= 5.0, Lower

π_T = temperature factor

$$= \exp\left(-4485\left(\frac{1}{T_j + 273} - \frac{1}{298}\right)\right), \quad T_j = \text{junction temperature } (^oC)$$

π_E = environmental factor (see Table 5.5-1)

The failure rate prediction model for GaAs power FETs (output power >100 mW) is as follows,

$$\lambda_p = \lambda_b \, \pi_A \, \pi_M \, \pi_Q \, \pi_T \, \pi_E$$

where

λ_p = predicted failure rate (failures/10^6 operating hours)

λ_b = base failure rate (failures/10^6 operating hours)
= .0093 exp(.429(f) + .486(P))

where

f = frequency (GHz)
P = output power (watts)

π_A = application factor
= 1.0, CW
= 5.0, pulsed

π_M = internal network factor
= 1.0, input and output internal matching
= 2.0, input internal matching
= 4.0, no internal matching

π_Q = quality factor
= 0.5, JANTXV or equivalent
= 1.0, JANTX or equivalent
= 2.0, JAN or equivalent
= 5.0, lower quality

π_T = temperature factor

$$= \exp\left(-5297\left(\frac{1}{T_j + 273} - \frac{1}{298}\right)\right), \quad T_j = \text{junction temperature } (^oC)$$

π_E = environmental factor (see Table 5.5-1)

5.5.2 Prediction Model Development

Failure rate prediction models were developed for microwave power transistors, GaAs FETs and GaAs power FETs. Additionally, data analysis was conducted on low noise RF transistor failure data to modify the transistor model (described in Section 5.2). Model development activities involved hypothesis of a theoretical model and analysis of field and life test data. Model development for microwave power transistors was based on a large set of data from field sources including PAVE PAWS, SEEK IGLOO, AN/TPS-59, DME and TACAN. Model development for GaAs FETs and GaAs power FETs was based primarily on life test data.

Application and construction variables that characterize high frequency transistors are presented in Table 5.5-2. These variables were based on a review of device specifications. They represent potential model input parameters.

Tables 5.5-3, 5.5-4 and 5.5-5 present the collected field and life test data for microwave power transistors, GaAs power FETs and GaAs FETs respectively. In addition to this data, 568 observed failures in 331.76 x 10^6 part hours were collected for low noise RF transistors. The field data for microwave power transistors represents a comprehensive covering of military and FAA usage of these devices, including the SEEK IGLOO, PAVE PAWS and other systems. The data for GaAs FETs and GaAs power FETs are from life testing programs.

TABLE 5.5-2. RF TRANSISTOR CHARACTERIZATION VARIABLES

I. Material

- A. Si
- B. GaAs

II. Type

- A. Bipolar Transistor
- B. FET

III. Output Power

IV. Frequency

V. Application (pulsed vs. CW, device function)

VI. Pulse Width

VII. Duty Factor

VIII. Junction Temperature

IX. Thermal Resistance

X. Quality

XI. Application Environment

TABLE 5.5-3. MICROWAVE POWER TRANSISTOR FIELD DATA

System	Failures	Part Hours ($x10^6$)	f(GHz)	P(W)	Duty Cycle	Pulse Width (Millisec)	T_j (^oC)	Env.
1. ITT VORTAC	1611	484.0	1.09	200	.04	.0035	125	GF
2. ITT VORTAC	402	124.0	1.09	200	.04	.0035	175	GF
3. R/C WXR	4	0.65	.85	200	.005	.020	165	Air
4. R/C WXR	18	1.3	.85	400	.005	.20	165	Air
5. R/C LRA	4	3.13	4	4	CW	CW	143	Air
6. R/C TPR	3	1.19	1	220	.01	.0008	155	Air
7. R/C TPR	1	0.74	1	60	.01	.0008	145	Air
8. R/C DME	2	3.24	1	300	.01	.0035	155	Air
9. R/C DME	1	1.62	1	200	.01	.0035	150	Air
10. R/C TACAN	8	7.4	1	25	.01	.0035	130	Air
11. PAVE PAWS	416	251.3	0.435	130	.296	15	140	GF
12. PAVE PAWS	49	125.7	0.435	42	.296	15	110	GF
13. PAVE PAWS	56	62.8	0.435	11	.296	15	100	GF
14. AN/TPS-59	14	14.4	1.3	45	.20	2	125	GM
15. SEEK IGLOO	11	20.49	1.3	45	.18	0.8	153	GF
16. B3D	12	36.74	1.3	45	.18	0.8	155	GF

TABLE 5.5-4. GaAs POWER FET LIFE TEST DATA

	Source	Failures	Part Hours	f(GHz)	P(watts)	Channel Temp. (°C)
1.	JPL/SD	8	13611	7.5	2	150
2.	JPL/SD	11	4209	7.5	2	190
3.	JPL/SD	6	1040	7.5	2	225
4.	JPL/SD	8	68962	7.5	6	180
5.	JPL/SD	8	27294	7.5	6	240
6.	JPL/SD	8	6561	7.5	6	270
7.	Raytheon SMD	4	8400	9.5	.11	228
8.	Raytheon SMD	7	840	9.5	.14	280
9.	Raytheon SMD	0	2600	9.5	.19	218
10.	Bell Labs	66	88000(1)	4	2.5	265
11.	Bell Labs	8	33000(1)	4	2.5	208
12.	Bell Labs	4	146000(1)	4	2.5	160
13.	Avantek	4	77184	4	1	225
14.	Avantek	10	104968	4	1	250
15.	Avantek	13	8534	4	1	275
16.	NRL(2)	(MTBF = 2200 hrs.)		8	.20	200
17.	Hughes/AFWAL(3)	(MTBF = 1800 hrs.)		9.5	.75	218
18.	Hughes/AFWAL(3)	(MTBF = 620 hrs.)		9.5	.75	249
19.	Hughes/AFWAL(3)	(MTBF = 220 hrs.)		9.5	.75	274
20.	Hughes/AFWAL(3)	(MTBF = 135 hrs.)		9.5	.75	274
21.	Hughes/AFWAL(3)	(MTBF = 470 hrs.)		9.5	.75	274

Notes: (1) Part hours estimated from figure (Ref. 13)
(2) Test results only available as MTBF (Ref. 76)
(3) Test results only available as MTBF (Ref. 77)

TABLE 5.5-5. GaAs FET (< 100 mW) LIFE TEST DATA

	Source	Failures	Part Hours	Channel Temperature (°C)	Frequency (GHz)
1.	RADC/Hughes	21	26,539	200	5.7
2.	RADC/Hughes	30	21,157	220	5.7
3.	RADC/Hughes	24	22,963	240	5.7
4.	RADC/Hughes	22	12,597	260	5.7
5.	RADC/Hughes	6	10,344	200	5.7
6.	RADC/Hughes	10	7,824	220	5.7
7.	RADC/Hughes	5	4,765	240	5.7
8.	RADC/Hughes	11	3,274	260	5.7
9.	Avantek (1)	(MTBF = 1,645)		230	6.0
10.	Avantek (1)	(MTBF = 254)		255	6.0
11.	Avantek (1)	(MTBF = 109)		275	6.0

Note: (1) Test results only available as MTBF (Ref. 18).

Microwave Power Transistors

Development and design of microwave power transistors involves a trade-off between the following parameters,

- Output power
- Frequency
- Pulse width
- Duty cycle

In the development process, performance is the first priority. When the desired performance levels can be demonstrated, reliability concerns become important. Of particular concern with microwave electronic devices, as opposed to other electronic devices, is the effect of operating frequency and power levels.

Higher power at microwave frequencies is attained by using larger junction areas. This practice, however, has limits. Less output power is observed as the collector base junction area is increased above a critical level, even though the device emitter periphery to base area ratio and base periphery figure of merit are maintained. Larger area devices exhibit grossly non-uniform current and temperature distributions.

To avoid hot spots, the collector-base junction area can be divided into paralleled "cells". By splitting up the active cell base areas, the base periphery is increased, thereby reducing the thermal resistance on a unit area basis. However, phase differences associated with package parasitics and physical die dimensions cause problems in the gigahertz frequency range. In general, the junction-temperature rise is approximately proportional to the ratio of the base area to the base periphery:

$$\Delta T_j \propto \frac{BA}{BP}$$

where

ΔT_j = change in junction temperature
BA = base area
BP = base periphery

The key design parameters are highly related. Conceptually, all possible combinations of design parameters form an "envelope" of physically attainable designs. Ideally, an equation could be determined defining the envelope, as

$$CV \geq K$$
$$K = f(\text{power, frequency, pulse width, duty cycle})$$

where

CV = critical value
K = design "figure-of-merit" based on key design parameters

Within a given range of values, an increase in the value of one of the key parameters can be compensated by a corresponding change in another variable to maintain an acceptable reliability level. For example the microwave power transistors in the JTIDS program operate at a low pulse width to maintain the desired power at a high duty factor. Above a certain range (i.e., approximately 500 watt output power), 'K' would increase above the critical value and no compensatory changes would be feasible. As the figure-of-merit (K) becomes less than the critical value, the failure rate would be anticipated to be low. Conversely, as the figure-of-merit approaches the critical value, the transistors would be expected to have a short life.

A theoretical model for microwave power transistors was developed based on the conceptual figure-of-merit discussions and observed failure mechanisms. Observed failure mechanisms include:

- Electromigration
- Gold diffusion through the barrier layer
- McDonald effect, reverse bias breakdown
- Chip cracking
- Metal restructuring
- Lead or bond failure
- Peeling metalization
- Carrier fracture due to mountdown
- Voids in carrier mountdown

Initially the theoretical model for microwave power transistors was given as a function of the following factors:

- Frequency (f) (GHz)
- Output power (P) (watts)
- Peak junction temperature (T_j) (^oC)
- Metalization
- V_{CE} (operating voltage) (volts)
- BV_{CES} (collector-emitter breakdown with base shorted to emitter) (volts)
- Operating mode (pulsed vs. CW)
- Duty factor (DF) (%)

- Pulse width (PW) (milliseconds)
- Internal matching
- Quality
- Environment

Grouping the independent variables into MIL-HDBK-217E style Pi factors results in the following conceptual model (f_i, g_i represent unknown functions).

$$\lambda_p = \lambda_b \pi_A \pi_{pw} \pi_m \pi_Q \pi_T \pi_E$$

where

λ_p = device failure rate (failures/10^6 operating hrs.)

λ_b = base failure rate
= $f_1(f, W)$

π_A = application factor
= f_3(pulsed vs. CW, DF)

π_{pw} = pulse width factor, based on PW

π_m = matching network factor

π_Q = quality factor

π_T = temperature factor
= f_2(metalization, V_{CE}, BV_{CES}, T_j)

$$= S_v \exp\left(-A\left(\frac{1}{T_j + 273} - \frac{1}{298}\right)\right)$$

where

S_v = voltage stress contribution
= $g_1(V_{CE}, BV_{CES})$

A = temperature constant
= g_2(metalization)

π_E = environmental factor (see Table 5.5-1)

The base failure rate was defined as a function of frequency and output power. These two parameters were identified as the two dominant factors affecting device failure rate. To optimize RF performance at high frequencies, the device designer must reduce line widths to improve gain and power capability. However, failure rate increases as the cross-sectional area decreases, thereby creating a design trade-off problem.

The temperature factor depends on metalization, V_{CE}, BV_{CES} and the peak junction temperature. The effect of temperature on microwave power transistor mean-time-to-failure (MTTF) has been predicted by use of Black's equation (Ref. 62).

$$MTTF = \frac{WT}{CJ^2} \exp(\phi/KT)$$

where

W = strip width of the metalization (cm)
T = strip thickness of the metalization (cm)
J = current density (amps/cm^2)
C = constant
ϕ = activation energy (eV)
K = Boltzman's constant
T = temperature (^oK)

Black's equation is in agreement with the equivalent Arrhenius equation regarding the relationship of temperature and failure rate. Black's equation also is dependent on width, thickness and current density. It was decided not to include these factors in the theoretical model because:

(1) These values would not be readily available to reliability engineers in the equipment design phase

(2) The frequency-power characteristics of the device determine the metalization geometries and thus, these factors are implicitly handled by the base failure rate.

The existing MIL-HDBK-217E microwave transistor model presents different temperature factors depending on the type of metalization (Al vs refractory Au). The debate of Al vs Au is no longer relevant because the consensus is that well controlled Au metalization systems are superior above 750 MHz (Ref. 63). Specifically, Au metalization is better regarding,

- o Electromigration resistance
- o Temperature stability
- o Corrosion resistance
- o Mechanical strength
- o Oxide step coverage
- o Manufacturability

The proposed temperature factor will only correspond to Au metalization since it is anticipated that all future designs will employ Au metalization. Additionally, this action will further discourage the use of Al metalization for RF power transistors.

The existing MIL-HDBK-217E temperature factor for refractory gold is as follows:

$$\pi_{T,217} = 2((V_{CE}/BV_{CES}) - .35), \; T_j < 100$$
$$\pi_{T,217} = 0.08(T_j - 75)((V_{CE}/BV_{CES}) - .35), \; 100 \geq T_j \geq 200$$

This model format is not in accordance with Black's equation or the equivalent Arrhenius equation, and therefore a change was proposed to provide agreement with published material, and to provide continuity with other MIL-HDBK-217E models. The proposed temperature factor is,

$$\pi_T = 6.7((V_{CE}/BV_{CES}) - .35) \exp(-2903(\frac{1}{T_j} - \frac{1}{373}))$$

This factor was determined by:

(1) Forcing an Arrhenius style equation through the values predicted by the previous equation

(2) Normalizing the factor to be equal to one when the peak junction temperature is 100°C and V_{CE}/BV_{CES} is 0.50. The equivalent activation energy will later be tested using the available data.

The application factor depends on whether the device operates under pulsed or CW conditions, and on the duty factor (if pulsed). This is consistent with the existing application factor except that the choice for oscillator has been deleted. This option is no longer required since devices operating as oscillators fit into the CW category.

Two other modifications to the application factor are recommended. First, the application factor for CW was lowered to allign with pulsed applications with a low duty factor (i.e., less than 5%). This recommendation is because of a much improved control of circuit parameters under CW applications. The second modification was to propose a continous equation for pulsed application factor based on the duty factor. The current factor was the three following discrete categories:

Category 1: $DF < 5\%$
Category 2: $5\% \leq DF \leq 30\%$
Category 3: $DF > 30\%$

A continous relationship provides the model with greater sensitivity. The proposed factor is:

$$\pi_A = K_1 + K_2(DF)$$

where

K_1, K_2 are constants.

The theoretical model included a factor for pulse width. This factor will be a new addition to the model and is considered to be important since pulse width is one of the key parameters involved in the design

trade-off for microwave power transistors. Pulse width was identified as one of several failure influencing factor by Poole and Walsha (Ref. 64).

The matching network factor from the existing MIL-HDBK-217E model was retained since a mismatch at the output will cause part of the output power to be reflected back into the chip. Under proper phase conditions this can reduce efficiency, increase dissipated power and junction temperature and increase internal local currents and voltages. The use of matching has significantly reduced the probability of RF transistor failure during amplifier development testing and field operation.

The matching factor from MIL-HDBK-217E is,

Matching	π_m
input and output internal matching	1
input internal matching	2
no internal matching	4

The theoretical model also included factors for quality and environment. Standardization of microwave power transistors is a problem impeding the development of appropriate quality factors. As a result, the current method of grouping the devices into equivalent categories was retained. The factor was normalized so that a JANTX device had a quality factor equal to one. This was done to improve the consistency of the document since all other discrete semiconductor devices had JANTX quality factors equal to one.

The next step in the model development process was the application of regression techniques to quantify the theoretical model. The collected dataset included failure data from most large military programs employing microwave power devices. However, there are only a small number of these systems, and thus, the dataset is fairly limited from a statistical perspective. Additionally, the independent variables were highly correlated preventing independent evaluation and quantification.

Generally, when independent variables are highly correlated, the most significant variable is selected as a model parameter. The regression solution for this variable implicitly includes the effects of the others. Unfortunately this was not a suitable approach for microwave power transistors. For example, the data collected by IITRI showed a high positive correlation between duty factor and pulse width. We know, however, that this is not consistently true. The power transistors in the JTIDS, one of the largest systems using microwave power transistors, have a high duty factor but a lower pulse width. If data had been available from this system, the observed correlation would have been less. The JTIDS example cannot be attributed to an abberation. As designers get more sophisticated and processes and material properties improve, it is anticipated that there will be even a greater variety of design options.

To compensate for the problems in the dataset, the temperature factor, the matching network factor and the quality factor presented in the theoretical model discussion were assumed correct.

Regression analysis was then applied to the data. Results of the regression analysis indicated that output power was the most significant variable affecting failure rate as expected. Frequency was also determined to be an important influencing factor. Pulse width, duty factor and environment were not found to be significant in this initial analysis and are discussed later in this section.

The regression solution is given by:

$$\lambda_p' = 0.439 \exp(.354(f) + .00558(P))$$

where

λ_p' = preliminary predicted failure rate (failure/10^6 operating hours)
f = frequency (GHz)
P = output power (watts)

Pulse width, duty factor and environment were not found to be significant despite strong theoretical reasons why they should be included in the model. If similar results had been found in a larger, more controlled dataset, these factors would have been removed. However, with the limitations of the available dataset, the regression solution was determined to be insufficient evidence to remove them. For the resulting model to be a useful design tool, these factors must be retained.

To study duty factor and pulse width, a two step approach was applied. The first step was to assume an application factor (dependent on duty factor) based on the MIL-HDBK-217E factor. The second step was to select data from three high-quality data sources, PAVE PAWS, SEEK IGLOO and B3D, with a range of pulse width of from 0.8 milliseconds for SEEK IGLOO and B3D to 15 milliseconds for PAVE PAWS.

IITRI had collected data with pulse widths as low as 0.8 microseconds; however, there were problems with these sources. The ITT VORTAC data was for microwave power transistors with a steadily decreasing failure rate with the passage of time (from 1983 to present). The high early failure rate is not indicative of the inherent reliability of these devices. The Rockwell/Collins data was also for low pulse width devices. These data records typically had low failure quantities, thereby, creating failure rate estimation uncertainties. It is hypothesized that this tended to mask any apparent effect caused by pulse width variations. Use of the high-quality dataset removed some of the possible sources of variation other than that caused by pulse width.

The resulting application and pulse width factor are,

$$\pi_A = .06(DF) + .40$$

$$\pi_{pw} = .937 + .127(PW), \quad PW > .5 \text{ ms}$$

$$= 1.0, \quad PW \leq .5 \text{ ms}$$

where

DF = duty factor (%)

PW = pulse width (milliseconds)

The remaining activities included determination of appropriate environmental factors and a base failure rate constant. By assuming all other factors to be correct, observed environmental factors were computed for ground fixed, ground mobile and airborne uninhabited categories. Factors for the remaining categories were computed by using the existing MIL-HDBK-217E factors as a scaling factor. The complete series of factors were presented in Table 5.5-1. The base failure rate constant was determined to be 0.032 by adjusting all observed failure rates by the previously determined factors. This resulted in a base failure rate equation given by,

$$\lambda_b = .032 \exp(.354(f) + .00558(P))$$

Adjustment of the base failure rate constant concluded the model development activities for microwave power transistors. Comparisons of this updated model with the existing MIL-HDBK-217E microwave transistor model are that:

(1) The model corresponds to higher power-frequency combinations

(2) The model results in overall lower failure rates

(3) The temperature factor has been modified to an equivalent Arrhenius style relationship

Low Noise RF Transistors

Failure data was also collected and analyzed for low noise RF transistors. All collected field data for these devices was from the AN/FPS-115 PAVE PAWS. A summary of the PAVE PAWS low noise RF transistor data is presented in Table 5.5-6. The failure quantities presented in Table 5.5-6 correspond to a total of 331.76×10^6 part hours accrued over calender years 1984 and 1985, and 7.5 months of 1986.

TABLE 5.5-6. PAVE PAWS LOW NOISE RF TRANSISTOR FAILURE DATA

Part Designation	Site	Failures	Hours ($x10^6$)
914592-1 (Q1)	Otis	72	82.94
914592-2 (Q2)	Otis	94	82.94
914592-1 (Q1)	Beale	173	82.94
914592-2 (Q2)	Beale	229	82.94
TOTAL		568	331.76

It was impossible to derive an independent low noise RF transistor model with data from only one source. Therefore, the data was used to evaluate the accuracy of the existing MIL-HDBK-217E failure rate predictions for low noise RF transistors. Given a ground fixed environment, case temperatures of 40°C, JANTX quality levels and worst case stress ratios of 0.70, the existing MIL-HDBK-217E failure rate predictions are as follows,

$$\lambda_{PNP} = .100 \text{ failures}/10^6 \text{ hours}$$

$$\lambda_{NPN} = .0626 \text{ failures}/10^6 \text{ hours}$$

The PAVE PAWS data therefore indicates that the existing failure rate prediction models are too low by a factor ranging from 17 to 27. Upon further researching this comparison, two other observations were made:

1) The failure data from Beale has historically exhibited a failure rate twice as high as similar transistors at Otis. While the specific cause for this discrepency has never been precisely resolved, it can be stated that the higher failure rates at Beale are due to the operation and/or maintenance of the system and not reflective of inherent differences in the transistors.

2) Previous attempts (Ref. 53) to model low noise RF transistors have yielded negligible data, far smaller quantities than were collected in this study. Therefore the existing model has never had a strong empirical backing.

Based on the two previous observations, it was decided to update the existing model with a higher resultant failure rate using the data from Otis only. With only the Otis data, the ratio between observed and predicted failure rate falls somewhere between 9.9 and 15.8 which is still a significant difference.

The environmental and quality factors for RF devices were applied to low noise RF transistors. Additionally the power rating and voltage stress factors were applied from the conventional transistor model. These factors are necessary to provide the model with proper discrimination against failure tendencies relating to derating and electrical stress levels.

A base failure rate was then determined from the Otis data by adjusting the observed failure rate with the pi factors corresponding to the PAVE PAWS data. Worst case electrical parameters were chosen. The resultant base failure rate was determined to be,

$$\lambda_b = 0.18 \text{ failures}/10^6 \text{ hours}$$

The low noise RF transistor model was therefore given by the following equation.

$$\lambda_p = \lambda_b \pi_r \pi_s \pi_Q \pi_T \pi_E$$

where

λ_b = base failure rate

π_r = power rating factor

π_s = voltage stress factor

π_Q = quality factor

π_T = temperature factor

π_E = environmental factor

GaAs Power FETs

Similar to the discussion for RF power transistors, the development of GaAs power FETs involves a trade-off of the key design parameters, including frequency and output power among others. The design and development of GaAs power FETs is still very much evolving and performance is still the primary design consideration. As required performance levels can be demonstrated, then reliability concerns become more important. The failure rate prediction model developed in this study effort represents an initial attempt to model GaAs power FET reliability. As designs mature and more development and testing work is completed, the model should be adjusted to reflect these advances.

An important observation from the leading organizations performing testing of GaAs power FETs is that lot-to-lot and manufacturer-to-manufacturer variations are the dominant factors influencing long-term reliability. Unfortunately, it is difficult or impossible to include those effects into the context of a MIL-HDBK-217E style failure rate prediction model. Therefore, the failure rate prediction models developed and presented in this report represent general reliability trends and it should be understood that individual cases can exist which deviate from the findings presented have.

The theoretical model for GaAs power FETS was determined to be:

λ_p = f(f, P, CW vs pulsed, T_{Ch}, screening, package type, environment, passivation)

where

λ_p = predicted failure rate (failures/10^6 hours)

f = frequency (GHz)

P = output power (watts)

T_{Ch} = channel temperature (^oC)

All collected GaAs power FET data (previously presented in Table 5.5-5) was from life testing programs. It was assumed that testing conditions were analagous to a ground benign environment with elevated temperatures.

An initial regression analysis was performed with all collected data except the Jet Propulsion Laboratories (JPL) 6 watt test results. This data was received very late in this study program and was therefore not available for analysis during the early and intermediate stages of model development. The results of this initial regression analysis seemed encouraging and are given by,

$$\lambda_p' = .00233\ (\exp(.546(f) + 1.348(P))\ \exp(-5473(\frac{1}{T_{ch}} - \frac{1}{298}))$$

where

λ_p' = preliminary predicted failure rate

Frequency, power and channel temperature were determined to be significant failure rate influencing variables at a 95% confidence limit. Detracting from the model, however, was the restriction that it was only valid for devices with output power less than or equal to 2.5 watt (the maximum in the dataset). When the model was extrapolated beyond 2.5 watts, the predicted failure rate increased dramatically.

The JPL 6-watt testing was on-going when this study program was initiated. It was important that IITRI obtain results of this testing to determine meaningful models, valid over a range of conceivable power requirements. When the test results were finally received during the last month of this study program (IITRI received the results from one of two device manufacturers being tested), the results were quickly grouped with the other data, and the analyses performed again. The unexpected result was then obtained that output power was no longer identified as a significant variable. These results seemed contradictory and it was concluded that the relatively lower failure rates observed in the 6-watt

devices was due to improved design and processing and not that output power was no longer an important failure influencing factor.

To quantify the effect of output power, it was assumed that the magnitude of the previously detected difference (from 0.1 W to 2.5 watt output power) was now appropriate for a range from 0.1 watt to 6.0 watt output power. The preliminary model coefficient for power was changed to account for this assumption. Mathematically, the assumed effect of output power is given by,

$$\lambda_p \propto \exp(.486(P))$$

The next step in the model development process was to re-access the effects of frequency and channel temperature given the assumed power relationship. Regression analysis was again performed and results of this step are given by,

$$\lambda_p' = .00929 \exp(.429(f) + .486(P)) \exp(-5297(\frac{1}{T_{ch}} - \frac{1}{298}))$$

The effects of frequency and power were incorporated into the base failure rate and a temperature factor was defined dependent on the channel temperature. Remaining model development activities involved assumption of quality, environment and matching network factors and determination of an application factor based on CW vs. pulsed operation.

The effects of passivation, channel material, overlay metal and back metal were also considered as potential failure rate model parameters. Testing and research performed by Hughes (Ref. 77) was useful to evaluate these factors. A control lot was life tested with no passivation. Other lots were then tested and compared to the control lot with varying combinations of passivation, channel material, overlay metal and back metal. The study findings did not reveal any dramatic failure rate enhancement caused by these design modifications. A maximum of a two-to-one improvement was achieved. However, given the large anticipated lot-

to-lot and manufacturer-to-manufacturer variation, it was not believed that the observed differences warrented expansion of the preliminary model to include these factors.

Since all GaAs power FET data was from life testing, it was impossible to empirically determine an independent environmental factor. Therefore, it was necessary to assume the environmental factor series used for other RF discrete semiconductor devices.

Development and testing of GaAs power FETs have not been standardized; thereby, inhibiting the development of an appropriate quality factor. Initially, it was felt that the model should not have a quality factor because of this lack of standardization. It was later decided, however, to include an assumed quality factor because a model without provisions for screening and packaging considerations would delude the final model users into believing that these factors are not important. It is acknowledged that the assumed factors are only approximate, but the model improves as a design trade-off tool by becoming more sensitive to quality considerations. The assumed factors were taken from the RF power transistor model.

The discussion of internal matching and the matching network factor which was presented for RF power transistors is also relevant to the reliability of GaAs power FETs. For those reasons, the same factor (π_m) was used for these devices.

The final model development activity for GaAs power FETs was the development of an application factor based on whether the device is operated in a CW or pulsed application. Physically, GaAs power FETs prefer CW and this should be reflected in the prediction model. It was difficult to determine an apropriate factor. However a five-to-one factor was determined based on the anticipated difference between CW and pulsed for GaAs power FETs, and an examination of existing MIL-HDBK-217E discrete semiconductor application factors.

Low Noise GaAs FETs

Separate models were developed for low noise GaAs FETs and GaAs power FETs due to the physical differences and different failure mechanisms. A GaAs power FET was defined for purposes of this study to be devices with output power greater than or equal to 100 mW. The GaAs FET model therefore corresponds to devices with less than 100 mW. Both models are restricted to devices $\leq$ 10 GHz due to data constraints.

The largest set of life test data for low noise GaAs FETs was from the testing program performed for RADC by Hughes (Ref. 22). Testing was performed on both packaged and chip devices under biased and unbiased conditions. Test temperatures were varied from 200°C to 260°C. Regression analysis was applied to both the biased and unbiased testing to ascertain temperature effects. The results are:

Biased: $\lambda_1 = e^{12.30} \exp(-2616(1/T))$
Unbiased: $\lambda_2 = e^{16.30} \exp(-6353(1/T))$
Together: $\lambda_3 = e^{16.05} \exp(-4485(1/T))$

The higher equivalent activation energy for unbiased than biased testing was attributed to a statistical abberation. It was concluded that the results from the overall regression analysis better represented temperature effects. A temperature factor was defined based on these findings and is given by:

$$\pi_T = \exp(-4485(\frac{1}{T_j} - \frac{1}{298}))$$

Data was also available from Avantek (Ref. 18). Results of analyses on this data revealed an extremely temperature dependent failure rate. The Avantek testing was for small signal GaAs FETs using TiW/Au gates. The observed failure mode was a decrease in the free carrier concentration in the channel. The results of this testing are typical of programs where

high temperatures are used to accelerate a single failure mechanism. The equivalent activation energies tend to be high but are not necessarily representative of lower temperatures, where other failure mechanisms begin to act.

The development of a unique temperature factor for GaAs FETs offers a distinct improvement. The existing MIL-HDBK-217E model assumes that temperature dependence is the same for Si and GaAs FETs.

Quality and environment factors were assumed for GaAs FETs. Derivation of these factors was discussed in Section 4.3 and 4.4 and in other model development sections.

It had been desired to develop a base failure rate equation for GaAs FETs as a function of operating frequency. However, this was not possible because of the limited frequency range found in the data. The base failure rate (.052) was therefore determined based on the available life test data and it's relationship to Si FET model. The final GaAs FET model is given by:

$$\lambda_p = \lambda_b \pi_Q \pi_T \pi_E$$

where

λ_p = GaAs FET predicted failure rate (failures/10^6 operating hours)

λ_b = base failure rate
= .052 failures/10^6 operating hours

π_Q = quality factor

π_T = temperature factor

π_E = environment factor

5.6 OPTO-ELECTRONIC DEVICES

This section presents the failure rate prediction models and describes model development activities for the following devices types:

- LED
- LED Alphanumeric Displays
- LED Emitting Diode Array
- Infrared Emitting Diode
- Phototransistors
- Photodiodes
- Opto-isolators
  - Photodiode Output
  - Phototransistor Output
  - Photo-Darlington Output
- Laser Diodes

5.6.1 Opto-Electronic Failure Rate Prediction Models

The models for opto-electronic devices are as follows. The devices are presented in a MIL-HDBK-217E format in Appendix A.

LEDs

The failure rate prediction model for LEDs is given by:

$$\lambda_p = \lambda_b \, \pi_Q \, \pi_T \, \pi_E$$

where

λ_p = device failure rate (failures/10^6 operating hours)

λ_b = base failure rate (failures/10^6 operating hours)
= .00023

π_Q = quality factor (see Table 5.6-1)

π_T = temperature factor

$$= \exp\left(-2650\left(\frac{1}{T_j} - \frac{1}{298}\right)\right)$$

where

T_j = junction temperature (^oK)

π_E = environmental factor (see Table 5.6-2)

LED Alpha-Numeric Displays (Segment Display)

$$\lambda_p = \lambda_b \pi_Q \pi_T \pi_E$$

where

λ_p = device failure rate (failures/10^6 operating hours)

λ_b = base failure rate (failures/10^6 operating hours)
= .00043(C) + λ_{1C}

where

C = number of characters (where each alpha-numeric character is comprised of a series of discrete LED segments)

λ_{1C} = logic chip failure rate contribution
= 0, displays without a logic chip
= .000043, displays with logic chip

π_Q = quality factor (see Table 5.6-1)

π_T = temperature factor

$$= \exp\left(-2650\left(\frac{1}{T_j} - \frac{1}{298}\right)\right)$$

where

T_j = junction temperature (^oK)

π_E = environmental factor (see Table 5.6-2)

LED Alpha-Numeric Displays (Diode Array Display)

$$\lambda_p = \lambda_b \pi_Q \pi_T \pi_E$$

where

λ_p = device failure rate (failures/10^6 operating hours)

λ_b = base failure rate (failures/10^6 operating hours)
= .000090 + .00017(C) + λ_{1C}

where

C = number of characters (where each alpha-numeric character is comprised of a series of diode array segments)

λ_{1C} = logic chip failure rate contribution
= 0, displays without a logic chip
= .000043, displays with logic chip

π_Q = quality factor (see Table 5.6-1)

π_T = temperature factor

$$= \exp(-2650(\frac{1}{T_j} - \frac{1}{298}))$$

where

T_j = junction temperature (^oK)

π_E = environmental factor (see Table 5.6-2)

Infrared Emitting Diode

$$\lambda_p = \lambda_b \pi_Q \pi_T \pi_E$$

where

λ_p = device failure rate (failures/10^6 operating hours)

λ_b = base failure rate (failures/10^6 operating hours)
= .0013

π_Q = quality factor (see Table 5.6-1)

π_T = temperature factor

$$= \exp(-2650(\frac{1}{T_j} - \frac{1}{298}))$$

where

T_j = junction temperature (^oK)

π_E = environmental factor (see Table 5.6-2)

Photo-detectors

$$\lambda_p = \lambda_b \pi_Q \pi_T \pi_E$$

where

λ_p = device failure rate (failures/10^6 operating hours)

λ_b = base failure rate (failures/10^6 operating hours)
= .0055, phototransistors
= .0040, photodiodes

π_Q = quality factor (see Table 5.6-1)

π_T = temperature factor

$$= \exp\left(-2790\left(\frac{1}{T_j} - \frac{1}{298}\right)\right)$$

where

T_j = junction temperature (^oK)

π_E = environmental factor (see Table 5.6-2)

Opto-Isolators

$$\lambda_p = \lambda_b \pi_Q \pi_T \pi_E$$

where

λ_p = device failure rate (failures/10^6 operating hours)

λ_b = base failure rate (failures/10^6 operating hours)
= .0025, photodiode output, single device
= .013, phototransistor output, single device
= .013, photodarlington output, single device
= .0064, light sensitive resistor, single device
= .0033, photodiode output, dual device
= .017, phototransistor output, dual device
= .017, photodarlington output, dual device
= .0086, light service resistor, dual device

π_Q = quality factor (see Table 5.6-1)

π_T = temperature factor

$$= \exp\left(-2790\left(\frac{1}{T_j} - \frac{1}{298}\right)\right)$$

where

T_j = junction temperature (^oK)

π_E = environmental factor (see Table 5.6-2)

Laser Diodes

$$\lambda_p = \lambda_b \pi_i \pi_A \pi_p \pi_Q \pi_T \pi_E$$

where

λ_p = laser diode failure rate (failures/10^6 operating hours)

λ_b = base failure rate (failures/10^6 operating hours)
= 3.23, GaAs/AlGaAs
= 5.65, InGaAs/InGaAsP

π_i = forward current factor
= $(I)^{0.68}$

where

I = forward peak current (amps)

π_A = application factor
= 4.4, CW
= (duty cycle)$^{0.5}$, pulsed

π_p = power degradation factor
= $0.5\ P_s/(P_s-P_r)$

where

P_s = rated optical power output (mW)
P_r = required optical power output (mW)

π_Q = quality factor
= 1.0, hermetic package
= 1.0, nonhermetic (with facet coating)
= 3.3, nonhermetic (without facet coating)

π_T = temperature factor

$= \exp(-A(\frac{1}{T_j} - \frac{1}{298}))$, T_j = junction temperature (^oK)

where

A = temperature constant
= 4635, AlGaAs/GaAs
= 5784, InGaAs/InGaAsP

π_E = environmental factor (see Table 5.6-2)

TABLE 5.6-1. OPTO-ELECTRONIC QUALITY FACTORS

Screen Class	π_Q
JANTXV	0.7
JANTX	1.0
JAN	2.4
Lower	5.5
Plastic	8.0

TABLE 5.6-2. OPTO-ELECTRONIC ENVIRONMENTAL FACTORS

Environment	π_E
GB	1
GMS	1.2
GF	2.4
GM	7.8
MP	7.7
NSB	3.7
NS	5.7
NU	12
NH	12
NUU	12
ARW	17
AIC	3.8
AIT	3.8
AIB	3.8
AIA	5.8
AIF	5.8
AUC	5.5
AUT	5.5
AUB	5.5
AUA	7.8
AUF	7.8
SF	1
MFF	7.8
MFA	11
USL	23
ML	26
CL	450

5.6.2 Opto-Electronic Device Model Development

Failure rate prediction models were developed for the following opto-electronic device types: LEDs, LED alpha-numeric displays, photodetectors, opto-isolators and laser diodes. The models were developed based on statistical analysis of field and life test data.

Initially, part application and construction variables were identified for opto-electronic devices. These variables represent potential failure rate model parameters and are presented in Table 5.6-3.

Field failure data was collected for a variety of opto-electronic device styles. Sufficient data was collected to thoroughly evaluate opto-electronic device reliability through use of data analysis techniques. Life test data was also collected to quantify the effects of temperature. Additionally, the results of life testing and failure analyses were the sole source of information for laser diodes. A summary of the collected data is presented in Tables 5.6-4 through 5.6-6 for field data, test data and laser diode test data respectively.

Quality factors and environmental factors were assumed for the opto-electronic device family. The series of quality factors determined for non-RF discrete semiconductor (described in Section 4.4) was assumed to be applicable for opto-electronic devices as well (except for laser diodes where an independent factor was developed). The existing MIL-HDBK-217E opto-electronic quality factors are the same on a relative scale (see Table 4.4-2) as other discrete semiconductor part types and there was no data to disprove this. Additionally, the existing series of MIL-HDBK-217E environmental factors for opto-electronic devices was retained. There was insufficient data to check the validity of these factors. However, there is no physical reason to believe that opto-electronic environmental sensitivity has changed since the last MIL-HDBK-217E revision.

TABLE 5.6-3. OPTO-ELECTRONIC CHARACTERIZATION VARIABLES

I. Device Type
- A. Emitter
  1. LED
  2. Infrared
  3. Laser Diode
- B. Sensor
  1. Photodiode
  2. Phototransistor
  3. Photodarlington
  4. Photothyristor
  5. Photocircuit
- C. Photocoupler (Opto-Isolator)
  1. Photodiode Output
  2. Phototransistor Output
  3. Photodarlington Output
  4. Photocircuit Output
- D. LED Display
  1. Segment Display
  2. Diode Array Display

II. Quality Level

III. Thermal Resistance

IV. Temperature

V. Material

A.	GaP:N	N.	Cd
B.	GaP:ZnO	O.	CdS
C.	GaSb	P.	CdSe
D.	Ge	Q.	CdSe:CdS
E.	InAs	R.	GaAs
F.	InGaAsP	S.	GaAs:Al
G.	InSb	T.	GaAs:P
H.	LiTa	U.	GaAs:P:N
I.	PbS	V.	GaAsS
J.	Se	W.	GaAsZn
K.	Si	X.	GaInAsP:In
L.	SiC	Y.	GaP
M.	ZnS		

VI. Application

VII. Environment

TABLE 5.6-4. OPTO-ELECTRONIC FIELD FAILURE DATA

Device Type	Style	Material	Environment	Failures	Part Hrs ($x10^6$)
LED	--	GaP	GB	0	9.81
LED	--	GaAsP	GB	22	4817.27
Infrared Emitting Diode	--	GaAs	GB	0	39.19
Alpha-numeric Display	Segment	Si	GB	0	0.86
Alpha-numeric Display	Segment	GaAsP	GB	144	636688.81
Alpha-numeric Display	Diode Array	GaP	GB	0	1.00
Alpha-numeric Display	Diode Array	GaAsP	GB	4	645.09
Photodetector	Photo-diode	Si	GB	0	0.28
Photodetector	Photo-tran-sistor	Si	GB	7	46.74
Opto-isolator	Photo-tran-sistor Output	Si	GB	126	482.36
Opto-isolator	Photo-tran-sistor Output	Si	AIF	0	1.11
Opto-isolator	Photo-tran-sistor Output	GaAs	GB	43	36.96
Opto-isolator	Photodar-lington Output	Si	GB	1	75.01
Opto-isolator	Photo-circuit Output	Si	GB	0	0.52

TABLE 5.6-5. OPTO-ELECTRONIC LIFE TEST DATA

Device Type	Material	Temperature(°C)	Failures	Part Hours (x10^6)
LED	GaAs	10	41	0.333
LED	GaAs	70	1	0.003
LED	GaAs	130	1	0.003
LED	Si	170	43	0.054
LED	GaAs	170	15	0.003
LED	GaAs	190	5	0.003
LED	Si	210	62	0.034
LED	Si	250	69	0.017
Infrared Emitting Diode	--	---	39	1.023
Opto-isolator	Si	10	103	0.647
Opto-isolator	Si	130	60	0.810
Opto-isolator	Si	190	53	0.256
Opto-isolator	Si	230	41	0.312
Opto-isolator	Si	250	80	0.128

TABLE 5.6-6. LASER DIODE LIFE TEST DATA

Material	Package	Application	Case Temperature(°C)	Failures	Part Hrs (x10^6)
AlGaAs	Plastic w/facet coat	CW	70	38	0.119
AlGaAs	Plastic w/facet coat	CW	70	37	0.187
AlGaAs	Plastic w/facet coat	CW	70	6	0.058
AlGaAs	Plastic w/facet coat	CW	22	7	0.750
AlGaAs	Plastic w/facet coat	CW	22	1	0.084
AlGaAs	Plastic w/facet coat	CW	22	0	0.018
AlGaAs	Plastic w/facet coat	CW	70	74	0.451
AlGaAs	Plastic w/facet coat	CW	22	2	0.154
AlGaAs	Plastic w/facet coat	CW	22	1	0.021
AlGaAs	Plastic w/facet coat	CW	22	2	0.008
GaAs	Hermetic	pulsed	22	0	0.637
GaAs	Hermetic	pulsed	65	0	0.091
AlGaAs	Plastic w/facet coat	CW	70	13	0.237
AlGaAs	Plastic w/facet coat	CW	70	0	0.120
AlGaAs	Plastic w/facet coat	pulsed	70	0	0.150
AlGaAs	Plastic w/facet coat	pulsed	70	0	0.070
AlGaAs	Plastic w/facet coat	pulsed	70	0	0.080
AlGaAs	Plastic w/facet coat	CW	70	30	0.180
AlGaAs	Plastic w/facet coat	CW	70	7	0.048

LEDs

The theoretical model for LEDs was determined based on physical failure mechanisms and findings from the literature search. The theoretical model for LEDs was:

$$\lambda_p = \lambda_b \pi_Q \pi_T \pi_E$$

where

λ_p = device failure rate (failures/10^6 hours)

λ_b = base failure rate
= f(material, application current)

π_Q = quality factor

π_T = temperature factor

$$= \exp\left(-A\left(\frac{1}{T_j} - \frac{1}{298}\right)\right)$$

where

A = constant
T_j = junction temperature (^oK)

π_E = environmental factor

The base failure rate was determined to be a function of device material and application current. The data collected for this study included devices with both GaP and GaAsP material. The data did not indicate any difference in failure rate between the two materials. However, there was only a very limited amount of GaP data and thus only a substantial difference in failure rate could have been detected. Since no difference could be detected and no alternative method was available to differentiate by material, it was assumed that the base failure rate was the same for these two materials.

Several references (Ref. 27,30) indicate that application current is an important factor influencing failure rate. One reference (Ref. 27),

however, also indicated that proper device screening can eliminate devices particularly sensitive to application current stress.

NASA Marshall Space Flight Center performed testing on LEDs and other opto-electronic device types (Ref. 65). The dominant observed failure mechanism was degraded LED output caused by dark spots. This mechanism was accelerated by current and temperature. Based on these findings, it was recommended that LEDs are operated at less than 50% of maximum rated current and at a junction temperature less than 80°C. This compares to the recommended RADC derating guidelines of 50% of maximum rated current and 95°C junction temperature.

There was an insufficient range of operating currents and a lack of detail (i.e., it is often difficult to identify operating currents from field data sources) to empirically determine the effects of current. As a result, a constant base failure rate was proposed.

The effects of temperature on LED failure rate have been studied and reported in several different sources. The Marshall Space Flight Center testing indicated an equivalent activation energy of .79 eV. Studies performed by Zipfel, et al (Ref. 27) indicated an equivalent activation energy from .67 to .75 eV for GaAlAs LEDs. IITRI collected life test data on LEDs with test temperature ranging from 10°C to 250°C. Data analysis revealed the following temperature factor,

$$\pi_T = \exp\left(-2650\left(\frac{1}{T_j} - \frac{1}{298}\right)\right), \quad T_j = \text{junction temperature } (^{\circ}K)$$

The LED base failure rate was determined from the collected field data and the factors for temperature quality and environment. The numerical value for base failure rate corresponds to ground fixed environment, JANTX screen class and 25°C, and is given by,

$$\lambda_b = .00023$$

Infrared Emitting Diode

Infrared emitting diodes are not presently included in MIL-HDBK-217E. IITRI collected failure data consisting of zero observed failures in 39.19 x 10^6 part hours. This was insufficient data to apply regression techniques. However, a model was developed based on similarities to LEDs and the available data.

An upper limit on failure rate was computed by assuming one failure. Additionally, the temperature, quality and environment factors for LEDs were assumed to be applicable for infrared devices, thereby completing model development activities for these devices. The infrared emitting diode base failure rate is,

$$\lambda_b = .0013$$

The base failure rate value was determined by normalizing the observed failure rate to a standard set of conditions (i.e., where the Pi factors are equal to one). This was accomplished by:

$$\lambda_b = \frac{\lambda_o}{\pi_T \, \pi_Q \, \pi_E} = \frac{.0255}{(3.21)(7.95)(1.0)} = .0013$$

where

λ_b = base failure rate
λ_o = observed upper limit failure rate = .0255
π_T = temperature factor for 70°C = 3.21
π_Q = quality factor for plastic devices = 7.95
π_E = environmental factor for GB = 1.0

LED Alphanumeric Display

The theoretical failure rate model for LED Alphanumeric displays was determined to be a function of the number of characters, display type (segment vs. diode array), temperature, quality and environment. Segment style alphanumeric displays generally consist of seven segments while a diode array alphanumeric display consists of many diodes forming the alphanumeric characters. IITRI collected data from a variety of device characteristics and quantified the theoretical model through data analysis.

The results of a two-dimensional regression of failure rate versus the number of characters was performed. The dataset included devices ranging from one character to 15 characters. It must be remembered that the number of characters in a display is the number of characters contained in a single sealed package and not the number of separately packaged single characters mounted together. The results of the analysis are:

Segment Display: $\lambda_p' = .0121(C)$
Diode Array: $\lambda_p' = .00229 + .00434(C)$

where C is the number of characters and λ_p' is the predicted failure rate.

LED alpha-numeric displays are available either with or without a logic chip to control display functions. An incremental failure rate contribution of .000043 was determined based on the present MIL-HDBK-217E model.

The effects of temperature on LED alpha-numeric display are similar to that of a single LED, and the same temperature factor was applied. Use of this factor, together with the quality and environmental factor for the

opto-electronic device family, were used to adjust the observed regression results. The resultant base failure rate equations are:

Segment Display: $\lambda_b = .00043(C) + \lambda_{lc}$

Diode Array: $\lambda_b = .000090 + .00017(C) + \lambda_{lc}$

where C is again the number of characters and λ_{lc} is the failure rate contribution of the logic chip (.000043), which assumes a value of zero when there is no logic chip.

Opto-Isolators

Currently, the MIL-HDBK-217E opto-isolator model depends on complexity (single vs. dual), temperature, quality and environment. Separate base failure rates are presented for light sensitive resistors, phototransistor output and photodiode output. IITRI retained this model format, but used the collected data to refine the temperature factor and base failure rate constants.

Opto-isolator life test data was collected for junction temperatures ranging from 130°C to 250°C. This was a sufficient range of temperatures to accurately quantify the equivalent Arhenius relationship constant. The resulting temperature factor is,

$$\pi_T = \exp(-2790(\frac{1}{T_j} - \frac{1}{298})), \quad T_j = \text{junction temperature } (^oK)$$

Field data was collected for phototransistor output and photodarlington output opto-isolators with Si and GaAs materials. The data did not indicate a significant difference between single and dual devices, but did indicate that photodarlington devices have a significantly lower failure rate than do phototransistors. Both of these results seem contrary to the anticipated relationships and are discussed further in the following paragraphs.

Physically, dual devices are expected to fail at a higher rate than single devices. However, no effect could be detected from analysis of the collected dataset. It was hypothesised that the difference between single and dual devices is not large enough to be modeled statistically with the available data. Nevertheless, the data analysis clearly did not disprove the current prediction technique which involves separating single from dual devices.

To evaluate the difference between single and dual devices, ratios from the existing MIL-HDBK-217E opto-electronic models were computed. The ratios between single and dual devices currently presented in MIL-HDBK-217E are as follows:

Device	λ single/λ dual
Photodiode Output	.67
Phototransistor Output	.74
Light Sensitive Resistor	.63
geometric mean	.68

Evaluation of these ratios confirmed the suspicion that the difference between single and dual devices was not large enough to be distinguished statistically. Generally, no influence can be detected from observed failure data which has less than a two-to-one effect. This is primarily due to natural variability in observed failure rates. Nevertheless, it is important that the failure rate prediction models are physically correct, and for that reason it was assumed that the ratio between single and dual opto-isolators is equal to 0.68.

Photodarlington output devices were found to have a lower failure rate than phototransistor devices. From an engineering perspective, this observation does not seem correct.

A comparison of phototransistor and photodarlington transistor failure mechanisms was conducted to understand the empirical results. The primary failure mechanism for phototransistors is ionic contamination.

Phototransistor failure is often accelerated by the comparitively high operating temperature which results from the greater power dissipation of these devices. Photodarlington transistors exhibit all of the failure mechanisms associated with phototransistors plus additional mechanisms from the additional transistor used in photodarlington transistor designs to amplify the output gain. A comparison of phototransistor and photodarlington designs is presented in Figure 5.6-1. The figure clearly indicates the more complex nature of photodarlington devices.

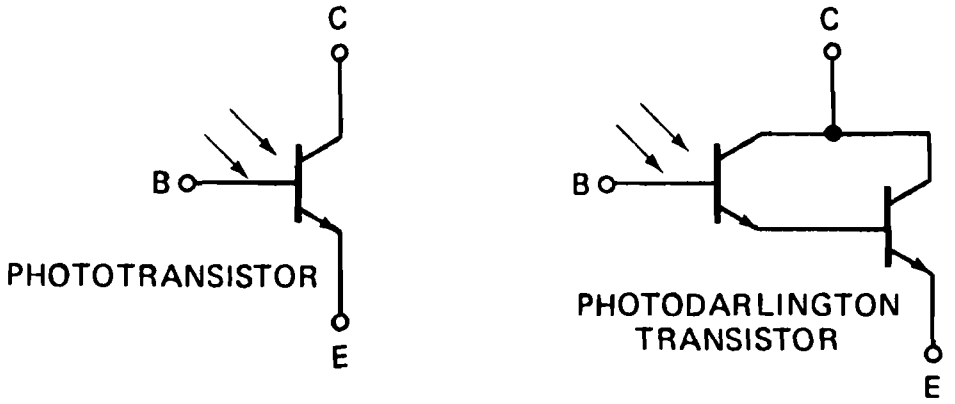

Figure 5.6-1. Comparison of Phototransistor and Photodarlington Transistor Designs

Based on the comparisons of failure mechanisms, it seemed illogical that photodarlington devices exhibted a lower failure rate. Upon further inspection of the data, it was revealed that only one observed failure was collected for photodarlington devices. It can therefore be concluded that the observed lower failure rate was a statistical aberration and not indicative of a failure rate trend. A single base failure rate for both phototransistor and photodarlington devices was then computed by merging the data together.

It had been desired to update the opto-isolator series of models to include devices with a photocircuit output. A small amount of data (0 failures in 0.52×10^6 hours) was collected to support this study effort. This was an insufficient amount to base a new factor and none is proposed.

However, it was not felt that the absence of a photocircuit output option seriously detracts from the utility of the discrete semiconductor reliability prediction models due to the relative infrequency of their usage.

The updated series of base failure rates were then determined based on:

(1) Observed failure rates for phototransistor output and photodarlington output devices

(2) Factors for temperature quality and environment

(3) Ratio between single and dual devices

(4) Existing relationship of photodiode output and light sensitive resistor failure rates to the phototransistor output failure rate

The revised base failure rate constants are:

Single Devices

photodiode output	.0025
phototransistor output	.013
photodarlington output	.013
light sensitive resistor	.0064

Dual Devices

photodiode output	.0033
phototransistor output	.017
photodarlington output	.017
light sensitive resistor	.0086

Photodetectors

The theoretical model developed for photodetectors was similar to those for other opto-electronic devices. The model presented failure rate as a function of device style, temperature, quality and environment. The temperature factor for opto-isolators was also applied to photodetectors.

The opto-electronic quality and environmental factors were applied as well.

Data collected for phototransistors consisted of seven observed failures in 46.74 x 10^6 part hours. A revised base failure rate for phototransistors was determined to be .0055, equal to the observed failure rate divided by the plastic package quality factor and the temperature factor for junction temperature equal to 70°C.

No data was available for photodiodes. A base failure rate of .0040 was determined based on the existing MIL-HDBK-217E ratio of photodiode to phototransistor failure rate (.73) and the previously determined base failure rate for phototransistors.

Laser Diodes

A failure rate prediction model for laser diodes was developed based on analysis of life test data and findings from the literature search. A thorough investigation of laser diode reliability was included in the IITRI study, RADC-TR-83-108, "Reliability Modeling of Critical Electronic Devices" (Ref. 66). The models presented in that document were refined using updated data sources.

The theoretical laser diode model was designed to provide sensitivity to known laser diode failure mechanisms. Generally, laser diode failure mechanisms are classified either as catastrophic, gradual degradation or functional degradation. Catastrophic failures are caused by optical flux density, metalization and bonding anomalies. Gradual degradation is related to the electron-hole recombination process and is dependent on the laser technology and operating conditions. Functional degradation failures are related to the ability of the laser to function in specific

design applications. Specifically laser diode failure mechanisms can be categorized as:

- o Catastrophic
  - P-side Metalization Breakdown (Ref. 52)
  - Catastrophic Facet Damage (Ref. 52,67,68)
- o Gradual Degradation
  - Dark Line Defects (Ref. 67)
  - Dark Spot Defects (Ref. 67)
  - Thermal Resistance Degradation (Ref. 67,68,69)
  - Homogeneous Degradation (Ref. 67)
  - Non-catastrophic Facet Deterioration (Ref. 52,67,68,70)
- o Functional Degradation
  - Intensity Pulsations (Ref. 52,67,71,72)
  - Optical Frequency Shifts (Ref. 67,71)
  - Light Intensity Changes (Ref. 67,71)

The theoretical model developed for laser diodes was,

$$\lambda = f(\text{material, application, facet coating, environment, package type, } I, T_C, P_S, P_r, DC)$$

where

T_C = case temperature (^oK)
P_s = rated optical power output (mW)
P_r = required optical power output (mW)
DC = duty cycle

Grouping the independent variables into MIL-HDBK-217E style modifying factors results in the following model format:

$$\lambda_p = \lambda_b \, \pi_T \, \pi_i \, \pi_A \, \pi_P \, \pi_Q \, \pi_E$$

where

λ_p = predicted failure rate (failures/10^6 operating hours)

λ_b = base failure rate, based on material

π_T = temperature factor

$= \exp(-A_t(\frac{1}{T_j} - \frac{1}{298}))$, A_t = constant, based on material

π_i = forward current factor
$= (I)^n$

where

I = forward peak current (amps)
n = constant

π_A = application factor
$= f_1$(pulsed vs. CW, DC)

π_p = power degradation factor
$= f_2(P_s, P_r)$

π_Q = quality factor
$= f_3$(facet coating, package type)

π_E = environmental factor

Laser diode failure mechanisms are accelerated by increasing temperature. The theoretical model assumes that failure rate can be predicted using the equivalent Arrhenius equation. The literature includes many estimates of laser diode activation energy. A summary is as follows:

Reference	Material	E_a(eV)
32	AlGaAs	.62
35	GaAs	.34
73	GaAs	.7-1.1
33	AlGaAs	.70
34	AlGaAs	.9-1.3
31	AlGaAs	.8
74	AlGaAs	.7-.9
29	---	.75
75	AlGaAs	.7-.9

Several observations regarding activation energies are relevant to this discussion of laser diode reliability. First, activation energies based on field data or from more extensive testing (with a large temperature range) invariably tend to produce lower activation energies than from less extensive testing. It is hypothesized that this is because at high temperatures, a single highly temperature sensitive mechanism (i.e., bulk diffusion) dominates. At lower temperatures additional mechanisms become more relevant. The second observation is that the presence of other Pi factors which correlate with temperature, tend to minimize or mask the apparent effects of temperature. Yoshida et al (Ref. 74), whose work indicated an activation energy of .7 to .9 eV, explained that the presence of a factor for forward current results in an estimated activation energy of .3 to .4 eV when degradation rate data was compensated (i.e., normalized) for the forward current effect. This is due to the natural correlation between temperature and forward current.

The literature strongly supports the necessity of an application factor (π_A) dependent on whether the laser operates under pulsed or CW conditions, and the duty cycle, if pulsed. The consensus is clearly that CW laser diodes fail more often that pulsed devices. Research by Barry and Mecherle (Ref. 35) indicates that the ratio between CW and pulsed failure rate is 21.6. This relationship is also supported by the findings presented by Yoshida et al (Ref. 74), which compared the degradation rates of (1) CW devices, (2) pulsed devices with 50% duty cycle, and (3) pulsed devices with 20% duty cycles. The testing clearly indicated that CW operations performed the worst, pulsed with low (20%) duty cycle performed the best and pulsed with high (50%) duty cycle fell between the extremes. These findings also support the contention that an application factor should depend on duty cycle for pulsed applications.

The laser diode model presented in RADC-TR-83-108 (Ref. 66) indicates a forward current factor of the form:

$\pi_I = (I)^{.68}$, where I = forward peak current (ma)

Several references support this model factor. In particular, Kumada et al (Ref. 32) concludes that operating current is among the dominant influences on laser diode lifetime. This reference pertained to testing of a 800 nm wavelength AlGaAs semiconductor laser.

There are no standardized screening or quality levels for laser diodes. Thus, it becomes difficult to determine an applicable quality factor. Clearly, several observed failure mechanisms can be avoided by proper screening (Ref. 71). However, due to the lack of quality standardization, quality factor development focused on physical characteristics including the presence of facet coating and the package type.

All data collected for laser diodes was life test data. As a result it was impossible to empirically determine environmental factors. It is recommended that laser diode reliability models use the same series of factors as the opto-electronic device family.

The life test data for laser diodes was previously presented in Table 5.6-5. Analysis of this data using regression techniques resulted in the following preliminary model.

$$\lambda_p' = \lambda_b' \pi_T' \pi_Q' \pi_A'$$

where

λ_p' = predicted failure rate (failures/10^6 hrs)

λ_b' = preliminary base failure rate
= 20.8, AlGaAs
= 19.1, GaAs

π_T' = preliminary temperature factor

$= \exp(-3270(\frac{1}{T_j} - \frac{1}{298}))$, T_j = junction temperature (^oC)

π_A' = preliminary application factor
= 1.0, CW
= .12, pulsed

π_Q' = preliminary quality factor
= 1.0 hermetic package
= 1.0 facet coating
= 4.2 nonhermetic package without facet coating

Each of these variables was significant with 90% confidence with the exception of material (AlGaAs vs. GaAs) which was insignificant. This variable was not included in subsequent analyses. Later in the development process, a separate base failure constant is proposed for InGaAs/InGaAsP.

The observed results are generally in agreement with the RADC-TR-83-108 model factors for quality and temperature activation energy, and the existing factors were retained. A cosmetic change was made to the temperature factor equation by introducing a reference temperature term (298°C). No data was available for InGaAs or InGaAsP laser diodes. The RADC-TR-83-108 temperature factor constant (-5784) for these materials was retained.

The observed relationship for application confirmed the conclusions from the literature that CW failure rates are higher than pulsed. There was insufficient data, however, to develop a factor for pulsed applications dependent on duty cycle. To provide the model with the required sensitivity, the RADC-TR-83-108 relationship for duty cycle was assumed to be correct. This factor (designated π_f in RADC-TR-83-109) is given by the following equation,

$$\pi_f = (\text{duty cycle})^{0.5}$$

An application factor for CW was then determined by:

(1) The average duty cycle was found from the pulsed device data records in Table 5.6-5. This average value was 28%.

(2) The RADC-TR-83-108 duty cycle factor (designated π_f in RADC-TR-83-108 but integrated into π_A in this study) was computed. π_f was equal to 0.53 for 28% duty factor.

(3) The ratio of CW-to-pulsed failure rate was taken from the regression results (1.0 ÷ .12 = 8.33).

(4) An application factor for CW applications was computed by multiplying the average duty cycle factor (0.53) by the CW-to-pulsed ratio (8.33) (8.33 x 0.53 = 4.4). These results indicate that CW devices fail at a rate 4.4 times higher than pulsed devices with a duty cycle of 100%, and 8.33 times higher then pulsed devices with a duty cycle of 28%. This step was necessary because a π_f value of one corresponds to a duty cycle of 100% and not 28% (i.e., the average from the collected data). Thus, the observed ratio of CW-to-pulsed could not be incorporated directly into π_A but had to be normalized.

(5) The resulting factor is therefore equal to 4.4 for CW applications and the square root of duty cycle (from RADC-TR-83-108) for pulsed applications. Duty cycle is measured as a decimal (i.e., .50) and not as a percentage (i.e., 50%).

The regression results did not indicate that forward peak current was a significant variable. However, this was primarily due to the presence of data records where the forward peak current was unknown. It was concluded that the regression results represented insufficient evidence to delete this factor and it was retained. A minor change was made to set the current factor equal to one when forward peak current is equal to one amp. It was believed that the corresponding range of factor values (.13 - 8.9) resulted in a more usable model format then the previous range (14 - 978) when forward peak current is varied from 50 milliamps to 25 amps. Since the models are multiplicative in nature, changes in any factor are compensated by corresponding inverse changes in the base failure rate. It was the goal of this study for base failure rate values to correspond to failure rates for a standard set of conditions, and therefore it is imperative that each Pi factor have one option where the factor is equal to one.

Given the refinements to the regression results the model takes the following form.

$$\lambda_p = \lambda_b \pi_T \pi_A \pi_i \pi_Q \pi_E$$

where

λ_p = laser diode failure rate (failures/10^6 operating hours)

λ_b = base failure rate
= 3.23, AlGaAs/GaAs

π_T = temperature factor

$$= \exp\left(-4635\left(\frac{1}{T_j} - \frac{1}{298}\right)\right), \text{ AlGaAs/GaAs}$$

π_A = application factor
= 4.4, CW
= (duty cycle)$^{0.5}$, pulsed

π_i = forward current factor
= $(I)^{.68}$, I = forward peak current (amps)

π_Q = quality factor
= 1.0 hermetic package
= 1.0 facet coating used
= 3.0 nonhermetic package without facet coating

π_E = environmental factor (see Table 5.6-2)

Two final modifications were made to conclude model development activities for laser diodes. First, the equivalent activation energy for InGaAsP devices was retained from the RADC-TR-83-108 model and a corresponding base failure rate computed. Second, a power degradation factor was determined from the RADC-TR-83-108 prediction methods.

The existing temperature constant for InGaAs/InGaAsP devices is -5784. The corresponding base failure rate is 5.65.

There is a fairly detailed procedure in RADC-TR-83-108 to compute failure rate. A summary follows:

STEP 1A: Compute average optical power output degradation rate

STEP 1B: Compute the mean life based on the rated optical power (P_s), the required optical power output (P_r) and the degradation rate from STEP 1A.

STEP 1C: Compute the average failure rate

STEP 2: Compute final failure rate

As part of this study effort, IITRI consolidated the procedure into one model requiring a single step. To accommodate the procedures from STEP 1B above, an additional factor was required. This factor was designated the power degradation factor and is given by

$$\pi_p = 0.5\ P_s/(P_s - P_r)$$

Derivation of the power degration factor concludes the model development activity for laser diodes. This model provides improved failure rate prediction accuracy and sensitivity to failure accelerating stresses.

5.7 NONOPERATING FAILURE RATES

As a complement to the development of operating failure rate prediction models, models were also developed to predict the failure rate of discrete semiconductor devices during nonoperating periods. The IITRI study RADC-TR-85-91, "Impact of Nonoperating Periods on Equipment Reliability" (Ref. 48) was used as a basis for model development activities.

5.7.1 Proposed Nonoperating Failure Rate Prediction Models

Failure rate prediction models were developed to predict the failure rate of discrete semiconductor devices during nonoperating periods. The proposed nonoperating failure rate model for diodes is:

$$\lambda_p = \lambda_{nb}\ \pi_{NT}\ \pi_{NQ}\ \pi_{NE}\ \pi_{cyc}$$

where

λ_p = predicted diode/thyristor nonoperating failure rate

λ_{nb} = nonoperating base failure rate (failure/10^6 operating hours)
= .000083, general purpose (switching, analog, rectifier)
= .00040, voltage reference, voltage regulator
= .00063, thyristor
= .0027, high frequency (Schottky, point contact, varactor, step recovery, tunnel/back, Gunn, IMPATT, PIN)

π_{NT} = nonoperating temperating factor

$$= \exp\left(-A_n\left(\frac{1}{T_n + 273} - \frac{1}{298}\right)\right)$$

where

T_n = nonoperating temperature (^oC)
A_n = temperature factor constant (see Table 5.7-1)

π_{NQ} = nonoperating quality factor (see Table 5.7-2)
π_{NE} = nonoperating environmental factor (see Table 5.7-3)
π_{cyc} = equipment power on-off cycling factor
$= 1 + .083(N_c)$

where

N_c = number of equipment power on-off cycles per 10^3 nonoperating hours

The nonoperating failure rate prediction model for transistors is:

$$\lambda_p = \lambda_{nb}\ \pi_{NT}\ \pi_{NQ}\ \pi_{NE}\ \pi_{cyc}$$

where

λ_p = predicted transistor nonoperating failure rate

λ_{nb} = nonoperating base failure rate (failure/10^6 operating hours)
= .000082, bipolar transistors
= .00039, FETs
= .0013, unijunction
= .041, microwave power transistors

π_{NT} = nonoperating temperature factor

$$= \exp\left(-A_n\left(\frac{1}{T_n + 273} - \frac{1}{298}\right)\right)$$

where

A_n = temperature factor coefficient (see Table 5.7-1)
T_n = nonoperating temperature (^oC)

π_{NQ} = nonoperating quality factor (see Table 5.7-2)

π_{NE} = nonoperating environmental factor (see Table 5.7-3)

π_{cyc} = equipment power on-off cycling factor
$= 1 + .050(N_c)$

where

N_c = number of equipment power on-off cycles per 10^3 nonoperating hours

The proposed nonoperating failure rate prediction model for opto-electronic semiconductor devices is the following equation:

$$\lambda_p = \lambda_{nb}\, \pi_{NQ}\, \pi_{NE}$$

where

λ_p = predicted opto-electronic semiconductor nonoperating failure rate

λ_{nb} = nonoperating base failure rate (failures/10^6 operating hours)
= .00016, LED
= .00070, Single Opto-Isolator
= .00089, Dual Opto-Isolator
= .00038, Phototransistor
= .00028, Photodiode
= .00025, Alphanumeric Displays

π_{NQ} = nonoperating quality factor (see Table 5.7-2)

π_{NE} = nonoperating environmental factor (see Table 5.7-3)

TABLE 5.7-1. NONOPERATING TEMPERATURE FACTOR CONSTANTS

Part	Style	A_n
Transistors	Bipolar, Si	2114
	Bipolar, Ge	3521
	FET	1925
	Unijunction	2483
	RF Power	2903
Diodes	GP, Si	3091
	GP, Ge	4914
	Voltage Reference/ Voltage Regulator	1718
	Thyristor	3082
	High Frequency	2100

5.7-2. NONOPERATING QUALITY FACTORS

Quality Level	π_{NQ}
JANTXV	0.7
JANTX	1.0
JAN	2.4
Lower	5.5
Plastic	8.0

5.7-3. NONOPERATING ENVIRONMENTAL FACTOR

Env.	π_{NE}	Env.	π_{NE}
G_B	1	A_{IA}	23
G_{MS}	1.5	A_{IF}	38
G_F	4.9	A_{UC}	20
G_M	18	A_{UT}	28
M_P	12	A_{UB}	55
N_{SB}	7.3	A_{UA}	38
N_S	7.3	A_{UF}	58
N_U	20	S_F	1.0
N_H	20	M_{FF}	12
N_{UU}	20	M_{FA}	17
A_{RW}	27	U_{SL}	36
A_{IC}	12	M_L	41
A_{IT}	18	C_L	690
A_{IB}	32		

5.7.2 Nonoperating Model Development

The method utilized to develop nonoperating failure rate prediction models consisted of analysis of data from long-term nonoperating or storage applications. The analysis methodology paralleled the methods described in RADC-TR-85-91 (Ref. 48) with the additional requirement that the predicted nonoperating failure rate always be less than the corresponding proposed operating failure rate. The nonoperating failure data is presented in Tables 5.7-4 and 5.7-5 for diodes and transistors, respectively. The dataset used for this study was the same as used in RADC-TR-85-91.

It was necessary to ensure that the operating failure rates were greater than the nonoperating failure rate for all cases. In the RADC-TR-85-91 program, there were infrequent instances when the resulting predicted nonoperating failure rate was larger than the corresponding MIL-HDBK-217E predicted operating failure rate. Primary reasons for this seemingly inconsistency were that:

(1) For some discrete semiconductor part types, both the operating and nonoperating failure rates are so low that prediction model precision is comparitively poor.

(2) Prediction models and the resultant reliability predictions, at best, represent a sampling mean of a diverse group of devices and applications. Since sampling means deviate from the true, unknown mean, there is always a small but finite probability that the mean computed from one population will exceed the mean computed from another population which actually has a higher true mean. The distribution of sampling means tends to be normal (due to the central limit theorem) and the variance is based on the sample size.

(3) Entirely different samples (i.e., different part numbers, equipments, data collection periods) were used for the MIL-HDBK-217E modeling process (RADC-TR-78-3) and the nonoperating failure rate prediction modeling process; thereby, introducing natural variation caused by uncontrolled samples.

TABLE 5.7-4. DIODE NONOPERATING FAILURE DATA

Diode Style/ Classification	Diode Application	Quality Level	App Env.	Part Hrs. ($\times 10^6$)	# Failed
Gen. Purpose	N/R	JAN	GB	25061.000	2
Si, Gen. Purpose	N/R	JAN	GF	20028.361	18
Si, Gen. Purpose	N/R	JAN	GB	6364.083	41
Si, Gen. Purpose	N/R	JANTX	GF	11717.907	2
Si, Gen. Purpose	N/R	N/R	GB	3462.338	0
Si, Gen. Purpose	N/R	N/R	GF	400.000	1
Si, Gen. Purpose	N/R	Plastic	GF	1558.000	40
Si, Gen. Purpose	Power Rectifier $\leq$500mA	JAN	GB	11276.200	1
Si, Gen. Purpose	Power Rectifier $\leq$500mA	JANTX	GF	241.075	0
Si, Gen. Purpose	Power Rectifier $\leq$500mA	N/R	GF	0.717	0
Si, Gen. Purpose	Power Rectifier H.V. Stacks	JANTX	GF	0.669	0
Si, Gen. Purpose	Switching <500mA	JAN	GB	180698.700	8
Si, Gen. Purpose	Switching <500mA	JAN	GF	76.562	0
Si, Gen. Purpose	Switching <500mA	JAN	N/R	293.489	0
Si, Gen. Purpose	Switching <500mA	JANTX	GF	1003.867	0
Si, Gen. Purpose	Switching <500mA	N/R	GF	164.870	0
Si, Gen. Purpose	Voltage Regulator	JAN	GB	5770.520	2
Si, Gen. Purpose	Voltage Regulator	JANTX	GF	2.124	0
Zener & Avalanche	N/R	JAN	GB	824.360	0
Zener & Avalanche	N/R	JAN	GF	954.000	3
Zener & Avalanche	N/R	JANTX	GF	175.000	1
Zener & Avalanche	N/R	Plastic	GF	47.000	5
Zener & Avalanche	Power Rectifier $\leq$500mA	JANTX	GF	2.282	0
Zener & Avalanche	Voltage Reference	JAN	GB	1154.100	0
Zener & Avalanche	Voltage Reference	JAN	N/R	607.000	0
Zener & Avalanche	Voltage Reference	JANTX	GF	1400.477	4
Zener & Avalanche	Voltage Reference	N/R	GF	0.496	0

TABLE 5.7-4. DIODE NONOPERATING FAILURE DATA (CONT'D)

Diode Style/ Classification	Diode Application	Quality Level	App Env.	Part Hrs. ($x10^6$)	# Failed
Zener & Avalanche	Voltage Regulator	JAN	GB	27368.730	0
Zener & Avalanche	Voltage Regulator	JAN	GF	306.248	0
Zener & Avalanche	Voltage Regulator	JANTX	GF	391.210	0
Thyristors	N/R	JAN	GF	165.000	1
Thyristors	N/R	JANTX	GF	509.157	1
Thyristors	N/R	Plastic	GF	11.500	16
Microwave Detector	N/R	JANTX	GF	170.147	0
Step Recovery	N/R	N/R	GF	17.015	0
Tunnel	N/R	JANTX	GF	2.000	0
Varactor	N/R	JANTX	GF	19.015	2

TABLE 5.7-5. TRANSISTOR NONOPERATING FAILURE DATA

Style/ Classification	Application	Complexity	Quality Level	Env.	Part Hours ($\times 10^6$)	# Failed
Ge, NPN	N/R	N/R	JANTX	N/R	21.000	0
Ge, PNP	N/R	N/R	JAN	GB	164.870	0
Ge, PNP	N/R	N/R	JANTX	GF	13.140	0
Ge, PNP	N/R	N/R	JANTX	N/R	45.000	0
Si, NPN	High Freq.	N/R	N/R	N/R	0.669	0
Si, NPN	Linear	Single	JAN	GB	3297.400	0
Si, NPN	Linear	Single	JAN	GF	319.010	1
Si, NPN	N/R	Dual (Matched)	JAN	GB	2308.200	0
Si, NPN	N/R	Dual (Unmatched)	JANTX	GF	102.088	0
Si, NPN	N/R	N/R	JAN	GB	20.760	12
Si, NPN	N/R	N/R	JAN	GF	4044.000	8
Si, NPN	N/R	N/R	JANTX	GF	2984.629	6
Si, NPN	N/R	N/R	JANTX	N/R	5329.000	7
Si, NPN	N/R	N/R	JANTXV	GF	1.886	0
Si, NPN	N/R	Single Device	JAN	GF	242.448	2
Si, NPN	N/R	Single Device	JANTX	GF	5138.436	6
Si, NPN	Switch	N/R	JAN	GB	3132.600	0
Si, NPN	Switch	Single Device	JAN	GB	57537.900	4
Si, NPN	Switch	Single Device	JAN	GF	76.562	1
Si, NPN	Linear	Single Device	JAN	GF	25.521	0
Si, PNP	N/R	Dual (Unmatched)	JANTX	GF	170.147	0
Si, PNP	N/R	N/R	JAN	GB	5.090	3
Si, PNP	N/R	N/R	JAN	GF	1961.000	6
Si, PNP	N/R	N/R	JAN	N/R	3.620	0

TABLE 5.7-5. TRANSISTOR NONOPERATING FAILURE DATA (CONT'D)

Style/ Classification	Application	Complexity	Quality Level	Env.	Part Hours ($x10^6$)	# Failed
Si, PNP	N/R	N/R	JANTX	GF	2031.016	4
Si, PNP	N/R	N/R	JANTX	N/R	1327.000	1
Si, PNP	N/R	N/R	JANTXV	GF	10.240	0
Si, PNP	N/R	N/R	N/R	GF	1.936	0
Si, PNP	N/R	Single Device	JANTX	GF	2331.014	2
Si, PNP	Switch	Single Device	JAN	GB	61662.300	1
FET	N/R	Dual (Unmatched)	JANTX	GF	340.294	1
FET	N/R	N/R	JANTX	GF	41.180	0
FET	N/R	N/R	JANTX	N/R	72.000	0
FET	N/R	Single Device	JANTX	GF	2160.866	2
Si, FET	Linear	Single Device	JAN	GB	2308.200	0
Si, FET	N/R	N/R	JAN	GF	1136.000	8
Si, FET	N/R	Single Device	JAN	GF	25.521	0
Unijunct	N/R	N/R	JAN	GF	5.000	0
Unijunct	N/R	N/R	JANTX	N/R	1.000	0
Unijunct	N/R	Single Device	JAN	GB	1483.800	0
Microwave	N/R	N/R	JANTX	GF	17.014	1

Several universal changes were made to the RADC-TR-85-91 nonoperating failure rate prediction models. They are:

(1) The nonoperating quality factors were updated to reflect improvements in processing and technology, as were the operating quality factors.

(2) The nonoperating equivalent activation energies were compared to the corresponding values developed in this study; if the RADC-TR-85-91 nonoperating values were larger, then the operating values were assumed.

(3) The environmental factor series were consolidated (to be consistent with the proposed series of operating environmental factors).

The first required modification was to assign the operating quality factors developed in this study to the nonoperating discrete semiconductor models. This modification is a result of the contention in RADC-TR-85-91 that the effect of screening is smaller for nonoperating failure rates than operating failure rates.

The second change was to compare operating and nonoperating equivalent activation energies. The operating value (A) was assumed to be applicable for the nonoperating case if it was larger than the RADC-TR-85-91 nonoperating temperature value (A_n). This represents a practical more than an engineering or physics-of-failure change. The failure mechanisms acting during operating and nonoperating states are different and thus, different equivalent activation energies should be acceptable. However, it was found from a thorough exercising of the RADC-TR-85-91 models that certain examples existed where the nonoperating failure rate stayed below the operating until a certain temperature range and then surpassed the operating failure rate. Since the field nonoperating data was for low temperatures, a relatively small estimation error in the equivalent activation energy can cause this conflict at higher temperatures. It was desired to remove this conflict by assuming similar activation energies for the operating and nonoperating states. Other research by IITRI (Ref.

78) for microcircuit nonoperating reliability indicates that operating and nonoperating activation energies are generally similar. If this is also true for discrete semiconductors, then assumption of the operating temperature factor constants does not negatively impact nonoperating failure rate estimation.

The nonoperating model development process was then performed with the following steps:

(1) Universal changes applied

(2) Nonoperating base failure rate estimated from collected data

(3) Comparison with operating failure rate

(4) Adjustment to base failure rate to ensure a minimum of two-to-one difference between operating and nonoperating failure rates (in most instances the ratio is much greater than two-to-one).

The adjustments to the base failure rates were only required for switching diodes and bipolar transistors. The changes were small enough so that nonoperating failure rate prediction accuracy would not be impaired, yet useful to provide a physically correct series of models.

6.0 CONCLUSIONS

Failure rate prediction models were developed for the discrete semiconductor family of devices. Existing MIL-HDBK-217E failure rate prediction models were evaluated and revised if deemed necessary. New failure rate prediction models were developed for parts not currently included in MIL-HDBK-217E.

The model development process consisted of collection and analysis of field reliability data and an in-depth investigation of physical failure modes/mechanisms. Significant parameters found to influence failure rate were device construction, semiconductor material, junction temperature, electrical stresses, environment, package type and screen class.

Results of the data analyses indicated a general reliability growth process for high frequency and high power devices. For these device types, the observed failure rates are lower than was previously indicated in MIL-HDBK-217E. For other device types there has been either a gradual decrease in failure rate or no apparent change.

A major effort was successfully completed to improve the usability of the discrete semiconductor section. The failure rate prediction process was made more efficient by:

- Consolidation of redundant quality factor tables
- Consolidation of redundant environmental factor tables
- Definition of a separate temperature factor
- Junction temperature estimation based on thermal resistances
- Elimination of insignificant model factors

New failure rate prediction models were developed for the following device types:

- GaAs power FETs
- Transient suppressors
- Infrared LEDs

- o Diode array displays
- o Current regulator diodes

Inclusion of these devices into MIL-HDBK-217E improves prediction capabilities for equipments utilizing them.

In several instances, the resultant failure rate prediction models are not as sophisticated or as sensitive as was orignally intended, resulting entirely from a lack of "hard" failure data. Improved data tracking capabilities or alternate methods of failure rate prediction model development will be required as failure rates continue to fall.

7.0 RECOMMENDATIONS

It is recommended that the updated discrete semiconductor failure rate prediction section (presented in Appendix A) be included in the next revision of MIL-HDBK-217E. Use of these revised failure rate prediction models will improve equipment reliability prediction accuracy and will provide a better tool for reliability engineers to use for design trade-off analyses.

Technological advancements are continually being made to improve the performance and to expand the power-frequency characteristics of GaAs power FETs, IMPATT diodes and other devices. These advancements will continue to result in lower failure rates as today's advanced performance requirements become standardized. Also, technological advancements will expand the set of conditions where the models should apply. For these reasons, it is recommended that the prediction models be evaluated on a continual basis and appropriate changes be made every three to five years to better reflect these advancements. Additionally, new device types such as HEMTs and GaAs MMICs need to be considered in future reliability studies.

It was noted during this study that many of the part and equipment manufacturers were reluctant to furnish uncontracted data free of charge. This reluctance may be attributed to material and manpower costs incurred in providing the data or to the proprietary nature of the data. The study contractor is normally not provided with sufficient funds to allow for the purchase of these data. The government should investigate methods for enforcing automatic distribution of the data to a central repository such as the Reliability Analysis Center (a DoD Information Analysis Center) that is available to all government contractors.

APPENDIX A1:

PROPOSED REVISION PAGES

FOR MIL-HDBK-217E

5.1.3 Discrete Semiconductor. The semiconductor transistor, diode and opto-electronic device sections present the failure rates on the basis of device type and construction. An analytical model of the failure rate is also presented for each device category.

The various types of discrete semiconductor devices require different failure rate models that vary to some degree. The semiconductor generic groups are shown in Table 5.1.3-1. The specific failure rate model and the π factor values for each group are shown in the section dealing with that particular group and at the end of the Discrete Semiconductor section.

TABLE 5.1.3-1: DISCRETE SEMICONDUCTOR GENERIC GROUPS

Part Type	Group
Low Frequency Diodes General Purpose Diodes Analog Switching Fast Recovery Power Rectifiers Voltage Regulator/Voltage Reference Varistor, Suppressor Diodes Current Regulator Diodes	I
High Frequency (Microwave, RF) Diodes PIN Gunn Tunnel, Back (including Mixers, Detectors) Si IMPATT Schottky Barrier (including Detectors) and Point Contact Varactor and Step Recovery	II
Low Frequency Transistors Bipolar FETs Unijunction Transistors	III IV V
High Frequency (Microwave, RF) Transistors Bipolar ($\geq$200 MHz) Low Power (< 1 W) High Power ($\geq$ 1 W) FETs GaAs ($\geq$1 GHz, Avg. Power <100 mW) GaAs ($\geq$1 GHz, Avg. Power $\geq$100 mW) Si (>400 MHz & Avg. Power <300 mW)	VI VII
Thyristors, SCRs	VIII
Opto-Electronics	IX

DISCRETE SEMICONDUCTORS

The initial grouping of discrete semiconductor device models is based on frequency, either Low Frequency or High Frequency. The definition of Low versus High Frequency varies depending on the part type. Table 5.1.3-2 presents frequency classifications to aid MIL-HDBK-217E users.

TABLE 5.1.3-2: FREQUENCY CLASSIFICATIONS

Part Type	High Frequency	Low Frequency
Diodes	The division of high and low frequency diodes is based on part construction, and application rather than a specified fequency level (see Table 5.1.3-1).	
Transistors		
Bipolar	<200 MHZ	≥200 MHz
FET		
Si	≤400 MHz	>400 MHz
GaAs	--	≥1 GHz

The applicable MIL specification for transistors, and opto-electronic devices diodes is MIL-S-19500. The quality levels (JAN, JANTX, JANTXV) are as defined in MIL-S-19500.

The general failure rate model for transistors, diodes and opto-electronic devices is:

$$\lambda_p = \lambda_b \, \pi_A \, \pi_r \, \pi_s \, \pi_c \, \pi_Q \, \pi_T \, \pi_E$$

where

λ_p = device failure rate (failures/10^6 operating hours)
λ_b = base failure rate (failures/10^6 operating hours)
π_A = application factor
π_r = electrical rating factor
π_s = electrical stress factor
π_c = construction factor
π_Q = quality factor
π_T = temperature factor
π_E = environmental factor

The temperature factor is based on the device junction temperature. Junction temperature is computed based on worst case power (or maximum power dissipation) and the thermal resistance (^oC). Determination of junction temperatures is explained in Section 5.1.3.10.2.

DISCRETE SEMICONDUCTORS

LOW FREQUENCY DIODES

5.1.3.1 Group I, Low Frequency Diodes

SPECIFICATION	DESCRIPTION
MIL-S-19500	Low Frequency Diodes; analog, switching, fast recovery, power rectifier, voltage regulator, voltage reference, varistor, transient suppressors, current regulator

Part operating failure rate model (λ_p):

$$\lambda_p = \lambda_b \pi_S \pi_C \pi_Q \pi_T \pi_E \text{ failures}/10^6 \text{ operating hours}$$

where

λ_b = base failure rate, Table 5.1.3.1-1

π_S = voltage stress factor, Table 5.1.3.1-2

π_C = contact construction factor
= 1.0, metallurgically bonded
= 2.0, non-metallurgically bonded and spring loaded contacts

π_Q = quality factor, Table 5.1.3.10.1-1 in Section 5.1.3.10.1

π_T = temperature factor, Table 5.1.3.10.1-3 in Section 5.1.3.10.1

π_E = environmental factor, Table 5.1.3.10.1-6 in Section 5.1.3.10.1

TABLE 5.1.3.1-1: LOW FREQUENCY DIODE BASE FAILURE RATE (λ_b)

Style/Application	base failure rate (λ_b)
Analog	.0038
Switching	.0023
Fast Recovery	.069
Power Rectifier/Schottky Power Diode	.011
Power Rectifier with H.V. Stacks	.019/Junction
Voltage Regulator	.0047
Voltage Reference	.0047
Transient Suppressor (Varistor)	.0013
Current Regulator	.0034

TABLE 5.1.3.1-2: VOLTAGE STRESS FACTOR (π_S)

Style	$\frac{\text{Voltage Applied}}{\text{Voltage Rated}}$	π_S
Voltage Regulator	--	1.0
Voltage Reference	--	1.0
Transient Suppressor (Varistor)	--	1.0
Current Regulator	--	1.0
All Other Diodes	$Vs \leq .3$	.054
	$.3 < Vs \leq .4$	.11
	$.4 < Vs \leq .5$	.19
	$.5 < Vs \leq .6$	.29
	$.6 < Vs \leq .7$	.42
	$.7 < Vs \leq .8$	.58
	$.8 < Vs \leq .9$	.77
	$.9 < Vs \leq 1.0$	1.0

π_S = 1.0, Voltage Regulator, Voltage Reference, Current Regulator, Transient Suppressor (Varistor)

$\pi_S = .054$, $Vs \leq .3$

$\pi_S = (Vs)^{2.43}$, $Vs > .3$

Vs = voltage stress = (Voltage Applied/Voltage Rated)

DISCRETE SEMICONDUCTORS

HIGH FREQUENCY DIODES

5.1.3.2 Group II, High Frequency Diodes

SPECIFICATION	DESCRIPTION
MIL-S-19500	Si IMPATT; Bulk Effect, Gunn; Tunnel, Back; Mixer, Detector; PIN; Schottky; Varactor, Step Recovery

Si IMPATT Diodes

Part operating failure rate model for IMPATT diodes (only applicable for frequencies $\leq$35 GHz) (λ_p):

$$\lambda_p = \lambda_b \pi_Q \pi_T \pi_E \quad \text{failure}/10^6 \text{ operating hours}$$

where

λ_b = base failure rate
= .2235

π_Q = quality factor, Table 5.1.3.10.1-1 in Section 5.1.3.10.1

π_T = temperature factor, Table 5.1.3.10.1-4 in Section 5.1.3.10.1

π_E = environmental factor, Table 5.1.3.10.1-6 in Section 5.1.3.10.1

DISCRETE SEMICONDUCTORS

HIGH FREQUENCY DIODES

Gunn/Bulk Effect Diodes

Part operating failure rate model for Gunn and Bulk Effect diodes (λ_p):

$$\lambda_p = \lambda_b \pi_Q \pi_T \pi_E \text{ failures}/10^6 \text{ operating hours}$$

where

λ_b = base failure rate
= .18

π_Q = quality factor, Table 5.1.3.10.1-1 in Section 5.1.3.10.1

π_T = temperature factor, Table 5.1.3.10.1-4 in Section 5.1.3.10.1

π_E = environmental factor, Table 5.1.3.10.1-6 in Section 5.1.3.10.1

DISCRETE SEMICONDUCTORS

HIGH FREQUENCY DIODES

Tunnel and Back Diodes (Including Mixers, Detectors)

Part operating failure rate model for Tunnel and Back diodes, including Mixers/Detectors (λ_p):

$$\lambda_p = \lambda_b \pi_Q \pi_T \pi_E \text{ failures}/10^6 \text{ operating hours}$$

where

λ_b = base failure rate
= .0023

π_Q = quality factor, Table 5.1.3.10.1-1 in Section 5.1.3.10.1

π_T = temperature factor, Table 5.1.3.10.1-4 in Section 5.1.3.10.1

π_E = environmental factor, Table 5.1.3.10.1-6 in Section 5.1.3.10.1

DISCRETE SEMICONDUCTORS

HIGH FREQUENCY DIODES

PIN Diodes

Part operating failure rate model for PIN diodes (λ_p):

$$\lambda_p = \lambda_b \pi_r \pi_Q \pi_T \pi_E \quad \text{failures}/10^6 \text{ operating hours}$$

where

λ_b = base failure rate
= .0081

π_r = power rating factor, Table 5.1.3.2-1

π_Q = quality factor, Table 5.1.3.10.1-1 in Section 5.1.3.10.1

π_T = temperature factor, Table 5.1.3.10.1-4 in Section 5.1.3.10.1

π_E = environmental factor, Table 5.1.3.10.1-6 in Section 5.1.3.10.1

TABLE 5.1.3.2-1: POWER RATING FACTOR (π_r)

Power Rating (watts)	π_r
$P_r \leq 10$	0.5
$10 < P_r \leq 100$	1.3
$100 < P_r \leq 1000$	2.0
$1000 < P_r \leq 3000$	2.4

$$\pi_r = .326 \ln(P_r) - .25$$

P_r = power rating (watts)

DISCRETE SEMICONDUCTORS

HIGH FREQUENCY DIODES

Schottky Diodes (Including Detectors)

Part operating failure rate model for Si Schottky and Point Contact diodes (operating frequencies between 200 MHz and 35 GHz) (λ_p):

$$\lambda_p = \lambda_b \pi_Q \pi_T \pi_E \quad \text{failures}/10^6 \text{ operating hours}$$

where

λ_b = base failure rate
= .027

π_Q = quality factor, Table 5.1.3.10.1-1 in Section 5.1.3.10.1

π_T = temperature factor, Table 5.1.3.10.1-4 in Section 5.1.3.10.1

π_E = environmental factor, Table 5.1.3.10.1-6 in Section 5.1.3.10.1

DISCRETE SEMICONDUCTORS

HIGH FREQUENCY DIODES

Varactor and Step Recovery Diodes

Part operating failure rate model for Varactors and Step Recovery diodes (λ_p):

$$\lambda_p = \lambda_b \pi_A \pi_Q \pi_T \pi_E \quad \text{failures}/10^6 \text{ operating hours}$$

where

λ_b = base failure rate
= .0025

π_A = application factor
= 0.5, varactor, voltage control
= 2.5, varactor, multiplier
= 1.0, step recovery

π_Q = quality factor, Table 5.1.3.10.1-1 in Section 5.1.3.10.1

π_T = temperature factor, Table 5.1.3.10.1-4 in Section 5.1.3.10.1

π_E = environmental factor, Table 5.1.3.10.1-6 in Section 5.1.3.10.1

DISCRETE SEMICONDUCTORS

LOW FREQUENCY TRANSISTORS, BIPOLAR

5.1.3.3 Group III, Low Frequency Transistors, Bipolar

SPECIFICATION	DESCRIPTION
MIL-S-19500	Si, NPN Si, PNP Ge, NPN Ge, PNP

Part operating failure rate model (λ_p) for Si and Ge NPN and PNP transistors is:

$$\lambda_p = \lambda_b \pi_A \pi_r \pi_S \pi_Q \pi_T \pi_E \quad \text{failures}/10^6 \text{ operating hours}$$

where

λ_b = base failure rate
= .00074

π_A = application factor
= 1.5, linear
= 0.7, switching

π_r = power rating factor, Table 5.1.3.3-1

π_S = voltage stress factor, Table 5.1.3.3-2

π_Q = quality factor, Table 5.1.3.10.1-1 in Section 5.1.3.10.1

π_T = temperature factor, Table 5.1.3.10.1-2 in Section 5.1.3.10.1

π_E = environmental factor, Table 5.1.3.10.1-6 in Section 5.1.3.10.1

DISCRETE SEMICONDUCTORS

LOW FREQUENCY TRANSISTORS, BIPOLAR

TABLE 5.1.3.3-1: POWER RATING FACTOR (π_r)

Power Rating (Watts)	π_r
0.1	0.43
0.5	0.77
1.0	1.0
5.0	1.8
10	2.3
50	4.3
100	5.5
500	10

$\pi_r = 0.43$, rated power $\leq .1$ W

$\pi_r = (\text{rated power})^{.37}$, rated power $> .1$ W

TABLE 5.1.3.3-2: VOLTAGE STRESS FACTOR (π_S)

Voltage Stress $(\frac{\text{Applied } V_{CE}}{\text{Rated } V_{CEO}})$	π_S
$0 < Vs \leq 0.3$	.10
$0.3 < Vs \leq 0.4$	.16
$0.4 < Vs \leq 0.5$	.21
$0.5 < Vs \leq 0.6$	.27
$0.6 < Vs \leq 0.7$	.39
$0.7 < Vs \leq 0.8$	.54
$0.8 < Vs \leq 0.9$	.73
$0.9 < Vs \leq 1.0$	1.0

$$\pi_S = .045 \exp\left(3.1\left(\frac{\text{Applied } V_{CE}}{\text{Rated } V_{CEO}}\right)\right)$$

DISCRETE SEMICONDUCTORS

LOW FREQUENCY TRANSISTORS, FET

5.1.3.4 Group IV, Low Frequency Transistors, FET

SPECIFICATION	DESCRIPTION
MIL-S-19500	Si, FET (frequency $\leq$400 MHz)

Part operating failure rate model (λ_p) for N-Channel and P-Channel Si Field Effect Transistors is:

$$\lambda_p = \lambda_b \pi_A \pi_Q \pi_T \pi_E \quad \text{failures}/10^6 \text{ operating hours}$$

where

λ_b = base failure rate
= .012, MOSFET
= .0045, JFET

π_A = application factor
= 1.5, linear
= 0.7, switching
= 10, power FET (average power >250W)

π_Q = quality factor, Table 5.1.3.10.1-1 in Section 5.1.3.10.1

π_T = temperature factor, Table 5.1.3.10.1-2 in Section 5.1.3.10.1

π_E = environmental factor, Table 5.1.3.10.1-6 in Section 5.1.3.10.1

5.1.3.5 Group V, Unijunction Transistors

SPECIFICATION	DESCRIPTION
MIL-S-19500	Unijunction Transistors

Part operating failure rate model (λ_p):

$$\lambda_p = \lambda_b \pi_Q \pi_T \pi_E \quad \text{failures}/10^6 \text{ operating hours}$$

where

λ_b = base failure rate
= .0083

π_Q = quality factor, Table 5.1.3.10.1-1 in Section 5.1.3.10.1

π_T = temperature factor, Table 5.1.3.10.1-2 in Section 5.1.3.10.1

π_E = environmental factor, Table 5.1.3.10.1-6 in Section 5.1.3.10.1

DISCRETE SEMICONDUCTORS

MICROWAVE, RF BIPOLAR TRANSISTORS

5.1.3.6 Group VI, High Frequency Transistors, Bipolar

SPECIFICATION	DESCRIPTION
MIL-S-19500	Bipolar Microwave RF transistor (frequencies above 200 MHz); Low Power (< 1 W) and High Power (≥ 1 W)

Low Noise RF Transistor (Average Power <1W)

Part operating failure rate model (λ_p) for Low Noise RF Transistors (average power <1W):

$$\lambda_p = \lambda_b \pi_r \pi_s \pi_Q \pi_T \pi_E \text{ failures/}10^6 \text{ operating hours}$$

where

λ_b = base failure rate
= .18

π_r = power rating factor, Table 5.1.3.6-1

π_s = voltage stress factor, Table 5.1.3.6-2

π_Q = quality factor, Table 5.1.3.10.1-1 in Section 5.1.3.10.1

π_T = temperature factor, Table 5.1.3.10.1-2 in Section 5.1.3.10.1

π_E = environmental factor, Table 5.1.3.10.1-6 in Section 5.1.3.10.1

DISCRETE SEMICONDUCTORS

MICROWAVE, RF BIPOLAR TRANSISTORS

TABLE 5.1.3.6-1: POWER RATING FACTOR (π_r)

Power Rating (Watts)	π_r
$\leq$.1	.43
.2	.55
.3	.64
.4	.71
.5	.77
.6	.83
.7	.88
.8	.92
.9	.96

π_r = .43, rated power $\leq$ .1W
π_r = (rated power)$^{.37}$, rated power > .1W

TABLE 5.1.3.6-2: VOLTAGE STRESS FACTOR (π_S)

Voltage Stress $(\frac{\text{Applied } V_{CE}}{\text{Rated } V_{CEO}})$	π_S
0 < Vs $\leq$ .3	.10
.3 < Vs $\leq$ .4	.16
.4 < Vs $\leq$ .5	.21
.5 < Vs $\leq$ .6	.27
.6 < Vs $\leq$ .7	.39
.7 < Vs $\leq$ .8	.54
.8 < Vs $\leq$ .9	.73
.9 < Vs $\leq$ 1.0	1.0

$$\pi_S = .045 \exp\left(3.1\left(\frac{\text{Applied } V_{CE}}{\text{Rated } V_{CEO}}\right)\right)$$

DISCRETE SEMICONDUCTORS

MICROWAVE, RF BIPOLAR TRANSISTORS

Power Microwave, RF Transistors (Average Power ≥1W)

Part operating failure rate model (λ_p) for Bipolar microwave, RF Transistors (average power ≥1W):

$$\lambda_p = \lambda_b \pi_A \pi_{pw} \pi_m \pi_Q \pi_T \pi_E \text{ failures/}10^6 \text{ operating hours}$$

where

λ_b = base failure rate, Table 5.1.3.6-3

π_A = application factor, Table 5.1.3.6-4

π_{pw} = pulse width factor, Table 5.1.3.6-5

π_m = matching network factor
= 1.0, input and output internal matching
= 2.0, input internal matching
= 4.0, no internal matching

π_Q = quality factor, Table 5.1.3.10.1-1 in Section 5.1.3.10.1

π_T = temperature factor, Table 5.1.3.6-6

π_E = environmental factor, Table 5.1.3.10.1-6 in Section 5.1.3.10.1

DISCRETE SEMICONDUCTORS

MICROWAVE/RF BIPOLAR TRANSISTORS

5.1.3.6-3: RF POWER TRANSISTOR BASE FAILURE RATE (λ_b)

Frequency (GHz)	Average Output Power (Watts)								
	1.0	5.0	10	50	100	200	300	400	500
0.5	.038	.039	.040	.050	.067	.12	.20	.36	.62
1	.046	.047	.048	.060	.080	.14	.24	.42	.74
2	.065	.067	.069	.086	.11	.20	.34		
3	.093	.095	.098	.12	.16	.28			
4	.13	.14	.14	.17	.23				
5	.19	.19	.20	.25					

$$\lambda_b = .032 \exp(.354(f) + .00558(P))$$

where

f = frequency (GHz)
P = average output power (watts)

NOTE: The average output power refers to the power level for the overall packaged device and not to individual transistors within the package (if more than one transistor is ganged together).

DISCRETE SEMICONDUCTORS

MICROWAVE/RF BIPOLAR TRANSISTORS

TABLE 5.1.3.6-4: APPLICATION FACTOR (π_A)

Application	Duty Factor	π_A
CW	N/A	.40
Pulsed	≤ 1%	.46
	5%	.70
	10%	1.0
	15%	1.3
	20%	1.6
	25%	1.9
	30%	2.2

π_A = .06(Duty Factor) + .40, pulsed

TABLE 5.1.3.6-5: PULSE WIDTH FACTOR

Application	Pulse Width (milliseconds)	π_{pw}
CW	N/A	1.0
Pulsed	≤ 0.5	1.0
	1.0	1.1
	5.0	1.6
	10	2.2
	15	2.8
	20	3.5
	25	4.1

π_{pw} = .127(PW) + .937, pulsed

PW = pulse width (milliseconds)

DISCRETE SEMICONDUCTORS

MICROWAVE/RF BIPOLAR TRANSISTORS

TABLE 5.1.3.6-6: RF POWER TRANSISTORS TEMPERATURE FACTOR (π_T)

Junction Temp. (°C)	V_{CE}/BV_{CES}			
	0.40	0.45	0.50	0.55
≤100	.34	.67	1.0	1.3
110	.41	.82	1.2	1.6
120	.50	1.0	1.5	2.0
125	.55	1.1	1.6	2.2
130	.60	1.2	1.8	2.4
140	.71	1.4	2.1	2.8
150	.84	1.7	2.5	3.4
160	.98	2.0	3.0	3.9
170	1.1	2.3	3.4	4.6
180	1.3	2.6	4.0	5.3
190	1.5	3.0	4.6	6.1
200	1.7	3.5	5.1	6.9

$$\pi_T = .34 \exp\left(-2903\left(\frac{1}{T_j + 273} - \frac{1}{373}\right)\right), \quad (V_{CE}/BV_{CES}) \leq 0.40$$

$$\pi_T = 6.7((V_{CE}/BV_{CES}) - .35) \exp\left(-2903\left(\frac{1}{T_j + 273} - \frac{1}{373}\right)\right), \quad (V_{CE}/BV_{CES}) > 0.40$$

DISCRETE SEMICONDUCTORS

MICROWAVE/RF FIELD EFFECT TRANSISTORS (FETS)

5.1.3.7 Group VII, High Frequency Transistors, FET

SPECIFICATION	DESCRIPTION
MIL-S-19500	GaAs Power FETs (Power ≥ 100 mW) GaAs FETs (Power < 100 mW) Si FETs (Power < 100 mW)

GaAs Power FET

Part operating failure rate model (λ_p) for GaAs power FETs (output power ≥ 100 mW):

$$\lambda_p = \lambda_b \pi_A \pi_m \pi_Q \pi_T \pi_E \quad \text{failures}/10^6 \text{ operating hours}$$

where

λ_b = base failure rate, Table 5.1.3.7-1

π_A = application factor
= 1.0, pulsed applications
= 5.0, CW applications

π_m = matching network factor
= 1.0, input and output internal matching
= 2.0, input internal matching
= 4.0, no internal matching

π_Q = quality factor, Table 5.1.3.10.1-1 in Section 5.1.3.10.1

π_T = temperature factor, Table 5.1.3.10.1-2 in Section 5.1.3.10.1

π_E = environmental factor, Table 5.1.3.10.1-6 in Section 5.1.3.10.1

DISCRETE SEMICONDUCTORS

GaAs FETs ($\geq$ 1 GHz)

5.1.3.7-1: GaAs POWER FET BASE FAILURE RATES (λ_b)

Operating Frequency (GHz)	Average Output Power (Watts)					
	.1	.5	1	2	4	6
4	.054	.066	.084	.14	.36	.96
5	.083	.10	.13	.21	.56	1.5
6	.13	.16	.20	.32	.85	2.3
7	.20	.24	.30	.50	1.3	3.5
8	.30	.37	.47	.76	2.0	
9	.46	.56	.72	1.2		
10	.71	.87	1.1	1.8		

$$\lambda_b = .0093 \exp(.429(f) + .486(P))$$

where

f = frequency (GHz)
P = Average Output Power (Watts)

DISCRETE SEMICONDUCTORS

GaAs FETs ($\geq$ 1 GHz)

GaAs FET

Part operating failure rate model (λ_p) for GaAs FETs (output power < 100 mW):

$$\lambda_p = \lambda_b \pi_A \pi_Q \pi_T \pi_E \quad \text{failures}/10^6 \text{ operating hours}$$

where

λ_b = base failure rate
= .052

π_A = application factor
= 1.0, low noise
= 7.1, driver

π_Q = quality factor, Table 5.1.3.10.1-1 in Section 5.1.3.10.1

π_T = temperature factor, Table 5.1.3.10.1-2 in Section 5.1.3.10.1

π_E = environmental factor, Table 5.1.3.10.1-6 in Section 5.1.3.10.1

DISCRETE SEMICONDUCTORS

MICROWAVE/RF Si FETs

Low Noise Si FETs (frequency > 400 MHz, avg. power < 300 mW)

Part operating failure rate model (λ_p) for Low Noise Microwave/RF Si FETs:

$$\lambda_p = \lambda_b \pi_Q \pi_T \pi_E \quad \text{failures}/10^6 \text{ operating hours}$$

where

λ_b = base failure rate
= .060, MOSFET
= .023, JFET

π_Q = quality factor, Table 5.1.3.10.1-1 in Section 5.1.3.10.1

π_T = temperature factor, Table 5.1.3.10.1-2 in Section 5.1.3.10.1

π_E = environmental factor, Table 5.1.3.10.1-6 in Section 5.1.3.10.1

DISCRETE SEMICONDUCTORS

THYRISTOR AND SCR

5.1.3.8 Group VIII, Thyristors and SCRs

SPECIFICATION	DESCRIPTION
MIL-S-19500	Thyristors SCRs

Part operating failure rate model for Thyristors and SCRs (λ_p):

$$\lambda_p = \lambda_b \pi_r \pi_s \pi_Q \pi_T \pi_E \quad \text{failures}/10^6 \text{ operating hours}$$

where

λ_b = base failure rate
= .0022

π_r = power rating factor, Table 5.1.3.8-1

π_s = voltage stress factor, Table 5.1.3.8-2

π_Q = quality factor, Table 5.1.3.10.1-1 in Section 5.1.3.10.1

π_T = temperature factor, Table 5.1.3.10.1-4 in Section 5.1.3.10.1

π_E = environmental factor, Table 5.1.3.10.1-6 in Section 5.1.3.10.1

DISCRETE SEMICONDUCTORS

THYRISTOR AND SCR

TABLE 5.1.3.8-1: THYRISTOR CURRENT RATING FACTOR (π_r)

Rated Forward (I_f(rms)) (amps)	π_r	Rated Forward (I_f(rms)) (amps)	π_r
.05	.31	80	5.5
0.1	.41	90	5.8
0.5	.76	100	6.0
1.0	1.0	110	6.2
5.0	1.9	120	6.5
10	2.5	130	6.7
20	3.2	140	6.9
30	3.8	150	7.1
40	4.2	160	7.2
50	4.6	170	7.4
60	4.9	175	7.5
70	5.2		

$$\pi_r = (I_f(rms))^{.40}$$

TABLE 5.1.3.8-2: THYRISTOR VOLTAGE STRESS FACTOR (π_S)

$\frac{\text{Blocking Voltage (Applied)}}{\text{Blocking Voltage (Rated)}}$	π_S
$Vs \leq 0.3$	.10
$0.3 < Vs \leq 0.4$	.17
$0.4 < Vs \leq 0.5$	.27
$0.5 < Vs \leq 0.6$	.38
$0.6 < Vs \leq 0.7$	.51
$0.7 < Vs \leq 0.8$	.65
$0.8 < Vs \leq 0.9$	.83
$0.9 < Vs \leq 1.0$	1.0

$\pi_S = .10$, $Vs \leq 0.3$

$\pi_S = (Vs)^{1.9}$, $Vs > 0.3$

$$Vs = \frac{\text{Blocking Voltage (Applied)}}{\text{Blocking Voltage (Rated)}}$$

5.1.3.9 Group IX, Opto-Electronics

SPECIFICATION	DESCRIPTION
MIL-S-19500	Photodetectors Opto-isolators Emitters Alphanumeric Displays Laser Diodes

Photodetectors

Part operating failure rate model for Photodetectors (λ_p):

$$\lambda_p = \lambda_b \pi_Q \pi_T \pi_E$$

where

λ_b = base failure rate,
= .0055, phototransistors
= .0040, photodiodes

π_Q = quality factor, Table 5.1.3.10.1-1 in Section 5.1.3.10.1

π_T = temperature factor, Table 5.1.3.10.1-5 in Section 5.1.3.10.1

π_E = environmental factor, Table 5.1.3.10.1-6 in Section 5.1.3.10.1

Opto-Isolators

Part operating failure rate model for Opto-Isolators (λ_p):

$$\lambda_p = \lambda_b \pi_Q \pi_T \pi_E$$

where

λ_b = base failure rate
- = .0025, Photodiode output, single device
- = .013, Phototransistor output, single device
- = .013, Photodarlington output, single device
- = .0064, Light sensitive resistor, single device
- = .0033, Photodiode output, dual device
- = .017, Phototransistor output, dual device
- = .017, Photodarlington output, dual device
- = .0086, Light sensitive resistor, dual device

π_Q = quality factor, Table 5.1.3.10.1-1 in Section 5.1.3.10.1

π_T = temperature factor, Table 5.1.3.10.1-5 in Section 5.1.3.10.1

π_E = environmental factor, Table 5.1.3.10.1-6 in Section 5.1.3.10.1

DISCRETE SEMICONDUCTORS

OPTO-ELECTRONICS

Emitters (LED, IRED)

Part operating failure rate model for Emitters (λ_p):

$$\lambda_p = \lambda_b \pi_Q \pi_T \pi_E$$

where

λ_b = base failure rate
= .0013, Infrared Light-Emitting Diode (IRED)
= .00023, Light-Emitting Diode (LED)

π_Q = quality factor, Table 5.1.3.10.1-1 in Section 5.1.3.10.1

π_T = temperature factor, Table 5.1.3.10.1-5 in Section 5.1.3.10.1

π_E = environmental factor, Table 5.1.3.10.1-6 in Section 5.1.3.10.1

Alphanumeric Displays

Part operating failure rate model for Alphanumeric Displays (λ_p):

$$\lambda_p = \lambda_b \pi_Q \pi_T \pi_E$$

where

λ_b = base failure rate, Table 5.1.3.9-1

π_Q = quality factor, Table 5.1.3.10.1-1 in Section 5.1.3.10.1

π_T = temperature factor, Table 5.1.3.10.1-5 in Section 5.1.3.10.1

π_E = environmental factor, Table 5.1.3.10.1-6 in Section 5.1.3.10.1

TABLE 5.1.3.9-1: ALPHANUMERIC DISPLAY BASE FAILURE RATE (λ_b)

Characters	Segment Display	Diode Array Display
1	.00043	.00026
1 w/logic chip	.00047	.00030
2	.00086	.00043
2 w/logic chip	.00090	.00047
3	.00129	.00060
3 w/logic chip	.00133	.00064
4	.00172	.00077
4 w/logic chip	.00176	.00081
5	.0022	.00094
6	.0026	.0011
7	.0031	.0013
8	.0035	.0015
9	.0039	.0016
10	.0043	.0018
11	.0048	.0020
12	.0052	.0021
13	.0056	.0023
14	.0060	.0025
15	.0065	.0026

$\lambda_b = .00043(C) + \lambda_{\ell C}$, segment displays

$\lambda_b = .00009 + .00017(C) + \lambda_{\ell C}$, diode array displays

where

C = number of characters

$\lambda_{\ell C}$ = .000043, displays with a logic chip
= 0, displays without a logic chip

NOTE: The number of characters in a display is the number of characters contained in a single sealed package. For example, a 4 character display comprising 4 separately packaged single characters mounted together would be 4-one character displays, not 1-four character display.

DISCRETE SEMICONDUCTORS

OPTO-ELECTRONICS

Laser Diodes

Part operating failure rate model for laser diodes (with optical flux densities < 3 mW/cm^2 and forward current < 25 amps) (λ_p):

$$\lambda_p = \lambda_b \pi_i \pi_A \pi_p \pi_Q \pi_T \pi_E$$

where

λ_b = base failure rate
= 3.23 GaAs/AlGaAs
= 5.65 InGaAs/InGaAsP

π_i = forward peak current factor, Table 5.1.3.9-2

π_A = application factor, Table 5.1.3.9-3

π_p = power degradation factor, Table 5.1.3.9-4

π_Q = quality factor
= 1.0, hermetic package
= 1.0, nonhermetic (with facet coating)
= 3.3, nonhermetic (without facet coating)

π_T = temperature factor, Table 5.1.3.10.1-5 in Section 5.1.3.10.1

π_E = environmental factor, Table 5.1.3.10.1-6 in Section 5.1.3.10.1

DISCRETE SEMICONDUCTORS

OPTO-ELECTRONICS

TABLE 5.1.3.9-2: LASER DIODE FORWARD CURRENT FACTOR (π_i)

Current (Amps)	π_i
.050	.13
.075	.17
.1	.21
.5	.62
1.0	1.0
2.0	1.6
3.0	2.1
4.0	2.6
5.0	3.0
10	4.8
15	6.3
20	7.7
25	8.9

$$\pi_i = (I)^{.68}$$

where

I = Forward Peak Current (amps), $I \leq 25$ amps

NOTE: For variable current sources use the initial current value

TABLE 5.1.3.9-3: LASER DIODE APPLICATION FACTOR (π_A)

Application	Duty Cycle	π_A
CW	--	4.4
Pulsed	0.1	0.32
	0.2	0.45
	0.3	0.55
	0.4	0.63
	0.5	0.71
	0.6	0.77
	0.7	0.84
	0.8	0.89
	0.9	0.95
	1.0	1.0

$\pi_A = 4.4$, CW

$\pi_A = (\text{duty cycle})^{0.5}$, pulsed

TABLE 5.1.3.9-4: POWER DEGRADATION FACTOR (π_p)

Ratio P_r/P_s	π_p
0.0	.50
.05	.53
.10	.56
.15	.59
.20	.63
.25	.67
.30	.71
.35	.77
.40	.83
.45	.91

Ratio P_r/P_s	π_p
.50	1.0
.55	1.1
.60	1.3
.65	1.4
.70	1.7
.75	2.0
.80	2.5
.85	3.3
.90	5.0
.95	10

$$\pi_p = \frac{0.5P_s}{(P_s - P_r)}$$

where

P_s = rated optical power output (mW)
P_r = required optical power output (mW)

NOTE: Each laser diode must be replaced when power output falls to P_r for failure rate prediction to be valid

5.1.3.10 Instructions for Use of Discrete Semiconductor Models

This section is divided into three subsections. First, common tables are presented which apply to more than one discrete semiconductor part style. Specifically, tables are presented for quality, temperature and environment. The second subsection provides detailed instructions to compute junction temperature and temperature factor. The third subsection includes sample failure rate calculations.

5.1.3.10.1 Common Tables

TABLE 5.1.3.10.1-1: QUALITY FACTORS (π_Q)

Part Type				
Quality Class	Non-R.F. Devices/ Opto-Electronics (Groups, I, III, IV, V, VIII, IX)	High Freq. Diodes (1) (Group II excluding Schottky)	RF Transistors(2) (Group VI, VII)	Schottky Diodes(1) (>200 MHz)
JANTXV	.7	0.5	0.5	.5
JANTX	1.0	1.0	1.0	1.0
JAN	2.4	5.0	2.0	1.8
Lower	5.5	25.0	5.0	2.5
Plastic	8.0	50.0	-	-

NOTES: (1) For high frequency part classes not specified to MIL-S-19500, equivalent quality classes are defined as devices meeting the same requirements provided in MIL-S-19500

(2) For RF Power Transistors ($\geq$200 MHz & avg. power $\geq$ watt), JANTXV quality class must include IR scan for die attach and screen for barrier layer pinholes on gold metallized devices.

TABLE 5.1.3.10.1-2: TEMPERATURE FACTOR FOR TRANSISTORS (π_T)

Junction/ Channel Temp. (°C)	Bipolar* NPN/PNP		Silicon FET	Unijunction	GaAs FETs	
	Si	Ge			<100mW	≥100mW
25	1.0	1.0	1.0	1.0	1.0	1.0
35	1.2	1.5	1.2	1.3	1.6	1.8
45	1.6	2.1	1.5	1.7	2.6	3.1
55	1.9	2.9	1.8	2.1	4.0	5.1
65	2.3	4.0	2.1	2.7	5.9	8.2
75	2.8	5.5	2.5	3.3	8.7	13
85	3.3	7.2	3.0	4.0	12	20
95	3.8	9.5	3.4	4.9	18	29
105	4.5	12	3.9	5.8	24	43
115	5.2	--	4.5	6.9	33	62
125	5.9	--	5.1	8.1	44	87
135	6.9	--	5.7	9.4	58	121
145	7.7	--	6.4	11	75	165
155	8.6	--	7.1	13	97	221
165	9.6	--	7.9	14	123	293
175	11	--	8.7	16	154	384

$$\pi_T = \exp\left(-A\left(\frac{1}{T_j + 273} - \frac{1}{298}\right)\right)$$

where

A = temperature coefficient (see Table 5.1.3.10.2-1)
T_j = junction/channel temperature (°C) (see Section 5.1.3.10.2 for junction temperature determination)

*NOTE:

This table does not apply to RF Power Transistors (see Table 5.1.3.6-6 in Section 5.1.3.6 for these devices)

TABLE 5.1.3.10.1-3: TEMPERATURE FACTOR FOR LOW FREQUENCY DIODES (<200 MHz) (π_T)

Junction Temp. (°C)	V. Regulator/ V. Reference	Current Regulator	Transient Suppressor	General Purpose	
				Si	Ge
25	1.0	1.0	1.0	1.0	1.0
35	1.2	1.2	1.5	1.4	1.7
45	1.4	1.5	2.2	1.9	2.8
55	1.7	1.8	3.2	2.5	4.5
65	2.0	2.1	4.5	3.4	7.0
75	2.3	2.5	6.3	4.4	11
85	2.6	3.0	8.5	5.7	16
95	3.0	3.4	11	7.2	23
105	3.4	3.9	15	9.0	--
115	3.8	4.5	19	11	--
125	4.3	5.1	25	14	--
135	4.7	5.7	31	16	--
145	5.2	6.4	39	20	--
155	5.8	7.1	49	23	--
165	6.3	7.9	60	28	--
175	6.9	8.7	72	32	--

$$\pi_T = \exp\left(-A\left(\frac{1}{T_j + 273} - \frac{1}{298}\right)\right)$$

where

A = temperature coefficient (see Table 5.1.3.10.2-1)

T_j = junction temperature (°C) (see Section 5.1.3.10.2 for junction temperature determination)

TABLE 5.1.3.10.1-4. TEMPERATURE FACTOR FOR HIGH FREQUENCY DIODES (≥200 MHz) AND THYRISTORS (π_T)

Junction Temp. (°C)	PIN/Tunnel Back	Thyristors/ SCR	Si IMPATT	Schottky Barrier	Varactor/ Step Recovery	Gunn
25	1.0	1.0	1.0	1.0	1.0	1.0
35	1.3	1.4	1.8	1.2	1.3	1.3
45	1.6	1.9	3.0	1.4	1.6	1.7
55	1.9	2.6	5.0	1.6	1.9	2.2
65	2.3	3.4	8.1	1.8	2.3	2.8
75	2.8	4.4	13	2.1	2.8	3.4
85	3.3	5.6	19	2.4	3.3	4.2
95	3.8	7.1	29	2.6	3.8	5.1
105	4.4	8.9	42	3.0	4.4	6.2
115	5.1	11	60	3.3	5.1	7.3
125	5.9	13	84	3.6	5.9	8.7
135	6.7	16	117	4.0	6.7	10
145	7.6	20	159	4.3	7.6	12
155	8.5	23	213	4.7	8.5	14
165	9.5	27	282	-	9.5	16
175	11	32	369	-	11	18

$$\pi_T = \exp\left(-A\left(\frac{1}{T_j + 273} - \frac{1}{298}\right)\right)$$

where

A = temperature coefficient (see Table 5.1.3.10.2-1)

T_j = junction temperature (°C) (see Section 5.1.3.10.2 for junction temperature determination)

DISCRETE SEMICONDUCTORS

TABLE 5.1.3.10.1-5: TEMPERATURE FACTOR FOR OPTO-ELECTRONIC DEVICES (π_T)

Temp. (°C)	LED & Displays (All Types)	Photo-detectors Opto-Isolators	Laser Diodes	
			GaAs/ AlGaAs	InGaAs/InGaAsp
5	.53	.51	.33	.25
15	.73	.72	.58	.51
25	1.0	1.0	1.0	1.0
35	1.3	1.4	1.7	1.9
45	1.7	1.8	2.7	3.4
55	2.3	2.4	4.1	5.9
65	2.9	3.0	6.3	9.9
75	3.6	3.8	9.3	16
85	4.4	4.8		
95	5.4	5.9		
105	6.6	7.3		
115	7.9	8.8		

$$\pi_T = \exp\left(-A\left(\frac{1}{T_j + 273} - \frac{1}{298}\right)\right)$$

where

A = temperature coefficient (see Table 5.1.3.10.2-1)

T_j = junction temperature (°C) (see Section 5.1.3.10.2 for junction temperature determination)

DISCRETE SEMICONDUCTORS

TABLE 5.1.3.10.1-6: ENVIRONMENTAL FACTORS FOR DISCRETE SEMICONDUCTOR DEVICES (π_E)

Env.	Non-RF Diodes Transistors, and Thyristors (Groups I, III, IV, V, VIII)	High Frequency Diodes and Transistors (Groups II, VI, VII)	Opto-Electronics (Group IX)
G_B	1.0	1.0	1.0
G_{MS}	1.6	1.1	1.2
G_F	5.5	2.0	2.4
G_M	17	4.9	7.8
M_P	13	4.9	7.7
N_{SB}	8.0	3.6	3.7
N_S	9.5	4.7	5.7
N_U	19	11	12
N_{UU}	19	11	12
N_H	19	11	12
A_{IC}	13	3.7	3.8
A_{IT}	13	3.7	3.8
A_{IB}	13	3.7	3.8
A_{IA}	30	4.6	5.8
A_{IF}	28	4.6	5.8
A_{UC}	20	7.0	5.5
A_{UT}	20	7.0	5.5
A_{UB}	20	7.0	5.5
A_{UA}	45	12	7.8
A_{UF}	41	12	7.8
A_{RW}	24	16	17
U_{SL}	30	22	23
S_F	1.0	1.0	1.0
M_{FF}	12	7.5	7.8
M_{FA}	16	11	11
M_L	33	55	26
C_L	320	250	450

5.1.3.10.2 Temperature Factor Determination

This section applies to all devices but RF bipolar power transistors (Group V Transistors). For RF bipolar power transistor temperature factor, see Section 5.1.3.6.

The temperature factor for discrete semiconductor devices is of the form:

$$\pi_T = \exp\left(-A\left(\frac{1}{T_j + 273} - \frac{1}{298}\right)\right)$$

where

A = equivalent activation energy divided by Boltzman's constant (given in Table 5.1.3.10.2-1)

T_j = device junction/channel temperature (^oC)

Determining the value of the temperature factor is a two stage process. First, determine the device junction temperature, and second, look up the π_T value corresponding to that device type and junction temperature in Tables 5.1.3.10.1-2 through 5.1.3.10.1-5.

STEP 1: Calculate T_j as follows:

STEP 1A: Determine ambient or case temperature. If unknown, assume the following default ambient values.

TYPICAL AMBIENT TEMPERATURES FOR ALL ENVIRONMENTS

Env.	T_A	Env.	T_A
G_B	30	U_{SL}	35
G_{MS}	31	A_{IA}	55
G_F	40	A_{IB}	55
G_M	55	A_{IC}	55
M_A	45	A_{IF}	55
M_{FF}	45	A_{IT}	55
M_L	55	A_{RW}	55
M_P	35	A_{UA}	71
N_H	40	A_{UB}	71
N_S	40	A_{UC}	71
N_{SB}	40	A_{UF}	71
N_U	75	A_{UT}	71
N_{UU}	20	C_L	40
S_F	30		

STEP 1B: Determine thermal resistance (θ) from junction-air (if ambient temperature is used) or junction-to-case (if case temperature is used).

In the case where a heat sink is used, total junction-to-ambient thermal resistance is given by:

$$\theta_{JA} = \theta_{JC} + \theta_{CA}$$

where

θ_{JA} = total junction-to-ambient thermal resistance

θ_{JC} = device junction-to-case thermal resistance

θ_{CA} = thermal resistance of heat sink to ambient

Device thermal resistances should be taken from manufacturer's specification sheets or MIL slash sheets whichever θ is greater. If the value is not given outright, it can be obtained by taking the inverse of the derating value.

Example 1:

Given: Derate a particular device at 3.33 mW/^{o}C for T_C > 25^{o}C.

Calculate θ_{JC}:

$$\theta_{JC} = 1/3.33 \text{ mW}/^{o}\text{C} = 300^{o}\text{C/W}$$

Example 2:

Given: A particular device has the following specifications:

$\overline{P_D}$ = 400 mW (maximum power)

$\overline{T_j}$ = 175^{o}C (maximum junction temperature)

T_A = 25^{o}C (maximum ambient temperature)

TABLE 5.1.3.10.2-1: TEMPERATURE FACTOR COEFFICIENTS

Part Class	A
Transistors	
Bipolar, Si	2,114
Bipolar, Ge	3,521
FET, Si	1,925
Unijunction	2,483
RF Power (2)	2,903
GaAs FET (3)	4,485
GaAs Power FET (3)	5,297
Diodes	
General Purpose, Si (4)	3,091
General Purpose, Ge (4)	4,914
Voltage Ref./Voltage Reg.	1,718
Current Regulator	1,925
Transient Suppressor/Varistor	3,810
Schottky/Barrier, Si	1,522
Varactor/Step Recovery/PIN	2,100
Tunnel/Back/Mixer/Detector	2,100
Gunn	2,562
IMPATT	5,260
Thyristor	3,082
Opto-Electronics	
Photodetectors	2,790
Opto-Isolators	2,790
Emitters (LEDs, IREDs)	2,650
Alphanumeric Displays	2,650
Laser Diodes, AlGaAs/GaAs	4,635
Laser Diodes, InGaAs/InGaAsP	5,784

Notes: (1) $\pi_T = \exp(-A(\frac{1}{T_j} - \frac{1}{298}))$,

where T_j = junction temperature (^oK)

(2) RF Power Transistor are defined as bipolar power transistors with frequency $\geq$200 MHz and average output $\geq$ 1 watt.

(3) GaAs Powers FETs are devices with output power $\geq$100mW. GaAs FETs have output power <100mW.

(4) General purpose diodes are diodes which perform the following functions: analog, switching, fast recovery, rectifier, power rectifier, HV stack.

Since the maximum power dissipation is calculated from the specified maximums at room temperature:

$$T_j = T_A + \theta_{JA} P_D$$

$$175^oC = 25^oC + (\theta_{JA})\ (.4)$$

$$\theta_{JA} = 375^oC/W.$$

where

T_j = junction temperature (^oC)
T_A = ambient temperature (^oC)
P_D = power dissipation

Table 5.1.3.10.2-2 gives approximate thermal resistances for devices in various package types, however, final estimates should come from military specifications or manufacturer's values, whichever is greater. If θ_{CA} for heatsink is unknown assume 9^oC/Watt as worst case.

STEP 1C: Determine maximum applied power or current for the device, depending upon the units of thermal resistance. If thermal resistance is in $^oC/W$, use power, if thermal resistance is in ^oC/Amp use current.

STEP 1D: Calculate T_j:

Case A: No heatsink

$$T_j = T_A + \theta_{JA}E$$

where

T_j = junction temperature (^oC)

T_A = ambient temperature (^oC)

θ_{JA} = junction-to-air thermal resistance ($^oC/W$ or ^oC/Amp)

E = Applied Electrical (power or current) value (Watts or Amps as in θ)

Case B: Heatsink present:

$$T_j = T_A + (\theta_{JC} + \theta_{CA})E$$

where

θ_{JC} = junction-to-case thermal resistance ($^oC/W$ or $^oC/Amp$)
θ_{CA} = case-to-ambient thermal resistance ($^oC/W$ or $^oC/Amp$) includes washer heatsink compound and heatsink.

STEP 2: Refer to Tables 5.1.3.10.1-2 through 5.1.3.10.1-5 for π_T value corresponding to the value of T_j calculated and the particular device type.

NOTE: The models are not applicable to devices at overstress conditions. If the calculated junction temperature is greater than the maximum rated junction temperature on the MIL slash sheets or the vendor's specifications, whichever is smaller, then the device is overstressed and these models ARE NOT APPLICABLE.

Typical maximum junction temperatures for discrete semiconductor devices are:

Si Diodes	175°C
Ge Diodes	100°C
Si Transistors	175°C
Ge Transistors	100°C
Ge Microwave Diodes	70°C
Si Microwave Diodes	150°C
Bipolar Microwave Power Transistors	200°C
GaAs Transistors	135°C
GaAs Diodes	135°C
Laser Diodes	100°C

Final values should be taken from Military specification sheets or vendor values, whichever is lower.

Case C: With or without heatsink:

$$T_j = T_C + \theta_{JC} E$$

where

T_C = case temperature (^oC)

TABLE 5.1.3.10.2-2: APPROXIMATE THERMAL RESISTANCE FOR SEMICONDUCTOR DEVICES IN VARIOUS PACKAGE SIZES (STILL AIR)*

PACKAGE TYPE	θ_{JA}(°C/W unless otherwise specified)	θ_{JC} (°C/W unless otherwise specified)
TO-1	2000	-
TO-3	50	10
TO-5	400	90
TO-8	100	7
TO-9	1250	-
TO-11	200	125
TO-12	1400	-
TO-18	500	250
TO-28	-	4.0
TO-33	650	320
TO-39	250	100
TO-41	-	2.0
TO-44	200	-
TO-46	600	125
TO-52	500	150
TO-53	50	5
TO-57	200	5
TO-59	100	5
TO-60	70	5
TO-61	50	5
TO-63	50	1.0
TO-66	50	10.0
TO-71	600	-
	400	-
TO-72	600	300
TO-83	-	.5
TO-89	700	250
	500	125
TO-92	400	200
TO-94	-	.5
TO-99	250	-
TO-126	-	5.0
TO-127	-	3.5
TO-204	-	2.0
TO-204AA	-	2.0

TABLE 5.1.3.10.2-2: APPROXIMATE THERMAL RESISTANCE FOR SEMICONDUCTOR DEVICES IN VARIOUS PACKAGE SIZES (STILL AIR)* (CONT'D)

PACKAGE TYPE	θ_{JA}(^{o}C/W unless otherwise specified)	θ_{JC} (^{o}C/W unless otherwise specified)
TO-205AD	200	25.0
TO-205AF	-	7.0
TO-220	-	5.0
DO-4	15	2.0
DO-5	-	3.0
DO-7	600	-
DO-8	-	1.0
DO-9	-	1.0
DO-13	500	-
DO-14	600	-
DO-29	200	-
DO-35	625	-
DO-41	200	-
DO-45	-	5.0
DO-204MB	600	-
DO-205AB	-	1.0
PA-42A,B	-	200
PD-36C	800	-
PD-50	-	200
PD-77	-	200
PD-180	-	200
PD-319	100	-
PD-262	600	200
PD-975	500	-
PD-280	300	-
PS-216	600	-
PT-2G	500	-
PT-6B	2000	-
PH-13	600	-
PH-16	400	-
PH-56	200	-
PY-58	1000	-
PY-373	1000	-

*When available, estimates must be based on military specification sheet or vendor values, whichever θ is higher.

5.1.3.10.3 Examples of Failure Rate Calculations

Example 1.

STEP 1: Given: Silicon NPN general purpose JAN grade transistor in linear service at 0.4 of its rated maximum power of 1 watt in fixed ground installation at 25 ^{o}C ambient, with T_{MAX} = 175^{o}C, and operated at 60 percent of maximum voltage. The transistor operates at less than 200 MHz. θ_{JA} for the device is 50^{o}C/W.

STEP 2: Since the device is a bipolar transistor operating at less than 200 MHz, the device falls into Group III and the correct model is given in Section 5.1.3.3. The model for these devices is,

$$\lambda_p = \lambda_b \pi_A \pi_r \pi_s \pi_Q \pi_T \pi_E$$

STEP 3: Referring to Section 5.1.3.10.2, the correct method to compute junction temperature is found to be:

$$T_j = T_A + \theta_{JA} P$$

STEP 4: Junction temperature is computed

$$T_j = 25 + (50)(.4) = 45^{o}C$$

STEP 5: From Table 5.1.3.10.1-2 for junction temperature = 45^{o}C, π_T = 1.6

STEP 6: From Table 5.1.3.10.1-6 Fixed Ground, π_E = 5.5

STEP 7: From Table 5.1.3.10.1-1 for JAN quality level, π_Q = 2.4

STEP 8: For Si NPN transistor

$$\lambda_b = .00074 \text{ failures}/10^6 \text{ hours}$$

STEP 9: For linear operation, π_A = 1.5

STEP 10: From Table 5.1.3.3-1 for 1 watt rating, π_r = 1.0

STEP 11: From Table 5.1.3.3-2 for rated power 1 watt and transistor at 60 percent of maximum voltage π_S = .27

STEP 12: Perform the calculation:

$$\lambda_p = \lambda_b \pi_A \pi_r \pi_s \pi_Q \pi_T \pi_E$$
$$\lambda_p = .00074 \times 1.5 \times 1.0 \times .27 \times 1.6 \times 2.4 \times 5.5$$
$$= .0063$$

Example 2.

STEP 1: Given: A Silicon J-Field Effect Transistor (JFET), JANTX grade, operating at 80 milliwatts at 500 MHz in airborne inhabited fighter service at 63°C case temperature. (Rated at 200 milliwatts, T_S = 25°C and T_{MAX} = 175°C). θ_{jc} is 25°C/W.

STEP 2: Since the device is a Silicon FET operating above 400 MHz, the device falls into Group VII and the correct section is 5.1.3.7. Within this section, there are models for Silicon, Low Power GaAs (<.1 W) and High Power GaAs (≥.1 W). This device is silicon and the model is given by,

$$\lambda_p = \lambda_b \pi_Q \pi_T \pi_E$$

STEP 3: From Section 5.1.3.10.2, select the correct equation for junction temperature

$$T_j = T_c + \theta_{jc} P$$

STEP 4: Compute junction temperature

$$T_j = 63 + (25)(.08) = 65°C$$

STEP 5: From Table 5.1.3.10.1-2 for junction temperature = 65°C, π_T = 2.1

STEP 6: For a silicon JFET,

$$\lambda_b = .023 \text{ failures}/10^6 \text{ hours}$$

STEP 7: From Table 5.1.3.10.1-6 for A_{IF} environment, π_E = 4.6

STEP 8: From Table 5.1.3.10.1-1 for JANTX grade, π_Q = 1.0

STEP 9: Perform the calculation:

$$\lambda_p = \lambda_b \pi_Q \pi_T \pi_E$$

$$\lambda_p = .023 \times 1 \times 2.1 \times 4.6$$

$$\lambda_p = 0.22 \text{ failures}/10^6 \text{ hours}$$

Example 3.

STEP 1: Given: Silicon diode, JAN grade, in ground mobile service operating at 0.4 rated maximum current, and at 25°C ambient in logic switching with 20 percent of rated voltage. Rated current is 1 amp at 25°C with T_{max} = 200°C. The device has a metallurgically bonded contact. θ_{JA} is 175°C/amp.

STEP 2: Since the device is functioning as a switching diode, it falls into the category of low frequency diode, Group I and the model is given in Section 5.1.3.1. The model for these devices is given by,

$$\lambda_p = \lambda_b \pi_S \pi_C \pi_Q \pi_T \pi_E$$

STEP 3: The correct equation for junction temperature was selected from Section 5.1.3.10.2.

$$T_j = T_A + \theta_{JA} I$$

STEP 4: Junction temperature was computed

$$T_j = 25 + (175)(.4) = 95^{\circ}C$$

STEP 5: From Table 5.1.3.10.1-3 for a junction temperature of 95°C, π_T = 7.2

STEP 6: From Table 5.1.3.1-1 for logic switching application,

$$\lambda_b = 0.0023 \text{ failures}/10^6 \text{ hours}$$

STEP 7: From Table 5.1.3.1-2 for 20 percent rated voltage, π_S = .054

STEP 8: From Table 5.1.3.10.1-6 for ground mobile service, π_E = 17

STEP 9: From Table 5.1.3.10.1-1 for JAN grade, π_Q = 2.4

STEP 10: For metallurgically bonded contacts, π_C = 1.0

STEP 11: Perform the calculation:

$$\lambda_p = \lambda_b \pi_S \pi_C \pi_Q \pi_T \pi_E$$

$$\lambda_p = .0023 \times .054 \times 1 \times 2.4 \times 7.2 \times 17$$

$$\lambda_p = .036 \text{ failures}/10^6 \text{ hours}$$

Example 4.

STEP 1: Given: Silicon dual transistor (complementary), JAN grade, rated for 0.25 W at 25°C, one side only, and 0.35 W at 25°C, both sides, with T_{max} = 200°C, operating in linear service at 55°C case temperature in a sheltered naval environment. Side one, NPN, operating at 0.1 W and 50 percent of rated voltage and side two, PNP, operating at 0.05 W and 30 percent of rated voltage. The device operates at less than 200 MHz. θ_{jc} is 100°C/W.

STEP 2: Since the device is a bipolar dual transistor operating at low frequency (<200 MHz), it falls into Group III and the appropriate model is given in Section 5.1.3.3. Since the device is a dual device, it is necessary to compute the failure rate of each side separately and sum them together.

STEP 3: For side one, junction temperature is,

$$T_j = T_C + \theta_{jc} P = 55 + (100)(.1) = 65^{\circ}C$$

STEP 4: From Table 5.1.3.10.1-2 for

$$T_j = 65^{\circ}C, \ \pi_T = 2.3$$

STEP 5: λ_b = .00074 failures/10^6 hours

STEP 6: From Table 5.1.3.10.1-6 naval sheltered, π_E = 9.5

STEP 7: For linear applications π_A = 1.5

STEP 8: From Table 5.1.3.10.1-1, JAN grade, π_Q = 2.4

STEP 9: From Table 5.1.3.3-1 for .25 watt, π_r = 0.60

STEP 10: From Table 5.1.3.3-2 at 50 percent of rated voltage, π_S = .21

STEP 11: Perform the calculation for side one:

$$\lambda_{p1} = \lambda_b \pi_A \pi_r \pi_s \pi_Q \pi_T \pi_E$$

$$\lambda_{p1} = .00074 \times 1.5 \times .6 \times .21 \times 2.4 \times 2.3 \times 9.5$$

$$= .0073$$

Example 4 Cont'd).

STEP 12: For side two, junction temperature is,

$$T_j = T_C + \theta_{jc} P = 55 + (100)(.05) = 60^oC$$

STEP 13: In Table 5.1.3.10.1-2, there is no listed value for 60°C. Using the equation below the table for $T_j = 60^oC$, $\pi_T = 2.1$

STEP 14: λ_b, λ_E, π_A, π_Q, π_r and π_C same as for side one.

STEP 15: From Table 5.1.3.3-2 at 30 percent of rated voltage, $\pi_S = .10$

STEP 16: Perform the calculation for side two:

$$\lambda_{p2} = \lambda_b \pi_A \pi_r \pi_s \pi_Q \pi_T \pi_E$$

$$\lambda_{p2} = .00074 \times 1.5 \times .6 \times .1 \times 2.4 \times 2.1 \times 9.5$$

$$= .0032$$

STEP 17: The device failure rate is,

$$\lambda_p = \lambda_{p1} + \lambda_{p2} = .0073 + .0032 = .011$$

Example 5.

STEP 1: Given: A microwave transistor, JANTX equivalent quality, is used in a mobile ground environment as a pulse amplifier at 20% duty factor with a pulse duration of 0.4 ms and an average power output of 50 watts at 2.0 GHz. The device package has input and output matching networks and uses refractory metal-gold metallization. V_{CE} = 28 volts and BV_{CES} = 56 volts. The operating peak temperature is 140°C.

STEP 2: The device is a microwave transistor operating at above 200 MHz and therefore the correct model is given in Group VI, Section 5.1.3.6. Within Section 5.1.3.6, there are models for Low Power (<1 W) and High Power (≥1 W). Since this device has an average power output of 50 W, the model for High Power microwave transistors is applicable. This model is given by,

$$\lambda_p = \lambda_b \pi_A \pi_{pw} \pi_m \pi_Q \pi_T \pi_E$$

STEP 3: From Table 5.1.3.6-3 with a peak output power of 50 watts at 2 GHz, λ_b = .086 failures/10^6 hrs.

STEP 4: From Table 5.1.3.6-4 pulse amplifier with 20% duty factor,

$$\pi_A = 1.6$$

STEP 5: From Table 5.1.3.6-5 with a pulse width of .4 ms, π_{pw} = 1.0

STEP 6: V_{CE}/BV_{CES} = 28/56 = 0.5. From Table 5.1.3.6-6 with V_{CE}/BV_{CES} = 0.5 and T_j = 140°C, π_T = 2.1

STEP 7: For input and output matching networks, π_m = 1.0

STEP 8: From Table 5.1.3.10.1-6 for mobile ground (G_M), π_E = 4.9

STEP 9: From Table 5.1.3.10.1-1 for JANTX equivalent, π_Q = 1.0

STEP 10: Perform the calculation:

$$\lambda_p = \lambda_b \pi_A \pi_{pw} \pi_m \pi_Q \pi_T \pi_E$$

$$= .086 \times 1.6 \times 1.0 \times 1.0 \times 1.0 \times 2.1 \times 4.9$$

$$= 1.4 \text{ failure}/10^6 \text{ hr.}$$

Example 6.

STEP 1: Given: Voltage reference diode, metallurgically bonded, JANTX quality, in ground fixed environment, operating at 25°C ambient. θ_{JA} is 175°C/watt. The diode is operating at .4 of rated power, which is 1 watt.

STEP 2: Voltage reference diodes fall into Group I and the model is given in Section 5.1.3.1. This model is given by,

$$\lambda_p = \lambda_b \pi_S \pi_C \pi_Q \pi_T \pi_E$$

STEP 3: The correct equation for junction temperature was selected from Section 5.1.3.10.2

$$T_j = T_A + \theta_{JA} P$$

STEP 4: The junction temperature was computed

$$T_j = 25 + 175(.4) = 95$$

STEP 5: From Table 5.1.3.10.1-3 for a junction temperature of 95°C, π_T = 3.0

STEP 6: From Table 5.1.3.1-1 for Voltage Reference applications, λ_b = .0047 failures/10^6 hours

STEP 7: From Table 5.1.3.1-2 π_S = 1.0 for voltage reference

STEP 8: From Table 5.1.3.10.1-6 for ground fixed service, π_E = 5.5

STEP 9: From Table 5.1.3.10.1-1 for JANTX quality grade, π_Q = 1.0

STEP 10: For metallurgically bonded contacts, π_C = 1.0

STEP 11: Perform the calculation:

$$\lambda_p = \lambda_b \pi_S \pi_C \pi_Q \pi_T \pi_E$$

$$\lambda_p = .0047 \times 1.0 \times 1.0 \times 1.0 \times 3.0 \times 5.5$$

$$\lambda_p = .078 \text{ failure}/10^6 \text{ hours}$$

Example 7.

STEP 1: Given: A discrete, hermetic light emitting diode (LED) procured in accordance with MIL-S-19500 is used in an Airborne, Inhabited, Trainer application environment. The device is a JANTX quality part operating at a case temperature of 60°C. Package case-to-junction thermal resistance is 500°C/Watt. The device dissipates 50mW.

STEP 2: LEDs are optoelectronic devices and therefore the series of models which fall into Group IX, Section 5.1.3.9 are applicable. The model for LEDs is,

$$\lambda_p = \lambda_b \pi_Q \pi_T \pi_E$$

STEP 3: The equation for junction temperature from Section 5.1.3.10.2 is

$$T_j = T_c + \theta_{jc} P$$

STEP 4: The junction temperature is

$$T_j = 60 + 500(.05) = 85^oC$$

STEP 5: From Table 5.1.3.10.1-5 for a T_j of 85°C, $\pi_T = 4.4$

STEP 6: From Section 5.1.3.9 for LEDs, $\lambda_b = .00023$ failures/10^6 hours

STEP 7: From Table 5.1.3.10.1-1 for JANTX, $\pi_Q = 1.0$

STEP 8: From Table 5.1.3.10.1-6 for A_{IT}, $\pi_E = 3.8$

STEP 9: Perform the calculation:

$$\lambda_p = \lambda_b \pi_Q \pi_T \pi_E$$

$$\lambda_p = .00023 \times 1.0 \times 4.4 \times 3.8$$

$$\lambda_p = .0038 \text{ failure}/10^6 \text{ hours}$$

Example 8.

STEP 1: Given: A 10 mW GaAs/AlGaAs Double Heterostructure (DH) stripe geometry laser diode is used in a Ground, Fixed environment, case temperature is 55°C. It is nonhermetic with a facet coat and has a fixed current source. The application is continuous wave (DC), the forward current is 100mA, and the minimum acceptable optical power output is 5mW. θ_{jc} is 170°C/A.

STEP 2: Laser diodes are classified as optoelectronic devices and therefore the models in Group IX, Section 5.1.3.9 are applicable. The model for laser diodes is,

$$\lambda_p = \lambda_b \pi_i \pi_A \pi_p \pi_Q \pi_T \pi_E$$

STEP 3: The correct equation for junction temperature was selected

$$T_j = T_c + \theta_{jc} A$$

STEP 4: The junction temperature was computed

$$T_j = 55 + 170(.1) = 72^oC$$

STEP 5: In Table 5.1.3.10.1-5 there is no listing for 72°C. Using the equation below the table for T_j = 72°C, π_T = 8.3

STEP 6: For GaAs/AlGaAs, λ_b = 3.23

STEP 7: From Table 5.1.3.9-2 for 100mA forward current, π_i = .21

STEP 8: From Table 5.1.3.9-3 for continuous wave (cw), π_A = 4.4

STEP 9: From Table 5.1.3.9-4 for P_r/P_s = 5/10 = .5, π_p = 1.0

STEP 10: For a nonhermetic device with a facet coating, π_Q = 1.0

STEP 11: From Table 5.1.3.10.1-6 for a ground fixed environment, π_E = 2.4

STEP 12: Perform the calculation:

$$\lambda_p = \lambda_b \pi_i \pi_A \pi_p \pi_Q \pi_T \pi_E$$

$$\lambda_p = 3.23 \times .21 \times 4.4 \times 1.0 \times 1.0 \times 8.3 \times 2.4$$

$$\lambda_p = 59.5 \text{ failure}/10^6 \text{ hours}$$

APPENDIX A2:

PROPOSED REVISION PAGES

NONOPERATING RELIABILITY PREDICTION MODELS

5.2.3 Discrete Semiconductors Nonoperating Failure Rate Prediction

This section includes the nonoperating failure rate prediction models for discrete semiconductors.

5.2.3.1 Transistor and Diode Semiconductor Devices

The general nonoperating failure rate prediction model for transistors and diodes is as follows:

$$\lambda_p = \lambda_{nb}\ \pi_{NT}\ \pi_{NE}\ \pi_{NQ}\ \pi_{cyc} \quad \text{failures}/10^6 \text{ nonoperating hours}$$

where

λ_p = predicted transistor or diode nonoperating failure rate

λ_{nb} = nonoperating base failure rate (See Table 5.2.3-1)

π_{NT} = nonoperating temperature factor, based on device style (See Table 5.2.3-2 for transistors, Table 5.2.3-3 a and b for diodes and Table 5.2.3-4 for temperature factor parameter)

π_{NE} = nonoperating environmental factor (See Table 5.2.3-5)

π_{NQ} = nonoperating quality factor (See Table 5.2.3-6)

π_{cyc} = equipment power on-off cycling factor (See Table 5.2.3-7 for transistors and Table 5.2.3-8 for diodes)

5.2.3.2 Opto-Electronic Semiconductors Devices

The general nonoperating failure rate prediction model for opto-electronic semiconductor devices is as follows:

$$\lambda_p = \lambda_{nb}\ \pi_{NE}\ \pi_{NQ} \quad \text{failures}/10^6 \text{ nonoperating hours}$$

where

λ_p = predicted nonoperating opto-electronic device failure rate

λ_{nb} = nonoperating base failure rate (See Table 5.2.3-1)

π_{NE} = nonoperating environmental factor (See Table 5.2.3-5)

π_{NQ} = nonoperating quality factor (See Table 5.2.3-6)

DISCRETE SEMICONDUCTORS

TABLE 5.2.3-1: DISCRETE SEMICONDUCTOR NONOPERATING BASE FAILURE RATE (λ_{nb})

Part Class	Part Type	λ_{nb} (Failures per 10^6 hrs)
A. Transistors	Bipolar Transistors	.000082
	FETs	.00039
	Unijunction	.0013
B. Diodes and Rectifiers	Gen. Purpose, (switching, analog rectifier)	.000083
	Zener/Avalanche	.00040
	Thyristors	.00063
C. Microwave Semiconductors and Special Devices	Detectors, Mixers	.0027
	Varactors, Step Recovery	.0027
	Microwave Transistors	.041
D. Opto-Electronic Devices	LED	.00016
	Single Isolator	.00070
	Dual Isolator	.00089
	Phototransistor	.00038
	Photo Diode	.00028
	Alpha-Numeric Displays	.00025

TABLE 5.2.3-2: TEMPERATURE FACTOR FOR TRANSISTORS (π_{NT})

Nonop Temp. (°C)	Bipolar NPN/PNP		RF Power	Silicon FET	Unijunction	GaAs FETs	
	Si	Ge				<100mW	≥100mW
25	1.0	1.0	1.0	1.0	1.0	1.0	1.0
35	1.2	1.5	1.4	1.2	1.3	1.6	1.8
45	1.6	2.1	1.8	1.5	1.7	2.6	3.1
55	1.9	2.9	2.4	1.8	2.1	4.0	5.1
65	2.3	4.0	3.2	2.1	2.7	5.9	8.2
75	2.8	5.5	4.1	2.5	3.3	8.7	13
85	3.3	7.2	5.1	3.0	4.0	12	20
95	3.8	9.5	6.4	3.4	4.9	18	29
105	4.5	12	7.9	3.9	5.8	24	43
115	5.2	--	9.6	4.5	6.9	33	62
125	5.9	--	12	5.1	8.1	44	87
135	6.9	--	14	5.7	9.4	58	121
145	7.7	--	16	6.4	11	75	165
155	8.6	--	19	7.1	13	97	221
165	9.6	--	23	7.9	14	123	293
175	11	--	26	8.7	16	154	384

$$\pi_{NT} = \exp\left(-A\left(\frac{1}{T_n + 273} - \frac{1}{298}\right)\right)$$

where

A = temperature coefficient
T_n = nonoperating temperature (°C)

TABLE 5.2.3-3a: TEMPERATURE FACTOR FOR LOW FREQUENCY DIODES (<200 MHz) (π_{NT})

Nonop Temp. (°C)	Zener/Avalanche (V. Regulator/ V. Reference)	Current Regulator	Transient Suppressor	General Purpose	
				Si	Ge
25	1.0	1.0	1.0	1.0	1.0
35	1.2	1.2	1.5	1.4	1.7
45	1.4	1.5	2.2	1.9	2.8
55	1.7	1.8	3.2	2.5	4.5
65	2.0	2.1	4.5	3.4	7.0
75	2.3	2.5	6.3	4.4	11
85	2.6	3.0	8.5	5.7	16
95	3.0	3.4	11	7.2	23
105	3.4	3.9	15	9.0	--
115	3.8	4.5	19	11	--
125	4.3	5.1	25	14	--
135	4.7	5.7	31	16	--
145	5.2	6.4	39	20	--
155	5.8	7.1	49	23	--
165	6.3	7.9	60	28	--
175	6.9	8.7	72	32	--

$$\pi_{NT} = \exp\left(-A\left(\frac{1}{T_n + 273} - \frac{1}{298}\right)\right)$$

where

A = temperature coefficient (see Table 5.1.3.10.2-1)

T_n = nonoperating temperature (°C)

TABLE 5.2.3-3b: TEMPERATURE FACTOR FOR HIGH FREQUENCY DIODES (≥200 MHz) AND THYRISTORS (π_{NT})

Nonop Temp. (°C)	PIN/Tunnel Back	Thyristors/ SCR	IMPATT	Schottky Barrier	Varactor/ Step Recovery
25	1.0	1.0	1.0	1.0	1.0
35	1.2	1.4	1.8	1.2	1.3
45	1.5	1.9	3.0	1.4	1.6
55	1.9	2.6	5.0	1.6	1.9
65	2.3	3.4	8.1	2.1	2.3
75	2.7	4.4	13	2.1	2.8
85	3.2	5.6	19	2.4	3.3
95	3.8	7.1	29	2.6	3.8
105	4.4	8.9	42	3.0	4.4
115	5.1	11	60	3.3	5.1
125	5.9	13	84	3.6	5.9
135	6.7	16	117	4.0	6.7
145	7.6	20	159	4.3	7.6
155	8.5	23	213	4.7	8.5
165	9.5	27	282	-	9.5
175	11	32	369	-	11

$$\pi_{NT} = \exp\left(-A\left(\frac{1}{T_n + 273} - \frac{1}{298}\right)\right)$$

where

A = temperature coefficient

T_n = nonoperating temperature (°C)

DISCRETE SEMICONDUCTORS

TABLE 5.2.3-4: DISCRETE SEMICONDUCTOR NONOPERATING TEMPERATURE FACTOR PARAMETERS

Group	Part Type	A_n
Transistors	Si, Bipolar	2,114
	Ge, Bipolar	3,521
	FET	1,925
	Unijunction	2,483
Diodes	Si, Gen. Purpose,	3,091
	Ge, Gen. Purpose	4,914
	Zener/Avalanche	1,718
	Thyristors	3,082
	Microwave	2,100
	IMPATT, Gunn, Varactor, PIN, Step Recovery & Tunnel	2,100
Transistors	RF/Microwave Power	2,903

$$\pi_{NT} = \exp\left(-A\left(\frac{1}{T_n + 273} - \frac{1}{298}\right)\right)$$

where

T_n = nonoperating temperature (^oC)

A_n = temperature factor constant (Table 5.2.3-4)

DISCRETE SEMICONDUCTORS

TABLE 5.2.3-5: DISCRETE SEMICONDUCTORS NONOPERATING ENVIRONMENTAL FACTOR (π_{NE})

Environment	π_{NE}
G_B	1
G_{MS}	1.5
G_F	4.9
G_M	18
M_P	12
N_{SB}	7.3
N_S	7.3
N_U	20
N_H	20
N_{UU}	20
A_{RW}	27
A_{IC}	12
A_{IT}	18
A_{IB}	32
A_{IA}	23
A_{IF}	38
A_{UC}	20
A_{UT}	28
A_{UB}	55
A_{UA}	38
A_{UF}	58
S_F	1
M_{FF}	12
M_{FA}	17
U_{SL}	36
M_L	41
C_L	690

TABLE 5.2.3-6: DISCRETE SEMICONDUCTORS NONOPERATING QUALITY FACTOR (π_{NQ})

Quality Level	π_{NQ}
JANTXV	.7
JANTX	1.0
JAN	2.4
Lower, Hermetic*	5.5
Plastic**	8.0

* applies to all hermetic packaged discrete semiconductors devices and to Non-JAN hermetic packaged devices.

** applies to all discrete semiconductor devices encapsulated with organic material

TABLE 5.2.3-7: TRANSISTOR EQUIPMENT POWER ON-OFF CYCLING FACTOR (π_{cyc})

Cycling Rate***(N_C) (Power Cycles/ 10^3 hrs.)	Mean-Time-Between Power Cycles	π_{cyc}
<1	>1000	1.00
1	1000	1.05
2	500	1.10
3	333	1.15
4	250	1.20
5	200	1.25
10	100	1.50
20	50	2.00
50	20	3.50

$$\pi_{cyc} = 1 + .050(N_C)$$

N_C = number of equipment power on-off cycles per 1000 nonoperating hours

*** An equipment power on-off cycle is defined as the state during which an electronic equipment goes from zero electrical activation level to the normal design activation level plus the state during which is returns to zero.

TABLE 5.2.3-8: DIODE EQUIPMENT POWER ON-OFF CYCLING FACTOR (π_{cyc})

Cycling Rate***(N_C) (Power Cycles/ 10^3 hrs.)	Mean-Time-Between Power Cycles	π_{cyc}
<0.6	>1667	1.00
1	1000	1.08
2	500	1.17
3	333	1.25
4	250	1.33
5	200	1.42
10	100	1.83
20	50	2.66
50	20	5.15

$\pi_{cyc} = 1 + .083(N_C)$

N_C = number of equipment power on-off cycles per 1000 nonoperating hours

*** An equipment power on-off cycle is defined as the state during which an electronic equipment goes from zero electrical activation level to the normal design activation level plus the state during which is returns to zero.

Example 1.

STEP 1: Given: Silicon NPN general purpose JAN grade transistor in fixed ground storage installation, at 25°C ambient being power cycled every 1,000 hours

STEP 2: From Table 5.2.3-1, for a bipolar transistor, λ_{nb} = .000082 failures/10^6 nonoperating hours

STEP 3: From Table 5.2.3-2, for T_a = 25°C, π_{NT} = 1.0

STEP 4: From Table 5.2.3-5 for ground fixed, π_{NE} = 4.9

STEP 5: From Table 5.2.3-6 for JAN quality, π_{NQ} = 2.4

STEP 6: From Table 5.2.3-7, for Mean-Time-Between-Power-Cycles of 1,000 hours, π_{cyc} = 1.08

STEP 7: Perform the calculation:

$$\lambda_p = \lambda_{nb}\ \pi_{NT}\ \pi_{NE}\ \pi_{NQ}\ \pi_{cyc}$$

$$\lambda_p = .000082 \times 1.0 \times 4.9 \times 2.4 \times 1.08$$

$$\lambda_p = .0010 \text{ failure}/10^6 \text{ nonoperating hours}$$

APPENDIX B:

DISCRETE SEMICONDUCTOR FAILURE DATA
(SUMMARY AND DETAILED DATA LISTINGS)

APPENDIX B-1:

DATA SUMMARIES

TABLE B1-1. DIODE FAILURE DATA SUMMARY

COMPONENT TYPE	SCREEN QUALITY	NO.# TESTED	FAILURES	PART HOURS
Switching Diode	JANTX	941,953	95	919,695,236
	Lower	2,011	6	2,614,300
General Purpose	JANTX	39,788	0	38,121,167
	Lower	17,913	1	23,286,900
	Plastic	19,795	2	25,733,500
Rectifier	JAN	364	3	1,155,635
	JANTX	45,474	7	35,523,386
	Lower	5,821,360	426	7,567,768,000
	Plastic	7,896	0	10,264,800
High Power Rectifier	JANTX	100,684	16	93,995,180
Fast Recovery	JANTX	114,720	24	103,388,095
	Lower	603	0	783,900
Bridge Rectifier, F. Wave	Unknown	1,524	0	829,055
Zener Diode	JANTX	20,692	3	27,890,467
	Lower	383,332	84	547,335,000
	Plastic	962	0	1,652,300
Voltage Regulator Diode	JANTX	257,783	36	243,430,923
	Plastic	642,906	192	911,651,000
Voltage Reference Diode	JANTX	31,043	1	31,550,488
	Lower	182,121	16	232,077,300
	Plastic	2,553,843	366	3,687,777,600
Avalanche Diode	Plastic	35,891	0	52,984,100
Current Regulator Diode	Plastic	9,342	2	13,542,100
Suppressor Diode	JANTX	1,948	0	,850,308
Transient Suppressor	JANTX	7,632	7	6,294,426
Tunnel Diodes	Lower	178,400	72	231,920,000
Schottky Barrier Diode	Unknown	150	52	62,313,038
	JANTX	85,260	6	81,688,215
PIN Diode	Unknown	52	348	146,607,740
	JAN	N/A	1298	8,292,439,319
	Lower	16	0	280,320
Varactor Diodes	Unknown	N/A	0	38,714,719
	JANTX	6,248	0	7,293,861
	Plastic	101,557	30	132,024,100
Gunn Effect Diode	Unknown	N/A	40	4,727,000
IMPATT Diode	Unknown	290	90	640,441
Thyristors	JANTX	1,316	4	4,178,065
	Plastic	138,433	44	179,962,900
Silicon Controlled Rect.	JANTX	22,754	102	21,783,524
	Plastic	593,628	103	771,716,400
TRIAC's	Plastic	30,755	27	39,981,500
Trigger Triode	Plastic	5,398	19	7,017,400
Multigate Thyristor	Plastic	4,356	1	5,662,800
Diode (NOC)	Unknown	1,524	0	829,055
	JANTX	64,048	111	60,733,746
	Lower	32	8	560,640

TABLE B1-2. TRANSISTOR FAILURE DATA SUMMARY

COMPONENT TYPE	SCREEN QUALITY	NO.* TESTED	FAILURES	PART HOURS
Lower Power Transistor	Plastic	451,815	25	587,359,500
Lower Power (Silicon)	Unknown	51	6	127,500
	JAN	1,960	15	6,055,619
	JANTX	1,030,941	405	1,005,222,839
	Plastic	18,224,725	2189	23,692,142,500
Lower Power (Germanium)	JANTX	28,424	12	27,294,178
	Plastic	46,579	19	60,606,700
High Power Transistor	Unknown	N/A	1367	1,471,680
	Plastic	20,306	15	26,397,800
High Power (Silicon)	JAN	336	0	1,066,740
	JANTX	156,342	124	149,080,340
	Plastic	809,333	274	1,052,132,900
High Power (Germanium)	Plastic	7,574	4	9,846,200
Field Effect (NOC)	Unknown	N/A	374	2434,123
JFET (N-Channel)	JANTX	91,365	29	82982,532
	Lower	8	0	140,160
	Plastic	3,815,194	835	4959752,200
JFET (P-Channel)	Unknown	1,016	1	552,697
	JANTX	5,684	5	5445,881
	Plastic	99,279	8	129062,700
MOSFET (IGFET) N-Channel	Unknown	445	153	9120840,431
	Plastic	271,826	182	353373,800
MOSFET (IGFET) P-Channel	Unknown	51	1	125,300
	Plastic	6,074	4	7896,200
Unijunction Transistors	JANTX	5,692	0	5586,041
	Plastic	48,183	19	62637,900
RF Transistor	Unknown	27	24	9,288
	JANTX	5,264	1	16712,260
	Lower	20	0	350,400
Multiple Trans. (Matched)	JANTX	520	1	486,598
	Lower	4	0	70,080
Complementary Transistors	JANTX	2,044	0	6,489,335
Darlington Transistors	JANTX	84,760	57	80,661,462
Chopper Transistors	Plastic	150,295	5	195,383,500
Transistor Arrays	Lower	28	0	490,560
Microwave Transistors	Unknown	74	2	1,089,640
	JANTX	2,296	0	7,289,390
Programmable Unijunction	Plastic	6,803	3	8,843,900
Transistors (NOC)	Unknown	508	0	276,358
	JANTX	26,674	11	23,611,674
	Lower	N/A	343	140,160

TABLE B1-3. OPTOELECTRONIC FAILURE DATA SUMMARY

COMPONENT TYPE	SCREEN QUALITY	NO.# TESTED	FAILURES	PART HOURS
Optoelectronic Emitter	Plastic	32,183	5	41,837,900
Light Emitting Diodes	Plastic	3,680,956	17	4,785,242,800
Infrared Emitting Diode	Unknown	60	39	1,022,660
LED Emitting Diode Array	Unknown	352	237	447,240
	Plastic	497,611	4	646,894,300
Infrared Diode Array	Plastic	3,0148	0	39,192,400
Laser Diode	Unknown	874	442	4,646,181
Photodiode Sensor	Unknown	16	0	76,800
	Plastic	158	0	205,400
Phototransistor Sensor	Plastic	35,956	7	46,742,800
Photocoupler (NOC)	Unknown	669	337	2,152,176
	Plastic	90,205	41	117,652,600
Phototransistor Output	JANTX	2,032	0	1,105,394
	Plastic	145,593	108	189,270,900
Photodarlington Output	Plastic	22,621	1	29,407,300
Photocircuit Output	Plastic	398	0	517,400
Dual Darlington	Plastic	156,964	61	204,053,200
Dual Transistor	Plastic	35,084	0	45,608,300
Optoelectronic Displays	Plastic	1,880	0	2,444,000
LED Displays	Plastic	3,228,612	144	636,682,158,900
Optoelectronics (NOC)	Plastic	3,194,606	10	4,153,432,400

APPENDIX B-2:

DIODE DATA LISTING

DEVICE TYPE	QUALITY	TESTED	FAILED	PART HOURS
Multigate Thyristor	Plastic	4356	1	5.662800
Programmable Unijunction	Plastic	6803	3	8.843900
Trigger Triode	Plastic	42	0	0.054600
Trigger Triode	Plastic	5356	19	6.962800
TRIAC	Plastic	29861	27	38.819300
TRIAC	Plastic	894	0	1.162200
Silicon Controlled (SCR)	Plastic	234261	24	304.539300
Silicon Controlled (SCR)	Plastic	167920	31	218.296000
Silicon Controlled (SCR)	Plastic	6366	0	8.275800
Silicon Controlled (SCR)	Plastic	2345	4	3.048500
Silicon Controlled (SCR)	Plastic	28192	3	36.649600
Silicon Controlled (SCR)	Plastic	68100	28	88.530000
Silicon Controlled (SCR)	Plastic	116	0	0.150800
Silicon Controlled (SCR)	Plastic	39828	4	51.776400
Silicon Controlled (SCR)	Plastic	7504	2	9.755200
Silicon Controlled (SCR)	Plastic	1959	4	2.546700
Silicon Controlled (SCR)	Plastic	36509	3	47.461700
Silicon Controlled (SCR)	*Plastic*	*528*	*0*	*0.686400*
Silicon Controlled (SCR)	JANTX	1880	16	2.763222
Silicon Controlled (SCR)	JANTX	4532	18	4.281518
Silicon Controlled (SCR)	JANTX	1302	7	1.009974
Silicon Controlled (SCR)	JANTX	4532	18	4.281518
Silicon Controlled (SCR)	JANTX	2920	8	1.699572
Silicon Controlled (SCR)	JANTX	1880	16	2.763222
Silicon Controlled (SCR)	JANTX	752	2	1.137476
Silicon Controlled (SCR)	JANTX	752	2	1.137476
Silicon Controlled (SCR)	JANTX	1302	7	1.009974
Silicon Controlled (SCR)	JANTX	2902	8	1.699572
Thyristor (NOC)	Plastic	138433	44	179.962900
Thyristor (NOC)	JANTX	1288	4	4.089170
Thyristor (NOC)	JANTX	28	0	0.088895
Thyristor (NOC)	JAN	28	0	0.088895
IMPATT Diode	Unknown	40	17	0.040000
IMPATT Diode	Unknown	42	32	0.064000
IMPATT Diode	Unknown	40	32	0.015081
IMPATT Diode	Unknown	20	3	0.100000
IMPATT Diode	Unknown	10	1	0.031200
IMPATT Diode	Unknown	10	0	0.031200
IMPATT Diode	Unknown	7	2	0.018710
IMPATT Diode	Unknown	45	0	0.142626
IMPATT Diode	Unknown	42	0	0.163354
IMPATT Diode	Unknown	24	1	0.005760
IMPATT Diode	Unknown	10	2	0.028510
Gunn Effect	Unknown	N/A	0	0.118000
Gunn Effect	Unknown	N/A	2	0.300000
Gunn Effect	Unknown	N/A	4	1.114000
Gunn Effect	Unknown	N/A	29	1.809000
Gunn Effect	Unknown	N/A	4	1.112000
Gunn Effect	Unknown	N/A	1	0.274000

MIL-HDBK-217E
DISCRETE SEMICONDUCTOR DATA SOURCE
(Diodes)

DEVICE TYPE	QUALITY	TESTED	FAILED	PART HOURS
Varactor Diode	Plastic	4340	4	5.642000
Varactor Diode	Plastic	11365	0	14.774500
Varactor Diode	Plastic	152	0	0.197600
Varactor Diode	Plastic	854	0	1.110200
Varactor Diode	Plastic	17360	9	22.568000
Varactor Diode	Plastic	18275	7	23.757500
Varactor Diode	Plastic	7718	2	10.033400
Varactor Diode	Plastic	622	0	0.808600
Varactor Diode	Plastic	1754	0	2.280200
Varactor Diode	Plastic	39117	8	50.852100
Varactor Diode	JANTX	392	0	1.244530
Varactor Diode	JANTX	4	0	0.070080
Varactor Diode	JANTX	56	0	0.177790
Varactor Diode	JANTX	2266	0	2.140759
Varactor Diode	JANTX	56	0	0.177790
Varactor Diode	JANTX	56	0	0.177790
Varactor Diode	JANTX	1451	0	0.849786
Varactor Diode	JANTX	940	0	1.381611
Varactor Diode	JANTX	651	0	0.504987
Varactor Diode	JANTX	376	0	0.568738
Varactor Diode	Unknown	N/A	0	0.033600
Varactor Diode	Unknown	N/A	0	0.091239
Varactor Diode	Unknown	N/A	0	35.170000
Varactor Diode	Unknown	N/A	0	2.583000
Varactor Diode	Unknown	N/A	0	0.027880
Varactor Diode	Unknown	N/A	0	0.809000
PIN Diode	Lower	16	0	0.280320
PIN Diode	JAN	N/A	0	0.588549
PIN Diode	JAN	N/A	1298	8291.840000
PIN Diode	JAN	N/A	0	0.010770
PIN Diode	Unknown	N/A	0	14.700000
PIN Diode	Unknown	N/A	0	0.020800
PIN Diode	Unknown	N/A	1	57.771900
PIN Diode	Unknown	48	320	0.840960
PIN Diode	Unknown	4	0	0.070080
PIN Diode	Unknown	N/A	25	63.054000
PIN Diode	Unknown	N/A	2	10.150000
Schottky Barrier	JANTX	21765	2	12.746790
Schottky Barrier	JANTX	5640	0	8.531070
Schottky Barrier	JANTX	14100	3	20.724165
Schottky Barrier	JANTX	9765	0	7.574805
Schottky Barrier	JANTX	33990	1	32.111385
Schottky Barrier	Unknown	N/A	0	1.503000
Schottky Barrier	Unknown	N/A	0	0.072566
Schottky Barrier	Unknown	N/A	1	16.546778
Schottky Barrier	Unknown	N/A	0	0.413330
Schottky Barrier	Unknown	50	16	0.263153
Schottky Barrier	Unknown	N/A	0	0.157000
Schottky Barrier	Unknown	50	23	0.108807

MIL-HDBK-217E
DISCRETE SEMICONDUCTOR DATA SOURCE
(Diodes)

DEVICE TYPE	QUALITY	TESTED	FAILED	PART HOURS
Schottky Barrier	Unknown	N/A	0	2.248000
Schottky Barrier	Unknown	50	10	0.263073
Schottky Barrier	Unknown	N/A	0	1.416300
Schottky Barrier	Unknown	N/A	0	0.091239
Schottky Barrier	Unknown	N/A	0	3.319992
Schottky Barrier	Unknown	N/A	1	4.181800
Schottky Barrier	Unknown	N/A	0	0.128000
Schottky Barrier	Unknown	N/A	1	31.600000
Tunnel Diode	Lower	1	0	0.001300
Tunnel Diode	Lower	36	0	0.046800
Tunnel Diode	Lower	39728	9	51.646400
Tunnel Diode	Lower	1	0	0.001300
Tunnel Diode	Lower	4915	1	6.389500
Tunnel Diode	Lower	13982	4	18.176600
Tunnel Diode	Lower	81647	39	106.141100
Tunnel Diode	Lower	38090	19	49.517000
Transient Suppressor	JANTX	1948	1	0.850308
Transient Suppressor	JANTX	376	0	0.568738
Transient Suppressor	JANTX	1451	4	0.848023
Transient Suppressor	JANTX	2266	1	2.140759
Transient Suppressor	JANTX	940	0	1.381611
Transient Suppressor	JANTX	651	1	0.504987
Suppressor (NOC)	JANTX	1948	0	0.850308
Current Regulator	Plastic	9342	2	13.542100
Avalanche	Plastic	3620	0	7.373600
Avalanche	Plastic	32271	0	45.610500
Voltage Reference	Plastic	64635	21	96.909800
Voltage Reference	Plastic	950609	138	1401.090600
Voltage Reference	Plastic	34301	7	49.162100
Voltage Reference	Plastic	29345	3	42.629600
Voltage Reference	Plastic	4018	0	6.201000
Voltage Reference	Plastic	96	0	0.163800
Voltage Reference	Plastic	141116	34	212.706000
Voltage Reference	Plastic	137421	10	186.576000
Voltage Reference	Plastic	476074	34	674.601200
Voltage Reference	Plastic	301411	39	421.621200
Voltage Reference	Plastic	1614	0	2.445300
Voltage Reference	Plastic	384143	78	553.234500
Voltage Reference	Plastic	29060	2	40.436500
Voltage Reference	Lower	53289	7	69.275700
Voltage Reference	Lower	3164	1	4.113200
Voltage Reference	Lower	1970	0	2.561000
Voltage Reference	Lower	4	0	0.005200
Voltage Reference	Lower	6200	0	8.060000
Voltage Reference	Lower	3790	0	4.927000
Voltage Reference	Lower	38406	2	45.247800
Voltage Reference	Lower	4	0	0.005200
Voltage Reference	Lower	7531	2	9.790300
Voltage Reference	Lower	74	0	0.096200

MIL-HDBK-217E
DISCRETE SEMICONDUCTOR DATA SOURCE
(Diodes)

DEVICE TYPE	QUALITY	TESTED	FAILED	PART HOURS
Voltage Reference	Lower	1894	0	2.462200
Voltage Reference	Lower	55873	2	72.634900
Voltage Reference	Lower	9922	2	12.898600
Voltage Reference	JANTX	487	0	0.212577
Voltage Reference	JANTX	140	0	0.444475
Voltage Reference	JANTX	376	0	0.568738
Voltage Reference	JANTX	2266	0	2.140759
Voltage Reference	JANTX	532	0	1.689005
Voltage Reference	JANTX	1880	0	2.763222
Voltage Reference	JANTX	1302	0	1.009974
Voltage Reference	JANTX	752	1	1.137476
Voltage Reference	JANTX	651	0	0.504987
Voltage Reference	JANTX	1451	0	0.849786
Voltage Reference	JANTX	940	0	1.381611
Voltage Reference	JANTX	308	0	0.977845
Voltage Reference	JANTX	2902	0	1.699572
Voltage Reference	JANTX	2902	0	1.699572
Voltage Reference	JANTX	28	0	0.088895
Voltage Reference	JANTX	112	0	0.355580
Voltage Reference	JANTX	1302	0	1.009974
Voltage Reference	JANTX	4532	0	4.281518
Voltage Reference	JANTX	1880	0	2.763222
Voltage Reference	JANTX	508	0	0.276358
Voltage Reference	JANTX	508	0	0.276348
Voltage Reference	JANTX	752	0	1.137476
Voltage Reference	JANTX	4532	0	4.281518
Voltage Regulator	Plastic	91373	34	127.153000
Voltage Regulator	Plastic	107602	22	161.367700
Voltage Regulator	Plastic	10094	0	13.993200
Voltage Regulator	Plastic	175675	33	250.191500
Voltage Regulator	Plastic	22690	2	33.551700
Voltage Regulator	Plastic	193998	97	266.514300
Voltage Regulator	Plastic	18593	2	28.697500
Voltage Regulator	Plastic	1658	0	2.579200
Voltage Regulator	Plastic	21223	2	27.602900
Voltage Regulator	JANTX	2540	0	1.381752
Voltage Regulator	JANTX	6798	1	6.422277
Voltage Regulator	JANTX	508	0	0.276358
Voltage Regulator	JANTX	2032	0	1.105397
Voltage Regulator	JANTX	13596	0	12.844554
Voltage Regulator	JANTX	1451	0	0.849786
Voltage Regulator	JANTX	1016	0	0.552698
Voltage Regulator	JANTX	2266	0	2.140759
Voltage Regulator	JANTX	487	0	0.212577
Voltage Regulator	JANTX	1451	0	0.849786
Voltage Regulator	JANTX	4	0	0.070080
Voltage Regulator	JANTX	1451	1	0.849786
Voltage Regulator	JANTX	2266	0	2.140759
Voltage Regulator	JANTX	508	1	0.276358

MIL-HDBK-217E
DISCRETE SEMICONDUCTOR DATA SOURCE
(Diodes)

DEVICE TYPE	QUALITY	TESTED	FAILED	PART HOURS
Voltage Regulator	JANTX	1451	0	0.849786
Voltage Regulator	JANTX	4532	1	4.281518
Voltage Regulator	JANTX	24	0	0.420480
Voltage Regulator	JANTX	487	0	0.212577
Voltage Regulator	JANTX	2266	0	2.140759
Voltage Regulator	JANTX	140	0	0.076234
Voltage Regulator	JANTX	15862	0	14.985313
Voltage Regulator	JANTX	2266	0	2.140759
Voltage Regulator	JANTX	508	1	0.276358
Voltage Regulator	JANTX	1451	0	0.849786
Voltage Regulator	JANTX	8	0	0.140160
Voltage Regulator	JANTX	487	1	0.212577
Voltage Regulator	JANTX	2266	2	2.140759
Voltage Regulator	JANTX	4532	0	4.281518
Voltage Regulator	JANTX	18506	0	8.077900
Voltage Regulator	JANTX	N/A	0	0.070080
Voltage Regulator	JANTX	3896	0	1.700600
Voltage Regulator	JANTX	2902	0	1.699572
Voltage Regulator	JANTX	4	0	0.070080
Voltage Regulator	JANTX	4	3	0.070080
Voltage Regulator	JANTX	3896	0	1.700600
Voltage Regulator	JANTX	1451	1	0.849786
Voltage Regulator	JANTX	2266	1	2.140759
Voltage Regulator	JANTX	20	0	0.350400
Voltage Regulator	JANTX	116	0	2.032320
Voltage Regulator	JANTX	2266	0	2.140759
Voltage Regulator	JANTX	10157	0	5.948502
Voltage Regulator	JANTX	6798	2	6.422277
Voltage Regulator	JANTX	1016	0	0.552697
Voltage Regulator	JANTX	1016	0	0.552697
Voltage Regulator	JANTX	2266	1	2.140759
Voltage Regulator	JANTX	2266	1	2.140759
Voltage Regulator	JANTX	4	0	0.070080
Voltage Regulator	JANTX	1451	0	0.849786
Voltage Regulator	JANTX	1016	4	0.552697
Voltage Regulator	JANTX	1451	0	0.849786
Voltage Regulator	JANTX	4532	0	4.281518
Voltage Regulator	JANTX	4	0	0.070080
Voltage Regulator	JANTX	651	0	0.504987
Voltage Regulator	JANTX	940	0	1.381611
Voltage Regulator	JANTX	752	0	1.137476
Voltage Regulator	JANTX	364	0	1.155635
Voltage Regulator	JANTX	1451	0	0.848023
Voltage Regulator	JANTX	2256	0	3.412428
Voltage Regulator	JANTX	1451	0	0.849786
Voltage Regulator	JANTX	28	0	0.088895
Voltage Regulator	JANTX	2902	0	1.696046
Voltage Regulator	JANTX	376	0	0.568738
Voltage Regulator	JANTX	4353	0	2.544951

MIL-HDBK-217E
DISCRETE SEMICONDUCTOR DATA SOURCE
(Diodes)

DEVICE TYPE	QUALITY	TESTED	FAILED	PART HOURS
Voltage Regulator	JANTX	504	1	2.489060
Voltage Regulator	JANTX	376	0	0.568738
Voltage Regulator	JANTX	392	0	1.244530
Voltage Regulator	JANTX	2266	0	2.140759
Voltage Regulator	JANTX	651	0	0.504987
Voltage Regulator	JANTX	8706	0	5.098716
Voltage Regulator	JANTX	752	0	1.137476
Voltage Regulator	JANTX	2266	1	2.140759
Voltage Regulator	JANTX	700	0	2.222375
Voltage Regulator	JANTX	3906	0	3.029922
Voltage Regulator	JANTX	1128	0	1.706214
Voltage Regulator	JANTX	940	0	2.691398
Voltage Regulator	JANTX	2820	0	4.144833
Voltage Regulator	JANTX	1880	0	2.763222
Voltage Regulator	JANTX	940	0	1.381611
Voltage Regulator	JANTX	168	0	0.533370
Voltage Regulator	JANTX	1880	0	2.763222
Voltage Regulator	JANTX	112	0	0.355580
Voltage Regulator	JANTX	168	0	0.533370
Voltage Regulator	JANTX	224	0	0.711160
Voltage Regulator	JANTX	5640	0	8.289666
Voltage Regulator	JANTX	376	0	0.568738
Voltage Regulator	JANTX	376	0	0.568738
Voltage Regulator	JANTX	376	1	0.568738
Voltage Regulator	JANTX	6580	0	9.671277
Voltage Regulator	JANTX	376	0	0.568738
Voltage Regulator	JANTX	940	0	1.381611
Voltage Regulator	JANTX	376	0	0.568738
Voltage Regulator	JANTX	940	0	1.381611
Voltage Regulator	JANTX	376	0	0.568738
Voltage Regulator	JANTX	940	0	1.381611
Voltage Regulator	JANTX	2632	0	3.981166
Voltage Regulator	JANTX	651	0	0.504987
Voltage Regulator	JANTX	651	0	0.504987
Voltage Regulator	JANTX	4353	2	2.549358
Voltage Regulator	JANTX	752	0	1.137476
Voltage Regulator	JANTX	1451	0	0.849786
Voltage Regulator	JANTX	940	0	1.381611
Voltage Regulator	JANTX	1451	0	0.848317
Voltage Regulator	JANTX	940	0	1.381611
Voltage Regulator	JANTX	376	0	0.568738
Voltage Regulator	JANTX	940	0	1.381611
Voltage Regulator	JANTX	2266	0	2.140759
Voltage Regulator	JANTX	1953	0	1.514961
Voltage Regulator	JANTX	651	0	0.504987
Voltage Regulator	JANTX	940	1	1.381611
Voltage Regulator	JANTX	651	0	0.504987
Voltage Regulator	JANTX	940	0	1.381611
Voltage Regulator	JANTX	1302	0	1.009974

MIL-HDBK-217E
DISCRETE SEMICONDUCTOR DATA SOURCE
(Diodes)

DEVICE TYPE	QUALITY	TESTED	FAILED	PART HOURS
Voltage Regulator	JANTX	651	0	0.504987
Voltage Regulator	JANTX	376	1	0.568738
Voltage Regulator	JANTX	1302	0	1.009974
Voltage Regulator	JANTX	376	0	0.568738
Voltage Regulator	JANTX	940	0	1.381611
Voltage Regulator	JANTX	1128	0	1.706214
Voltage Regulator	JANTX	651	1	0.504987
Voltage Regulator	JANTX	1451	0	0.849786
Voltage Regulator	JANTX	2820	0	8.074194
Voltage Regulator	JANTX	4557	1	3.534909
Voltage Regulator	JANTX	651	0	0.504987
Voltage Regulator	JANTX	1880	1	2.763222
Voltage Regulator	JANTX	651	0	0.504987
Voltage Regulator	JANTX	376	0	0.568738
Voltage Regulator	JANTX	940	0	1.381611
Voltage Regulator	JANTX	2902	0	1.696046
Voltage Regulator	JANTX	651	0	0.504987
Voltage Regulator	JANTX	1302	0	1.009974
Voltage Regulator	JANTX	376	0	0.568738
Voltage Regulator	JANTX	508	5	0.276358
Voltage Regulator	JANTX	376	0	0.568738
Voltage Regulator	JANTX	1953	0	1.514961
Voltage Regulator	JANTX	651	0	0.504987
Voltage Regulator	JANTX	651	0	0.504987
Voltage Regulator	JANTX	2266	0	2.140759
Zener Diode (NOC)	Plastic	962	0	1.652300
Zener Diode (NOC)	Lower	1805	0	2.849600
Zener Diode (NOC)	Lower	42004	0	57.140200
Zener Diode (NOC)	Lower	6114	1	8.444800
Zener Diode (NOC)	Lower	2518	0	3.273400
Zener Diode (NOC)	Lower	38207	37	49.669100
Zener Diode (NOC)	Lower	33	0	0.042900
Zener Diode (NOC)	Lower	19882	7	28.230800
Zener Diode (NOC)	Lower	7368	1	9.578400
Zener Diode (NOC)	Lower	160	0	1.757600
Zener Diode (NOC)	Lower	266	0	0.360100
Zener Diode (NOC)	Lower	3042	3	3.954600
Zener Diode (NOC)	Lower	12559	1	18.733000
Zener Diode (NOC)	Lower	31136	0	45.715800
Zener Diode (NOC)	Lower	687	0	0.839100
Zener Diode (NOC)	Lower	22509	13	29.261700
Zener Diode (NOC)	Lower	980	0	1.409200
Zener Diode (NOC)	Lower	32073	5	41.694900
Zener Diode (NOC)	Lower	26042	4	33.854600
Zener Diode (NOC)	Lower	29666	0	43.602000
Zener Diode (NOC)	Lower	22777	5	33.571700
Zener Diode (NOC)	Lower	1783	0	2.444000
Zener Diode (NOC)	Lower	602	0	0.915200
Zener Diode (NOC)	Lower	13578	3	19.518200

MIL-HDBK-217E
DISCRETE SEMICONDUCTOR DATA SOURCE
(Diodes)

DEVICE TYPE	QUALITY	TESTED	FAILED	PART HOURS
Zener Diode (NOC)	Lower	2855	1	4.323800
Zener Diode (NOC)	Lower	707	0	10.838200
Zener Diode (NOC)	Lower	940	0	1.222000
Zener Diode (NOC)	Lower	3462	0	5.062200
Zener Diode (NOC)	Lower	18109	1	30.175600
Zener Diode (NOC)	Lower	41468	2	58.852300
Zener Diode (NOC)	JANTX	476	0	1.511215
Zener Diode (NOC)	JANTX	420	0	1.333425
Zener Diode (NOC)	JANTX	28	0	0.088895
Zener Diode (NOC)	JANTX	84	0	0.266685
Zener Diode (NOC)	JANTX	392	0	1.244530
Zener Diode (NOC)	JANTX	28	0	0.088895
Zener Diode (NOC)	JANTX	112	0	0.355580
Zener Diode (NOC)	JANTX	448	1	1.422320
Zener Diode (NOC)	JANTX	224	0	0.711160
Zener Diode (NOC)	JANTX	56	0	0.177790
Zener Diode (NOC)	JANTX	420	0	1.333425
Zener Diode (NOC)	JANTX	651	0	0.504987
Zener Diode (NOC)	JANTX	28	0	0.088895
Zener Diode (NOC)	JANTX	644	0	2.044585
Zener Diode (NOC)	JANTX	376	0	0.568738
Zener Diode (NOC)	JANTX	196	0	0.622265
Zener Diode (NOC)	JANTX	28	0	0.088895
Zener Diode (NOC)	JANTX	2266	0	2.140759
Zener Diode (NOC)	JANTX	56	0	0.177790
Zener Diode (NOC)	JANTX	1451	0	0.849786
Zener Diode (NOC)	JANTX	1880	0	2.763222
Zener Diode (NOC)	JANTX	752	0	1.137476
Zener Diode (NOC)	JANTX	940	0	1.381611
Zener Diode (NOC)	JANTX	1302	0	1.009974
Zener Diode (NOC)	JANTX	4532	2	4.281518
Zener Diode (NOC)	JANTX	2902	0	1.696046
Full Wave Bridge Rect.	Unknown	1524	0	0.829055
Fast Recovery	Lower	603	0	0.783900
Fast Recovery	JANTX	6604	0	3.592520
Fast Recovery	JANTX	376	0	0.568738
Fast Recovery	JANTX	10157	0	5.948502
Fast Recovery	JANTX	508	2	0.276400
Fast Recovery	JANTX	1451	0	0.849786
Fast Recovery	JANTX	10157	4	5.948502
Fast Recovery	JANTX	752	0	1.137476
Fast Recovery	JANTX	508	0	0.276358
Fast Recovery	JANTX	2632	0	3.981166
Fast Recovery	JANTX	6580	2	9.671277
Fast Recovery	JANTX	940	0	1.381611
Fast Recovery	JANTX	651	0	0.504987
Fast Recovery	JANTX	1302	0	1.009974
Fast Recovery	JANTX	2902	0	1.696046
Fast Recovery	JANTX	2902	0	1.699572

MIL-HDBK-217E
DISCRETE SEMICONDUCTOR DATA SOURCE
(Diodes)

DEVICE TYPE	QUALITY	TESTED	FAILED	PART HOURS
Fast Recovery	JANTX	651	0	0.504987
Fast Recovery	JANTX	752	0	1.137476
Fast Recovery	JANTX	1451	0	0.849786
Fast Recovery	JANTX	2632	0	3.981166
Fast Recovery	JANTX	940	0	1.381611
Fast Recovery	JANTX	4532	5	4.281518
Fast Recovery	JANTX	15862	0	14.985313
Fast Recovery	JANTX	15862	5	14.985313
Fast Recovery	JANTX	2266	0	2.140759
Fast Recovery	JANTX	4557	1	3.534909
Fast Recovery	JANTX	1880	0	2.763222
Fast Recovery	JANTX	4532	0	4.281518
Fast Recovery	JANTX	376	0	0.568738
Fast Recovery	JANTX	1880	4	2.763222
Fast Recovery	JANTX	4557	0	3.534909
Fast Recovery	JANTX	1302	1	1.009974
Fast Recovery	JANTX	2266	0	2.140759
High Power Rectifier	JANTX	2902	0	1.696634
High Power Rectifier	JANTX	18128	1	17.126072
High Power Rectifier	JANTX	3008	0	4.549904
High Power Rectifier	JANTX	7520	0	11.052888
High Power Rectifier	JANTX	2604	0	2.019948
High Power Rectifier	JANTX	1302	0	1.009974
High Power Rectifier	JANTX	4532	1	4.281518
High Power Rectifier	JANTX	9064	1	8.563036
High Power Rectifier	JANTX	2902	1	1.699572
High Power Rectifier	JANTX	1880	0	5.382796
High Power Rectifier	JANTX	1302	0	1.009974
High Power Rectifier	JANTX	4532	6	4.281518
High Power Rectifier	JANTX	752	0	1.137476
High Power Rectifier	JANTX	1504	0	2.274952
High Power Rectifier	JANTX	1880	2	2.763222
High Power Rectifier	JANTX	752	0	1.137476
High Power Rectifier	JANTX	5208	2	4.039896
High Power Rectifier	JANTX	9740	0	4.251500
High Power Rectifier	JANTX	11608	1	6.798288
High Power Rectifier	JANTX	3760	0	5.526444
High Power Rectifier	JANTX	5804	1	3.392092
Rectifier	Plastic	3948	0	5.132400
Rectifier	Plastic	3948	0	5.132400
Rectifier	Lower	62178	3	80.831400
Rectifier	Lower	3810	0	4.953000
Rectifier	Lower	2535	3	3.295500
Rectifier	Lower	4230	0	5.499000
Rectifier	Lower	511460	22	664.898000
Rectifier	Lower	2893	2	3.760900
Rectifier	Lower	7909	5	10.281700
Rectifier	Lower	38594	0	50.172200
Rectifier	Lower	4317707	250	5613.019100

MIL-HDBK-217E
DISCRETE SEMICONDUCTOR DATA SOURCE
(Diodes)

DEVICE TYPE	QUALITY	TESTED	FAILED	PART HOURS
Rectifier	Lower	239135	50	310.875500
Rectifier	Lower	87550	16	113.815000
Rectifier	Lower	11606	3	15.087800
Rectifier	Lower	1285	0	1.670500
Rectifier	Lower	1024	0	1.331200
Rectifier	Lower	21260	10	27.638000
Rectifier	Lower	11885	0	15.450500
Rectifier	Lower	334476	22	434.818800
Rectifier	Lower	6550	0	8.515000
Rectifier	Lower	155273	40	201.854900
Rectifier	JANTX	651	0	0.504987
Rectifier	JANTX	1288	0	4.089170
Rectifier	JANTX	18506	4	8.077900
Rectifier	JANTX	504	0	1.600110
Rectifier	JANTX	56	0	0.177790
Rectifier	JANTX	3034	0	0.165812
Rectifier	JANTX	1624	0	5.155910
Rectifier	JANTX	2266	0	2.140759
Rectifier	JANTX	112	0	0.355580
Rectifier	JANTX	376	0	0.568738
Rectifier	JANTX	2032	0	1.105432
Rectifier	JANTX	3556	0	1.934416
Rectifier	JANTX	112	0	0.355580
Rectifier	JANTX	5844	1	2.550000
Rectifier	JANTX	940	0	1.381611
Rectifier	JANTX	116	0	2.032320
Rectifier	JANTX	84	2	0.266685
Rectifier	JANTX	1451	0	0.849786
Rectifier	JANTX	2922	0	2.210800
Rectifier	JAN	364	3	1.155635
General Purpose	Plastic	19795	2	25.733500
General Purpose	Lower	4	0	0.005200
General Purpose	Lower	15319	0	19.914700
General Purpose	Lower	2590	1	3.367000
General Purpose	JANTX	10157	0	5.948502
General Purpose	JANTX	6580	0	9.671277
General Purpose	JANTX	4557	0	3.534909
General Purpose	JANTX	2632	0	3.981166
General Purpose	JANTX	15862	0	14.985313
Switching	Lower	2011	6	2.614300
Switching	JANTX	12220	0	17.960943
Switching	JANTX	14322	3	11.109714
Switching	JANTX	2632	0	3.981166
Switching	JANTX	6580	2	18.839786
Switching	JANTX	49852	12	47.096698
Switching	JANTX	8272	2	12.512236
Switching	JANTX	64449	1	49.993713
Switching	JANTX	4888	0	7.393594
Switching	JANTX	752	0	1.137476

MIL-HDBK-217E
DISCRETE SEMICONDUCTOR DATA SOURCE
(Diodes)

DEVICE TYPE	QUALITY	TESTED	FAILED	PART HOURS
Switching	JANTX	10157	1	5.938219
Switching	JANTX	20680	10	30.395442
Switching	JANTX	1880	0	2.763222
Switching	JANTX	103244	23	45.066000
Switching	JANTX	28	0	0.088895
Switching	JANTX	31922	3	18.656506
Switching	JANTX	8708	2	27.646345
Switching	JANTX	753	9	0.409407
Switching	JANTX	6384	0	20.268060
Switching	JANTX	28	0	0.490560
Switching	JANTX	1302	3	1.009974
Switching	JANTX	224334	1	211.940000
Switching	JANTX	37224	1	56.305062
Switching	JANTX	2902	2	1.699572
Switching	JANTX	4557	1	3.534909
Switching	JANTX	2032	0	1.105394
Switching	JANTX	11200	0	35.558000
Switching	JANTX	93060	1	136.780000
Switching	JANTX	8463	0	6.564831
Switching	JANTX	15862	1	14.985313
Switching	JANTX	18863	0	11.047218
Switching	JANTX	28	15	0.490560
Switching	JANTX	29458	0	27.829867
Switching	JANTX	252	0	4.415040
Switching	JANTX	1016	1	0.552700
Switching	JANTX	143649	1	84.128814
Diodes (NOC)	Lower	4	4	0.070080
Diodes (NOC)	Lower	16	4	0.280320
Diodes (NOC)	Lower	12	0	0.210240
Diodes (NOC)	JANTX	940	2	1.381611
Diodes (NOC)	JANTX	2820	0	4.144833
Diodes (NOC)	JANTX	2902	8	1.699572
Diodes (NOC)	JANTX	940	3	1.381611
Diodes (NOC)	JANTX	1880	0	2.763222
Diodes (NOC)	JANTX	1880	4	2.763222
Diodes (NOC)	JANTX	1880	4	2.763222
Diodes (NOC)	JANTX	1451	1	0.849786
Diodes (NOC)	JANTX	1302	4	1.009974
Diodes (NOC)	JANTX	1302	6	1.009974
Diodes (NOC)	JANTX	1451	1	0.849786
Diodes (NOC)	JANTX	4353	0	2.549358
Diodes (NOC)	JANTX	1953	0	1.514961
Diodes (NOC)	JANTX	1302	3	1.009974
Diodes (NOC)	JANTX	651	1	0.504987
Diodes (NOC)	JANTX	651	2	0.504987
Diodes (NOC)	JANTX	1524	0	0.829055
Diodes (NOC)	JANTX	2902	4	1.699572
Diodes (NOC)	JANTX	2902	0	1.699572
Diodes (NOC)	JANTX	4532	39	4.281518

MIL-HDBK-217E
DISCRETE SEMICONDUCTOR DATA SOURCE
(Diodes)

DEVICE TYPE	QUALITY	TESTED	FAILED	PART HOURS
Diodes (NOC)	JANTX	752	0	1.137476
Diodes (NOC)	JANTX	6798	0	6.422277
Diodes (NOC)	JANTX	752	3	1.137476
Diodes (NOC)	JANTX	2266	5	2.140759
Diodes (NOC)	JANTX	376	0	0.568738
Diodes (NOC)	JANTX	4532	2	4.281518
Diodes (NOC)	JANTX	2266	2	2.140759
Diodes (NOC)	JANTX	4532	7	4.281518
Diodes (NOC)	JANTX	376	0	0.568738
Diodes (NOC)	JANTX	752	10	1.137476
Diodes (NOC)	JANTX	1128	0	1.706214
Diodes (NOC)	Unknown	1016	0	0.552697
Diodes (NOC)	Unknown	508	0	0.276358
Diodes (NOC)	JANTX	487	1	0.212577
Diodes (NOC)	JANTX	487	0	0.212577
***** Totals *****		12483602	3646	24680.627898

APPENDIX B-3:

TRANSISTOR DATA LISTING

DEVICE TYPE	QUALITY	TESTED	FAILED	PART HOURS
Programmable Unijunction	Plastic	6803	3	8.843900
Microwave Transistor	JANTX	2296	0	7.289390
Microwave Transistor	Unknown	60	0	0.505140
Microwave Transistor	Unknown	5	1	0.232500
Microwave Transistor	Unknown	9	1	0.352000
Transistor Array	Lower	4	0	0.070080
Transistor Array	Lower	24	0	0.420480
Chopper Transistor	Plastic	139045	2	180.758500
Chopper Transistor	Plastic	11250	3	14.625000
Darlington	JANTX	376	0	0.568738
Darlington	JANTX	940	1	1.381611
Darlington	JANTX	651	2	0.504987
Darlington	JANTX	2266	0	2.140759
Darlington	JANTX	1451	2	0.848023
Darlington	JANTX	3399	7	3.211138
Darlington	JANTX	977	1	0.757481
Darlington	JANTX	977	1	0.757481
Darlington	JANTX	1451	0	0.848023
Darlington	JANTX	564	0	0.853107
Darlington	JANTX	376	0	0.568738
Darlington	JANTX	1410	1	2.072416
Darlington	JANTX	376	0	0.568738
Darlington	JANTX	1088	1	0.636017
Darlington	JANTX	2266	0	2.140759
Darlington	JANTX	2177	0	1.272034
Darlington	JANTX	940	3	1.381611
Darlington	JANTX	564	0	0.853107
Darlington	JANTX	651	0	0.504987
Darlington	JANTX	1410	1	2.072416
Darlington	JANTX	1451	1	0.848023
Darlington	JANTX	1088	1	0.636017
Darlington	JANTX	376	0	0.568738
Darlington	JANTX	705	0	1.036208
Darlington	JANTX	2266	0	2.140759
Darlington	JANTX	488	0	0.378740
Darlington	JANTX	940	1	1.381611
Darlington	JANTX	488	0	0.378440
Darlington	JANTX	651	0	0.504987
Darlington	JANTX	705	1	1.036208
Darlington	JANTX	1451	2	0.848023
Darlington	JANTX	488	1	0.378740
Darlington	JANTX	2266	0	2.140759
Darlington	JANTX	282	0	0.426553
Darlington	JANTX	1880	1	2.763222
Darlington	JANTX	1574	1	1.605569
Darlington	JANTX	1303	1	1.009974
Darlington	JANTX	651	0	0.504987
Darlington	JANTX	2902	1	1.696046
Darlington	JANTX	3399	4	3.211138

MIL-HDBK-217E
DISCRETE SEMICONDUCTOR DATA SOURCE
(Transistors)

DEVICE TYPE	QUALITY	TESTED	FAILED	PART HOURS
Darlington	JANTX	752	0	1.137476
Darlington	JANTX	282	0	0.426553
Darlington	JANTX	752	0	1.137476
Darlington	JANTX	1574	2	1.605569
Darlington	JANTX	4532	5	4.281518
Darlington	JANTX	1574	1	1.605569
Darlington	JANTX	1303	1	1.009974
Darlington	JANTX	1088	0	0.636017
Darlington	JANTX	1880	2	2.763222
Darlington	JANTX	1088	1	0.636017
Darlington	JANTX	2902	0	1.696046
Darlington	JANTX	940	0	1.381611
Darlington	JANTX	4532	1	4.281518
Darlington	JANTX	488	0	0.378740
Darlington	JANTX	940	0	1.381611
Darlington	JANTX	282	0	0.426553
Darlington	JANTX	651	0	0.504987
Darlington	JANTX	1574	0	1.605569
Darlington	JANTX	705	1	1.036208
Darlington	JANTX	282	1	0.426553
Darlington	JANTX	705	3	1.036208
Darlington	JANTX	1451	1	0.848023
Darlington	JANTX	376	0	0.568738
Darlington	JANTX	2266	1	2.140759
Darlington	JANTX	2177	2	0.272034
Complementary	JANTX	2044	0	6.489335
Multiple (MATCHED)	Lower	4	0	0.070080
Multiple (MATCHED)	JANTX	12	0	0.210240
Multiple (MATCHED)	JANTX	508	1	0.276358
MOSFET RF	Plastic	44609	15	57.991700
MOSFET RF	Plastic	53094	108	69.022200
MOSFET RF	Plastic	25416	2	33.040800
MOSFET RF	JANTX	896	1	2.844640
MOSFET RF	JANTX	1504	3	2.274952
MOSFET RF	JANTX	784	0	2.489060
MOSFET RF	JANTX	4	0	0.070080
MOSFET RF	JANTX	16	0	0.280320
MOSFET RF	JANTX	9064	1	8.563036
MOSFET RF	JANTX	3760	0	5.526444
MOSFET RF	JANTX	5804	2	3.399144
MOSFET RF	JANTX	212	0	3.714240
MOSFET RF	JANTX	2604	0	2.019948
Bipolar RF	Plastic	20172	7	26.223600
Bipolar RF	Plastic	4140	3	5.382000
RF Transistor (NOC)	Lower	4	0	0.070080
RF Transistor (NOC)	Lower	16	0	0.280320
RF Transistor (NOC)	JANTX	5264	1	16.712260
RF Transistor (NOC)	Unknown	9	8	0.000648
RF Transistor (NOC)	Unknown	9	8	0.004320

MIL-HDBK-217E
DISCRETE SEMICONDUCTOR DATA SOURCE
(Transistors)

DEVICE TYPE	QUALITY	TESTED	FAILED	PART HOURS
RF Transistor (NOC)	Unknown	9	8	0.004320
RF Transistor (NOC)	Unknown	N/A	0	0.000000
Unijunction Transistor	Plastic	29368	14	38.178400
Unijunction Transistor	Plastic	10275	0	13.357500
Unijunction Transistor	Plastic	5218	3	6.783400
Unijunction Transistor	Plastic	3322	2	4.318600
Unijunction Transistor	JANTX	1451	0	0.849786
Unijunction Transistor	JANTX	8	0	0.140160
Unijunction Transistor	JANTX	2266	0	2.140759
Unijunction Transistor	JANTX	940	0	1.381611
Unijunction Transistor	JANTX	376	0	0.568738
Unijunction Transistor	JANTX	651	0	0.504987
MOSFET - P-Channel	Plastic	6074	4	7.896200
MOSFET - P-Channel	Unknown	17	0	0.042500
MOSFET - P-Channel	Unknown	17	1	0.040300
MOSFET - P-Channel	Unknown	17	0	0.042500
MOSFET - N-Channel	Plastic	8576	2	11.148800
MOSFET - N-Channel	Plastic	139756	97	181.682800
MOSFET - N-Channel	Plastic	13058	1	16.975400
MOSFET - N-Channel	Plastic	23899	15	31.068700
MOSFET - N-Channel	Plastic	N/A	0	0.000000
MOSFET - N-Channel	Plastic	8380	1	10.894000
MOSFET - N-Channel	Plastic	76197	66	99.056100
MOSFET - N-Channel	Plastic	1960	0	2.548000
MOSFET - N-Channel	Unknown	17	0	0.042500
MOSFET - N-Channel	Unknown	17	2	0.039500
MOSFET - N-Channel	Unknown	17	0	0.042500
MOSFET - N-Channel	Unknown	4	4	0.003674
MOSFET - N-Channel	Unknown	5	4	0.004603
MOSFET - N-Channel	Unknown	10	10	0.002851
MOSFET - N-Channel	Unknown	4	4	0.001272
MOSFET - N-Channel	Unknown	5	5	0.004637
MOSFET - N-Channel	Unknown	17	0	0.042500
MOSFET - N-Channel	Unknown	5	5	0.005474
MOSFET - N-Channel	Unknown	17	1	0.042500
MOSFET - N-Channel	Unknown	4	4	0.002133
MOSFET - N-Channel	Unknown	17	3	0.036300
MOSFET - N-Channel	Unknown	4	4	0.002133
MOSFET - N-Channel	Unknown	17	0	0.042500
MOSFET - N-Channel	Unknown	2	2	0.002551
MOSFET - N-Channel	Unknown	17	0	0.042500
MOSFET - N-Channel	Unknown	10	10	0.011580
MOSFET - N-Channel	Unknown	17	0	0.042500
MOSFET - N-Channel	Unknown	2	2	0.002446
MOSFET - N-Channel	Unknown	17	0	0.042500
MOSFET - N-Channel	Unknown	10	9	0.014150
MOSFET - N-Channel	Unknown	10	10	0.012231
MOSFET - N-Channel	Unknown	20	3	0.046300
MOSFET - N-Channel	Unknown	2	2	0.000096

MIL-HDBK-217E
DISCRETE SEMICONDUCTOR DATA SOURCE
(Transistors)

DEVICE TYPE	QUALITY	TESTED	FAILED	PART HOURS
MOSFET - N-Channel	Unknown	2	2	0.002190
MOSFET - N-Channel	Unknown	5	5	0.000240
MOSFET - N-Channel	Unknown	17	0	0.042500
MOSFET - N-Channel	Unknown	4	4	0.001704
MOSFET - N-Channel	Unknown	17	2	0.038596
MOSFET - N-Channel	Unknown	11	10	0.006075
MOSFET - N-Channel	Unknown	17	0	0.042500
MOSFET - N-Channel	Unknown	3	2	0.005741
MOSFET - N-Channel	Unknown	1	1	0.000024
MOSFET - N-Channel	Unknown	17	0	0.042500
MOSFET - N-Channel	Unknown	17	0	0.042500
MOSFET - N-Channel	Unknown	17	9	0.032072
MOSFET - N-Channel	Unknown	17	4	0.037300
MOSFET - N-Channel	Unknown	12	12	0.012389
MOSFET - N-Channel	Unknown	3	1	0.000777
MOSFET - N-Channel	Unknown	5	4	0.001104
MOSFET - N-Channel	Unknown	9	9	9120.000000
MOSFET - N-Channel	Unknown	4	4	0.000288
JFET - P-Channel	Plastic	77127	3	100.265100
JFET - P-Channel	Plastic	149	0	0.193700
JFET - P-Channel	Plastic	22003	5	28.603900
JFET - P-Channel	JANTX	651	1	0.504987
JFET - P-Channel	JANTX	376	0	0.568738
JFET - P-Channel	JANTX	940	0	1.381611
JFET - P-Channel	JANTX	2266	2	2.140759
JFET - P-Channel	JANTX	1451	2	0.849786
JFET - P-Channel	Unknown	1016	1	0.552697
JFET - N-Channel	Plastic	4093	0	5.320900
JFET - N-Channel	Plastic	792122	137	1029.758600
JFET - N-Channel	Plastic	20916	20	27.190800
JFET - N-Channel	Plastic	467	0	0.607100
JFET - N-Channel	Plastic	1485011	419	1930.514300
JFET - N-Channel	Plastic	4072	0	5.293600
JFET - N-Channel	Plastic	39108	0	50.840400
JFET - N-Channel	Plastic	336155	127	437.001500
JFET - N-Channel	Plastic	1071301	93	1392.691300
JFET - N-Channel	Plastic	1654	1	2.150200
JFET - N-Channel	Plastic	59924	38	77.901200
JFET - N-Channel	Plastic	371	0	0.482300
JFET - N-Channel	Lower	8	0	0.140160
JFET - N-Channel	JANTX	11201	15	4.889270
JFET - N-Channel	JANTX	5859	1	4.544883
JFET - N-Channel	JANTX	20394	7	19.266831
JFET - N-Channel	JANTX	8460	3	12.434499
JFET - N-Channel	JANTX	7255	1	4.248930
JFET - N-Channel	JANTX	4700	1	6.908055
JFET - N-Channel	JANTX	252	0	0.800055
JFET - N-Channel	JANTX	28	0	0.088895
JFET - N-Channel	JANTX	13059	0	7.632207

MIL-HDBK-217E
DISCRETE SEMICONDUCTOR DATA SOURCE
(Transistors)

DEVICE TYPE	QUALITY	TESTED	FAILED	PART HOURS
JFET - N-Channel	JANTX	1880	0	2.843690
JFET - N-Channel	JANTX	3384	0	5.118642
JFET - N-Channel	JANTX	11330	1	10.703795
JFET - N-Channel	JANTX	56	0	0.177790
JFET - N-Channel	JANTX	252	0	0.800055
JFET - N-Channel	JANTX	3255	0	2.524935
Field Effect	Unknown	7	7	0.000900
Field Effect	Unknown	7	3	0.031620
Field Effect	Unknown	16	0	0.097800
Field Effect	Unknown	16	0	0.063500
Field Effect	Unknown	14	9	0.017193
Field Effect	Unknown	12	11	0.024353
Field Effect	Unknown	4	0	0.005839
Field Effect	Unknown	36	0	0.015320
Field Effect	Unknown	4	0	0.000500
Field Effect	Unknown	139	1	1.059500
Field Effect	Unknown	7	4	0.014387
Field Effect	Unknown	8	4	0.001900
Field Effect	Unknown	12	8	0.014610
Field Effect	Unknown	6	0	0.134100
Field Effect	Unknown	24	0	0.147800
Field Effect	Unknown	16	12	0.034312
Field Effect	Unknown	14	0	0.028100
Field Effect	Unknown	16	12	0.034312
Field Effect	Unknown	N/A	0	0.002600
Field Effect	Unknown	N/A	4	0.146000
Field Effect	Unknown	N/A	8	0.033000
Field Effect	Unknown	N/A	1	0.000109
Field Effect	Unknown	N/A	1	0.000254
Field Effect	Unknown	N/A	1	0.001645
Field Effect	Unknown	N/A	11	0.003300
Field Effect	Unknown	N/A	5	0.004765
Field Effect	Unknown	N/A	8	0.014000
Field Effect	Unknown	N/A	6	0.010000
Field Effect	Unknown	N/A	4	0.077100
Field Effect	Unknown	N/A	6	0.001040
Field Effect	Unknown	N/A	10	0.105000
Field Effect	Unknown	N/A	8	0.027300
Field Effect	Unknown	N/A	13	0.008500
Field Effect	Unknown	N/A	4	0.008400
Field Effect	Unknown	N/A	1	0.002200
Field Effect	Unknown	N/A	66	0.088000
Field Effect	Unknown	N/A	22	0.012600
Field Effect	Unknown	N/A	1	0.001800
Field Effect	Unknown	N/A	11	0.004200
Field Effect	Unknown	N/A	8	0.006560
Field Effect	Unknown	N/A	7	0.000840
Field Effect	Unknown	N/A	10	0.007800
Field Effect	Unknown	N/A	8	0.068960

MIL-HDBK-217E
DISCRETE SEMICONDUCTOR DATA SOURCE
(Transistors)

DEVICE TYPE	QUALITY	TESTED	FAILED	PART HOURS
Field Effect	Unknown	N/A	1	0.000620
Field Effect	Unknown	N/A	3	0.000825
Field Effect	Unknown	N/A	21	0.026539
Field Effect	Unknown	N/A	30	0.021160
Field Effect	Unknown	N/A	24	0.022960
High Power Germanium	Plastic	1068	0	1.388400
High Power Germanium	Plastic	3010	1	3.913000
High Power Germanium	Plastic	3496	3	4.544800
High Power Silicon	Plastic	96215	32	125.079500
High Power Silicon	Plastic	65595	5	85.273500
High Power Silicon	Plastic	13812	0	17.955600
High Power Silicon	Plastic	29544	65	38.407200
High Power Silicon	Plastic	2872	1	3.733600
High Power Silicon	Plastic	86563	16	112.531900
High Power Silicon	Plastic	50642	12	65.834600
High Power Silicon	Plastic	1854	0	2.410200
High Power Silicon	Plastic	178668	48	232.268400
High Power Silicon	Plastic	68210	6	88.673000
High Power Silicon	Plastic	36081	3	46.905300
High Power Silicon	Plastic	15793	10	20.530900
High Power Silicon	Plastic	51931	51	67.510300
High Power Silicon	Plastic	28208	3	36.670400
High Power Silicon	Plastic	62	0	0.080600
High Power Silicon	Plastic	16206	1	21.067800
High Power Silicon	Plastic	4616	0	6.000800
High Power Silicon	Plastic	12939	2	16.820700
High Power Silicon	Plastic	4398	12	5.717400
High Power Silicon	Plastic	27061	7	35.179300
High Power Silicon	Plastic	4616	0	6.000800
High Power Silicon	Plastic	7636	0	9.926800
High Power Silicon	Plastic	18	0	0.023400
High Power Silicon	Plastic	3242	0	4.214600
High Power Silicon	Plastic	2551	0	3.316300
High Power Silicon	JANTX	2435	19	1.062800
High Power Silicon	JANTX	487	0	0.212575
High Power Silicon	JANTX	376	0	0.568738
High Power Silicon	JANTX	376	7	0.568738
High Power Silicon	JANTX	376	1	0.568738
High Power Silicon	JANTX	376	0	0.568738
High Power Silicon	JANTX	940	0	1.381611
High Power Silicon	JANTX	940	1	1.381611
High Power Silicon	JANTX	376	0	0.568738
High Power Silicon	JANTX	1451	1	0.849786
High Power Silicon	JANTX	4700	4	6.908055
High Power Silicon	JANTX	508	0	0.276358
High Power Silicon	JANTX	7520	2	11.052888
High Power Silicon	JANTX	2266	0	2.140759
High Power Silicon	JANTX	651	0	0.504987
High Power Silicon	JANTX	2266	0	2.140759

MIL-HDBK-217E
DISCRETE SEMICONDUCTOR DATA SOURCE
(Transistors)

DEVICE TYPE	QUALITY	TESTED	FAILED	PART HOURS
High Power Silicon	JANTX	2266	0	2.140759
High Power Silicon	JANTX	5804	1	3.399144
High Power Silicon	JANTX	940	0	2.691398
High Power Silicon	JANTX	1451	0	0.848317
High Power Silicon	JANTX	11608	1	6.798288
High Power Silicon	JANTX	11330	4	10.703795
High Power Silicon	JANTX	376	0	0.568738
High Power Silicon	JANTX	940	0	1.381611
High Power Silicon	JANTX	3008	2	4.549904
High Power Silicon	JANTX	3255	2	2.524935
High Power Silicon	JANTX	651	0	0.504987
High Power Silicon	JANTX	2266	0	2.140759
High Power Silicon	JANTX	1016	0	0.552697
High Power Silicon	JANTX	1451	0	0.849786
High Power Silicon	JANTX	9064	3	8.563036
High Power Silicon	JANTX	2266	8	2.140759
High Power Silicon	JANTX	940	1	1.381611
High Power Silicon	JANTX	2266	16	2.140759
High Power Silicon	JANTX	2266	1	2.140759
High Power Silicon	JANTX	1008	3	3.200220
High Power Silicon	JANTX	376	1	0.568738
High Power Silicon	JANTX	2604	0	2.019948
High Power Silicon	JANTX	4	0	0.070080
High Power Silicon	JANTX	940	0	0.000000
High Power Silicon	JANTX	3048	0	1.658110
High Power Silicon	JANTX	18128	2	17.126072
High Power Silicon	JANTX	2032	4	1.105394
High Power Silicon	JANTX	1451	1	0.849786
High Power Silicon	JANTX	2266	2	2.140759
High Power Silicon	JANTX	508	0	0.276358
High Power Silicon	JANTX	940	0	1.381611
High Power Silicon	JANTX	1016	17	0.552697
High Power Silicon	JANTX	1451	0	0.849786
High Power Silicon	JANTX	376	0	0.568738
High Power Silicon	JANTX	940	1	1.381611
High Power Silicon	JANTX	7255	1	4.248930
High Power Silicon	JANTX	508	2	0.276358
High Power Silicon	JANTX	1504	0	2.274952
High Power Silicon	JANTX	1451	0	0.849786
High Power Silicon	JANTX	4	0	0.070080
High Power Silicon	JANTX	1451	0	0.849786
High Power Silicon	JANTX	1880	2	2.843690
High Power Silicon	JANTX	728	0	2.311270
High Power Silicon	JANTX	3760	2	5.526444
High Power Silicon	JANTX	940	0	1.381611
High Power Silicon	JANTX	1451	8	0.849786
High Power Silicon	JANTX	651	0	0.504987
High Power Silicon	JANTX	651	2	0.504987
High Power Silicon	JANTX	651	1	0.504987

MIL-HDBK-217E
DISCRETE SEMICONDUCTOR DATA SOURCE
(Transistors)

DEVICE TYPE	QUALITY	TESTED	FAILED	PART HOURS
High Power Silicon	JANTX	651	0	0.504987
High Power Silicon	JANTX	651	0	0.504987
High Power Silicon	JANTX	5208	1	4.039896
High Power Silicon	JANTX	651	0	0.504987
High Power Silicon	JAN	56	0	0.177790
High Power Silicon	JAN	168	0	0.533370
High Power Silicon	JAN	112	0	0.355580
High Power Transistor	Plastic	20306	15	26.397800
High Power Transistor	Unknown	48	1053	0.840960
High Power Transistor	Unknown	24	154	0.420480
High Power Transistor	Unknown	12	160	0.210240
Lower Power Germanium	Plastic	8894	8	11.562200
Lower Power Germanium	Plastic	28440	10	36.972000
Lower Power Germanium	Plastic	6851	1	8.960300
Lower Power Germanium	Plastic	2394	0	3.112200
Lower Power Germanium	JANTX	752	0	1.137476
Lower Power Germanium	JANTX	1302	0	1.009974
Lower Power Germanium	JANTX	1880	0	2.763222
Lower Power Germanium	JANTX	2902	0	1.699572
Lower Power Germanium	JANTX	4	0	0.070080
Lower Power Germanium	JANTX	4532	0	4.281518
Lower Power Germanium	JANTX	1451	0	0.848023
Lower Power Germanium	JANTX	940	0	1.381611
Lower Power Germanium	JANTX	1451	1	0.848023
Lower Power Germanium	JANTX	2266	5	2.140759
Lower Power Germanium	JANTX	376	0	0.568738
Lower Power Germanium	JANTX	1451	0	0.848023
Lower Power Germanium	JANTX	940	0	1.381611
Lower Power Germanium	JANTX	651	0	0.504981
Lower Power Germanium	JANTX	2266	0	2.140759
Lower Power Germanium	JANTX	2266	5	2.140759
Lower Power Germanium	JANTX	376	0	0.568738
Lower Power Germanium	JANTX	651	1	0.504981
Lower Power Germanium	JANTX	940	0	1.381611
Lower Power Germanium	JANTX	651	0	0.504981
Lower Power Germanium	JANTX	376	0	0.568738
Lower Power Silicon	Plastic	1614	0	2.098200
Lower Power Silicon	Plastic	46486	4	60.431800
Lower Power Silicon	Plastic	497906	36	647.277800
Lower Power Silicon	Plastic	2902019	199	3772.624700
Lower Power Silicon	Plastic	6333208	628	8233.170400
Lower Power Silicon	Plastic	38797	0	50.436100
Lower Power Silicon	Plastic	1054499	355	1370.848700
Lower Power Silicon	Plastic	1224732	187	1592.151600
Lower Power Silicon	Plastic	87376	1	113.588800
Lower Power Silicon	Plastic	2372	0	3.083600
Lower Power Silicon	Plastic	284005	77	369.206500
Lower Power Silicon	Plastic	105779	12	137.512700
Lower Power Silicon	Plastic	1247549	99	1621.813700

MIL-HDBK-217E
DISCRETE SEMICONDUCTOR DATA SOURCE
(Transistors)

DEVICE TYPE	QUALITY	TESTED	FAILED	PART HOURS
Lower Power Silicon	Plastic	22302	3	28.992600
Lower Power Silicon	Plastic	1380502	218	1794.652600
Lower Power Silicon	Plastic	20040	0	26.052000
Lower Power Silicon	Plastic	6986	0	9.081800
Lower Power Silicon	Plastic	183495	12	238.543500
Lower Power Silicon	Plastic	1113506	89	1447.557800
Lower Power Silicon	Plastic	1534067	258	1994.287100
Lower Power Silicon	Plastic	7208	1	9.370400
Lower Power Silicon	Plastic	14122	5	18.358600
Lower Power Silicon	Plastic	116155	5	151.001500
Lower Power Silicon	JANTX	9064	0	8.563036
Lower Power Silicon	JANTX	11330	4	10.703795
Lower Power Silicon	JANTX	1960	0	6.222650
Lower Power Silicon	JANTX	504	0	1.600110
Lower Power Silicon	JANTX	56	0	0.177790
Lower Power Silicon	JANTX	420	0	1.333425
Lower Power Silicon	JANTX	2032	3	1.105401
Lower Power Silicon	JANTX	7305	0	3.188632
Lower Power Silicon	JANTX	4116	3	13.067565
Lower Power Silicon	JANTX	1451	0	0.849785
Lower Power Silicon	JANTX	84	0	0.266685
Lower Power Silicon	JANTX	29458	1	27.829867
Lower Power Silicon	JANTX	420	0	1.333425
Lower Power Silicon	JANTX	448	0	1.442320
Lower Power Silicon	JANTX	5804	0	3.399144
Lower Power Silicon	JANTX	7255	2	4.248930
Lower Power Silicon	JANTX	5804	1	3.399144
Lower Power Silicon	JANTX	5804	3	3.399144
Lower Power Silicon	JANTX	18863	2	11.047218
Lower Power Silicon	JANTX	651	1	0.504987
Lower Power Silicon	JANTX	196	0	0.622265
Lower Power Silicon	JANTX	4532	0	4.281518
Lower Power Silicon	JANTX	5804	0	3.399144
Lower Power Silicon	JANTX	2266	1	2.140759
Lower Power Silicon	JANTX	9064	0	8.563036
Lower Power Silicon	JANTX	2256	0	3.412428
Lower Power Silicon	JANTX	1880	0	2.843690
Lower Power Silicon	JANTX	8706	1	5.088138
Lower Power Silicon	JANTX	7255	0	4.240115
Lower Power Silicon	JANTX	13059	1	7.632207
Lower Power Silicon	JANTX	13596	0	12.844554
Lower Power Silicon	JANTX	24	0	0.420480
Lower Power Silicon	JANTX	2902	0	1.696634
Lower Power Silicon	JANTX	476	0	1.511215
Lower Power Silicon	JANTX	7255	2	4.241585
Lower Power Silicon	JANTX	3384	0	5.118642
Lower Power Silicon	JANTX	376	1	0.568738
Lower Power Silicon	JANTX	39934	55	17.431300
Lower Power Silicon	JANTX	8	0	0.140160

MIL-HDBK-217E
DISCRETE SEMICONDUCTOR DATA SOURCE
(Transistors)

DEVICE TYPE	QUALITY	TESTED	FAILED	PART HOURS
Lower Power Silicon	JANTX	2266	3	8.563036
Lower Power Silicon	JANTX	752	0	1.137476
Lower Power Silicon	JANTX	1880	1	2.843690
Lower Power Silicon	JANTX	1880	0	5.382796
Lower Power Silicon	JANTX	487	0	0.212575
Lower Power Silicon	JANTX	4700	0	13.456990
Lower Power Silicon	JANTX	5640	0	8.289666
Lower Power Silicon	JANTX	4700	1	6.908055
Lower Power Silicon	JANTX	8460	0	12.434499
Lower Power Silicon	JANTX	940	6	1.381611
Lower Power Silicon	JANTX	8706	1	5.098716
Lower Power Silicon	JANTX	20	0	0.350400
Lower Power Silicon	JANTX	4532	1	4.281518
Lower Power Silicon	JANTX	2266	2	8.563036
Lower Power Silicon	JANTX	11330	1	10.703795
Lower Power Silicon	JANTX	13596	1	12.844554
Lower Power Silicon	JANTX	11330	3	10.703795
Lower Power Silicon	JANTX	20394	2	19.266831
Lower Power Silicon	JANTX	2266	39	2.140759
Lower Power Silicon	JANTX	2435	4	1.062800
Lower Power Silicon	JANTX	5859	1	4.544883
Lower Power Silicon	JANTX	12	0	0.210240
Lower Power Silicon	JANTX	651	4	0.504987
Lower Power Silicon	JANTX	2435	5	1.062800
Lower Power Silicon	JANTX	3906	1	3.029922
Lower Power Silicon	JANTX	3255	0	2.524935
Lower Power Silicon	JANTX	1302	0	1.009974
Lower Power Silicon	JANTX	3255	0	2.524935
Lower Power Silicon	JANTX	974	0	0.425151
Lower Power Silicon	JANTX	92	0	1.611840
Lower Power Silicon	JANTX	7112	38	3.868867
Lower Power Silicon	JANTX	3760	0	5.526444
Lower Power Silicon	JANTX	4700	3	6.908055
Lower Power Silicon	JANTX	508	1	0.276358
Lower Power Silicon	JANTX	940	4	1.381611
Lower Power Silicon	JANTX	4572	7	2.487079
Lower Power Silicon	JANTX	9253	6	4.038962
Lower Power Silicon	JANTX	3760	0	5.526444
Lower Power Silicon	JANTX	5640	0	8.289666
Lower Power Silicon	JANTX	2902	0	1.699572
Lower Power Silicon	JANTX	84	0	0.266685
Lower Power Silicon	JANTX	1016	0	0.552697
Lower Power Silicon	JANTX	1036	0	3.289115
Lower Power Silicon	JANTX	2256	0	3.412428
Lower Power Silicon	JANTX	1504	0	2.274952
Lower Power Silicon	JANTX	3906	0	3.029922
Lower Power Silicon	JANTX	16	0	0.280320
Lower Power Silicon	JANTX	88	4	1.541760
Lower Power Silicon	JANTX	12220	1	17.960943

MIL-HDBK-217E
DISCRETE SEMICONDUCTOR DATA SOURCE
(Transistors)

DEVICE TYPE	QUALITY	TESTED	FAILED	PART HOURS
Lower Power Silicon	JANTX	1	1	5.526444
Lower Power Silicon	JANTX	2604	0	2.019948
Lower Power Silicon	JANTX	3760	5	5.526444
Lower Power Silicon	JANTX	20	0	0.350400
Lower Power Silicon	JANTX	752	0	1.137476
Lower Power Silicon	JANTX	1504	1	2.274952
Lower Power Silicon	JANTX	1504	2	2.274952
Lower Power Silicon	JANTX	4888	1	7.393594
Lower Power Silicon	JANTX	1880	0	2.763222
Lower Power Silicon	JANTX	1504	0	2.274952
Lower Power Silicon	JANTX	1880	1	2.843690
Lower Power Silicon	JANTX	376	1	0.568738
Lower Power Silicon	JANTX	1573	0	0.920602
Lower Power Silicon	JANTX	1018	0	1.496745
Lower Power Silicon	JANTX	705	1	0.347069
Lower Power Silicon	JANTX	407	0	0.616133
Lower Power Silicon	JANTX	2455	0	2.319556
Lower Power Silicon	JANTX	1573	0	0.920602
Lower Power Silicon	JANTX	1018	0	1.496745
Lower Power Silicon	JANTX	705	0	0.347069
Lower Power Silicon	JANTX	407	0	0.616133
Lower Power Silicon	JANTX	2455	0	2.319556
Lower Power Silicon	JANTX	1573	0	0.920602
Lower Power Silicon	JANTX	1018	0	1.496745
Lower Power Silicon	JANTX	705	0	0.347069
Lower Power Silicon	JANTX	407	0	0.616133
Lower Power Silicon	JANTX	2455	1	2.319556
Lower Power Silicon	JANTX	1573	0	0.920602
Lower Power Silicon	JANTX	1018	2	1.496745
Lower Power Silicon	JANTX	705	1	0.547069
Lower Power Silicon	JANTX	705	0	0.547069
Lower Power Silicon	JANTX	407	0	0.616133
Lower Power Silicon	JANTX	407	0	0.616133
Lower Power Silicon	JANTX	1573	1	0.920602
Lower Power Silicon	JANTX	2455	2	2.319156
Lower Power Silicon	JANTX	2821	2	2.188277
Lower Power Silicon	JANTX	1572	1	0.920602
Lower Power Silicon	JANTX	2455	0	2.319156
Lower Power Silicon	JANTX	1018	2	1.496745
Lower Power Silicon	JANTX	1018	0	1.496745
Lower Power Silicon	JANTX	4073	0	5.986981
Lower Power Silicon	JANTX	1629	0	2.464531
Lower Power Silicon	JANTX	1572	0	0.920602
Lower Power Silicon	JANTX	9819	4	9.276223
Lower Power Silicon	JANTX	705	0	0.547069
Lower Power Silicon	JANTX	407	0	0.616133
Lower Power Silicon	JANTX	2455	0	2.319156
Lower Power Silicon	JANTX	407	0	0.616133
Lower Power Silicon	JANTX	2455	1	2.319556

MIL-HDBK-217E
DISCRETE SEMICONDUCTOR DATA SOURCE
(Transistors)

DEVICE TYPE	QUALITY	TESTED	FAILED	PART HOURS
Lower Power Silicon	JANTX	705	0	0.347069
Lower Power Silicon	JANTX	3144	0	1.841203
Lower Power Silicon	JANTX	1411	1	1.094138
Lower Power Silicon	JANTX	2455	0	2.319156
Lower Power Silicon	JANTX	2037	1	2.993491
Lower Power Silicon	JANTX	1018	0	1.496745
Lower Power Silicon	JANTX	815	0	1.232266
Lower Power Silicon	JANTX	407	0	0.616133
Lower Power Silicon	JANTX	2455	0	2.319156
Lower Power Silicon	JANTX	1018	0	1.496745
Lower Power Silicon	JANTX	1573	0	0.920602
Lower Power Silicon	JANTX	705	1	0.547069
Lower Power Silicon	JANTX	1018	0	1.496745
Lower Power Silicon	JANTX	2455	0	2.319156
Lower Power Silicon	JANTX	407	0	0.616133
Lower Power Silicon	JANTX	1018	0	1.496745
Lower Power Silicon	JANTX	705	0	0.347069
Lower Power Silicon	JANTX	407	0	0.616133
Lower Power Silicon	JANTX	2455	0	2.319156
Lower Power Silicon	JANTX	2455	0	2.319556
Lower Power Silicon	JANTX	1573	0	0.920602
Lower Power Silicon	JANTX	705	0	0.547069
Lower Power Silicon	JANTX	1018	0	1.496745
Lower Power Silicon	JANTX	705	1	0.347069
Lower Power Silicon	JANTX	407	0	0.616133
Lower Power Silicon	JANTX	1573	0	0.920602
Lower Power Silicon	JANTX	705	0	0.347069
Lower Power Silicon	JANTX	4910	0	4.638311
Lower Power Silicon	JANTX	2455	0	2.319156
Lower Power Silicon	JANTX	407	0	0.616133
Lower Power Silicon	JANTX	705	0	0.347069
Lower Power Silicon	JANTX	1572	0	0.920602
Lower Power Silicon	JANTX	4910	0	4.638311
Lower Power Silicon	JANTX	3144	0	1.841203
Lower Power Silicon	JANTX	815	0	1.232266
Lower Power Silicon	JANTX	1411	0	1.094138
Lower Power Silicon	JANTX	2037	0	2.993491
Lower Power Silicon	JANTX	1573	0	0.920602
Lower Power Silicon	JANTX	1018	1	1.496745
Lower Power Silicon	JANTX	1573	0	0.920602
Lower Power Silicon	JANTX	1572	0	0.920602
Lower Power Silicon	JANTX	1018	0	1.496745
Lower Power Silicon	JANTX	407	0	0.616133
Lower Power Silicon	JANTX	1018	1	1.496745
Lower Power Silicon	JANTX	407	0	0.616133
Lower Power Silicon	JANTX	705	0	0.347069
Lower Power Silicon	JANTX	1018	0	1.496745
Lower Power Silicon	JANTX	1573	0	0.920602
Lower Power Silicon	JANTX	2455	0	2.319556

MIL-HDBK-217E
DISCRETE SEMICONDUCTOR DATA SOURCE
(Transistors)

DEVICE TYPE	QUALITY	TESTED	FAILED	PART HOURS
Lower Power Silicon	JANTX	407	1	0.616133
Lower Power Silicon	JANTX	705	0	0.547069
Lower Power Silicon	JANTX	705	1	0.347069
Lower Power Silicon	JANTX	1703	0	1.320735
Lower Power Silicon	JANTX	2455	0	2.319556
Lower Power Silicon	JANTX	4917	0	7.226888
Lower Power Silicon	JANTX	1573	0	0.920602
Lower Power Silicon	JANTX	11852	0	11.197816
Lower Power Silicon	JANTX	705	0	0.347069
Lower Power Silicon	JANTX	1967	0	2.974937
Lower Power Silicon	JANTX	407	0	0.616133
Lower Power Silicon	JANTX	3405	0	2.641470
Lower Power Silicon	JANTX	1018	0	1.496745
Lower Power Silicon	JANTX	492	0	0.743734
Lower Power Silicon	JANTX	2455	0	2.319556
Lower Power Silicon	JANTX	1229	0	1.806722
Lower Power Silicon	JANTX	1410	0	1.094138
Lower Power Silicon	JANTX	2963	2	2.799454
Lower Power Silicon	JANTX	3144	0	1.841203
Lower Power Silicon	JANTX	851	1	0.660368
Lower Power Silicon	JANTX	1222	1	1.848398
Lower Power Silicon	JANTX	2963	0	2.799454
Lower Power Silicon	JANTX	3055	0	4.490236
Lower Power Silicon	JANTX	1229	1	1.806722
Lower Power Silicon	JANTX	7365	0	6.957467
Lower Power Silicon	JANTX	1897	1	1.108953
Lower Power Silicon	JANTX	705	0	0.347069
Lower Power Silicon	JANTX	851	0	0.660367
Lower Power Silicon	JANTX	1573	0	0.920602
Lower Power Silicon	JANTX	492	0	0.743734
Lower Power Silicon	JANTX	407	0	0.616133
Lower Power Silicon	JANTX	3795	1	2.217906
Lower Power Silicon	JANTX	1018	0	1.496745
Lower Power Silicon	JANTX	2458	0	3.613444
Lower Power Silicon	JANTX	2458	0	3.613444
Lower Power Silicon	JANTX	5926	0	5.598908
Lower Power Silicon	JANTX	1573	0	0.920600
Lower Power Silicon	JANTX	983	0	1.487468
Lower Power Silicon	JANTX	1897	1	1.108953
Lower Power Silicon	JANTX	1703	0	1.320735
Lower Power Silicon	JANTX	2963	40	2.799454
Lower Power Silicon	JANTX	1451	8	0.848023
Lower Power Silicon	JANTX	851	2	0.660368
Lower Power Silicon	JANTX	2266	39	2.140759
Lower Power Silicon	JANTX	2458	0	3.613445
Lower Power Silicon	JANTX	2455	0	2.319556
Lower Power Silicon	JANTX	983	0	1.487686
Lower Power Silicon	JANTX	407	0	0.616133
Lower Power Silicon	JANTX	1018	0	1.496745

MIL-HDBK-217E
DISCRETE SEMICONDUCTOR DATA SOURCE
(Transistors)

DEVICE TYPE	QUALITY	TESTED	FAILED	PART HOURS
Lower Power Silicon	JANTX	705	0	0.347069
Lower Power Silicon	JANTX	1573	0	0.920602
Lower Power Silicon	JANTX	1018	0	1.996745
Lower Power Silicon	JANTX	815	0	1.232266
Lower Power Silicon	JANTX	1573	0	0.920602
Lower Power Silicon	JANTX	4910	0	4.638311
Lower Power Silicon	JANTX	2455	0	2.319556
Lower Power Silicon	JANTX	4716	0	2.761804
Lower Power Silicon	JANTX	705	0	0.347069
Lower Power Silicon	JANTX	1018	0	1.496745
Lower Power Silicon	JANTX	1018	0	1.496745
Lower Power Silicon	JANTX	705	0	0.347069
Lower Power Silicon	JANTX	1573	0	0.920602
Lower Power Silicon	JANTX	5926	0	5.598908
Lower Power Silicon	JANTX	2455	0	2.319556
Lower Power Silicon	JANTX	1229	3	1.806722
Lower Power Silicon	JANTX	407	0	0.616133
Lower Power Silicon	JANTX	3795	1	2.217906
Lower Power Silicon	JANTX	2455	1	2.319556
Lower Power Silicon	JANTX	407	0	0.616133
Lower Power Silicon	JANTX	3255	2	2.524935
Lower Power Silicon	JANTX	705	0	0.347069
Lower Power Silicon	JANTX	2604	0	2.019948
Lower Power Silicon	JANTX	2116	0	1.641208
Lower Power Silicon	JANTX	407	0	0.616133
Lower Power Silicon	JANTX	2455	0	2.319556
Lower Power Silicon	JANTX	705	1	0.347069
Lower Power Silicon	JANTX	1703	0	1.320735
Lower Power Silicon	JANTX	1018	0	1.496745
Lower Power Silicon	JANTX	5926	0	5.598908
Lower Power Silicon	JANTX	1302	0	1.009974
Lower Power Silicon	JANTX	2037	0	2.993491
Lower Power Silicon	JANTX	1573	0	0.920602
Lower Power Silicon	JANTX	492	1	0.743734
Lower Power Silicon	JANTX	2455	1	2.319556
Lower Power Silicon	JANTX	407	0	0.616133
Lower Power Silicon	JANTX	1573	0	0.920602
Lower Power Silicon	JANTX	2455	0	2.319556
Lower Power Silicon	JANTX	407	0	0.616133
Lower Power Silicon	JANTX	2604	2	2.019948
Lower Power Silicon	JANTX	2604	3	2.019948
Lower Power Silicon	JANTX	8463	3	6.564831
Lower Power Silicon	JANTX	1572	0	0.920602
Lower Power Silicon	JANTX	1018	0	1.496745
Lower Power Silicon	JANTX	983	0	1.487469
Lower Power Silicon	JANTX	2756	0	2.603626
Lower Power Silicon	JANTX	792	0	0.614173
Lower Power Silicon	JANTX	2756	0	2.603626
Lower Power Silicon	JANTX	792	0	0.614173

MIL-HDBK-217E
DISCRETE SEMICONDUCTOR DATA SOURCE
(Transistors)

DEVICE TYPE	QUALITY	TESTED	FAILED	PART HOURS
Lower Power Silicon	JANTX	1143	0	1.680338
Lower Power Silicon	JANTX	457	0	0.691708
Lower Power Silicon	JANTX	457	0	0.691708
Lower Power Silicon	JANTX	1765	0	1.033523
Lower Power Silicon	JANTX	1143	0	1.680338
Lower Power Silicon	JANTX	1143	0	1.680338
Lower Power Silicon	JANTX	2756	0	2.603626
Lower Power Silicon	JANTX	792	0	0.614173
Lower Power Silicon	JANTX	1765	0	1.033523
Lower Power Silicon	JANTX	2756	0	2.603626
Lower Power Silicon	JANTX	792	0	0.614173
Lower Power Silicon	JANTX	457	0	0.691708
Lower Power Silicon	JANTX	457	0	0.691708
Lower Power Silicon	JANTX	1765	0	1.033523
Lower Power Silicon	JANTX	1143	0	1.680338
Lower Power Silicon	JANTX	1143	0	1.680338
Lower Power Silicon	JANTX	2756	0	2.603626
Lower Power Silicon	JANTX	792	0	0.614173
Lower Power Silicon	JANTX	1765	1	1.033523
Lower Power Silicon	JANTX	2756	0	2.603626
Lower Power Silicon	JANTX	792	0	0.614173
Lower Power Silicon	JANTX	457	0	0.691708
Lower Power Silicon	JANTX	457	0	0.691708
Lower Power Silicon	JANTX	1765	0	1.033523
Lower Power Silicon	JANTX	1143	0	1.680338
Lower Power Silicon	JANTX	1143	1	1.680338
Lower Power Silicon	JANTX	16536	3	15.621797
Lower Power Silicon	JANTX	792	0	0.614173
Lower Power Silicon	JANTX	10588	1	6.201141
Lower Power Silicon	JANTX	2756	0	2.603626
Lower Power Silicon	JANTX	792	0	0.614173
Lower Power Silicon	JANTX	457	0	0.691708
Lower Power Silicon	JANTX	457	0	0.691708
Lower Power Silicon	JANTX	1765	0	1.033523
Lower Power Silicon	JANTX	1143	1	1.680338
Lower Power Silicon	JANTX	1143	0	1.680338
Lower Power Silicon	JANTX	2756	0	2.603626
Lower Power Silicon	JANTX	792	0	0.614173
Lower Power Silicon	JANTX	1765	1	1.033523
Lower Power Silicon	JANTX	2756	2	2.603626
Lower Power Silicon	JANTX	792	0	0.614173
Lower Power Silicon	JANTX	457	4	0.691708
Lower Power Silicon	JANTX	457	0	0.691708
Lower Power Silicon	JANTX	1765	3	1.033523
Lower Power Silicon	JANTX	1143	0	1.680338
Lower Power Silicon	JANTX	1143	1	1.680338
Lower Power Silicon	JANTX	2756	0	2.603626
Lower Power Silicon	JANTX	792	0	0.614173
Lower Power Silicon	JANTX	1765	0	1.033523

MIL-HDBK-217E
DISCRETE SEMICONDUCTOR DATA SOURCE
(Transistors)

DEVICE TYPE	QUALITY	TESTED	FAILED	PART HOURS
Lower Power Silicon	JANTX	2756	0	2.603626
Lower Power Silicon	JANTX	792	0	0.614173
Lower Power Silicon	JANTX	457	0	0.691708
Lower Power Silicon	JANTX	457	0	0.691708
Lower Power Silicon	JANTX	1765	0	1.033523
Lower Power Silicon	JANTX	1143	0	1.680338
Lower Power Silicon	JANTX	1143	0	1.680338
Lower Power Silicon	JANTX	457	0	0.691708
Lower Power Silicon	JANTX	792	0	0.614173
Lower Power Silicon	JANTX	1143	0	1.680338
Lower Power Silicon	JANTX	2756	1	2.603626
Lower Power Silicon	JANTX	792	1	0.614173
Lower Power Silicon	JANTX	457	0	0.691708
Lower Power Silicon	JANTX	457	0	0.691708
Lower Power Silicon	JANTX	1765	0	1.033523
Lower Power Silicon	JANTX	1143	0	1.680338
Lower Power Silicon	JANTX	1143	0	1.680338
Lower Power Silicon	JANTX	2756	0	2.603626
Lower Power Silicon	JANTX	792	0	0.614173
Lower Power Silicon	JANTX	1765	0	1.033523
Lower Power Silicon	JANTX	2756	0	2.603626
Lower Power Silicon	JANTX	792	0	0.614173
Lower Power Silicon	JANTX	457	0	0.691708
Lower Power Silicon	JANTX	1765	0	1.033523
Lower Power Silicon	JANTX	1765	0	1.033523
Lower Power Silicon	JANTX	457	1	0.691708
Lower Power Silicon	JANTX	1143	0	1.680338
Lower Power Silicon	JANTX	2756	0	2.603626
Lower Power Silicon	JANTX	792	0	0.614173
Lower Power Silicon	JANTX	792	1	0.614173
Lower Power Silicon	JANTX	2756	0	2.603626
Lower Power Silicon	JANTX	1143	0	1.680338
Lower Power Silicon	JANTX	457	0	0.691708
Lower Power Silicon	JANTX	1765	0	1.033523
Lower Power Silicon	JANTX	1765	0	1.033523
Lower Power Silicon	JANTX	2744	0	4.150250
Lower Power Silicon	JANTX	1143	0	1.680338
Lower Power Silicon	JANTX	2756	1	2.603626
Lower Power Silicon	JANTX	1584	0	1.228347
Lower Power Silicon	JANTX	792	0	0.614173
Lower Power Silicon	JANTX	5512	1	5.207252
Lower Power Silicon	JANTX	1143	0	1.680338
Lower Power Silicon	JANTX	915	0	1.383417
Lower Power Silicon	JANTX	1765	0	1.033523
Lower Power Silicon	JANTX	3529	0	2.067047
Lower Power Silicon	JANTX	457	0	0.691708
Lower Power Silicon	JANTX	2286	0	3.360675
Lower Power Silicon	JANTX	2756	0	2.603626
Lower Power Silicon	JANTX	792	0	0.614173

MIL-HDBK-217E
DISCRETE SEMICONDUCTOR DATA SOURCE
(Transistors)

DEVICE TYPE	QUALITY	TESTED	FAILED	PART HOURS
Lower Power Silicon	JANTX	2756	0	2.603626
Lower Power Silicon	JANTX	2756	0	2.603626
Lower Power Silicon	JANTX	792	0	0.614173
Lower Power Silicon	JANTX	457	1	0.691708
Lower Power Silicon	JANTX	1765	0	1.033523
Lower Power Silicon	JANTX	1143	0	1.680338
Lower Power Silicon	JANTX	457	0	0.691708
Lower Power Silicon	JANTX	792	0	0.614173
Lower Power Silicon	JANTX	2756	1	2.603626
Lower Power Silicon	JANTX	2756	0	2.603626
Lower Power Silicon	JANTX	1143	0	1.680338
Lower Power Silicon	JANTX	457	0	0.691708
Lower Power Silicon	JANTX	457	0	0.691708
Lower Power Silicon	JANTX	1765	0	1.033523
Lower Power Silicon	JANTX	4750	1	3.685040
Lower Power Silicon	JANTX	1143	0	1.680338
Lower Power Silicon	JANTX	1765	0	1.033523
Lower Power Silicon	JANTX	792	0	0.614173
Lower Power Silicon	JANTX	2756	0	2.603626
Lower Power Silicon	JANTX	2756	1	2.603626
Lower Power Silicon	JANTX	1143	0	1.680338
Lower Power Silicon	JANTX	457	0	0.691708
Lower Power Silicon	JANTX	1765	0	1.033523
Lower Power Silicon	JANTX	1765	0	1.033523
Lower Power Silicon	JANTX	792	0	0.614173
Lower Power Silicon	JANTX	1143	0	1.680338
Lower Power Silicon	JANTX	792	0	0.614173
Lower Power Silicon	JANTX	792	0	0.614173
Lower Power Silicon	JANTX	2756	0	2.603626
Lower Power Silicon	JANTX	2756	0	2.603626
Lower Power Silicon	JANTX	457	0	0.691708
Lower Power Silicon	JANTX	457	0	0.691708
Lower Power Silicon	JANTX	1765	0	1.033523
Lower Power Silicon	JANTX	1765	0	1.033523
Lower Power Silicon	JANTX	1143	0	1.680338
Lower Power Silicon	JANTX	6859	1	10.082026
Lower Power Silicon	JANTX	792	0	0.614173
Lower Power Silicon	JANTX	2756	0	2.603626
Lower Power Silicon	JANTX	1765	0	1.033523
Lower Power Silicon	JANTX	1143	0	1.680338
Lower Power Silicon	JANTX	792	0	0.614173
Lower Power Silicon	JANTX	2756	1	2.603626
Lower Power Silicon	JANTX	457	0	0.691708
Lower Power Silicon	JANTX	1765	0	1.033523
Lower Power Silicon	JANTX	457	0	0.691708
Lower Power Silicon	JANTX	1765	0	1.033523
Lower Power Silicon	JANTX	1143	0	1.680338
Lower Power Silicon	JANTX	792	0	0.614173
Lower Power Silicon	JANTX	2756	0	2.603626

MIL-HDBK-217E
DISCRETE SEMICONDUCTOR DATA SOURCE
(Transistors)

DEVICE TYPE	QUALITY	TESTED	FAILED	PART HOURS
Lower Power Silicon	JANTX	1143	0	1.680338
Lower Power Silicon	JANTX	1765	1	1.033523
Lower Power Silicon	JANTX	457	0	0.691708
Lower Power Silicon	JAN	84	14	0.099654
Lower Power Silicon	JAN	1792	0	5.689280
Lower Power Silicon	JAN	84	1	0.266685
Lower Power Silicon	Unknown	17	6	0.042500
Lower Power Silicon	Unknown	17	0	0.042500
Lower Power Silicon	Unknown	17	0	0.042500
Lower Power Transistor	Plastic	17821	9	23.167300
Lower Power Transistor	Plastic	114	0	0.148200
Lower Power Transistor	Plastic	433880	16	564.044000
Transistors (NOC)	Lower	4	142	0.070080
Transistors (NOC)	Lower	4	201	0.070080
Transistors (NOC)	JANTX	2266	0	2.140759
Transistors (NOC)	JANTX	1451	0	0.849786
Transistors (NOC)	JANTX	940	1	1.381611
Transistors (NOC)	JANTX	940	1	1.381611
Transistors (NOC)	JANTX	1880	0	2.763222
Transistors (NOC)	JANTX	1451	0	0.849786
Transistors (NOC)	JANTX	376	0	0.568738
Transistors (NOC)	JANTX	2902	0	1.699572
Transistors (NOC)	JANTX	752	1	1.137476
Transistors (NOC)	JANTX	4532	3	4.281518
Transistors (NOC)	JANTX	376	1	0.568738
Transistors (NOC)	JANTX	2266	2	2.140759
Transistors (NOC)	JANTX	974	0	0.425151
Transistors (NOC)	JANTX	974	0	0.425151
Transistors (NOC)	JANTX	974	0	0.425151
Transistors (NOC)	JANTX	1016	0	0.552697
Transistors (NOC)	JANTX	651	2	0.504987
Transistors (NOC)	JANTX	1302	0	1.009974
Transistors (NOC)	JANTX	651	0	0.504987
Transistors (NOC)	Unknown	508	0	0.276358
Transistors (NOC)	JANTX	974	0	0.425151
Transistors (NOC)	JANTX	974	0	0.425151
***** Totals *****		25576997	6655	41915.231532

APPENDIX B-4:

OPTO-ELECTRONIC DEVICE

DATA LISTING

MIL-HDBK-217E
DISCRETE SEMICONDUCTOR DATA SOURCE
(Optoelectronics)

DEVICE TYPE	QUALITY	TESTED	FAILED	PART HOURS
LED Display	Plastic	7941	0	10.323300
LED Display	Plastic	20894	1	27.162200
LED Display	Plastic	205730	4	267.449000
LED Display	Plastic	17498	0	22.747400
LED Display	Plastic	3450	1	4.485000
LED Display	Plastic	20550	1	26.715000
LED Display	Plastic	69715	6	90.629500
LED Display	Plastic	660	0	0.858000
LED Display	Plastic	43633	2	56.722900
LED Display	Plastic	1980	0	2.574000
LED Display	Plastic	15881	0	20.645300
LED Display	Plastic	1058	2	1.375400
LED Display	Plastic	486054	14	631.870200
LED Display	Plastic	6748	0	8.772400
LED Display	Plastic	3819	0	4.964700
LED Display	Plastic	369	0	0.479700
LED Display	Plastic	351966	17	457.555800
LED Display	Plastic	78272	9	101.753600
LED Display	Plastic	487014	16	633118.200000
LED Display	Plastic	146721	1	190.737300
LED Display	Plastic	21339	1	27.740700
LED Display	Plastic	228639	6	297.230700
LED Display	Plastic	548252	28	712.727600
LED Display	Plastic	23105	2	30.036500
LED Display	Plastic	288102	17	374.532600
LED Display	Plastic	11974	3	15.566200
LED Display	Plastic	9053	0	11.768900
LED Display	Plastic	128195	13	166.535000
Optoelectronic Displays	Plastic	72	0	0.093600
Optoelectronic Displays	Plastic	872	0	1.133600
Optoelectronic Displays	Plastic	936	0	1.216800
Dual Transistor	Plastic	1841	0	2.393300
Dual Transistor	Plastic	33243	0	43.215000
Dual Darlington	Plastic	156964	61	204.053200
Photocircuit (IC) Output	Plastic	398	0	0.517400
Photodarlington Output	Plastic	22621	1	29.407300
Phototransistor Output	Plastic	33	0	0.042900
Phototransistor Output	Plastic	4872	0	6.333600
Phototransistor Output	Plastic	2464	0	3.203200
Phototransistor Output	Plastic	22183	34	28.837900
Phototransistor Output	Plastic	232	0	0.301600
Phototransistor Output	Plastic	315	0	0.409500
Phototransistor Output	Plastic	21018	14	27.323400
Phototransistor Output	Plastic	3785	9	4.920500
Phototransistor Output	Plastic	90691	51	117.898300
Phototransistor Output	JANTX	1016	0	0.552697
Phototransistor Output	JANTX	1016	0	0.552697
Photocoupler (NOC)	Plastic	90205	41	117.652600

MIL-HDBK-217E
DISCRETE SEMICONDUCTOR DATA SOURCE
(Optoelectronics)

DEVICE TYPE	QUALITY	TESTED	FAILED	PART HOURS
Photocoupler (NOC)	Unknown	45	37	0.094312
Photocoupler (NOC)	Unknown	117	30	0.404880
Photocoupler (NOC)	Unknown	45	27	0.131840
Photocoupler (NOC)	Unknown	45	41	0.312488
Photocoupler (NOC)	Unknown	45	39	0.076680
Photocoupler (NOC)	Unknown	120	29	0.458000
Photocoupler (NOC)	Unknown	45	26	0.123944
Photocoupler (NOC)	Unknown	117	30	0.404880
Photocoupler (NOC)	Unknown	45	37	0.094312
Photocoupler (NOC)	Unknown	45	41	0.050840
Phototransistor Sensor	Plastic	30148	0	39.192400
Phototransistor Sensor	Plastic	5808	7	7.550400
Photodiode Sensor	Plastic	5	0	0.006500
Photodiode Sensor	Plastic	148	0	0.192400
Photodiode Sensor	Plastic	5	0	0.006500
Photodiode Sensor	Unknown	16	0	0.076800
Laser Diode	Unknown	8	2	0.154000
Laser Diode	Unknown	1	1	0.021000
Laser Diode	Unknown	2	2	0.008000
Laser Diode	Unknown	20	0	0.010000
Laser Diode	Unknown	12	0	0.120000
Laser Diode	Unknown	15	0	0.150000
Laser Diode	Unknown	7	0	0.070000
Laser Diode	Unknown	8	0	0.080000
Laser Diode	Unknown	40	29	0.080000
Laser Diode	Unknown	100	74	0.450506
Laser Diode	Unknown	9	1	0.102000
Laser Diode	Unknown	40	38	0.300000
Laser Diode	Unknown	103	64	0.006180
Laser Diode	Unknown	N/A	0	0.000000
Laser Diode	Unknown	15	9	0.195000
Laser Diode	Unknown	15	9	0.168000
Laser Diode	Unknown	24	7	0.560000
Laser Diode	Unknown	72	20	0.720000
Laser Diode	Unknown	95	47	0.005700
Laser Diode	Unknown	40	0	0.336120
Laser Diode	Unknown	23	13	0.107977
Laser Diode	Unknown	15	7	0.097053
Laser Diode	Unknown	16	5	0.109872
Laser Diode	Unknown	76	37	0.230605
Laser Diode	Unknown	N/A	17	0.015300
Laser Diode	Unknown	40	29	0.080000
Laser Diode	Unknown	17	12	0.060318
Laser Diode	Unknown	45	11	0.318576
Laser Diode	Unknown	16	8	0.089974
Infrared Diode Array	Plastic	30148	0	39.192400
LED Diode Array	Plastic	8977	0	11.670100
LED Diode Array	Plastic	74864	0	97.323200
LED Diode Array	Plastic	44137	1	57.378100

MIL-HDBK-217E
DISCRETE SEMICONDUCTOR DATA SOURCE
(Optoelectronics)

DEVICE TYPE	QUALITY	TESTED	FAILED	PART HOURS
LED Diode Array	Plastic	80463	2	104.601900
LED Diode Array	Plastic	1158	0	1.505400
LED Diode Array	Plastic	281	0	0.365300
LED Diode Array	Plastic	149	0	0.193700
LED Diode Array	Plastic	3795	0	4.933500
LED Diode Array	Plastic	104	0	0.135200
LED Diode Array	Plastic	257496	1	334.744800
LED Diode Array	Plastic	6184	0	8.039200
LED Diode Array	Plastic	8904	0	11.575200
LED Diode Array	Plastic	624	0	0.811200
LED Diode Array	Plastic	6908	0	8.980400
LED Diode Array	Plastic	446	0	0.579800
LED Diode Array	Plastic	2058	0	2.675400
LED Diode Array	Plastic	160	0	0.208000
LED Diode Array	Plastic	160	0	0.208000
LED Diode Array	Plastic	3	0	0.003900
LED Diode Array	Plastic	740	0	0.962000
LED Diode Array	Unknown	11	1	0.003162
LED Diode Array	Unknown	10	1	0.003162
LED Diode Array	Unknown	36	14	0.028640
LED Diode Array	Unknown	30	14	0.081000
LED Diode Array	Unknown	36	28	0.020488
LED Diode Array	Unknown	12	5	0.003162
LED Diode Array	Unknown	36	35	0.007456
LED Diode Array	Unknown	30	18	0.060000
LED Diode Array	Unknown	30	9	0.189000
LED Diode Array	Unknown	13	15	0.003162
LED Diode Array	Unknown	36	34	0.009840
LED Diode Array	Unknown	36	29	0.024976
LED Diode Array	Unknown	36	34	0.013192
Infrared (IRED)	Unknown	20	10	0.386560
Infrared (IRED)	Unknown	20	18	0.516020
Infrared (IRED)	Unknown	20	11	0.120080
Light Emitting Diode	Plastic	19044	0	24.757200
Light Emitting Diode	Plastic	225	0	0.292500
Light Emitting Diode	Plastic	1182	0	1.536600
Light Emitting Diode	Plastic	75	0	0.097500
Light Emitting Diode	Plastic	20478	8	26.621400
Light Emitting Diode	Plastic	1067	0	1.387100
Light Emitting Diode	Plastic	702	0	0.912600
Light Emitting Diode	Plastic	1937741	4	2519.063300
Light Emitting Diode	Plastic	5348	0	6.952400
Light Emitting Diode	Plastic	8148	0	10.592400
Light Emitting Diode	Plastic	750	0	0.975000
Light Emitting Diode	Plastic	8867	0	11.527100
Light Emitting Diode	Plastic	1439050	0	1870.765000
Light Emitting Diode	Plastic	5756	0	7.482800
Light Emitting Diode	Plastic	22249	5	28.923700
Light Emitting Diode	Plastic	7052	0	9.167600

MIL-HDBK-217E
DISCRETE SEMICONDUCTOR DATA SOURCE
(Optoelectronics)

DEVICE TYPE	QUALITY	TESTED	FAILED	PART HOURS
Light Emitting Diode	Plastic	9698	0	12.607400
Light Emitting Diode	Plastic	426	0	0.553800
Light Emitting Diode	Plastic	193098	0	251.027400
Emitter (Single LED)	Plastic	32183	5	41.837900
Optoelectronics (NOC)	Plastic	36	0	0.046800
Optoelectronics (NOC)	Plastic	2248	0	2.922400
Optoelectronics (NOC)	Plastic	8143	0	10.585900
Optoelectronics (NOC)	Plastic	725361	2	942.969300
Optoelectronics (NOC)	Plastic	19522	7	25.378600
Optoelectronics (NOC)	Plastic	347929	0	452.307700
Optoelectronics (NOC)	Plastic	1129	0	1.467700
Optoelectronics (NOC)	Plastic	104	1	0.135200
Optoelectronics (NOC)	Plastic	38	0	0.494000
Optoelectronics (NOC)	Plastic	1626	0	2.113800
Optoelectronics (NOC)	Plastic	2088470	0	2715.011000
***** Totals *****		11156978	1453	646994.111051

REFERENCES

1. Kern, G.A. and T. M. Drnas, Operational Influences on Reliability, RADC-TR-76-366, December 1976. (A035 016)

2. Coit, D., K. Dey, and W. Turkowski, "Practical Reliability Data and Analysis," Reliability Engineering, January 1986.

3. Sellberg, F., P. Weissglas, and G. Anderson, "A Study of Failure Mechanisms in Si IMPATT Diodes," IEEE Transactions on Electron Devices, Vol. ED-25, No. 6, June 1978, pp. 742-745.

4. Sinnaduri, F.N., "Accelerated Aging of IMPATT Diodes," Microelectronics Reliability, Vol. 21, No. 2, 1981, pp. 209-219.

5. Staecker, P., et.al, "Reliability of Si and GaAs K_A-Band IMPATT Diodes," 12th Annual Proceedings, Reliability Physics, April 1974, pp. 293-295.

6. Ballamy, W.C., and L.C. Kimerling, "Premature Failure in Pt-GaAs IMPATTS - Recombination Assisted Diffusion as a Failure-Mechanism," IEEE Transactions on Electron Devices, Vol. ED-25, No. 6, June 1978, pp. 746-752.

7. Heaton, J.L., Reliability Study of High Efficiency GaAs IMPATT Devices, RADC-TR-78-203, Microwave Associates Incorporated, January 1979. (A067 223)

8. Reith, T.M., "Aging Effects in Si-doped Al Schottky Barrier Diodes," Applied Physics Letters, Vol. 28, No. 1, February 1976, pp. 152-154.

9. Croft, D.C., "The Construction and Reliability of Schottky Diodes," Microelectronics Reliability, Vol. 17, July 1977, pp. 445-455.

10. Omori, M., "Metallic Contact on GaAs Microwave Devices," 15th Annual Proceedings, Reliability Physics, April 1977, pp. 232-239.

11. White, P.M., C.G. Rogers, and B.S. Hewitt, "Reliability Ku-Band GaAs Power FETs Under Highly Stressed RF Operation," 21st Annual Proceedings, Reliability Physics, April 1983, pp. 297-301.

12. Fukui, H., et.al., "Reliability of Improved Power GaAs FETs," 18th Annual Proceedings, Reliability Physics, April 1980, pp. 151-158.

13. Jordan, A.S., et.al., "A Large Scale Reliability Study of Burnout Failure In GaAs Power FETs," 18th Annual Proceedings, Reliability Physics, April 1980, pp. 123-130.

14. Moskowitz, S., "Power GaAs FETs Show Great Expectations for Longevity," Microwaves, Vol. 20, No. 12, November 1980, pp. 20-31.

REFERENCES (CONT'D)

15. Christou, A., "GaAs Device Reliability Workshop Summary," 21st Annual Proceedings, Reliability Physics, April 1983, p. 292.

16. Christou, A., "Report on the 1982 GaAs Device Reliability Workshop," 20th Annual Proceedings, Reliability Physics, April 1982.

17. Irie, T., et.al., "Reliability Study of GaAs MESFETS," IEEE Transactions on Microwave Theory and Techniques, Vol. MTT-24, No. 6, June 1976, pp. 110-119.

18. Omori, M., J. Wholey, and J.F. Gibbons, "Accelerated Active Life Tests of GaAs FET and a New Failure Mode," 18th Annual Proceedings, Reliability Physics, April 1980, pp.134-139.

19. Lundgren, R., Reliability Study of GaAs FET, RADC-TR-78-213, Hughes Research Laboratories, October 1978. (A061 473)

20. Macksey, H., Reliability Evaluation of GaAs FETs, RADC-TR-80-390, 1980. (A096 306)

21. Brydon, G.M., and B.G. Caplen, "Reliability Evaluation of Plessey Low Noise GaAs FETs," 21st Annual Proceedings, Reliability Physics, April 1983, pp. 302-311.

22. Bowman, L., and W. Tarn, Reliability Investigation of Low Noise GaAs FETs, RADC-TR-81-181, Hughes Aircraft Co., July 1981. (A108 396)

23. Zoroglu, D.S., High Reliability 225-400 MHz 50-Watt Si Transistor, TR-ECOM-0172, Motorola Inc., November 1971.

24. Herr, E.A., A. Poe, and A. Fox, "Reliability Evaluation and Prediction of Discrete Semiconductors," IEEE Transactions on Reliability, Vol. R-29, No. 3, August 1980, pp. 208-216.

25. Sim, S.P., "The Reliability of Si Avalanche Photodiodes for Use in Optical-Fiber Transmission Systems," IEEE Transactions on Electron Devices, Vol. ED-29, No. 10, October 1982, pp. 1611-1616.

26. Flint, S., Failure Rates for Fiber Optic Assemblies, RADC-TR-80-322, IIT Research Institute, October 1980. (A092 315)

27. Zipfel, C.C., et.al., "Reliability of DH $Ga_{1-x}Al_xAs$ LEDs for Lightwave Communications," 19th Annual Proceedings, Reliability Physics, April 1981, pp. 124-129.

28. Pommer, K., "Reliability Study of $GaAs_{63}P_{37}$ LEDs," 13th Annual Proceedings, Reliability Physics, April 1985, pp. 200-206.

REFERENCES (CONT'D)

29. Woolhouse, G.R., "Degradation in Injection Lasers," IEEE Journal of Quantum Electronics, Vol. QE-11, No. 7, July 1975, pp. 556-561.

30. Ralston, J.M., and J.W. Mann, Temperature and Current Dependence of Degradaton In Red-Emitting GaP LEDs, June 1978.

31. Todoroki, S., et.al., "A New Failure Mechanism Related to the Formation of Dark Defects," 21st Annual Proceedings, Reliability Physics, April 1983, pp. 160-166.

32. Kumada, S., H. Shimizu and K. Itoh, "Lifetimes of 800nm-Wavelength GaAlAs Semiconductor Lasers," 21st Annual Proceedings, Reliability Physics, April 1983, pp. 153-159.

33. Hartman, R.L., N.E. Shumaker, and R.W. Dixon, "Continuously Operated (AlGa)As DH Lasers with 70°C Lifetimes as Long as Two Years," Semiconductor Injection Lasers, IEEE Press, 1980, pp. 323-326.

34. Kressel, H., et.al., "Accelerated Step-Temperature Aging of $Al_xGa_{1-x}As$ Heterojunction Laser Diodes," Semiconductor Injection Lasers, IEEE Press, 1980, pp. 327-331.

35. Barry, J., and G. Mecherle, Laser Diode Life/Reliability Testing, SD-TR-84-07, Hughes Aircraft Company, October 1983.

36. Electronic Engineer's Handbook, 2nd, Edition, edited by D. Fink and D. Christiansen, McGraw Hill, New York 1982.

37. Eskin, D.J. and C.R. McCanless, Reliability Derating Procedures, RADC-TR-84-254, Martin Marietta Aerospace, December 1984. (153 744)

38. Macksey, H. and L. Joy, Reliability Evaluation of GaAs Power FETs, RADC-TR-80-124, April 1980. (A086 668)

39. Clarke, R., and B. Stallard, Reliability Study of Microwave Power Transistors, RADC-TR-75-18, TRW, Inc., January 1975. (A007 788)

40. Manchester, K.F., "Thermal Resistance - A Reliability Consideration," Proceedings, 1980 Electronic Components Conference, Sprague Electric Co., April 1980, pp. 362-370.

41. Ito, C.R., et.al., 240 GHz IMPATT Diode Development Program, Hughes Aircraft Company, June 1979.

42. Kahn, S.R., Effects of EMP Testing on Semiconductor Long Term Reliability, IIT Research Institute, November 1977.

43. Dey, K.A., Practical Statistical Analysis for the Reliability Engineer, Reliability Analysis Center Publication, SOAR-2, 1983.

REFERENCES (CONT'D)

44. Ayyagari, M.S., J.L. Heaton, and N. Jansen, Reliability of High-Power Pulsed IMPATT Diodes, RADC-TR-81-315, Microwave Associates, Inc., November 1981. (A110 798)

45. Yamamoto, T., K. Sakai, and S. Akiba, "10,000-h Continuous CW Operation of $In_{1-x}Ga_xAs_yP_{1-y}$/InP DH Lasers at Room Temperatures," IEEE Journal of Quantum Electronics, Vol. QE-15, No. 8, August 1979, pp. 684-687.

46. Derated Application of Parts for ESD Systems Development, ESD-TR-85-148, Rome Air Development Center, March 1985.

47. Butler, T.W., D.F. Cottrell, and W.M. Maynard, Failure Rate Mathematical Models for Discrete Semiconductors, RADC-TR-78-3, Martin Marietta Corporation, January 1978. (A050 181)

48. Coit, D.W. and M.G. Priore, Impact of Nonoperating Periods on Equipment Reliability, RADC-TR-85-91, IIT Research Institute, May 1985. (A158 843)

49. Herr, E, et.al., Failure Mechanisms in Semiconductor Diodes, RADC-TR-68-123, General Electric Company, September 1968. (839885)

50. Priore, M.G., IC Quality Grades: Impact on System Reliability and Life Cycle Cost, RAC Publication (SOAR-3), Winter 1984/85.

51. Somos, I.L., L.O. Eriksson, and W.H. Tobin, "Understanding di/dt Ratings and Life Expectancy for Thyristors," Power Conversion and Intelligent Motion, February 1986, pp. 56-59.

52. Reliability and Degradation, Semiconductor Devices and Circuits, Edited by M.J. Howes and D.V. Morgan, John Wiley & Sons, New York, 1981.

53. Guth, G.F., Reliability Prediction Models for Microwave Solid State Devices, RADC-TR-79-50, Martin Marietta Corporation, April 1979. (A069 386)

54. Mallorarpu, R. and G. MacMaster, 100W X-Band Spatial Field Power Combiner/Amplifier, Raytheon Company, November 1985.

55. Dominick, F., "How Much Pulsed Power Can a PIN Diode Handle?," Microwaves, February 1976, pp. 54-59.

56. Heaton, J.L., R.E. Walline, and J.F. Carroll, "Reliability Study of High Efficiency Gallium Arsenide Avalanche Diodes," 16th Annual Proceedings, Reliability Physics, April 1978, pp. 261-267.

57. Ramachandran, T.B., J.L. Heaton, and E.B. Hakin, "Reliability Studies of Gunn Diodes," 12th Annual Proceedings, Reliability Physics, Microwave Assoc., Inc., April 1971, pp. 284-289.

REFERENCES (CONT'D)

58. Christou, A., and Y. Anand, "GaAs Mixer Diode Burn-out Mechanisms at 36-94 GHz," 18th Annual Proceedings, Reliability Physics, April 1980, pp. 140-144.

59. Johnson, R.A., "Operating Diodes at mm-Wave Frequencies," Microwaves and RF, April 1984, p. 143.

60. Yen, H.C., W.F. Thorwer, M.M. Morishita, Millimeter-Wave Silion Diode Technology, AFWAL-TR-82-1032, March 1982.

61. Draper, N.R. and H. Smith, Applied Regression Analysis, John Wiley & Sons, New York, 1966.

62. Black, J.R., "Electromigration-A Brief Survey and Some Recent Results," IEEE Transactions on Electronic Devices, April 1969, pp. 338-347.

63. Utter, B., et.al., "Defect Free Transistors Demand Attention to Detail," Microwaves and RF, December 1985, pp. 65-68.

64. Poole, W.E. and L.G. Walsha, "Median-Time-to-Failure (MTF) of an L-Band Power Transistor Under RF Conditions," 12th Annual Proceedings, Reliability Physics, April 1974, pp. 109-115.

65. Hamiter, L. and F. Villella, "Identification of Failure Mechanisms and Activation Energy of Opto-Devices," 15th Annual Proceedings, Reliability Physics, April 1977, pp. 240-243.

66. Coit, D.W. and J.J. Steinkirchner, Reliability Modeling of Critical Electronic Devices, RADC-TR-83-108, May 1983. (A135 705)

67. Ettenberg, M. and H. Kressel "The Reliability of (AlGa)As CW Laser Diodes," IEEE Journal of Quantum Electronics, Vol. QE-16, No. 2., February 1980, pp. 186-196.

68. Newman, D.H. and S. Ritchie, "Degradation Pnenomena in Gallium Aluminium Arsenide Stripe Geometry Lasers," Cgechoslovak Journal of Physics, Vol. B30, 1980, pp. 336-344.

69. Goddard Space Flight Center, Product Assurance Briefs, PAB No. 82-01, March 31, 1982.

70. Ladany, I., M. Ettenberg, et.al., "Al_2O_3 Half-Wave Films for Long-life CW Lasers," Applied Physics Letters, Vol. 30, January 1977, pp. 87-88.

71. Paoli, L., "Changes in the Optical Properties of CW (AlGa)As Junction Lasers During Accelerated Aging," IEEE Journal of Quantum Electronics, Vol. QE-113, May 1977, pp. 351-359.

REFERENCES (CONT'D)

72. Channin, D.J., M. Ettenberg, and H. Kressel, "Self-Sustained Oscillations in (AlGa)As Oxide-Defined Stripe Lasers," Journal of Applied Physics, Vol. 50, No. 11, November 1979, pp. 6700-6706.

73. Hartman, R.L. and R.W. Dixon, "Reliability of DH GaAs Lasers at Elevated Temperatures," Semiconductor Injection Lasers, IEEE Press, 1980, pp. 302-305.

74. Yoshida, J., K. Chino and K. Wakita, et.al., "Degradation Behavior of AlGaAs Double-Heterostructure Laser Diodes Aged Under Pulsed Operating Conditions," IEEE Journal of Quantum Electronics, Vol. QE-18, No. 5, May 1982, pp. 879-884.

75. Ritchie, S., R. Godfrey, et.al., "The Temperature Dependence of Degradation Mechanisms in Long-Lived (GaAl)As DH Lasers," Journal of Applied Physics, June, 1978, p. 3127-3132.

76. Christou, A., E. Cohen and A. Macpherson, "Failure Modes in GaAs Power FETs: Ohmic Contact Electromigration and Formation of Refractory Oxides," 18th Annual Proceedings, Reliability Physics, April 1980.

77. Wang, S.K., E.A. Athey, et.al., "GaAs Power FET Technology Improvement", AFWAL-TR-86-1060, July 1986.

78. Priore, M. and D. Coit, "Impact of Nonoperating Periods on Monolithic Microcircuit Failure Rates," Proceedings, Government Microcircuits Application Conference (GOMAC), November 1986.

MISSION
of
Rome Air Development Center

RADC plans and executes research, development, test and selected acquisition programs in support of Command, Control, Communications and Intelligence (C^3I) activities. Technical and engineering support within areas of competence is provided to ESD Program Offices (POs) and other ESD elements to perform effective acquisition of C^3I systems. The areas of technical competence include communications, command and control, battle management, information processing, surveillance sensors, intelligence data collection and handling, solid state sciences, electromagnetics, and propagation, and electronic, maintainability, and compatibility.